Bulletin
of
The Geological Society of America

VOLUME 67 March 1956 NUMBER 3

CONTENTS

	Pages
Geology of the Blue Ridge near Harpers Ferry, West Virginia. By Richard P. Nickelsen	239–270
Late Wisconsin chronology of the Lake Michigan basin correlated with pollen studies. By James H. Zumberge and John E. Potzger	271–288
Structure of lopoliths. By H. D. Wilson	289–300
Paleomagnetic survey in Arizona and Utah: Preliminary results. By S. Keith Runcorn	301–316
Mineralogy and petrology of the Sittampundi complex, Salem district, Madras State, India. By A. P. Subramaniam	317–390
Short Note	
Cambro-Ordovician age of the "Inwood" limestone and "Manhattan" schist near Peekskill, New York. By Sidney Paige	391–394

Subscription $15.00 per year.

Printing Office: Mt. Royal & Guilford Aves., Baltimore 2, Md.

Communications for publications should be addressed to The Geological Society of America, Dr. H. R. Aldrich, Secretary, 419 West 117 Street, New York, N. Y.

Please give notice of change of address 4 weeks in advance. Claims for non-receipt of the Bulletin of a given month must be sent to the Secretary of the Society before the end of the second succeeding month.

Entered as second-class matter at the Post Office at Baltimore, Md.
under the Act of Congress of July 16, 1894.
Accepted for mailing at special rate of postage provided for in Section 1103
Act of October 3, 1917, authorized on July 8, 1918.

PAPERS IN PRESS FOR FORTHCOMING ISSUES

Geology and Structure of the Franklin-Sterling Area, New Jersey. By J. M. Hague, J. L. Baum, L. A. Hermann, and R. J. Pickering

Geology and Petrology of Enchanted Rock Batholith, Llano and Gillespie Counties, Texas. By Robert M. Hutchinson

Seismic-Refraction Measurements in the Atlantic Ocean. Part VII. By Samuel Katz and Maurice Ewing

Origin of the Chuska Sandstone, Arizona-New Mexico. By H. E. Wright, Jr.

Direct Radiometric Measurement by Gamma-Ray Scintillation Spectrometer. Parts 1 and 2. By Patrick M. Hurley

Evolution of Drainage Systems and Slopes in Badlands at Perth Amboy, New Jersey. By S. A. Schumm

Quantitative Slope Analysis. By A. N. Strahler

Physical Limnology and Sedimentation in a Glacial Lake. By W. H. Mathews

Gravity Survey of Puerto Rico. By G. Lynn Shurbet and Maurice Ewing

Geomorphology and Glacial History of Southernmost Baffin Island. By J. H. Mercer

Structures of Porphyritic Granite and Associated Metamorphic Rocks of East Manbhum, Bihar, India. By S. Sen

BULLETIN OF THE GEOLOGICAL SOCIETY OF AMERICA
VOL. 67, PP. 239-270, 11 FIGS., 3 PLS. MARCH 1956

GEOLOGY OF THE BLUE RIDGE NEAR HARPERS FERRY, WEST VIRGINIA

BY RICHARD P. NICKELSEN

ABSTRACT

The stratigraphy and geologic structure of Precambrian to Lower Cambrian rocks of the Blue Ridge province of northwestern Virginia was established by mapping. Major rock divisions are: Precambrian gneiss, Precambrian and Lower Cambrian metasedimentary and metavolcanic rocks, and Lower Cambrian quartzites, phyllites, and carbonate rocks. The sedimentary-volcanic sequence consists of local sediments and subaerial basalts, deposited unconformably upon the gneiss. Thinning of this sequence toward the north may be due either to original variations in thickness or to erosion prior to deposition of overlying rocks. Widespread Lower Cambrian sediments of the platform facies were deposited in a shallow sea that covered the older rocks.

Blue Ridge and Short Hill are parts of the west limb of the Catoctin Mountain-Blue Ridge anticlinorium, formed by Paleozoic deformation. Each contains an overturned anticline and syncline. During deformation, flexure folding graded into shear folding at different times in rocks of different competency. Near the close of deformation, flow cleavage, formed earlier during the shear folding of incompetent rocks, was folded, and slip cleavage developed. No major thrust faults are recognized in the area; but the west limb of the Catoctin Mountain-Blue Ridge anticlinorium is repeated by a fault, here interpreted as a normal fault of Triassic age. The rocks, including the gneiss, which underwent retrogressive changes during Paleozoic folding, are in the greenschist facies of metamorphism.

CONTENTS

TEXT

	Page
Introduction	240
Acknowledgments	240
Previous work	240
Stratigraphy	242
General	242
Precambrian rocks	242
Gneissic basement	242
Swift Run formation	243
Catoctin formation	244
Stratigraphic relationships and age of the Swift Run and Catoctin formations	246
Lower Cambrian rocks	247
Chilhowee group	247
Age of the Chilhowee group	253
Quaternary deposits	253
Stream deposits	253
Slope mantle	253
Summary of sedimentary features	254
Metamorphism	255
Structural geology	256
Planar and linear structures	256
Folds	259
Faults	263
Description of key areas	265
The eastern side of Blue Ridge	265
Area north of Purcell Knob	265
Potomac River: South Mountain-Short Hill gap	265
Conclusions	267
References cited	268

ILLUSTRATIONS

Figure	Page
1. Index map of Blue Ridge Province in the Potomac River region	241
2. Generalized stratigraphic section of Weverton quartzite	248
3. Columnar sections of Antietam quartzite and parts of adjacent formations	252

Page

4. Composite diagrams of planar and linear structures 258
5. Histogram showing angle between slip cleavage and flow cleavage 260
6. Generalized cross section of the Catoctin Mountain-Blue Ridge anticlinorium 261
7. Schematic sketch of outcrop distribution on south (Virginia) side of Potomac River gorge through South Mountain-Short Hill 262
8. Fold on flow cleavage in Harpers formation 262
9. Enlarged drawing of upper part of fold shown in Figure 8 263
10. Outcrop map of lower quartzite member of Weverton quartzite on east slope of Blue Ridge south of cross-section line D-D′ .. 264
11. Cross sections of Purcell Knob area 266

Plate — Facing page

1. Geologic map of Blue Ridge from Harpers Ferry, West Virginia, to Purcellville, Virginia 239
2. Photomicrographs 246
3. Cleavage and bedding in outcrop 247

TABLES

Table — Page

1. Correlation of Precambrian and Lower Cambrian rocks, adapted from King (1949, p. 519) 242
2. Some features of Precambrian and Lower Cambrian sediments 254

Introduction

Different interpretations of the structure and stratigraphic relations of the Blue Ridge of northern Virginia and Maryland have suggested the need for additional detailed field work. In an effort to provide new data from a poorly known area a study was made in northwestern Loudoun County, Virginia, and adjoining parts of Jefferson County, West Virginia. The map area of approximately 80 square miles is bounded by Short Hill on the east, the Potomac River on the north, the Shenandoah River on the west and extends 12 miles south of the Potomac River (Fig. 1). It was chosen to relate the abrupt termination of Short Hill, 11 miles south of the Potomac River, to the regional structure as interpreted by previous workers.

New facts were sought by splitting long-established formations into members and mappable beds to permit detailed mapping at a scale of 1:25,000 on 7½-minute quadrangles of the Army Map Service. Structurally complex areas were mapped at a scale of 1:6000 by pace and compass traverse. Aerial photographs helped in locating outcrops and following persistent beds across poorly exposed areas. Field work was done during the summers of 1951 and 1952.

Acknowledgments

The writer thanks Dr. Ernst Cloos, whose teaching fostered an interest in the problem, and Drs. Thomas W. Amsden, Aaron C. Waters, and Francis J. Pettijohn who offered much valuable criticism and instruction. The helpful comments of Dr. Robert B. Neuman of the United States Geological Survey are very much appreciated. Financial assistance from The Johns Hopkins University through University Scholarships during 1950–1951, 1951–1952, and 1952–1953 and Student Assistantships during 1951–1952 and 1952–1953 is gratefully acknowledged.

Previous Work

Keith (1893; 1894) first mapped the area, described the rocks, and interpreted the broader structural features. His formational divisions and lithologic descriptions have been changed little by subsequent workers but there has been controversy over his structural interpretations. Stose and Stose (1946), who mapped an adjacent area north of the Potomac River in Frederick County, Maryland followed Keith's interpretation of the Harpers Ferry overthrust and internal synclinal structure of the Blue Ridge and South Mountain. They added information on the rock units and clarified and expanded Keith's structural concepts. Cloos (1947; 1951) worked north of the area in Washington County, Maryland, and offered an alternative structural hypothesis. He believed the structure of the Blue Ridge province to be dominated by a large anticlinorium having its overturned limb in the Blue Ridge and South Mountain and its normal limb in Catoctin Mountain (Fig. 1). He discarded the Harpers Ferry overthrust, mapped a normal fault west of South Mountain, and described the in-

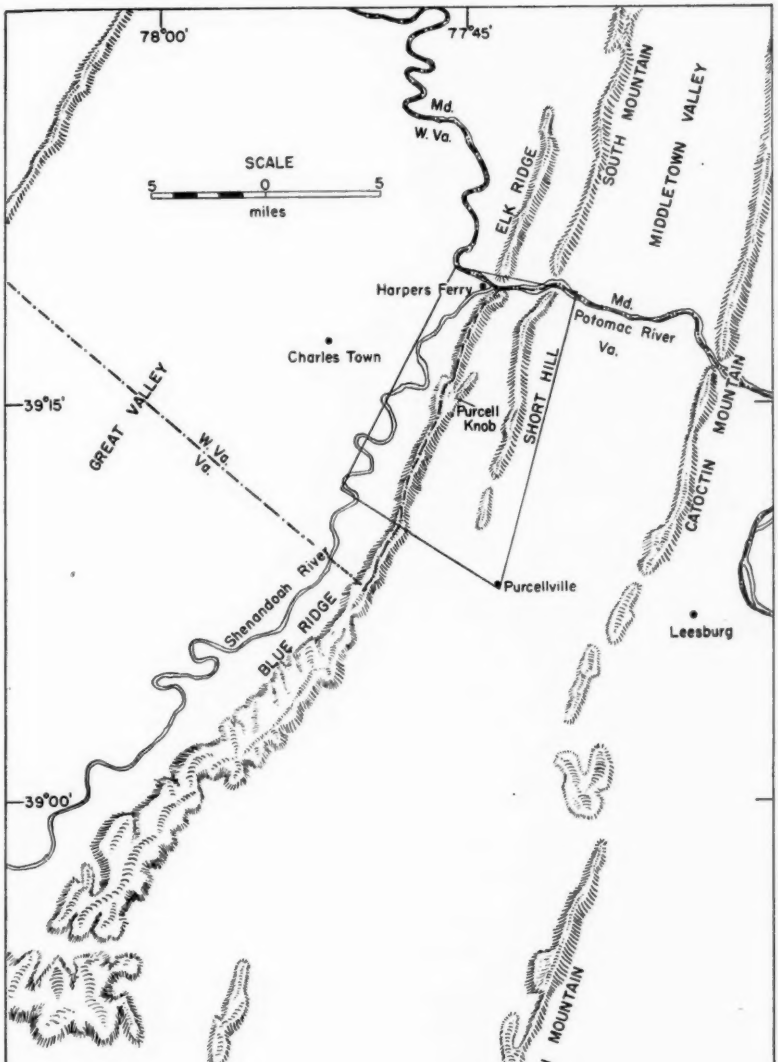

FIGURE 1.—INDEX MAP OF BLUE RIDGE PROVINCE IN THE POTOMAC RIVER REGION

ternal structure of South Mountain as anticlinal. Stose and Stose (1949, Fig. 8) did reconnaissance mapping on the Swift Run formation in Loudoun County, Virginia, and chose rock relations in the Purcell Knob area as an example of evidence for an erosional break between the late Precambrian and Lower Cambrian (1949, p. 311, 314).

TABLE 1.—CORRELATION OF PRECAMBRIAN AND LOWER CAMBRIAN ROCKS, ADAPTED FROM KING (1949, p. 519)

		Northeastern Tennessee	Potomac River region
Lower Cambrian		Shady dolomite	Tomstown formation
	Chilhowee group	Erwin quartzite	Antietam quartzite
		Hamptom shale	Harpers formation
		Unicoi formation	Weverton quartzite / Loudoun formation
Precambrian		Volcanics of Mt. Rogers area	Catoctin formation / Swift Run formation
		Cranberry granite	Gneissic basement

STRATIGRAPHY

General

Rocks of the area include indurated and metamorphosed Precambrian and Lower Cambrian and unconsolidated Cenozoic units. Resistant Lower Cambrian quartzites form Blue Ridge and Short Hill, while Precambrian metamorphosed igneous and sedimentary rocks underlie the intervening valley. Cenozoic deposits are restricted to the lower slopes of the ridges and flood plains of streams. Table 1 summarizes the stratigraphic sequence in the area and shows equivalents to the south. Lower Cambrian sediments were deposited in a shallow sea which inundated a low land mass of subaerial basalt flows, local sedimentary rocks, and a gneissic basement. These sediments resemble the foreland or platform facies as described by Pettijohn (1949, p. 451-456). Approximately 2000 feet of rock below the fossiliferous Antietam quartzite are included in the Lower Cambrian on the basis of stratigraphic conformity.

The area contains type sections of the Loudoun formation, Weverton quartzite, and Harpers formation that have not been restudied since their designation.

All available sections were measured, and other thicknesses were estimated on a basis of mapped outcrop width. Symbols following rock colors in the text refer to the Rock Color Chart published by the National Research Council (Goddard *et al.*, 1948). Where such symbols are not used, color names do not comply with this chart.

Precambrian Rocks

Gneissic basement.—The gneissic basement was called granite by Keith (1893, p. 299–304; Pl. XXIV) who mapped its textural and compositional variations. Stose and Stose (1946, p. 16) who refer to this unit as the Injection complex, differentiated granodiorite and biotite granite gneiss in the Middletown Valley of Maryland. Cloos (1951, p. 95–96) concluded, on the basis of cleavage and lineation in the gneiss, that it had been folded along with the overlying Paleozoic sediments.

The gneiss has had a complex history not fully deciphered here. Any attempt to describe it should be preceded by detailed mapping in an area of better exposures. Only the granodiorite gneiss of Stose and Stose is present within the area. It is commonly greenish gray with white to pinkish augen of potash feldspar. The weathered rock is rusty brown with dull-white spots. Garnet and biotite are present at a few places but typically the rock is a medium- to fine-grained, cataclastically deformed aggregate of quartz, chlorite, plagioclase, sericite, and potash feldspar (Pl. 2, fig. 1). Relic gneissic banding of Precambrian origin is commonly masked by flow cleavage formed later as the gneiss and overlying Cambrian sediments were folded. Grain size varies with the amount of cataclastic deformation during flow cleavage formation.

In fresh exposures along the Potomac River there are zones of intense shearing where the gneiss is fine-grained and phyllitic. Where poorly exposed, these zones resemble phyllites of the Swift Run formation. The augen are uncrushed remnants or porphyroclasts.

In thin section remnants of granoblastic texture are present but are generally masked by cataclastic or porphyroclastic structures.

Three kinds of feldspar were noted. Early plagioclase, perhaps originally a calcic-oligoclase or andesine, is saussuritized and now is albite (An_{8-8}). Twinned, oriented remnants of this early plagioclase are commonly enclosed within microcline-perthite porphyroclasts. The third feldspar is a clear untwinned albite, common as rims on the early plagioclase and as replacements of microcline-perthite. Apparently the sequence of feldspar formation was: (1) early plagioclase; (2) microcline-perthite; (3) saussuritization of early plagioclase and development of clear albite. Quartz blebs within early plagioclase near the border of microcline-perthite are suggestive of myrmekite.

Two biotites are present; an early biotite which is rarely preserved, and a late biotite formed during the last period of metamorphism. In one thin section early biotite has yellowish-brown to greenish-brown pleochroism and sagenite webs of rutile. This biotite is usually coated by a thin border of sphene. In other slides sheared and bent interlaminated books of sphene, chlorite, and epidote are all that remain of early biotite. Late biotite occurs as tiny radiating fibrous growths usually associated with fractures, but in strongly deformed rocks it lies along the flow cleavage.

Quartz is strained and in places has crushed borders.

Red garnet with a refractive index of 1.80 is present at the south end of the Potomac River bridge. It has been crushed and the fractures are now filled with sericite and some quartz (Pl. 2, fig. 1). Accessories are ilmenite with sphene borders, apatite, and zircon.

Sericite abundance is related to deformation. Phyllitic zones show much sericite within bent and broken plagioclase. In places plagioclase is almost completely gone, and the rock is a phyllonite with angular grains of relic microcline-perthite and strained quartz. Finely divided leucoxene is abundant in some sericitic phyllonites. Chlorite is common in zones formerly rich in early biotite. Calcite in small amounts fills cracks and fissures.

No attempt is made by the writer to definitely establish the original nature of the rock. Stose and Stose (1946, p. 16) state that it was a granodiorite, basing their conclusions mainly upon work further south in Virginia.

The following history of the gneiss is tentatively suggested:

(1) Intrusion of granodiorite or quartz diorite, or else the high grade metamorphism of a preexisting rock to produce a gneiss composed of calcic-oligoclase, quartz, biotite, garnet, pyroxene (?) and potash feldspar (?).

(2) Development of clear albite, saussuritization of calcic-oligoclase, and development of sphene borders on biotite and ilmenite.

(3) Intense deformation with production of cataclastic structure and phyllonite zones, retrogression of early biotite to chlorite and sphene, development of sericite and new biotite, straining and granulation of quartz and garnet, and introduction of calcite. This step also produced the low-grade metamorphism of the overlying sediments and is discussed in the section on metamorphism.

Swift Run formation.—Jonas and Stose (1939, p. 585) named this unit for exposures near Swift Run Gap in Rockingham County, Virginia. It was later traced northward to Loudoun County, Virginia, and Frederick County, Maryland (Stose and Stose, 1946, p. 18; 1949, p. 311, Fig. 8). Keith (1893; 1894) mapped it as part of the Loudoun formation.

The lithology of the formation is extremely variable. It contains blebby phyllites of probable tuffaceous origin, sericitic phyllites, quartzites, chloritic phyllites, and local lenses of marble. Two members were mapped in the area.

The lower member is a highly sericitic quartzite, white or greenish white to dark brownish green which grades into a white sericitic phyllite with scattered grains of quartz. Thin sections show varying amounts of 1–2 mm grains of detrital quartz enclosed in a matrix of sericite and fine quartz. Chlorite is rare or absent and accessories are apatite, zircon, tourmaline, magnetite, hematite, and leucoxene. No feldspar occurs in any of the thin sections although it would be expected in a sediment derived from the gneiss. Its absence may be due

to intense chemical weathering at the time of deposition or deformation or a combination of both. Clots of sericite and quartz that appear to have been detrital grains occur. Perhaps they were deposited as grains of kaolinized feldspar that has been converted to sericite and quartz by low grade metamorphism, or they may be fragments of rhyolite tuff. Quartzite beds in the Swift Run formation may be distinguished from the Weverton quartzite by their lenticular occurrence and greater abundance of sericite. These quartzites may contain cobbles of quartz up to 4 inches in diameter and purplish phyllite pebbles suspended in a matrix of sericite and quartz sand. Such suspended cobbles occur in a 15-foot bed of quartzite found at the base of the Swift Run section in the area north of Purcell Knob and 1.3 miles west of Mechanicsville in the area south of Route 9, east of the Blue Ridge. A small pod of marble about 4 feet thick and 50 feet long, is present north of Purcell Knob and State Route 685. It is dark brown on weathered surfaces and banded pink, white, and green on fresh surfaces. A thin section shows pale green mica, quartz, and recrystallized calcite alternating in thin contorted bands.

The lower member is thought to be a local deposit upon the irregular erosion surface of the gneiss. At several localities between the Potomac River and the north end of Purcell Knob and 1.1 miles southwest of Mt. Olivet Church, east of Short Hill, it grades into gneiss through a transition zone 50–75 feet wide. This interval is never well exposed but blocks of float from it are more highly cleaved than the gneiss and lack bedding. It may be an ancient regolith or fossil soil similar to the one described by Bloomer (1950, p. 771) at the same stratigraphic horizon in Nelson County, Virginia, or it may be phyllonite developed from the gneiss due to concentration of movement here. The lower member is estimated on the basis of mapped outcrop width to range from 0 to 150 feet thick.

The upper member is primarily phyllitic with scattered grains of quartz. It varies from light green to grayish red purple (5 RP 4/2). Bedding laminae 1–3 mm thick seen in a few places indicate the original sediment was water-laid but most primary structures are concealed by flow cleavage. Dark-bluish-gray phyllite with white sericitic blebs up to 1 inch long is common in the upper parts. Chlorite is more abundant then sericite, and accessories are the same as in the lower member.

This phyllite cannot be distinguished from phyllites within the Catoctin formation or at the base of the Loudoun formation, except on the basis of stratigraphic position. Probably all are tuffaceous sediments as suggested by purplish color, poorly sorted nature, irregular distribution, and intercalation with Catoctin metabasalt flows. Sericite, both in the blebs mentioned above and in the groundmass of parts of the rock, probably indicates the presence of rhyolitic volcanic material.

Although it was never seen in direct contact with the gneiss the upper member apparently rests directly upon the gneiss in areas where the lower member is absent. The lower member crops out so well over most of the area that its absence in outcrop is taken to mean that it has pinched out along the strike, probably owing to original variation in thickness upon the irregular erosion surface of the gneiss. The thickness of the upper member is estimated, on the basis of mapped outcrop width, to range from 50 to 200 feet.

Catoctin formation.—This sequence of volcanic flows and tuffs was named the Catoctin schist by Geiger and Keith (1891, Pl. IV). Williams (1892, p. 482–496) first recognized the altered volcanic nature of the unit. Its volcanic flows have been termed metabasalt by Stose and Stose (1946, p 20) in Frederick County, Maryland, and prophyllite or altered andesite by Bloomer and Bloomer (1947, p. 99–100) in central Virginia.

The principal rock of the Catoctin formation is grayish-green (5G 5/2) metabasalt but many shades of green, gray, and purple are present. No primary structures (flow structures, columnar jointing, pillow structures) are visible within the metabasalt of this area. Most rock is fine-grained to aphanitic with an even texture, but phenocrysts of feldspar 1–3 mm long occur south of the Potomac River east of Short Hill and at several places south of Route 9 east of the Blue Ridge. The rock is massive to well cleaved. Amygdules filled with epidote, quartz, or chlorite occur at numerous places. In cleaved areas the amygdules are flattened to ellipses lying in the plane of flow cleavage and elongated down the dip.

The most common well-cleaved rock is an even-grained green-schist composed of albite, epidote, chlorite, some actinolite, sericite, or quartz, and disseminated ilmenite and leucoxene. More rarely the schistose rock is spotted with dark-green uralitic actinolite in a lighter-green groundmass composed of chlorite, epidote, quartz, and plagioclase.

Thin sections from massive areas show relic intergranular textures with saussuritized plagioclase laths surrounded by interstitial chlorite, epidote, ilmenite, and actinolite (Pl. 2, fig. 2). Plagioclase, probably originally labradorite, is now albite (An_{3-9}). Original pyroxene is recrystallized to chlorite and actinolite. Chlorite has anomalous interference colors in blue, purple, and brown. Ilmenite, altered to leucoxene and sphene, is abundant. Epidote has pinkish and light-green pleochroism and a negative sign. Optic angles on eleven grains ranged from 58° to 84°, but 5 of the grains had optic angles between 75° and 78°. This epidote probably contains some manganese and therefore the diagram of Winchell and Winchell (1951, p. 449) cannot be applied.

Dikes that may be feeders of the basalt flows cut the gneiss and the Swift Run formation. They range from 1 to 50 feet in width but few are more than 10 feet wide. They are distinguished from Catoctin flows by coarser grain, darker color and complete lack of amygdules. They have the same east-dipping flow cleavage found in all rocks of the area. In good exposures they show chilled contacts and intrusive relationships with the gneiss.

Thin sections from the dikes show subophitic texture, with large grains of uralitized pyroxene enclosing laths of saussuritized plagioclase of albitic (An_{3-9}) composition. One slide contains pyroxene grains varying in composition from ferroaugite to augite (optic angles 42°–61°; extinction angle 38°–51°). Uralitic actinolite has a negative sign, optic angle of 80° and a 15-degree extinction angle. Other minerals are iron-rich chlorite, sphene, epidote, rutile, zoisite, and carbonate.

Several areas of sericitic phyllite occur within the Catoctin formation south of Route 9 and east of Blue Ridge. This rock is white to very light green with white blebs up to 4 or 5 mm in length. Poor exposures and obliteration of primary structures by flow cleavage prevent continuous tracing of this phyllite. However, its occurrence along the regional strike and fairly uniform position within the Catoctin formation indicates that it probably occurs at one horizon. It is apparently a lensing bed ranging from 0 to 50 feet thick. Thickness estimates are based on outcrop width of highly cleaved rock. In thin sections, sericite and quartz are most abundant but epidote and leucoxene are also present. Apatite and tourmaline which appear in blebby phyllites in the Catoctin, Swift Run, and Loudoun formations are not present. White blebs consist of aggregates of quartz, sericite, and albitic feldspar which were probably crystals and rock fragments in the original rock. The mineralogy of both the phyllite and the blebs indicate that this rock was derived from a rhyolite tuff.

Phyllitic sediments occur within the Catoctin formation but are not well exposed. Blebby, gray, blue, or green phyllite is the most common rock but locally, south of Short Hill and east of Blue Ridge, south of Route 9, feldspathic and phyllitic quartzites occur. A conglomerate or breccia exposed north of State Route 712, 1 mile west of its junction with State Route 719, is composed of 1–3 inch cobbles of metabasalt in a matrix of detrital quartz, feldspar, and chlorite. The metabasalt cobbles are elongated down the dip of the cleavage and flattened in the cleavage plane. These sediments are interpreted as tuffs deposited locally between metabasalt flows. The estimated thickness of the Catoctin formation ranges from 0 to 50 feet at the Potomac River to 500 to 1000 feet at the southern end of the Blue Ridge belt of outcrop. East of Short Hill the thickness is an estimated 300–600 feet. Estimates of thickness are based upon mapped outcrop width.

Cloos (1951, p. 25–28) attributes thickness variations of the Catoctin formation to the original irregular distribution of the volcanic rocks, while Stose and Stose (1946, p. 28-29) suggest uplift and erosion at the end of Catoctin time before deposition of the Loudoun formation. Detailed mapping revealed no conclusive evidence in support of either hypothesis. Stose and Stose (1946, p. 28-29) state that, "In Purcell Knob and north-eastward to Potomac River, the Loudoun formation overlaps the Catoctin metabasalt and Swift Run tuff and rests directly on granodiorite of the injection

complex of early Pre-Cambrian age". Relations mapped by the writer in this area suggest that erosion did not necessarily follow the deposition of the Catoctin formation since both the Loudoun formation and Swift Run formation can be traced continuously through the area. The Catoctin flows are thin and lensing owing to lack of deposition or post-Catoctin erosion. If thinning is due to post-Catoctin uplift and erosion, it is unusual that the erosion level should have stopped within the Catoctin formation leaving a thin veneer of flow rock and the Swift Run formation untouched. An alternative explanation is that the Catoctin flows thinned out against local hills or a gentle southeast regional slope. On the other hand King's (1951, p. 13) work in the Elkton region indicates an unconformity above the Catoctin and a northwestward overlap of the Loudoun formation upon the eroded edges of the Swift Run formation and injection complex. His description from Fultz Run (p. 13), "a few lenticular bodies of greenstone between the (Swift Run and Loudoun formations)", sounds very similar to relations observed north of Purcell Knob and it is entirely possible that here a similar unconformity and overlap would be recognized if exposures were available to the northwest.

Relict textures indicate that Stose and Stose (1946, p. 20) are probably correct in stating that the Catoctin flows are basalt. The writer thinks they were subaerial as suggested by columnar jointing, which is well preserved in the Catoctin formation along the Skyline Drive further south in Virginia (John Reed, Jr., personal communication). In addition, pillow lavas, expectable in subaqueous flows, have not been reported from the Catoctin formation. Since pillow lavas are commonly preserved through intense deformation, their absence also suggests subaerial flows.

Stratigraphic relationships and age of the Swift Run and Catoctin formations.—Within the map area the Swift Run formation rests unconformably upon the gneiss and grades upward, through tuffaceous beds, into the Catoctin formation. These units are clearly younger than the gneiss and are probably conformable with each other. Regionally, it is suggested by both Bloomer (1950, p. 770) and King (1951, p. 12, Fig. 4) that sediments in the position of the Swift Run formation may vary in age due to deposition transgressively upon the sloping eroded surface of the gneiss. The lower part of the Catoctin formation may thus be older, at places, than parts of the Swift Run formation. No evidence for or against this hypothesis was found in the area mapped.

The writer considers the Catoctin and Swift Run formations to be Precambrian. They consist of locally derived and deposited sediments and probably subaerial basalt flows. Overlying them is the marine Chilhowee group which contains lower Cambrian fossil in its upper

---

PLATE 2.—PHOTOMICROGRAPHS

FIGURE 1.—GNEISS, × 60, CROSSED NICOLS

Saussuritized, bent and fractured plagioclase on east and center of photograph; microcline-perthite in northwest corner; opaque grain in southeast corner is fractured garnet with sericite filling cracks.

FIGURE 2.—CATOCTIN METABASALT, × 60, CROSSED NICOLS

Relic intergranular texture; saussuritized plagioclase laths in matrix of chlorite, ilmenite, actinolite, and epidote; amygdule in southeast corner filled with euhedral epidote.

FIGURE 3.—LOWER QUARTZITE MEMBER OF WEVERTON QUARTZITE, × 60, CROSSED NICOLS

Quartz grains showing undulatory extinction are elongated northwest-southeast parallel to flow cleavage. Matrix consists of aligned sericite and crush quartz.

FIGURE 4.—UPPER QUARTZITE MEMBER OF WEVERTON QUARTZITE, × 60, CROSSED NICOLS

Grains more angular and less well sorted than lower quartzite member (Fig. 3). Flow cleavage northwest-southeast as shown by orientation of sericite in matrix.

FIGURE 5.—PHYLLITIC UPPER MEMBER OF THE SWIFT RUN FORMATION, × 100, CROSSED NICOLS

Flow cleavage oriented northwest-southeast is cut by north-northeast–south-southwest-trending shear zones which are slip cleavage. Sericite, quartz, and chlorite from earlier flow cleavage have been rotated into slip cleavage.

FIGURE 6.—HARPERS FORMATION, × 100, PLANE LIGHT

Phyllite with chlorite porphyroblasts elongated in flow cleavage; cleavage in porphyroblasts approximately perpendicular to flow cleavage

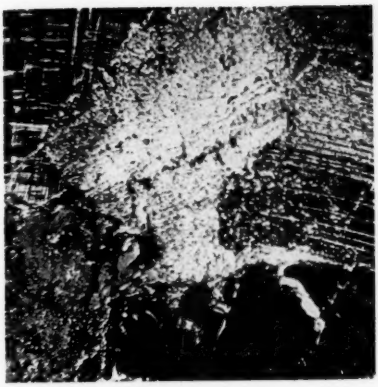

FIGURE 1

FIGURE 2

FIGURE 3

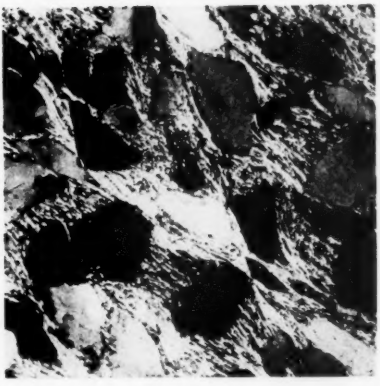

FIGURE 4

FIGURE 5

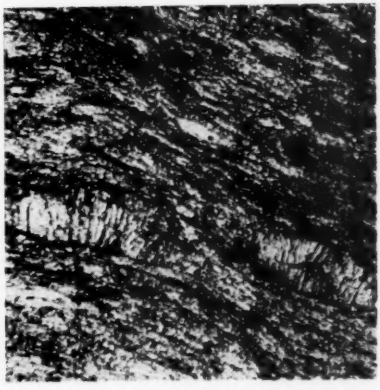

FIGURE 6

PHOTOMICROGRAPHS

FIGURE 1

FIGURE 2

CLEAVAGE AND BEDDING IN OUTCROP

part. Although no unconformity is definitely established between the Catoctin-Swift Run formations and Chilhowee group in this area, deposition of the two is marked by a change from nonmarine to marine sedimentation and a change from local to distant source of material.

King (1951, p. 12, 14) also considers the Catoctin and Swift Run formations Precambrian, basing this conclusion upon a post-Catoctin pre-Chilhowee unconformity present in the Elkton, Virginia, area. On similar evidence, Stose and Stose (1949, p. 315) also believe the Catoctin and Swift Run formations to be Precambrian. Conversely, Bloomer and Bloomer (1947, p. 106) and Cloos (1951, p. 25–28) emphasize lithologic gradations between the Catoctin-Swift Run sequence and the Chilhowee group, recognize no unconformity, and suggest a Cambrian age for the Catoctin formation.

Lower Cambrian Rocks

Chilhowee group.—Safford (1856, p. 152–153) named the sequence of Lower Cambrian quartzites and shales on Chilhowee Mountain, Blount County, Tennessee, the Chilhowee group, and the name has been applied throughout Virginia to a similar group of rocks (Table 1). In northern Virginia the Chilhowee group includes the Loudoun formation, Weverton quartzite, Harpers formation, and Antietam quartzite.

LOUDOUN FORMATION: The Loudoun formation was named by Keith (1892, p. 365; 1893, p. 324; 1894) who indicated only Loudoun County, Virginia, as the type locality. Stose and Stose (1946, p. 19) recognized both the Swift Run formation and Loudoun formation in Loudoun County and adjacent Maryland and showed that many of Keith's "Loudoun" localities actually were the lithologically similar Swift Run formation. Some of the Loudoun of this area, as restricted by Stose and Stose, was later shown to be lower Harpers formation by Cloos (1951, p. 29). This led Cloos to question the validity of the Loudoun as a unit. King (1950, p. 9, 16) recognized the Loudoun and Swift Run formations near Elkton, Virginia, but due to the above ambiguities in definition, questioned whether the "Loudoun" was a valid name (1950, p. 16). The writer found both the Swift Run formation and Loudoun formation present in Loudoun County, Virginia, and thinks that the name Loudoun should be retained in the original sense of Keith for characteristic beds occurring between the Catoctin formation and Weverton quartzite.

Two members of the Loudoun formation are present but were not mapped owing to lack of exposures. The lower member is very dusky-red-purple (5 RP 2/2) to dark-bluish-gray (5 G 4/1) phyllite with a well-developed cleavage that obliterates primary structures in all but a few outcrops. Oval green spots similar to those described by King (1950, p. 16) are well displayed on cleavage planes in outcrops of the lower member north of Purcell Knob. The phyllite consists mainly of sericite and magnetite or hematite, but chlorite and detrital quartz are present, and tourmaline is an abundant accessory. Its lower contact is at the top of the highest metabasalt in the underlying Catoctin formation. The lower member of the Loudoun formation and the upper member of the Swift Run formation are identical in character, and can be differentiated only in the presence of the intervening metabasalts of the Catoctin formation. These two phyllites appear to be in contact east and northeast of Purcell Knob where metabasalt occurs in thin lenticular bodies. Estimates based upon mapped outcrop width of the lower member indicate a thickness of 50–100 feet.

PLATE 3.—CLEAVAGE AND BEDDING IN OUTCROP

FIGURE 1.—"GUN-METAL" BLUE BEDS OF UPPER QUARTZITE MEMBER OF WEVERTON QUARTZITE

Looking north; bedding dips east (overturned), flow cleavage dips east parallel to hammer handle. Overturned cross-bedding is visible below hammer. South of Hillsboro, Virginia, .1 mile north of fire tower on Short Hill.

FIGURE 2.—CALCAREOUS BANDED HARPERS FORMATION

Looking north; bedding dips east (overturned) parallel to hammer handle. Flow cleavage dips gently west and shows slight bending in phyllitic parts of outcrop but sharp folds in sandstone beds near hammer. Road on north side of Shenandoah River south of Harpers Ferry, West Virginia.

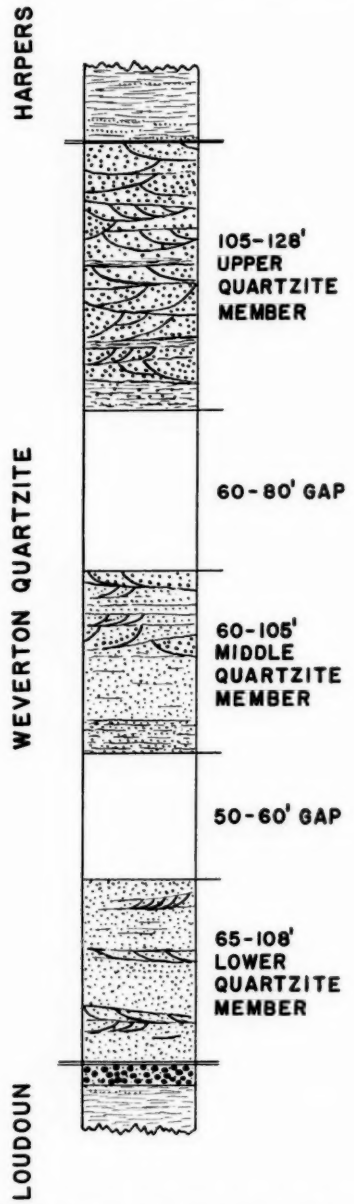

FIGURE 2.—GENERALIZED STRATIGRAPHIC SECTION OF WEVERTON QUARTZITE

The upper member of the Loudoun formation is a conglomerate with 1–2 inch pebbles of white quartz, red jasper, blue-black or grayish phyllite, creamy-white phyllite consisting of sericite and leucoxene, and yellowish-white kaolinized feldspar. The matrix is a greenish to purplish-black phyllite containing abundant small grains of magnetite and leucoxene and zircon and tourmaliue as accessories. Feldspar is rare and no gneiss or metabasalt pebbles were seen. The contact with the Weverton quartzite is abrupt. Sericitic matrix and phyllite pebbles disappear and the grain size decreases through a transition zone of 2 or 3 feet. At the north end of Purcell Knob the Loudoun conglomerate member reaches a maximum thickness of 10 feet. Along the eastern base of Blue Ridge it averages 5 feet in thickness and it is absent or very thin east of Short Hill.

The Loudoun formation is transitional between the Weverton quartzite and Catoctin formation. It separates terrestrial Catoctin deposits from marine sediments derived from a more distant source during Weverton time. The lower member was formerly an iron-rich shale containing tuffaceous material. The conglomerate appears to be an accumulation of mature weathering products (quartz and jasper) mixed with contemporaneously eroded and redeposited shale fragments and volcanic debris.

WEVERTON QUARTZITE: The Weverton quartzite was named by Keith (1882, p. 365; 1893, p. 329; 1894), who established a type section for the formation at Weverton, Maryland, just north of the map area of this report (Pl. 1). Stose and Stose (1946, p. 37) recognized two ledge-making quartzite members in this section and Cloos (1951, p. 30) found that part of their section had been described in reverse order. The writer has distinguished three quartzite members within the formation (Fig. 2). They form three subordinate ridges that are readily visible on aerial photographs of Short Hill and the southern part of Blue Ridge. Between ridges are depressions with few outcrops that are occupied by interbedded phyllite and quartzite.

The lower quartzite member is white to light gray on fresh surfaces and weathers darker gray. Bluish-black to dark-gray bands 1 or 2 mm thick occur at intervals of ¼–4 inches and locally outline small-scale cross-bedding. Quartz grains are blue, white, or pink and range in grain size from 2 mm to .2 mm. This member shows the best sorting to be found in the Weverton quartzite (Pl. 2, fig. 3). Thin sections contain an estimated 90–95 per cent quartz consisting of original grains, peripheral growth quartz

in optical continuity with the original grains and crush quartz, needle quartz and recrystallized quartz produced by metamorphism (Fellows, 1943, p. 1414). Original grains and peripheral-growth quartz could usually not be differentiated owing to deformation. The remainder of the rock consists of ilmenite, magnetite, zircon, tourmaline, and sericite. Ilmenite and magnetite make up less than 1 per cent of the rock and commonly are concentrated along bluish-black bedding planes. Sericite makes up 5–10 per cent of the rock. Zircon is more abundant than tourmaline but their combined total makes up less than 1 per cent of the rock.

At the north end of Purcell Knob the contact between the lower quartzite member and the conglomeratic Loudoun is well exposed. Here the overturned lower quartzite member is 75 feet thick. Other localities where this member is exposed are: (1) above and to the northeast of the stone quarry east of Weverton, Maryland, where 65 feet are exposed in an overturned section, (2) at the east end of the Potomac River gorge through Blue Ridge, (3) on Short Hill, north of Hillsboro, Virginia where 108 feet were measured in an overturned section.

The rock between the lower and middle quartzite members is known from a few widely scattered outcrops and from float. It is best exposed at the Weverton, Maryland, section in the steep slope above the stone quarry. Here the rock is a greenish-white phyllite with some scattered quartz grains up to 1 mm in diameter. Quartzite interbeds 4–6 inches thick, similar to quartzite from the quartzite members of the formation, are the only part of this interval commonly preserved as float. One thin section of the phyllite was estimated to contain 40 per cent quartz, 57 per cent sericite, and 3 per cent zircon, tourmaline, magnetite, and ilmenite.

The middle quartzite member is similar to both the upper and lower quartzite members but is less well sorted than the lower member and better sorted than the upper member. Many exposures contain bluish-black and white bands of approximately equal thickness. Cross-bedding is more common and larger than in the lower member. Although the predominant grain size is 1 or 2 mm, grains up to 3 or 5 mm are common. Estimated composition is similar to the lower quartzite member. In the stone quarry at Weverton, Maryland, it is 86 feet thick and on Short Hill just north of Hillsboro, Virginia, 105 feet were measured.

Magnetite-rich, conglomeratic quartzite that is more poorly sorted than the lower and middle quartzite members is characteristic of the upper quartzite member. At least three lithologies are present. The lower 10 feet is a silty phyllite, containing abundant euhedral magnetite crystals, that weathers to a light brown. Scattered coarse-grained quartz is present. Most of the member above this phyllite is well cross-bedded, conglomeratic, and magnetite-rich with a "gun metal" blue color on both fresh and weathered surfaces (Pl. 3, fig. 1). Larger blue and red quartz grains average 5 or 6 mm and occasionally are 10 mm. Phyllitic partings 1–3 inches thick are spaced at intervals of ½–4 feet. Above the "gun metal" blue beds the upper 20–30 feet of the member is greenish-gray and contains less magnetite and more sericite. Conglomerate beds here contain 75–80 per cent quartz and considerable ilmenite, magnetite, and sericite (Pl. 2, fig. 4). Sericite and small amounts of chlorite make up 10–15 per cent of the rock. Euhedral crystals of magnetite replace quartz and sericite and occur as irregular masses along bedding planes. Needles of sphene coated with leucoxene penetrate quartz grains and appear to be of metamorphic origin. Zircon and tourmaline are more abundant in the upper member.

The upper quartzite member is exposed back of the first house west of the stone quarry at Weverton, Maryland, where 128 feet were measured; at many points along the summit of Short Hill north of Hillsboro, Virginia, where sections 75–105 feet thick were measured; and west of the summit of the Blue Ridge along Route 9.

A composite section drawn from partial sections mentioned above indicates a total thickness of from 340 to 481 feet (Fig. 2). Measured sections are all overturned with the angle between cleavage and bedding rarely exceeding 20°. Each section, measured normal to bedding, is probably less than the true stratigraphic thickness, owing to flowage along cleavage (Gair, 1950, p. 872). This factor plus difficulty of making measurements between the three quartzite members makes thickness comparisons between measured sections difficult. The Weverton quartzite is estimated to be roughly 500 feet thick.

Gradation into the Harpers formation takes

place by a gradual increase in the amount of phyllite. In this part of the section there are phyllite pebbles, the rock is poorly sorted and the color ranges from grayish black to bluish black. These beds were probably mistaken for the Loudoun formation by Keith (1893; 1894) and Stose and Stose (1946) when they mapped Blue Ridge and South Mountain as synclines. The Weverton-Harpers contact is best exposed east of Chestnut Hill Church, West Virginia, and on the south side of the Potomac River gorge, east of Short Hill.

The Weverton quartzite falls within the quartzite field of Pettijohn's triangular diagram for classification of the arenites (1949, p. 227). It is a metaquartzite, but prior to metamorphism was a sedimentary quartzite or orthoquartzite (Pettijohn, 1949, p. 237).

No fossils have been found in the Weverton quartzite but it is conformable with the Harpers formation and the fossilferous, Lower Cambrian, Antietam quartzite.

HARPERS FORMATION: This unit was described by Keith (1892, p. 365) who later named it the Harpers shale (1893, p. 333). The type section is along the Potomac River or Shenandoah River at Harpers Ferry, West Virginia, within the map area of this report (Pl. 1). Study of this section by the writer has shown it to be incomplete and so highly cleaved in many places that bedding is obliterated or distorted beyond use in section measurement. At one place along the road bordering the left bank of the Shenandoah River south of Harpers Ferry overturned bedding dips 45° northwest and has been rotated more than 225° by recumbent folding. In view of the complexity of this type section and because no better sections are available within the map area, lithologic variations are described in correct relative position as established by mapping.

The base of the Harpers formation is light-brownish-gray (5 YR 7/1) to light-greenish-gray (5 G 7/1) phyllite probably derived from a silty claystone. These beds are exposed near Chestnut Hill Church in West Virginia. Next there is a great thickness of bedded phyllite, well exposed on both sides of the Shenandoah River from the west end of the Blue Ridge gap west to the bridge across the Shenandoah River near Harpers Ferry. The rock here is predominantly silty and dark greenish gray (5 G 4/1). It contains darker-green beds ½–1½ inches thick, spaced at intervals of 3–8 inches, or thicker calcareous, fine-grained quartzite beds, which are very light gray (N 8) on fresh surfaces and weather to light brown (5 YR 7/4). Calcite is disseminated through the dark-greenish-gray silty beds. In weathered rock the former presence of calcite is indicated by dusky-brown (5 YR 2/2) porous bands and lenses. Next in the section is light-greenish-gray (5 G 7/1) phyllite. Silty areas occur here but clay-size material probably predominated in the original sediment. Thin beds of fine-grained quartzite or color bands reveal bedding locally, but in most places cleavage obscures bedding. This phyllite is exposed on Route 9 between Blue Ridge School and Mountain Mission in West Virginia, and in the large road cut west of the Shenandoah River bridge on Route 340. The upper several hundred feet of the Harpers formation is silty. Thin fine-grained quartzite beds become more abundant in the upper parts of the Harpers formation. The rock here is light-greenish-gray (5 G 7/1) with darker-green and light-gray beds. Good exposures occur in cliffs on the south face of Snyder Hill, 1.6 miles northeast of Bloomery Bridge.

In thin section the Harpers formation shows a well-aligned matrix of sericite and less abundant chlorite with detital grains of quartz and feldspar elongated in the plane of flow cleavage. Porphyroblasts of chlorite from .1 to .8 mm in length occur in all but the upper 300–400 feet (Pl. 2, fig. 6). Quartz and feldspar make up 50 or 60 per cent of the silty beds but less than 20 per cent of the fine-grained beds. Calcite occurs in anhedral masses and as small disseminated rhombs. Feldspar increases in abundance upward into the Antietam quartzite. Plagioclase was the only feldspar recognized in the lower Harpers, but in the upper part microcline is at least twice as abundant as plagioclase. Accessories are zircon, magnetite, tourmaline, and ilmenite.

East of Waynesboro, Pennsylvania, Cloos (1951, p. 35) measured a Harpers section 3100 feet thick, but believed this thickness to be too great owing to its position on the crest of the South Mountain fold. Keith (1893, p. 334) estimated 1200 feet at Harpers Ferry, and Stose and Stose (1946, p. 40) estimated 2000 feet for the Pennsylvania-Maryland-Virginia area.

Judging from outcrop width and known thickening and repetition due to folding, the writer estimates a thickness of 1500–2000 feet in the Harpers Ferry area.

Scolithus tubes up to 3 inches in length have been collected from the upper Harpers, but the formation is otherwise unfossiliferous. It is considered Lower Cambrian because it is overlain conformably by the fossiliferous, Lower Cambrian, Antietam quartzite.

ANTIETAM QUARTZITE: The Antietam quartzite, differentiated by Keith (1892, p. 365), was later named the Antietam sandstone by him (1893, p. 335) and Williams and Clark (1893, p. 68). It is predominantly an interbedded sequence of white, well-sorted, fine- to very fine-grained quartzite and somewhat darker, more poorly sorted silty phyllite or sericitic quartzite. Beds are 1–6 inches thick with either lithology predominating. Fresh quartzite is very light gray (N8) to yellowish gray (5 Y 7/2) and commonly shows limonite specks. Sericitic quartzite and phyllite vary from darker hues of gray and brown to dark greenish gray (5 G 4/1) near the base of the section. Coarse-grained quartzite is scattered through the section in beds 4–16 inches thick. Locally quartz pebbles up to 8 mm in diameter appear, and at one place there is a ferruginous pebble conglomerate bed 16 inches thick with pebbles averaging 3–6 mm. Coarse-grained quartzite beds are most common near the middle and at the top of the Antietam section.

Typical Antietam quartzite contains approximately 80 per cent quartz ranging from 90 per cent in coarser beds to 60 per cent in sericitic interbeds. Feldspar commonly ranges from 9 to 20 per cent, but locally increases to 35 per cent. In quartzite beds the total of sericite and heavy minerals does not exceed 3 per cent. Shaly interbeds may once have contained 20–30 per cent of a clay-size matrix, now recrystallized to sericite, quartz, and, rarely, chlorite. Heavy minerals in order of abundance are: tourmaline, zircon, magnetite, apatite. Feldspar is detrital microcline, orthoclase, and, rarely, plagioclase. Original well-rounded boundaries are visible. Microcline and orthoclase have been enlarged since deposition by aprons of authigenic feldspar that is not in optical continuity with the detrital grain. More than half of the feldspars are rhombic or subrhombic in outline, and in some the boundary between the detrital grain and the overgrowth may be seen owing to differences in alteration. Rounded grains of green or blue tourmaline commonly show unabraded authigenic overgrowths of clear or paler-blue tourmaline similar to those reported by Krynine (1946, p. 71–74, Fig. 3). In places the upper 15 or 20 feet of the Antietam quartzite contains up to 10 per cent carbonate. Carbonate rhombs and irregular masses replace feldspar and quartz. These unweathered rhombs do not effervesce with HCl and staining with $Cu(NO_3)_2$ (Rodgers, 1940, p. 790) revealed no calcite. Rhomb-shaped cavities, partially filled with limonite, are scattered through other parts of the quartzite, suggesting that the original carbonate was ferriferous dolomite or ankerite. These weathered, limonite-filled rhombs effervesce with cold dilute HCl. They have been seen as far down as the middle of the section where they form the limonite specks found on the white Antietam surfaces. In summary, the Antietam quartzite is a well-rounded, well-sorted arenite many beds of which can be classified as feldspathic quartzite (Pettijohn, 1949, p. 227).

The total thickness of the Antietam quartzite, based on the composite section is 450 feet (Fig. 3). It grades downward into the Harpers formation by a decrease in quartzite and increase in greenish phyllite interbeds. The lower contact of the Antietam quartzite is placed at the base of the lowest sequence of interbedded quartzite and phyllite below the fine-grained quartzite beds. It is best exposed in the stream bed of Furnace Run where section 1 of Figure 3 was measured. The upper 20 feet of the Antietam quartzite shows an upward gradation from typical fine-grained quartzite into dolomitic and ferruginous coarse-grained quartzite before the contact with the sandy dolomite of the lower Tomstown formation is reached.

Fossil fragments occur most commonly in coarse-grained quartzite although fine-grained quartzite contains some fossils. They are mostly molds, partially or completely filled with ferruginous material. Poorly preserved fragments of trilobites (mainly genal spines, thoracic segments, and fragments of the cephalon), valves of inarticulate brachiopods, and well-defined worm tubes have been found by the writer. Fragments of trilobites collected in float from

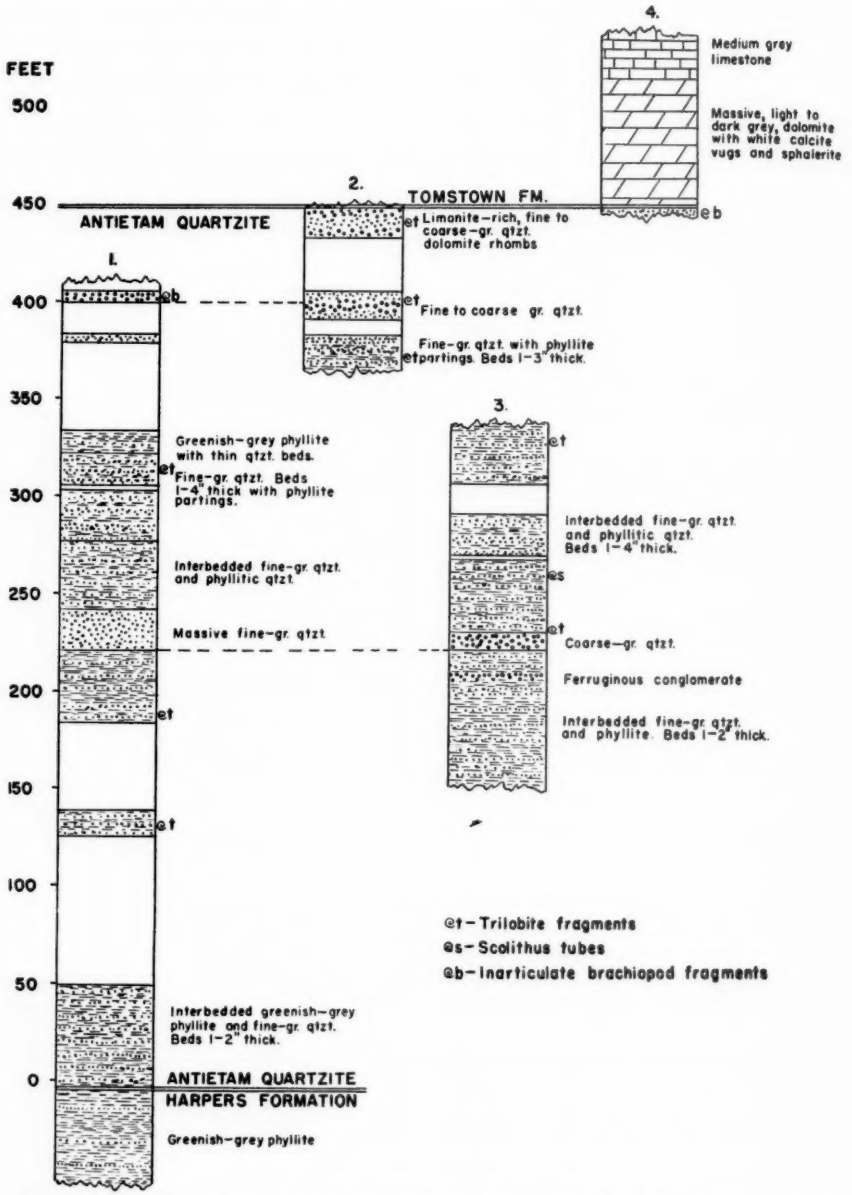

FIGURE 3.—COLUMNAR SECTIONS OF ANTIETAM QUARTZITE AND PARTS OF ADJACENT FORMATIONS

Section 1.—Stream bed and bank of Furnace Run in West Virginia; 2.6 miles south of Route 9 and .5 mile south of cross section C-C′

Section 2.—Stream bed of small stream entering Shenandoah River 4.6 miles south of Route 9 in West Virginia

Section 3.—Cuts along Baltimore and Ohio Railroad and Shenandoah River .5 mile east of Millville, West Virginia

Section 4.—River bank and gulley .8 mile northeast of Bloomery Bridge, West Virginia

the upper part of the Antietam quartzite along Route 9, near Mountain Mission in West Virginia, were studied by A. R. Palmer of the United States Geological Survey. He indicates an early Cambrian age for this fossil material (Personal communication).

TOMSTOWN FORMATION: The Tomstown formation was named by Stose (1906, p. 208; 1909, p. 5). According to Butts (1940, p. 40), the formation correlates with the Shady dolomite of Virginia, which was named earlier. The writer retains the name Tomstown owing to the proximity of the area mapped to the type section of the Tomstown.

Two distinct lithologic units were recognized: a lower white to dark gray (N 3) vuggy, saccharoidal dolomite which weathers to a moderate brown (5 Y 4/4), and an upper highly cleaved, white to medium-gray (N 5), commonly dolomitic or siliceous, limestone that weathers light gray (N 7). Sixty-five feet of the lower dolomitic unit were measured on a slope southeast of the Shenandoah River .8 of a mile northeast of Bloomery bridge; the total thickness of the upper limestone was not determined (section 4, Pl. 3). Sphalerite mineralization occurred in the measured section of the lower dolomite as a lining of calcite vugs, and similar mineralization was found in the same stratigraphic position at several points southward. These units seem to correlate with the two lithologies described by Currier (1935, p. 20) in the Patterson limestone member of the Shady dolomite in southwestern Virginia.

No fossils were found within the area mapped, but Resser (1938, p. 6–7) assigns a lower Cambrian age to the formation.

Age of the Chilhowee group.—Age of the Chilhowee group must be considered in the light of recent discussions of the base of the Cambrian problem by Snyder (1947), Wheeler (1947), and King (1949). These writers advocate varying procedures in fixing the base of the Cambrian in areas where considerable thicknesses of strata conformably underly the lowest fossiliferous zone. Wheeler (1947, p. 157) places the base of the Cambrian at the base of the *Olenellus* zone, Snyder (1947, p. 142) advocates putting the base of the Cambrian at the base of the lowest fossiliferous formation, and King (1949, p. 636–638), in the southern Appalachians, favors extending the Cambrian down through conformable strata to the first unconformity or significant change in lithology beneath the lowest Cambrian fossil.

In the southern and central Appalachians early Cambrian fossils have not been collected below the Antietam quartzite (or Erwin quartzite) at the top of the Chilhowee group. Resser and Howell (1938, p. 199) have advocated placing the base of the Cambrian below the Antietam and Erwin quartzites, but King (1950, p. 24) and Stose and Stose (1946, p. 29) favor placing it at the base of the Loudoun formation, 2000 or more feet below the Antietam, thus including all the Chilhowee group in the Cambrian. As was noted, Cloos (1951, p. 25–28) and Bloomer (1950, p. 781) suggest that the Cambrian may be extended still further to include the Catoctin formation. The writer considers the Chilhowee group Cambrian, because of conformity and lithologic similarity of its formations with the Antietam quartzite.

Quaternary Deposits

Stream deposits.—Stream deposits occupy relatively small areas along the Shenandoah and Potomac rivers. The Shenandoah is largely enclosed in rock walls and mappable deposits of alluvium are restricted to the insides of intrenched meanders and embayments where tributaries enter the river. These deposits were not observed more than 15 feet above the river. They consist of sands and silts with small amounts of gravel.

Slope mantle.—Deposits of slope mantle cover the base and lower slopes of Blue Ridge and Short Hill and extend ¼–½ mile into the valleys. This material is at least 15 feet thick at the base of the ridges and thins valleyward to a feather edge where it loses identity in the residual soil. Most of the slope mantle is composed of angular blocks of Weverton quartzite in a matrix of sand, silt, and pebbles of other less resistant formations. In some places no matrix is present and blocks are arranged in rock streams where they are firmly wedged together and lichen covered. No recent movement is indicated and Smith and Smith (1945, p. 1198) have suggested that similar features in Pennsylvania, Virginia, and Maryland formed under periglacial conditions in Pleistocene time.

TABLE 2.—SOME FEATURES OF PRECAMBRIAN AND LOWER CAMBRIAN SEDIMENTS

Formation	Per cent of feldspar	Kind of feldspar	Sorting	Per cent of quartz	Heavy minerals
Antietam	9–20 locally 35	microcline and orthoclase, rarely plagioclase	good	60–90	zircon, tourmaline
Harpers					
Upper part	5–10	microcline 2× plagioclase	.....	variable	zircon, tourmaline
Lower part	5–10	plagioclase	.....	variable	zircon, tourmaline
Weverton					
Upper qtzt. member	.....	.....	poor—some beds fair to good	75–80	zircon, tourmaline
Middle qtzt. member	.....	.....	fair to good	90–95	zircon, tourmaline
Lower qtzt. member	.....	.....	good	90–95	zircon, tourmaline
Loudoun—conglomerate	trace ?	.....	poor	variable	zircon, tourmaline
Swift Run—lower member	trace ?	.....	fair	variable	zircon, tourmaline

Summary of Sedimentary Features

Features suggesting source-area conditions and environment of deposition of sediments are summarized in Table 2. Percentage estimates were made by visual comparison with a chart by Folk (1951, p. 32). Sorting was described in the following manner: 1–3 Wentworth size grades, sorting was described as good; 4–6 Wentworth size grades, sorting was described as fair; and 7 or more Wentworth size grades, sorting was described as poor. The accuracy of sorting estimates is impaired by recrystallization of assumed clay-size material to sericite and chlorite and by metamorphic distortion and granulation of quartz grains. This is not thought to affect the value of the general comparison shown in Table 2.

Feldspar in sediments is an indicator of rate of erosion and deposition, both of which may be dependant upon intensity of diastrophism (Pettijohn, 1949, p. 94-95). The abundance of feldspar in the Precambrian and Lower Cambrian sediments of the Harpers Ferry area is not the same as reported from areas 60–100 miles to the south. Consequently, variations in the character of the source area and conditions of deposition are indicated.

Only traces of feldspar were found in the Swift Run formation of the Harpers Ferry region, whereas feldspar is an abundant constituent of the Swift Run formation in the Elkton, Virginia, area (King, 1949, p. 526; 1950, p. 10-11) and the correlative Oronoco formation (Bloomer, 1950, p. 770) in central Virginia. Field relations indicate that the underlying gneissic basement which contains abundant feldspar was the primary source of the Swift Run formation. Rarity of feldspar in the Harpers Ferry region is attributed to intense chemical weathering of the source area. Southward, an area with the same climate but higher local relief causing more vigorous erosion could have contributed the feldspar.

The Loudoun formation of the Elkton, Virginia, area contains thin layers of arkose (King, 1950, p. 16–17) whereas in the Harpers Ferry area only traces of feldspar are present. This difference is probably due to local variations in relief such as produced similar feldspar variation in the Swift Run formation. The efficiency of chemical weathering in the Potomac River region is illustrated by the contribution of only mature weathering products (quartz and jasper pebbles) by the pre-Loudoun rocks to the Loudoun conglomerate.

No feldspar is present in the Weverton quartzite of the Harpers Ferry area but further south in Virginia it is described as a feldspathic or even arkosic sandstone (King, 1949, p. 526; 1950, p. 19) and the correlative Unicoi formation contains many arkosic beds (Butts, 1940, p. 30–31). King (1949, p. 526), on the basis of differences in mineralogy and type of quartz,

suggests that the Swift Run and Weverton formations of the Elkton area have been laid down under different geographic conditions and may have come from different sources. A different source for the Weverton of the Harpers Ferry region is suggested by its better sorting and lack of shale pebbles and other locally derived materials. These factors suggest greater distance of transport and more opportunity for reworking before deposition than is evidenced in the Swift Run formation. In the Elkton area, feldspar was supplied by a local source of high relief despite the influx of new material.

The oldest rock unit of the Harpers Ferry area with appreciable feldspar is the Harpers formation. The predominance of plagioclase over microcline in the lower Harpers may be the result of additions from volcanic activity taking place during Harpers deposition in such nearby areas as Sugarloaf Mountain, Maryland, 15 miles to the east (Scotford, 1951, p. 50). Microcline is most abundant in the upper Harpers and increases in abundance upward into the Antietam quartzite.

The Antietam quartzite is the best-sorted arenite of the area and yet contains more feldspar than any other unit. Feldspar abundance can thus not be explained by lack of sorting or abrasion. Feldspar in the Antietam may indicate a change in the character of the same source area which provided the Weverton quartzite or an influx of material from a totally different area. King (1950, p. 22) reports only "a few grains of white feldspar" from the basal beds of the Antietam quartzite of the Elkton, Virginia, area.

The only abundant heavy minerals in the sequence are tourmaline and zircon. Because zircon and tourmaline are the most stable heavy minerals in the weathering environment (Pettijohn, 1949, Table 12), their preponderance in these sediments may be further evidence that the source area was deeply weathered before erosion, transportation and deposition. However, zircon and tourmaline are the only heavy minerals that show no decrease in abundance with increasing age (Pettijohn, 1949, p. 488). Their prominence may be due either to conditions in the source area, as suggested above, or removal of other heavy minerals by interstratal solutions (Pettijohn, 1949, p. 485–497). Abundance of zircon and tourmaline in the heavy mineral suite of other orthoquartzites has been observed by Theil (1935) and Krynine (1941),

Sediments of the Swift Run and Loudoun formations are fair to poorly sorted owing to lack of lengthy transportation. The basal beds of the Weverton show good sorting which contrasts sharply with the Loudoun formation only a few feet lower in the section. This has been cited as evidence for a different, more distant source for the Weverton. Proceeding upward in the Weverton section, sorting decreases in perfection and grain size increases. These changes indicate increasingly rapid sedimentation during upper Weverton time. This interpretation differs from that of Keith (1894, p. 335) and King (1950, p. 19) who postulate gradual upward change to more stable conditions. Phyllite pebbles which were apparently contemporaneously eroded from areas of shale deposition are found at the Weverton-Harpers contact. This may be further evidence for tectonic instability responsible for changes in the upper Weverton. The Antietam quartzite shows the best sorting and marks a return to very stable conditions paralleling those existent during lower Weverton time.

Metamorphism

The rocks of the region are within the greenschist facies of metamorphism as defined by Eskola (1920, p. 162-165) and Turner and Verhoogen (1951, p. 465–473). Metamorphism was dynamic or regional (Harker, 1939), unrelated to any known igneous intrusion.

Cataclastic deformation of the gneiss has been briefly discussed. Thin sections of gneiss show destruction of higher temperature minerals not in equilibrium with the new pressure-temperature conditions and growth of new minerals characteristic of the greenschist facies. Relic minerals of earlier high-grade metamorphism or igneous intrusion are crushed garnets (Pl. 2, fig. 1) and bent early biotite with sagenite webs and sphene borders. New minerals of the late metamorphism are: chlorite, sericite, biotite, epidote, zoisite, sphene, and albite. Albite and epidote or zoisite develop from earlier more calcic feldspar but potash feldspar has undergone no apparent chemical change. If the gneiss was originally a metamorphic rock, the degrading of higher temperature minerals to the equi-

librium assemblage of the greenschist facies is retrograde metamorphism in the sense of Schwartz and Todd (1941, p. 188). Retrograde metamorphism is recognized by the relic garnet and biotite.

The Harpers formation was originally a pelitic to silty sediment. It is now a phyllite containing chlorite, sericite, quartz, albite and, less commonly, calcite and microcline. Chlorite, as already reported by Scotford (1951, p. 58) occurs both in the fine-felted groundmass and as porphyroblasts several millimeters long. Porphyroblasts are elongated in the plane of flow cleavage, but their cleavage is roughly perpendicular to their elongation (Pl. 2, fig. 6). Albite is common in the Harpers formation. Scotford (1951, p. 58) noted the uniformity of the plagioclase in the area between Sugarloaf Mountain, Maryland, and Harpers Ferry, and believed that it was the product of widespread low-grade metamorphism. The plagioclase is mainly detrital, but has reached equilibrium within the greenschist facies by being converted to albite. Detrital microcline, common near the top of the formation, has not recrystallized. The Harpers formation is assigned to the muscovite-chlorite subfacies of the greenschist facies because of the presence of calcite, chlorite, and sericite, and the lack of antinolite and biotite (Turner and Verhoogen, 1951, p. 469).

Basalt flows of the Catoctin formation have been metamorphosed to the greenschist facies. The mineral assemblage is chlorite, epidote, albite, quartz, actinolite, and small amounts of sericite and sphene.

Metamorphic rocks of the region probably belong chiefly to the chlorite-muscovite subfacies of the greenschist facies. This conclusion is based upon the mineral assemblage developed in the Harpers formation, a sediment probably similar to the pelitic rocks used by Turner and Verhoogen (1951, p. 465) in their definition of the subfacies. Local appearance of biotite in the gneiss and actinolite in the Catoctin formation is thought to indicate compositional variations rather than higher metamorphic grade.

Structural Geology

Planar and Linear Structures

A total of eight linear and planar structures were observed and recorded: bedding, two cleavages, gneissic foliation, joints, and three lineations. Some planar structures are referred to as *S*-planes (Sander, 1930); bedding is S_1, flow cleavage is S_2 and slip cleavage S_3. As explained by Cloos (1937, p. 62), Sander's terminology is purely descriptive and expresses the inferred sequence of development of structures without genetic implications. Where possible, structures were described in terms of the three mutually perpendicular co-ordinate axes defined by Sander (1930, p. 57) and described by Cloos (1946, p. 6). The following definition of axes was used: *b*—the fold axis, *a*—perpendicular to *b* in the movement plane, *c*—perpendicular to *ab*. Composite diagrams illustrate trends of some of these structures (Fig. 4). These diagrams are stereographic net projections of linear structures or the poles of planar structures. The plane of projection is a map with north at the top.

BEDDING (S_1): Bedding was observed in all formations except the gneiss and the Catoctin formation. It is best preserved in the Weverton and Antietam quartzites where it is seen as color banding or changes in grain size that may be paralleled by large partings. In rocks with dominant cleavage it appears as color bands or disconnected lenticular pods, elongated in the cleavage and stacked upon one another in the direction of the former bedding plane. Commonly these pods have been sheared out along flow cleavage (S_2) planes and can only be recognized as bedding in large exposures. The relationship between flow cleavage (S_2) and bedding (S_1) (Nevin, 1949, p. 171) and the attitude of current cross-bedding were used to distinguish overturned from normal beds.

GNEISSIC FOLIATION: A foliation may have existed in the gneiss prior to deposition of the overlying formations, but has since been largely destroyed. Alternate bands of dark and light minerals, probably a relic foliation, were recognized in some fresh exposures of gneiss.

FLOW CLEAVAGE (S_2): All rocks show a flow cleavage that varies in degree of development with the kind of rock. It is the dominant planar structure of phyllites, where all planes parallel to the cleavage are possible planes of parting (Pl. 3, fig. 2). Cleavage surfaces are shiny owing to a microscopic parallel orientation of sericite and chlorite. In quartzites, flow cleavage shows best on weathered surfaces. Elongation and flattening of quartz grains result in an indis-

tinct planar structure. Quartzites do not break parallel to this planar structure unless sericite exceeds 20 or 30 per cent. Thin sections cut in *ac* show quartz elongation parallel to *a* in the cleavage plane and shortening in the *c* direction (Pl. 2, fig. 3). Sericite flakes parallel the cleavage plane. In the gneiss, flow cleavage similar in orientation to that in the overlying rocks is related to cataclastic deformation. Cleavage is not uniformly developed but almost all outcrops contain some planes of parting along which blebs and porphyroclasts are flattened. In thin section, sericite is most abundant and best oriented along shear planes which are the flow cleavage. The flow cleavage is the *ab* plane or plane of movement. A plot of 375 poles of unfolded flow cleavage reveals a dominant low easterly dip and northeasterly strike (Fig. 4, a).

SLIP CLEAVAGE (S_3): Slip cleavage (Dale, 1896, p. 561) occurs in fine-grained phyllites and quartzose phyllites with a sericite content of greater than 30 or 40 per cent. Slip cleavage is a parallel set of close-spaced (.2–3 mm) microfaults that grade into crinkles on flow cleavage. Crinkles are the incipient stage of development of slip cleavage. Where deformation has not produced fractures, the axial planes of these crinkles may be taken as the slip cleavage. Slip cleavage is generally not paralleled by platy minerals, but the cleavage surface may possess a dull sheen, owing either to incipient sericite crystallization in the cleavage plane or to the bending of well-oriented sericite from an earlier flow cleavage into the slip-cleavage plane (Pl. 2, fig. 5). A composite diagram of 97 slip-cleavage observations from all formations shows a dominant northeast strike and either a steep northwest or gentle southeast dip (Fig. 4, b). Slip cleavage (S_3) commonly intersects flow cleavage (S_2) at a large angle (Fig. 5) but shows no uniform relationship to bedding. In diagrams c and d of Figure 4, flow cleavage and slip cleavage were plotted for each outcrop where both occurred. Slip cleavage associated with "normal" southeast dipping flow cleavage dips steeply northwest (Diagram d) and slip cleavage associated with flat or northwest-dipping flow cleavage dips southeast (Diagram c). Flat or northwest-dipping flow cleavage has been folded since its formation and slip cleavage is oriented approximately parallel to axial planes of these folds.

JOINTS: Joints of the Weverton quartzite in Short Hill were studied in detail. Cross-(*ac*) joints and longitudinal (*bc*) joints, perpendicular to bedding and cleavage, predominate. Oblique joints, midway between longitudinal and cross-joints, occur but show no consistent angular relationship to tectonic coordinates. Diagram e of Figure 4 is a plot of joints from Weverton outcrops on Short Hill. Maxima on the periphery of the net approximately 90° from the cleavage maxima represent cross-joints. Longitudinal and oblique joints form an incomplete girdle with several 5 per cent maxima around the periphery of the net.

LINEATIONS: Three lineations were observed. One of these is an elongation of quartz grains, phyllite pebbles in conglomerates, amygdules, chlorite porphyroblasts, porphyroclasts in gneiss, silty dolomite lenses in the Tomstown formation or other streaked impurities lying in the flow-cleavage plane and oriented down its dip. The other two are lines produced by the intersection of planes; one the intersection of bedding (S_1) and flow cleavage (S_2) and the other an intersection of flow cleavage (S_2) and slip cleavage (S_3).

The elongation lineation is present in almost every exposure. Lineated particles are flattened perpendicular to the flow-cleavage plane but within the plane have apparently suffered little distortion perpendicular to the lineation. A plot of 140 observations on this lineation from all formations shows that it is oriented approximately perpendicular to the regional strike and plunges southeast except in cases where flow cleavage (S_2) has been rotated, in which case it plunges northwest (Fig. 4, f). Cloos (1946, p. 26, Pl. 10; 1951, p. 146) described this lineation in Maryland and Pennsylvania, designated it as an *a* lineation, and attributed its origin to shear and transport along flow-cleavage planes during the folding of the South Mountain anticlinorium. In this paper also it is termed the *a* lineation since its character and orientation approximately perpendicular to fold axes indicate that it is elongated in the probable direction of transport within the flow-cleavage planes.

Intersections of bedding and flow cleavage parallel the northeast regional strike of the beds and plunge slightly northeast or southwest (Fig. 4, f). This lineation is difficult to measure in this region owing to the small angle between overturned bedding and flow cleavage. Most direct measurements are from rarely exposed

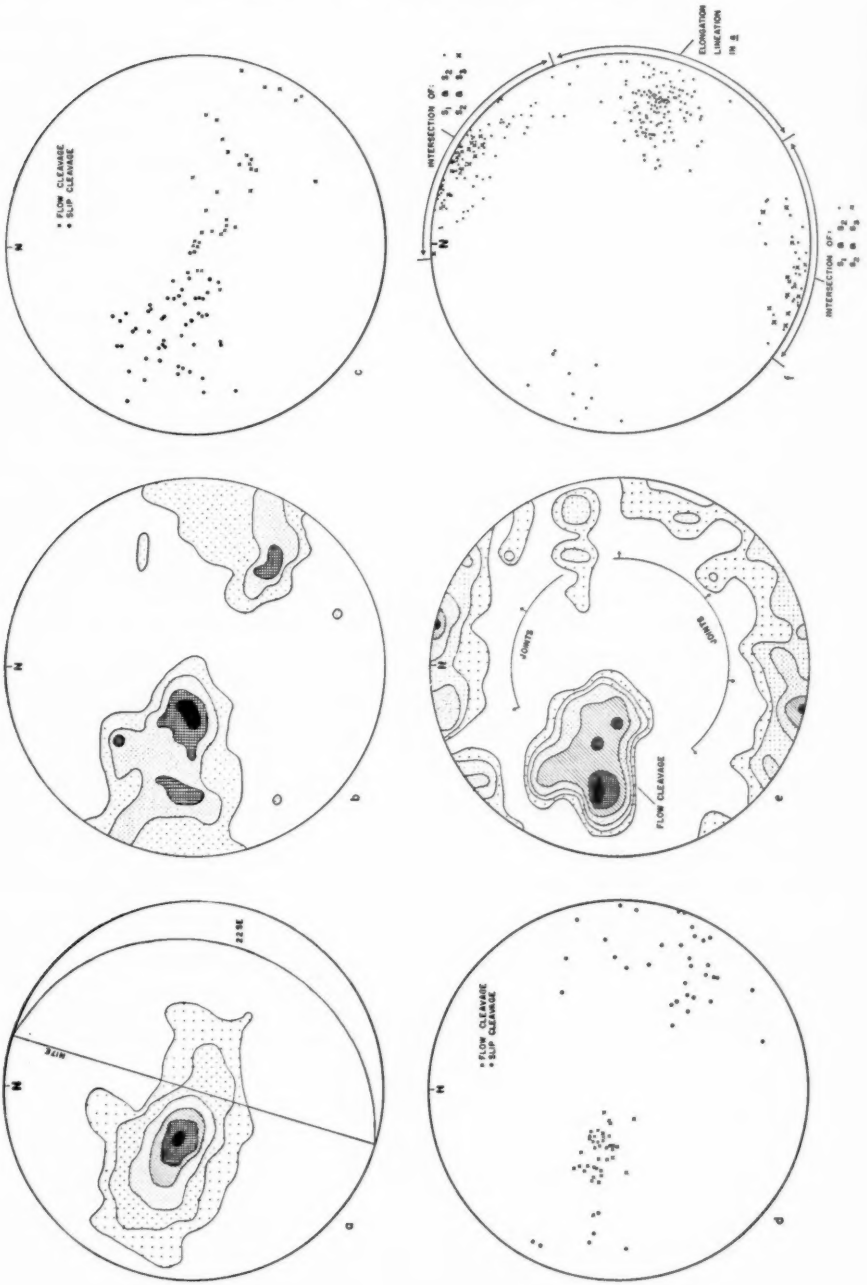
FLOW CLEAVAGE
SLIP CLEAVAGE
N
c
INTERSECTION OF:
ELONGATION LINEATION IN E
f
b
JOINTS
BANDS
FLOW CLEAVAGE
e
228°
N 31° W
a
FLOW CLEAVAGE
SLIP CLEAVAGE
d

FIGURE 4.—COMPOSITE DIAGRAMS OF PLANAR AND LINEAR STRUCTURES

Diagram	Structure	Formation	Area	No. of observations	Contours %
a.	Poles to unfolded flow cleavage	All formations	Whole area	375	23-15-10-5-2-½
b.	Poles to slip cleavage	All formations	Whole area	97	7-5-3-1
c.	Poles to flat or NW-dipping (folded) flow cleavage and related slip cleavage	All formations	Whole area	54 slip cl. 34 flow cl.	.....
d.	Poles to "normal" SE-dipping flow cleavage and related slip cleavage	All formations	Whole area	39 slip cl. 39 flow cl.	.....
e.	Poles to flow cleavage and joint surfaces	Weverton quartzite	Short Hill	33 flow cl. 74 joints	20-15-9-5-3-1
f.	Lineations	All formations	Whole area	Int. S_1 and S_2—94 Int. S_2 and S_3—36 *a* lineation—140	.....

anticlinal crests and synclinal troughs where the angle is large; but even here irregularities in strike and plunge are produced by fanning cleavage, forward movement along cleavages during shear folding, differences in competency of material, and inaccuracies of measurements. The intersection is suitable, however, for approximating the direction and plunge of fold axes and is termed the *b* lineation. Northeast plunge is most common because the area is on the northern end of the Catoctin Mountain-Blue Ridge anticlinorium.

Lineation owing to intersection of flow cleavage (S_2) and slip cleavage (S_3) is distinct only in phyllites. It shows as fractures or coarse to fine crinkles on the flow cleavage. The attitude of this lineation with respect to *b* can rarely be determined because bedding has been obliterated in most of the lineated rocks. It approximately parallels the regional strike and plots in the same areas of the stereographic net as the *b* lineation (Fig. 4, f). However, since it is commonly associated with crinkling of flow cleavage it cannot be assumed to parallel the plunge of bedding folds. It may parallel *b* in nonplunging portions of folds, but must vary considerably from *b* on the nose of plunging folds.

Folds

Two categories of folds are recognized in the area; folds on bedding and folds on flow cleavage. The largest bedding fold in the Blue Ridge province of Maryland, southern Pennsylvania, and Virginia, is in the Catoctin Mountain—Blue Ridge anticlinorium (Stose and Stose, 1946, p. 98) with limbs forming Catoctin Mountain and Bull Run Mountain on the east and South Mountain, Short Hill, and Blue Ridge on the west (Fig. 6). Several categories of smaller bedding folds on this structure relate to the same deformational plan. They have been divided into major folds, mapped on the limbs of the anticlinorium, and minor folds, ranging from an inch to 30 feet in amplitude, but too small to be shown on the geologic map.

Folds on flow cleavage range from several millimeters to 3 inches in amplitude and are found only in phyllites at a few localities.

CATOCTIN MOUNTAIN-BLUE RIDGE ANTICLINORIUM: This structure extends southward from southern Pennsylvania into Virginia (King,

1951, p. 132), becoming higher and exposing deeper parts of the gneissic basement to the south. It is asymmetric or overturned; normal east-dipping beds appear on Catoctin Mountain, but vertical to overturned east-dipping beds appear on Blue Ridge and Short Hill (Fig. 6). Normal faulting duplicates the western overturned limb in southern Maryland and northern Virginia. The northward plunge of the anticlinorium is shown by the plunge of major folds in the Weverton and Antietam quartzites at Chestnut Hill Church and north of Bloomery Bridge.

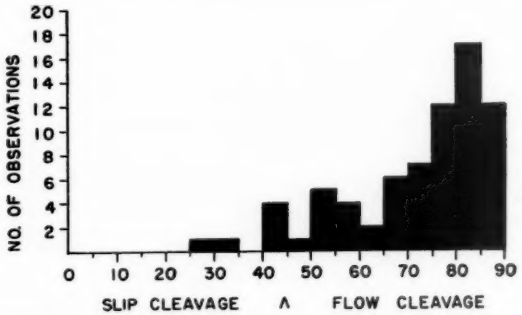

FIGURE 5.—HISTOGRAM SHOWING ANGLE BETWEEN SLIP CLEAVAGE AND FLOW CLEAVAGE

A combination of flexure folding (Billings, 1942, p. 87) and shear folding (Billings, 1942, p. 90) was responsible for its development. All gradations between folding by flexure and shear probably exist. The dominance of either type is a function of competency of material, position within the area, and position on the fold. Regardless of competency, shear folding was dominant near the end of deformation as evidenced by the flow cleavage in all rocks. Cloos first (1947, p. 908–910) interpreted the anticlinorium as a large shear fold formed predominantly by shearing and laminar flow along flow-cleavage planes; but later (1951, p. 148), pointed out its complexity and also described flexure folding in competent beds. This multiple origin for the folds in the anticlinorium accords with the writer's interpretation.

MAJOR FOLDS: All observed major folds lie in the western vertical or overturned limb of the anticlinorium and are commonly recumbent or have axial planes that dip gently east. Folds in Blue Ridge and Short Hill are almost isoclinal, but west of Blue Ridge in the Antietam quartzite they are more open. In the Potomac River region both Blue Ridge and Short Hill contain an overturned syncline and anticline of Weverton quartzite. These folds are schematically shown in Figure 7 which also illustrates the general flow-cleavage–bedding relationship. Cleavage and bedding intersect at a large angle near the troughs of synclines, crests of anticlines, and on normal east-dipping limbs. On overturned limbs dipping 20°–35° E., cleavage is commonly parallel to bedding. Flow cleavage is approximately parallel to the axial planes of folds. Generally, it fans slightly on the limbs, and is parallel to the axial plane in the crests or troughs.

Folds show the following features: thickened crests and troughs and thinned limbs, stretched blebs and elongated quartz grains lying in the flow cleavage perpendicular to the fold axis, and slickensided and boudinaged beds. Thickened crests and troughs are produced by plastic flowage of material and shear along subparallel cleavage planes (Cloos, 1947, p. 904–905, Fig. 19). Bedding-plane slip and slightly fanning cleavage are remnants of flexure folding. Folds may have started as flexure folds produced by bending and slip between bedding planes, accompanied by the development of fanning cleavage at a large angle to bedding. Axial planes of these folds were probably vertical or steeply east dipping. As folding continued, slippage along bedding planes was accompanied by slight displacement along closely spaced cleavage planes or shear directions. During this stage, cleavage planes on the limbs rotated

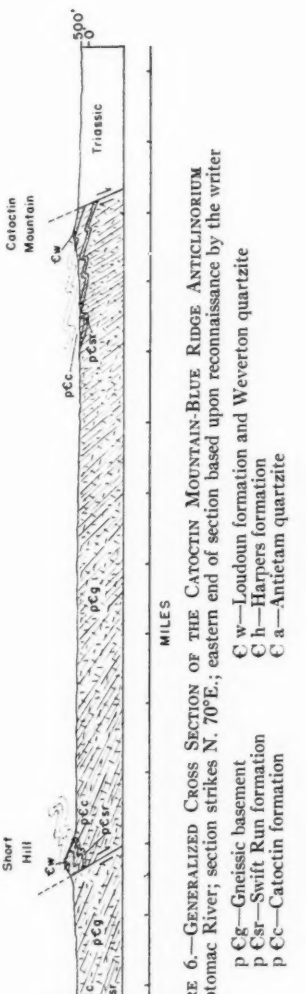

FIGURE 6.—GENERALIZED CROSS SECTION OF THE CATOCTIN MOUNTAIN-BLUE RIDGE ANTICLINORIUM
Four miles south of Potomac River; section strikes N. 70°E.; eastern end of section based upon reconnaissance by the writer

p €g—Gneissic basement
p €sr—Swift Run formation
p €c—Catoctin formation
€ w—Loudoun formation and Weverton quartzite
€ h—Harpers formation
€ a—Antietam quartzite

toward parallelism with the axial plane of the fold and axial planes rotated westward. Simultaneously, there was elongation of quartz grains in the cleavage, produced either by "plastic" flow or shear along intersecting sets of fractures. With continued deformation, flow-cleavage planes would probably attain nearly perfect parallelism with the axial plane and continued folding would be by shear along these planes.

Folds in the Antietam quartzite are thought to have formed by flexure, shear, and some flowage of material, but deformation was not carried as far as in the Weverton quartzite further east. Bedding-plane slip during flexure folding was facilitated by repeated lithology changes. Cleavage planes have not rotated as far toward the axial planes, and shear folding along cleavage planes has been largely restricted to shaly interbeds and thin quartzite beds. Thin sections of quartzite beds reveal some elongation of quartz in the cleavage plane, but most flowage and recrystallization has taken place in less competent beds.

Less competent formations such as the Harpers, Loudoun, Catoctin, and Swift Run have been folded predominantly by shear along flow-cleavage planes. Sections from the base of the Antietam quartzite into the Harpers formation reveal a transition in type of folding, as quartzite beds become thinner and less numerous. Thin beds are commonly displaced along flow cleavage, and cleavage planes are paralleled by color banding and lithologic differences caused by sheared out remnants of bedding. Bedding is visible only on the crests and troughs of folds and is parallel to cleavage on the limbs.

MINOR FOLDS: Minor folds are rare in all formations. Their sparseness is probably due to obliteration or distortion by shear folding. In the Tomstown formation and middle member of the Weverton quartzite drag folds were found. They were in places used to tell top from bottom, although they are not completely reliable in this regard.

FOLDS ON FLOW CLEAVAGE: These folds are present only in phyllites where flow cleavage is well developed. They are symmetrical and chevronlike in cross section. Flow cleavage is bent and fracture cleavage (S_3) occurs approximately parallel to the axial planes. They were probably developed at a late stage in the same

deformation that folded bedding and formed flow cleavage because:

(1) The forces which produced bedding folds operated in the same direction as the forces that produced folds on flow cleavage. Figure 4, a, b, c, f indicate development of flow cleavage and fracture cleavage along the same axis of folding.

(2) Folds on flow cleavage appear only in phyllites in which flow cleavage was well developed at an early stage of deformation and bedding was no longer active as a slip plane. With continued deformation, this early flow cleavage was folded at the same time that more-competent beds were still deforming by slip along bedding (flexure folding) and by shear along flow cleavage (shear folding).

In the writer's opinion, at least three kinds of folding progressed simultaneously near the end of deformation: (1) folding of competent beds (quartzites) by a combination of flexure and shear, (2) folding of bedding in less competent phyllites by shear along closely spaced flow-cleavage planes, (3) folding of flow cleavage by a combination of flexure and shear.

Several polished surfaces cut perpendicular to the axis of folds on flow cleavage have been studied. Figure 8 shows the orientation of bedding (S_1), flow cleavage (S_2), and slip cleavage (S_3) in these folds. The inferred sequence of events is as follows:

(1) Bedding, which is now vertical, was folded by shear along flow-cleavage planes. Slices of bedding are elongated and tailed out in the flow-cleavage plane, and separated by bands of other material which has been sheared into place between the slices.

(2) Flow cleavage was then folded and crinkled by flexure, with slip taking place between flow-cleavage planes.

(3) Later, slip cleavage developed as the axial planes of crinkles on flow cleavage and some slip took place along these fractures.

(4) Deformation continued by a combination

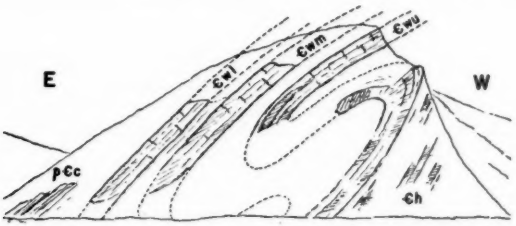

FIGURE 7.—SCHEMATIC SKETCH OF OUTCROP DISTRIBUTION ON SOUTH (VIRGINIA) SIDE OF POTOMAC RIVER GORGE THROUGH SOUTH MOUNTAIN-SHORT HILL
Width of sketch approximately 2200 feet

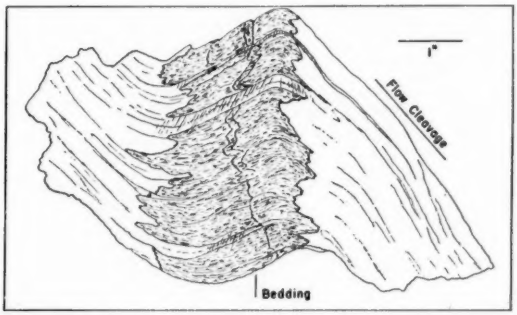

FIGURE 8.—FOLD ON FLOW CLEAVAGE IN HARPERS FORMATION
Tailing out of bedding along flow cleavage indicates shear folding. Following shear folding flow cleavage has been folded and slip cleavage developed. Drawing is traced from polished surface perpendicular to fold axis of specimen collected along road paralleling Shenandoah River south of Harpers Ferry.

of slip between flow-cleavage planes (flexure folding) and movement on slip-cleavage planes (shear folding).

Slip cleavage converges upward as shown in Figure 9. It is believed that it was originally parallel to the axial plane of the fold and has since been rotated inward by relative slip along flow-cleavage planes in response to flexure folding. Relative movements as shown by Billings (1947, Fig. 77, A) during flexure folding would cause an originally vertical plane to lean inward on both limbs of the anticline.

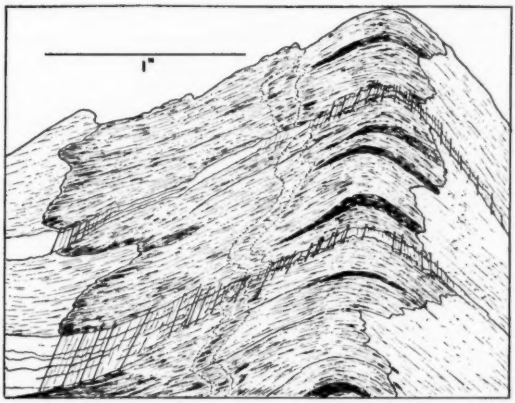

FIGURE 9.—ENLARGED DRAWING OF UPPER PART OF FOLD SHOWN IN FIGURE 8
Slip cleavage is oriented n-s almost parallel to axial plane of fold, but converges upward owing to relative slip along flow cleavage planes as they were folded.

Bedding parallels the axial planes of three folds on flow cleavage which were cut and polished for study. Although it was no longer a plane of active slip, it served as a plane of discontinuity which controlled the location of later folds of flow cleavage.

Faults

A normal fault lies along the west side of Short Hill and in Maryland was mapped by Cloos (1951) along the west side of South Mountain. Near Hillsboro, Virginia, it is estimated to dip 50° or 60° E., on the basis of its map pattern (Pl. 1). The abrupt ending of Short Hill 2 miles south of Hillsboro, Virginia, is caused by this fault plus a northward plunge of fold axes. Here, folds in the lower and middle quartzite members of the Weverton quartzite plunge 11° northward and are cut off at an acute angle. To the south the fault enters the gneiss and cannot be recognized. Since this fault is later than folding and has the same relative displacement as the border fault of the Triassic basin to the east (Fig. 6) it is probably Triassic in age.

A small normal fault located 1½ miles south of the Potomac River on the east side of Short Hill produces a duplication of the Weverton-Loudoun sequence.

Keith (1893; 1894) and Stose and Stose (1946) mapped large overthrusts in the Potomac River region. Cloos (1951) has shown that relations in Maryland are better explained by folding and normal faulting. The writer found no evidence of large-scale overthrusting in the area, although small thrusts probably occur. The Harpers Ferry overthrust which Stose and Stose (1946, p. 111) claim to have traced from Harpers Ferry southwestward into Clarke County, Virginia, along the west side of the Blue Ridge is not present. Four miles south of the Potomac River near Chestnut Hill Church, West Virginia, the Harpers formation overlies the Weverton quartzite in a normal, west-dipping sequence. No fault separates these formations here. Similar normal relationships between the Harpers and Weverton may be seen as far south as Wilson Gap at the southern end of the area. If a thrust fault is present on the

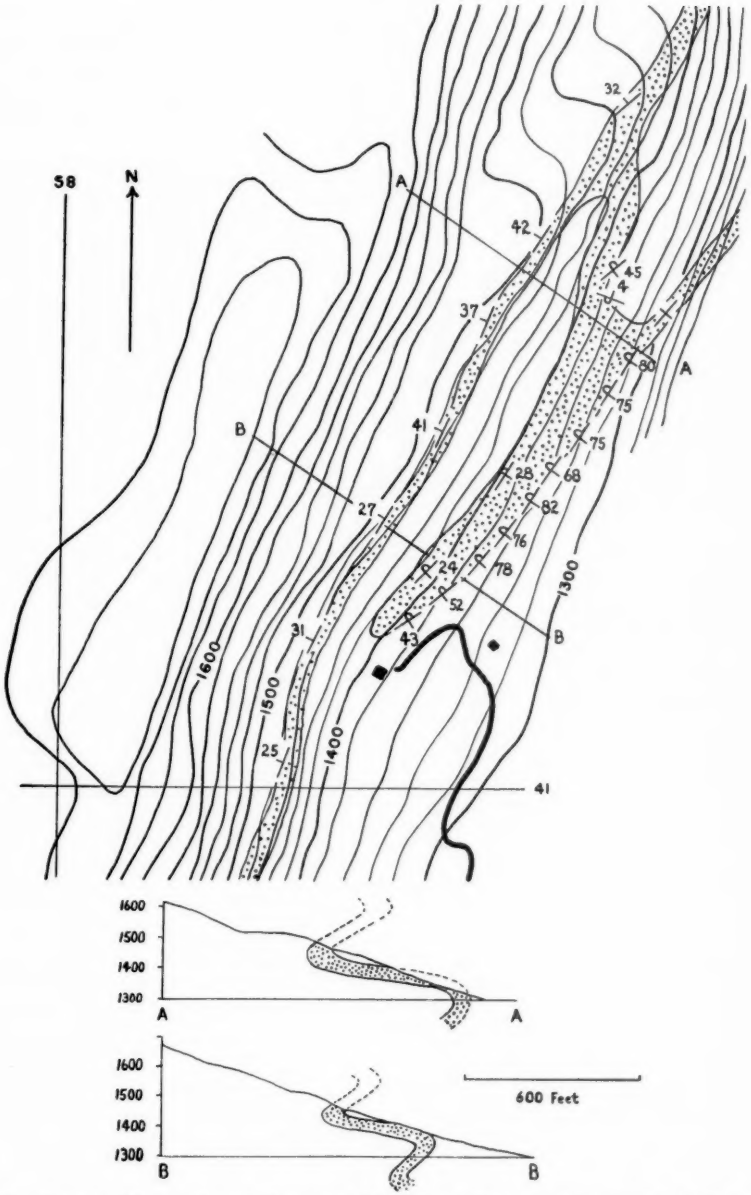

FIGURE 10.—OUTCROP MAP OF LOWER QUARTZITE MEMBER OF WEVERTON QUARTZITE ON EAST SLOPE OF BLUE RIDGE SOUTH OF CROSS-SECTION LINE D-D'

Recumbent anticline and syncline and relation of topography produce complex outcrop pattern. Bedding in easternmost outcrop is folded back into slope and appears up slope to the west, dipping 30° or 40°NW

western side of the Blue Ridge, it must lie to the south of the area mapped by the writer.

Description of Key Areas

The eastern side of Blue Ridge.—This area is a dip slope developed upon the overturned lower or middle Weverton quartzite members. Most outcrops are parts of minor folds upon the overturned limb that makes up the slope. In these outcrops bedding dips west or vertically, but in places may be seen to fold back into the slope as shown in Figure 10.

Wide outcrop belts of the lower and middle Weverton quartzite members north and south of Route 9 are due to parallelism of overturned bedding and topography. The wide belt of the lower Weverton quartzite member 2 miles south of Route 9 probably contains inliers of the middle Weverton quartzite member. They were not mapped because lithologies in the lower and middle Weverton quartzite members are not distinctive. The lower Weverton quartzite member extends overturned and dipping east up the east side of the Blue Ridge and crops out at the summit.

Area north of Purcell Knob.—North of Purcell Knob on the east side of Blue Ridge rock units from the gneiss to the Weverton quartzite were folded recumbently and subsequently bent. In phyllites bedding is obliterated, flow-cleavage planes are folded, and slip cleavage is well developed. The structural pattern is shown by the lower Weverton quartzite member (Pl. 1). Purcell Knob and the ridge extending northeastward are on the trough of a recumbent syncline overturned to the west and plunging approximately 18° NE. Bedding along this ridge varies abruptly from normal west dipping to overturned east dipping. At the north end of the ridge the strike of overturned bedding swings northwest and then west. Here, the Weverton quartzite dips 25° or 30° N. under phyllites and conglomerate of the Loudoun formation. Judging from topography, the quartzite then swings south and dips overturned westward under the Loudoun formation. Bedding along the west side of the ridge has thus been rotated more than 180° by folding (Fig. 11, section X-X′). The quartzite is next seen on a ridge to the west where it is overturned dipping east and is again overlain by the Loudoun formation. At some places bedding is flat and overturned, and flow cleavage dips west. North of the ridge the quartzite crops out on the east slope of Blue Ridge and retains this position northward to the Potomac River. Northward from the Weverton quartzite, younger formations dip under older formations, and proceeding down the plunge of the structure successively older formations appear. The gneiss overlies the Swift Run formation in a large outcrop at the end of road number 685, .7 mile west of the Church of the Nazarene. Here flow cleavage and bedding are essentially parallel and both dip west or vertically, paralleling the dip of flow cleavage in the overlying gneiss. Slip cleavage dips gently east.

Two stages of folding occurring in close sequence during one deformation, account for the map pattern. The stages are:

(1) Recumbent folding of bedding by flexure and shear

(2) Gentle warping or bending of bedding and previously formed flow-cleavage planes accompanied by the formation of slip cleavage in phyllites.

The first stage of folding produced a recumbent anticline with its crest approximately in the Blue Ridge, overlying a recumbent syncline with its trough in Purcell Knob (Fig. 11). The second stage produced a small upright syncline and an anticline in the flow cleavage and overturned beds of the first stage. The trough of the syncline passes through the isolated mass of gneiss just east of Blue Ridge. The anticlinal axis extends northeastward from the north end of Purcell Knob. Vertical to east-dipping lines near the eastern end of section X-X′ (Fig. 11) represent slip cleavage in this anticline. The second stage of folding is recorded by the attitude of flow cleavage and fracture cleavage, as well as the map pattern. Diagram d of Figure 4 shows normal orientation of flow and slip cleavage. In the Purcell Knob area, however, flow cleavage commonly dips west and slip cleavage east. Most of the readings recorded in diagram c of Figure 4 were obtained here. The writer interprets this to mean that an originally east-dipping or flat-lying flow cleavage was folded after formation. Fracture cleavage developed in an abnormal orientation (east dipping) in response to the same force that produced this folding.

Potomac River: South Mountain-Short Hill gap.—Cliff exposures on both sides of the Potomac River gorge were mapped by pace and compass traverse. Figure 7 illustrates the writer's interpretation of the structure of the Weverton quartzite here. The folds are major folds upon the steeply west-dipping limb of the Catoctin Mountain-Blue Ridge anticlinorium. Three members of the Weverton quartzite are shown in Figure 7. The upper Weverton quartzite member is at the west end of the figure and is the only bed which is folded within the ridge above river level. The middle and lower Weverton quartzite members crop out to the east of the upper member as two unfolded beds which are overturned and dip east. On the north (Maryland) side of the Potomac River gorge, overturned beds of the upper Weverton quartzite member crop out behind a

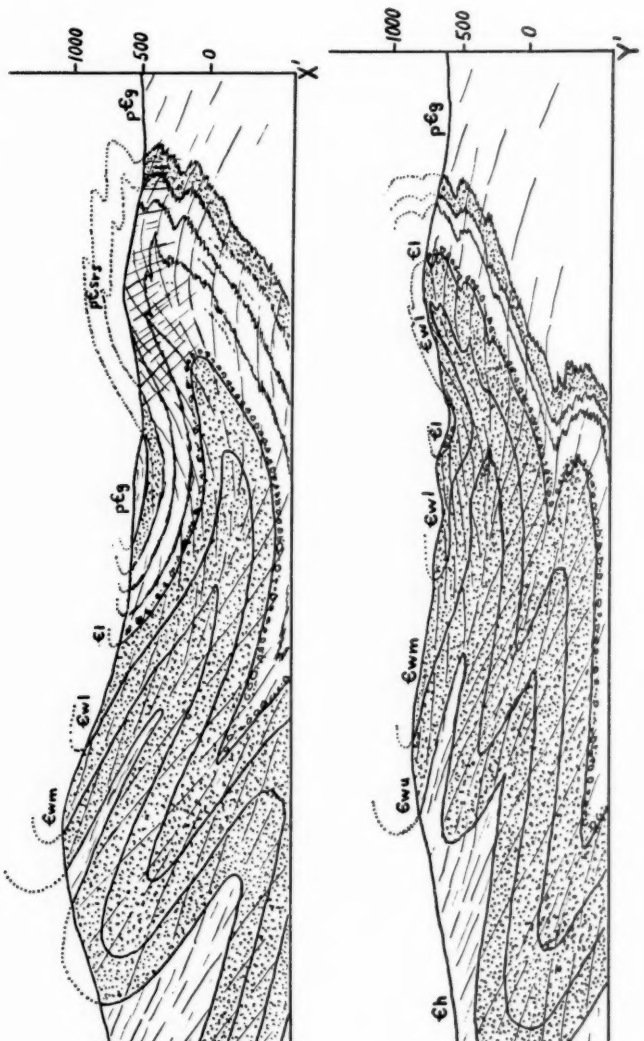

FIGURE 11.—CROSS SECTIONS OF PURCELL KNOB AREA
Plate 1 shows location of sections; scale of sections twice that of geologic map

house on Route 340 east of Weverton, Maryland. Here bedding dips 40° E. Bedding steepens to vertical 100 feet above the house and then folds very abruptly to the east forming a small asymmetric anticline. Three hundred feet east of the crest of this anticline bedding folds back to vertical or overturned and can be traced up the face of the cliff to the summit of the ridge. The shallow asymmetric syncline formed here is partially covered by talus.

In a quarry near the east end of the section the middle Weverton quartzite member dips 30°–35° E. and is overturned. Here boudinage, slippage between beds, and tension joints perpendicular to bedding may be seen. Bedding is paralleled by cleavage, but overturned cross-bedding and stratigraphic succession indicate the attitude of beds. This member may be traced as an overturned bed dipping 30° or 40° E., up the face of the cliff to the summit of the ridge where it forms a line of outcrops 300 feet east of the upper Weverton quartzite member. The middle Weverton quartzite member probably folds back to the west beneath the floor of the quarry.

The lower member of the Weverton quartzite crops out above and to the northeast of the quarry at the east end of the section. It is overturned, dips east, and parallels the middle member on the face of the bluff. Cross-bedding is absent or poorly developed, but the member is interpreted to be overturned on the basis of its parallelism with the middle Weverton quartzite member and its stratigraphic position above that member.

Figure 7, a schematic sketch of the south (Virginia) side of the Potomac River gorge, shows structure similar to the north side of the river. The anticline and syncline at the west end of the section are deeper and more nearly isoclinal. The upper overturned limb of the syncline dips as little as 16° E. Eastward this limb steepens to a dip of 57° E. and is cut by flow cleavage dipping 29° E., indicating overturned bedding. The middle and lower Weverton quartzite members crop out east of the upper member as overturned beds dipping 30° or 40° E. that make up the eastern dip slope of the ridge. Bedding in the lower two members is paralleled by cleavage, and the attitude of the beds is established by cross-bedding and stratigraphic sequence.

West of the Weverton quartzite vertical to overturned east-dipping beds of the Harpers formation are present. The western boundary of the Harpers formation is a normal fault described by Cloos (1951, p. 132) that brings Harpers against gneiss. East of the Weverton quartzite there is an overturned sequence, including, in succession, the Loudoun formation, Catoctin formation, Swift Run formation, and gneiss. There is no evidence for a fault on the eastern side of the ridge as suggested by Cloos (1951, p. 132).

Other authors have interpreted the structure of South Mountain differently. Stose and Stose (1946, p. 102–104, Fig. 22) believe it is a syncline and illustrate their description with a highly schematic diagram of the bluff on the north side of the Potomac River. Stose and Stose incorrectly correlate different beds within the Weverton quartzite and miss the vertical to overturned beds of the upper Weverton quartzite member at the western end of the section. As already pointed out by Cloos (1951, p. 34), they incorrectly assign the beds of the Harpers formation at the western end of the section to the Loudoun formation. Their interpretation of the eastern slope of South Mountain as a dip slope on overturned beds is essentially correct, however.

Cloos (1951, Fig. 22) published a sketch correctly illustrating the distribution of outcrops on the north wall of the Potomac River gorge. He states (Cloos, 1951, p. 134, Fig. 10 on p. 21) that South Mountain is an anticline, based upon the assumption that the east-dipping beds on the east slope of the ridge are right side up. This interpretation requires a normal fault at the east end of the section since the right-side-up Weverton quartzite dips under the Catoctin formation (Cloos, 1951, p. 132).

Work by the writer has revealed that the east dipping Weverton quartzite beds are overturned as indicated by overturned cross-bedding and stratigraphic sequence. The same overturned sequence has been mapped for 11 miles southward along the eastern slope of Short Hill. It is concluded that Short Hill is neither an anticline nor a syncline but the steeply dipping limb of the Catoctin Mountain-Blue Ridge anticlinorium, here made up of an anticline and syncline.

For most of its length the structure of Short Hill is essentially the same as is shown in Figure 7. From 1 mile north of Hillsboro, Virginia, to the southern end of Short Hill, however, the normal fault west of Short Hill has cut off part or all of the second order anticline shown in Figure 7. This is especially evident 1 mile north of Hillsboro where a syncline of Weverton quartzite is in fault contact with the gneiss.

Conclusions

The following major conclusions have resulted from this work:

(1) The gneissic basement is made up of meta-igneous or meta-sedimentary rocks that were retrograded to the greenschist facies at

the same time that later sedimentary and volcanic rocks were folded. All rocks of the area are in the greenschist facies of metamorphism.

(2) The volcanic and sedimentary rocks between the gneiss and the Weverton quartzite are local deposits from local sources that were not well sorted during deposition. Basalt flows of the Catoctin formation were subaerial. In contrast, the Weverton quartzite and overlying formations are widespread units derived from a distant source and deposited in a shallow sea after much sorting and reworking.

(3) The Weverton quartzite is divided into three quartzite members that may be useful for correlation southward.

(4) Feldspar is not present in the Weverton quartzite, but is fairly abundant in the Antietam quartzite. This may indicate a different source for the two formations or different conditions in the same source area.

(5) Short Hill and Blue Ridge both contain an asymmetric anticline and syncline of Weverton quartzite that are folds upon the western limb of the Catoctin Mountain-Blue Ridge anticlinorium. This limb has here been repeated by a normal fault west of Short Hill that is of Triassic age.

(6) Folding during the Paleozoic was the dominant mode of deformation. The Harpers Ferry thrust fault is not present in northern Virginia between the Potomac River and Clarke County. Recumbent folds, overturned to the northwest, of a magnitude not previously recognized in this area have been mapped.

(7) Several kinds of folding are recognized. Folding probably started by flexure and graded into shear during the late stages of deformation. Some quartzites still show evidence of flexure folding, but in the incompetent phyllites only shear folding along flow-cleavage planes can be recognized. In phyllites, where bedding was no longer an active slip plane and flow cleavage dominated, the flow cleavage was folded, and a later slip cleavage developed. Folding of flow cleavage probably took place in response to the same directive stress at a later time in the same period of folding. Late folds are upright anticlines and synclines upon the limbs of recumbent folds formed earlier.

References Cited

Billings, M. P., 1942, Structural geology: N. Y., Prentice-Hall, 473.

Bloomer, R. O., 1950, Late Pre-Cambrian or Lower Cambrian formations in Central Virginia: Am. Jour. Sci. v. 248, p. 753–783.

Bloomer, R. O., and Bloomer, R. R., 1947, The Catoctin formation in Central Virginia: Jour. Geology, v. 55, p. 94–106.

Butts, C., 1940, Geology of the Appalachian Valley in Virginia, pt. 1: Virginia Geol. Survey Bull. 52, p. 1–519.

Cloos, E., 1937, The application of recent structural methods in the interpretation of the crystalline rocks of Maryland: Maryland Geol. Survey, v. 13, pt. 1, p. 25–108.

—— 1946, Lineation; a critical review and annotated bibliography: Geo. Soc. America Mem. 18, p. 1–122.

—— 1947, Oölite deformation in the South Mountain Fold, Maryland: Geo. Soc. America Bull., v. 58, p. 843–918.

—— 1951, Washington County, State of Md.: Dept. of Geol. Mines and Water Res., p. 1–333.

Currier, L. W., 1935, Zinc and lead region of Southwestern Virginia: Virginia Geol. Survey Bull. 43, p. 1–122.

Dale, T. N., 1896, Structural features in the Green Mountain region and in eastern New York: U. S. Geol. Survey 16th Ann. Rept., pt. 1, p. 543–570.

Eskola, P., 1920, The mineral facies of rocks: Norsk Geol. Tids., v. 6, p. 143–194.

Fellows, R. E., 1943, Recrystallization and flowage in Appalachian quartzite: Geol. Soc. America Bull., v. 54, p. 1399–1432.

Folk, R. L., 1951, A comparison chart for visual percentage estimation: Jour. of Sed. Petrology, v. 21, p. 32–33.

Gair, J. E., 1950, Some effects of deformation in the Central Appalachians: Geo. Soc. America Bull., v. 61, p. 857–876.

Geiger, H. R., and Keith, A., 1891, The structure of the Blue Ridge near Harpers Ferry: Geo. Soc. America Bull., v. 2, p. 155–164.

Goddard, E. N., *et al.*, 1948, Rock color chart: Natl. Research Council, Washington, D. C.

Harker, A., 1939, Metamorphism: London, Methuen, 362 p.

Keith, A., 1892, The geologic structure of the Blue Ridge in Maryland and Virginia: Am. Geologist, v. 10, p. 362–368.

—— 1893, Geology of the Catoctin Belt: U. S. Geol. Survey, 14th Ann. Report, pt. II, p. 285–395.

—— 1894, Harpers Ferry folio: U. S. Geol. Survey Geol. Atlas, folio 10.

King, P. B., 1949, The base of the Cambrian in the Southern Appalachians: Am. Jour. Sci., v. 247, p. 513–530, 622–645.

—— 1950, Geology of the Elkton area, Virginia: U. S. Geol. Survey Prof. Paper 230, 82 p.

—— 1951, The tectonics of Middle North America: Princeton, N. J., Princeton Univ. Press, 203 p.

Krynine, P. D., 1941, Paleogeographic and tectonic significance of sedimentary quartzites (Abstract): Geo. Soc. America Bull., v. 52, p. 1915–1916.

Krynine, P. D., 1946, The Tourmaline group in sediments: Jour. Geology, v. 54, p. 65–87.
Nevin, C. M., 1949, Principles of structural geology, 4th Ed.: N. Y., John Wiley and Sons, 410 p.
Pettijohn, F. J., 1949, Sedimentary rocks: N. Y., Harpers Brothers, 526 p.
Resser, C. E., 1938, Cambrian system of the Southern Appalachians: Geol. Soc. America Spec. Papers, no. 15, 140 p.
Resser, C. E., and Howell, B. F., 1938, Lower Cambrian Olenellus zone of the Appalachians: Geol. Soc. America Bull., v. 49, p. 195–248.
Rodgers, J., 1940, Distinction between calcite and dolomite on polished surfaces: Am. Jour. Sci., v. 238, p. 788–793.
Safford, J. M., 1856, A geological reconnaissance of the State of Tennessee: 1st Bienn. Rept., Tenn. State Geologist.
Sander, B., 1930, Gefüge Kunde der Gesteine: Wien, Julius Springer, 352 p.
Schwartz, G. M., and Todd, J. H., 1941, Comments on retrograde metamorphism: Jour. Geology v. 49, p. 177–189.
Scotford, D. M., 1951, Structure of the Sugarloaf Mountain area, Maryland, as a key to Piedmont stratigraphy: Geo. Soc. America Bull., v. 62, p. 45–76.
Smith, H. T. U., and Smith, A. P., 1945, Periglacial rock streams in the Blue Ridge area (Abstract): Geol. Soc. America Bull., v. 56, p. 1198.
Snyder, F. G., 1947, The problem of the Lipalian interval: Jour. Geology, v. 55, p. 146–152.
Stose, A. I., and Stose, G. W., 1946, Geology of Carroll and Frederick counties: State of Md. Dept. of Geol. Mines, and Water Res., p. 11–128.
Stose, G. W., 1906, The sedimentary rocks of South Mountain, Pennsylvania: Jour. Geology, v. 14, p. 201–220.
—— 1909, Mercersburg-Chambersburg folio: U. S. Geol. Survey Geol. Atlas, folio 170.
Stose, G. W., and Jonas, A. I., 1939, Age relations of the Pre-Cambrian rocks in the Catoctin Mountain-Blue Ridge and Mount Rodgers Anticlinoria in Virginia: Am. Jour. Sci., v. 237, p. 575–593.
Stose, G. W., and Stose, A. I., 1949, Ocoee series of the Southern Appalachians: Geo. Soc. America Bull., v. 60, p. 267–320.
Thiel, G. A., 1935, Sedimentary and petrographic analysis of the St. Peter sandstone: Geo. Soc. America Bull., v. 46, p. 559–614.
Turner, F. J., and Verhoogen, J., 1951, Igneous and metamorphic petrology: N. Y., McGraw-Hill, 602 p.
Wheeler, H. E., 1947, Base of the Cambrian: Jour. Geology, v. 55, p. 153–159.
Williams, G. H., 1892, The volcanic rocks of South Mountain in Pennsylvania and Maryland: Am. Jour. Sci., v. 44, 3rd ser., p. 482–496.
Williams, G. H., and Clark, W. B., 1893, Maryland, its resources, industries and institutions: Baltimore.
Winchell, A. N., and Winchell, H., 1951, Elements of optical mineralogy, pt. II: N. Y., John Wiley and Sons, 551 p.

Department of Geology Pennsylvania State University, University Park, Pa.

Manuscript Received by the Secretary of the Society May 10, 1954
Contribution No. 55-24 from the College of Mineral Industries, The Pennsylvania State University

BULLETIN OF THE GEOLOGICAL SOCIETY OF AMERICA
VOL. 67, 271-288, 6 FIGS., 1 PL. MARCH 1956

LATE WISCONSIN CHRONOLOGY OF THE LAKE MICHIGAN BASIN CORRELATED WITH POLLEN STUDIES

BY JAMES H. ZUMBERGE AND JOHN E. POTZER*

ABSTRACT

Geological interpretation and radio carbon dating of an excellent exposure in a wave-cut cliff on the shore of Lake Michigan near South Haven, Michigan, permits the establishment of the following absolute chronology of events for the Lake Michigan Basin: Two Creeks-Bowmanville low-water stage, 11,000 years ago; end of Lake Algonquin, 8000 years ago; Lake Chippewa low-water stage, 5000 years ago; and beginning of the Nipissing Great Lakes, a little less than 4000 years ago.

Pollen profiles from the South Haven section and from a bog near Hartford, Michigan, on the Valparaiso ground moraine reveal the following forest succession in southwestern Michigan from Two Creeks time to the present: spruce-fir to Jack pine to white-red pine to oak to oak-hemlock-broad-leaved forest to oak-pine. Radiocarbon dating indicates that the close of the spruce-fir period was 8000 years ago; the Jack pine period, 7000 years ago; the white-red pine period, 6000 years ago; the oak-pine period, 5000 years ago; and the oak-hemlock-broad-leaved forest (Xerothermic), 4000 to 3500 years ago.

The difference in time between Lake Algonquin and the Nipissing Great Lakes was 4000 years. The Xerothermic is correlated with the Nipissing Great Lakes at 4000–3500 years ago.

CONTENTS

TEXT

	Page
Introduction	272
Acknowledgments	272
Résumé of the Late Wisconsin history of the Lake Michigan basin	272
Previous work	272
Glacial Lake Chicago	272
Lake Algonquin	273
Later "Algonquin" stages	273
Nipissing Great Lakes	273
Algoma Great Lakes	273
Low-water stages in the Lake Michigan basin	273
Geologic section near South Haven, Michigan	274
Description	274
Geologic interpretation	277
Summary of geologic events as indicated by the South Haven section	279
Radiocarbon chronology	280
Previous work	280
Discussion of South Haven radiocarbon dates	280
Pollen studies of the South Haven and Hartford sites	281
Introduction	281
Methods of collecting and preparing samples for pollen analysis	281
Pollen profiles	283
Discussion	283
Summary of pollen studies at South Haven and Hartford bog	286
References cited	287

ILLUSTRATIONS

Figure	Page
1. Index map	274
2. Wave-cut cliff exposure along Lake Michigan shore near South Haven, Michigan	275
3. Chart showing geologic section and radiocarbon dates from the South Haven site	276
4. Correlation chart of geologic events with forest succession	277
5. Pollen diagram of the South Haven section	278
6. Pollen diagram of the Hartford bog	282

Plate	Facing page
1. Views of the South Haven section	274

TABLES

Table	Page
1. Comparison of Antevs, Flint, and Zumberge-Potzger chronologies	283
2. Pollens of shrubs, trees, and herbaceous plants, and spores of ferns counted at South Haven	284
3. Pollens of shrubs, trees, and herbaceous plants, and spores of ferns, Hartford bog	285
4. Climatic change inferred from forest history in southwestern Michigan	286

* Deceased, September 18, 1955

Introduction

For more than 50 years geologists have been studying the late Pleistocene history of the Lake Michigan basin. From this mass of information a detailed sequence has been deciphered, ranging from the earliest impounding of glacial water (Lake Chicago) to modern Lake Michigan. Fluctuations of the ice front, shifts in outlets, and differential uplift of the land have contributed to the changes in elevation of the water plane during the final wastage and disappearance of the last Wisconsin ice sheet.

One of the more striking later contributions to this history has been discovery of extreme low-water stages. Prior to the recognition of these stages in lake history, geologists assumed that modern Lake Michigan attained its present level through a series of consecutive steplike lowerings (owing to various causes).

This paper presents further evidence in support of these low-water stages of the Lake Michigan basin and integrates the generally accepted chronology into an absolute time scale based on radiocarbon age determinations. A further aim is to correlate climatic changes as indicated by forest succession in southwestern Michigan during late Wisconsin time. Pollen studies by J. E. Potzger have been employed as the basis for this correlation. J. H. Zumberge made the geological investigations and interpretations.

Acknowledgments

During the field investigations, geologists, palynologists, and ecologists visited the exposures near South Haven. Among these were J Harlen Bretz, the late Leland Horberg, Bjorn Andersen, Pierre Dansereau, and Stanley A. Cain. Their discussions at the site and examination of results is greatly appreciated. J Harlen Bretz and the late Leland Horberg read the manuscript and gave the writers valuable criticism.

Appreciation is also expressed to Charles Shinn and William Grable of Larchmoor for their co-operation in providing access to the site itself, and to the Michigan Congregational Christian Conference for hospitality extended and for permission to work on the Pilgrim Haven property. Mr. Harvey Franz of Benton Harbor, Michigan, deserves credit for the initial discovery of the South Haven exposures.

Finally, the authors wish to express their sincere appreciation to the following who provided the C14 dates appearing in this paper: Richard Crane, University of Michigan Phoenix Project Radiocarbon Laboratory; W. F. Libby, University of Chicago Radiocarbon Laboratory; Hans Suess and Meyer Rubin, U. S. Geological Survey Radiocarbon Laboratory, and Wallace Broecker and J. Laurence Kulp, Columbia University Lamont Geological Observatory.

Résumé of the Late Wisconsin History of the Lake Michigan Basin

Previous Work

The framework of the present concept of late Wisconsin history of the Lake Michigan basin had its inception with the report of T. C. Chamberlin in 1877. Since then, additional findings by other workers have added much to the sequence of events. (*See* Taylor, 1894; Leverett, 1899; Alden, 1902; 1906; 1918; J. W. Goldthwait, 1906; 1907; 1908; Leverett and Taylor, 1915; Wright, 1918.) More recent contributions by Stanley (1938), Bretz (1951), and Hough (1952; 1953; 1955) are especially important in that they supply evidence bearing on low-water stages below the present level of Lake Michigan.

Glacial Lake Chicago

The proglacial lake that formed at the southern margin of the retreating Lake Michigan lobe was named Glacial Lake Chicago by Leverett (1897, p. 65). Three stages of this lake are recorded by shore features above the modern lake: the Glenwood stage, 60 feet above the present lake; the Calumet, 40 feet above modern lake level; and the Toleston at 20 feet above the modern water plane. The reasons for the changes in level were discussed by Bretz (1951) and need not be considered here.

The term "Calumet stage" as used in this paper is the same as Bretz's "second attained Calumet level" (Bretz, 1951, p. 427) and Calumet II as used by Hough (1953, p. 99).

Lake Algonquin

Lake Algonquin was the first body of water to occupy the entire Lake Michigan basin. The position of the ice border at the time of the inception of the Algonquin stage is not known, but Hough (1953, p. 101) believes that it was somewhere in the Northern Peninsula of Michigan and that much of the eastern end of Lake Superior was ice-blocked at that time. This would not permit Lake Algonquin to communicate with any part of the Lake Superior basin as supposed by Leverett (1929, p. 65) and Sharp (1953, p. 120). In either interpretation Lake Algonquin ("highest Algonquin" of Stanley, 1936, p. 1954) used the St. Clair-Detroit River and the Des Plaines River outlets. The reconciliation of these two ideas is not critical to this study. Lake Algonquin in the Lake Michigan basin was at about the same elevation as Lake Toleston (605 feet A.T.). The exact relationship of the Toleston stage of Lake Chicago to Lake Algonquin is not completely resolved, although Hough (1953), p. 37) considered that the Toleston stage ended when the Valders ice retreated sufficiently far north to open the Traverse Bay lowland or the Strait of Mackinac. Apparently no appreciable change in level occurred when this event took place

Later "Algonquin" Stages

As shown by Stanley in his work in the Georgian Bay area (1936; 1937), four prominent beaches lie below the highest or main Algonquin beach. Stanley demonstrated that these beaches are essentially parallel to the Algonquin beach and were produced by successively lower elevations of the water surface as lower eastward outlets were uncovered by ice recession. Chapman (1953) disagrees with this interpretation, but, since the present study is concerned primarily with the Lake Michigan basin, the writers can add no new data in support of either interpretation. For the sake of consistency, the four "lower Algonquin" stages (Wyebridge, Penetang, Cedar Point, and Payette in order of decreasing age) are used as originally defined by Stanley and followed by Hough (1953, p. 68–9).

Nipissing Great Lakes

The Nipissing Great Lakes occupied the area now covered by Lakes Superior, Michigan, and Huron. Most of the earlier students of Lake Nipissing considered its level to have been about 15 feet above modern Lake Michigan (Alden, 1918, p. 337; Leverett and Taylor, 1915, p. 449; Tague, 1946, p. 17) or about 595 feet A.T. in the southern Lake Michigan basin, but Hough (1953, p. 89–90) concluded that the Nipissing and Algonquin water planes were both at 605 feet A.T. before upwarping. This difference in interpretation is not critical to this study although the writers prefer Hough's reconstruction of the Algonquin-Nipissing history.

Algoma Great Lakes

Younger beaches 10–15 feet above the present level of Lakes Michigan and Huron were ascribed to the Algoma stage of lake history by Leverett and Taylor (1915, p. 449). Tague (1946, p. 18) followed Leverett and Taylor's interpretation, but Hough's interpretation (1953, p. 92) required all beaches referred to the Nipissing Great Lakes by his predecessors to be of Algoma age.

Low-Water Stages in the Lake Michigan Basin

Into the general scheme of events just outlined, two low-water phases have been injected. At least one lake stage below the Nipissing level was recognized by Alden (1918, p. 332), recorded in buried peat deposits near Sheboygan, Wisconsin. He was not certain, however, when this low-water phase occurred with respect to the other known stages. Baker (1910, p. 715) also noted a buried peat deposit under Calumet beach gravels near Bowmanville, north of Chicago, which he considered evidence for a pre-Calumet low-water stage. However, Leverett (1915, p. 356) did not consider the Bowmanville exposure conclusive in this respect.

Bretz (1951, p. 410), after Baker's interpretation, correlated the Bowmanville lower-water phase with the Two Creeks interstadial. The lowest water level of the Bowmanville stage is unknown, but it must have been lower than the present level of Lake Michigan, and Hough

(1953, p. 34) has suggested that it was at least 100 feet below the present lake level. The Bowmanville-Two Creeks correlation is now a generally accepted part of the "standard" chronology of events and occurs in time between the Glenwood and Calumet stages of Lake Chicago (Bretz, 1951, p. 427).

Stanley (1936; 1937; 1938) postulated a low-water stage in the Lake Huron and Lake Michigan basin between Algonquin and Nipissing time with a connecting channel through the strait of Mackinac. Hough's studies of bottom sediments verified an extreme low-water phase in the Lake Michigan basin (350 feet below present lake level or 230 feet A.T.) which he named Lake Chippewa (Hough, 1952). It fits the "standard" chronology between the Algonquin and Nipissing stages and would occur in time after the Payette stage of Stanley (1936, p. 1948).

FIGURE 1.—INDEX MAP

The major events of the history of the Lake Michigan basin are thus well established, although several details remain to be added. Some of these details are added here.

GEOLOGIC SECTION NEAR SOUTH HAVEN, MICHIGAN

Description

Between May 1952 and June 1954 the writers made several joint visits to an excellent section

PLATE 1.—VIEWS OF THE SOUTH HAVEN SECTION

FIGURE 1.—BURIED SAND DUNE ON LACUSTRINE SANDS
Looking south; *see* Figure 2 D for location; Melhorn (1954, Ph.D. thesis, Univ. Michigan)

FIGURE 2.—BURIED SOIL PROFILE ON LACUSTRINE SANDS WITH AN ORGANIC LAYER HIGHER IN THE SECTION
Looking east; *see* Figure 2 C for location

FIGURE 3.—CLOSE VIEW OF BURIED SOIL PROFILE
Same location as Figure 2

FIGURE 4.—BURIED PEAT LAYER
Looking east; *see* Figure 2 B for location

FIGURE 2

FIGURE 4

FIGURE 1

FIGURE 3

VIEWS OF THE SOUTH HAVEN SECTION

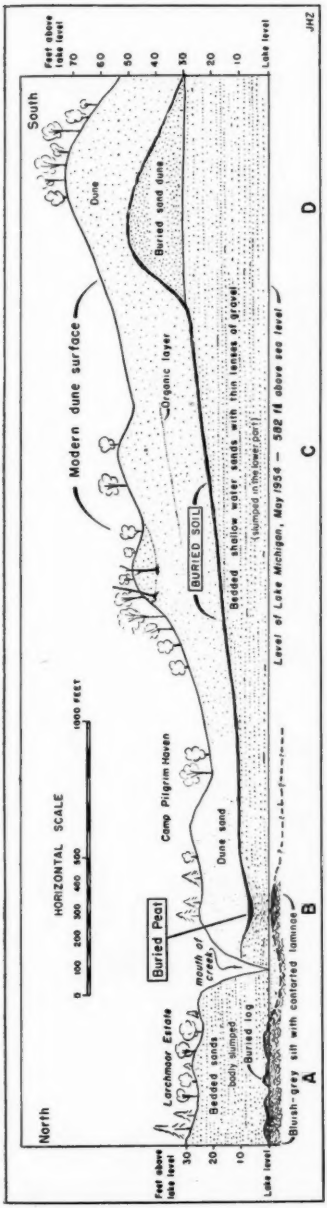

FIGURE 2.—WAVE-CUT CLIFF EXPOSURE ALONG LAKE MICHIGAN SHORE NEAR SOUTH HAVEN, MICHIGAN

near South Haven, Michigan, exposed as a wave-cut cliff along the east shore of Lake Michigan (Fig. 1). The locality lies in SW¼ NE¼ sec. 28, T. 1 S., R. 17 W., Van Buren County, Michigan (South Haven Quadrangle, U. S. Geological Survey). Figure 2 is a diagrammatic cross section showing the major features of the exposure. The vertical scale is exaggerated to emphasize the stratigraphic relationships.

The basal formation consists of a laminated, compact, blue-gray silt. The laminae are contorted and deformed. The base of the silt layer is not exposed anywhere in the area and it presumably lies below the present lake level. It probably rests on till. The top of the silt is irregularly exposed at or near the lake level of May 1952 (approximately 582 feet A.T.). The contact with the overlying deposits is unconformable and is marked in many places by an accumulation of organic material, which ranges in thickness from a few inches (Fig. 2, B) to over a foot (Fig. 2, A). Wood fragments were removed at B (Fig. 2) at the top of the silt layer. The South Haven pollen profile (Fig. 5) begins in this organic layer (Fig. 3) at the 107-inch level.

Unconformably on top of the silt is a unit of bedded littoral sand with fine lenses and stringers of gravel. Medium to coarse sand and fine to medium gravel is characteristic of the formation. At B (Fig. 2) the sands contain thin lenses and streaks of organic matter. These streaks were sampled for pollen and constitute the part of the South Haven pollen profile between the 30-inch and 107-inch levels. The thickness ranges from 8 to 30 feet in half a mile of length. At D (Fig. 2) a sand dune lies above this formation. The contact between the dune and the underlying bedded sands is shown in Figure 1 of Plate 1.

The top of the lacustrine sands is marked by a buried soil zone (Fig. 2). It can be traced continuously from the mouth of the creek near the north end of the section for about 3000 feet south along the exposure. It truncates the bedding of the sands and rises up over the buried sand dune near the south end of the section (Fig. 2; Pl. 1, fig. 1). This buried soil profile is developed in a high-quartz parent material and has a well-developed B horizon (Pl. 1, figs. 2, 3). No trace of calcium carbonate could be

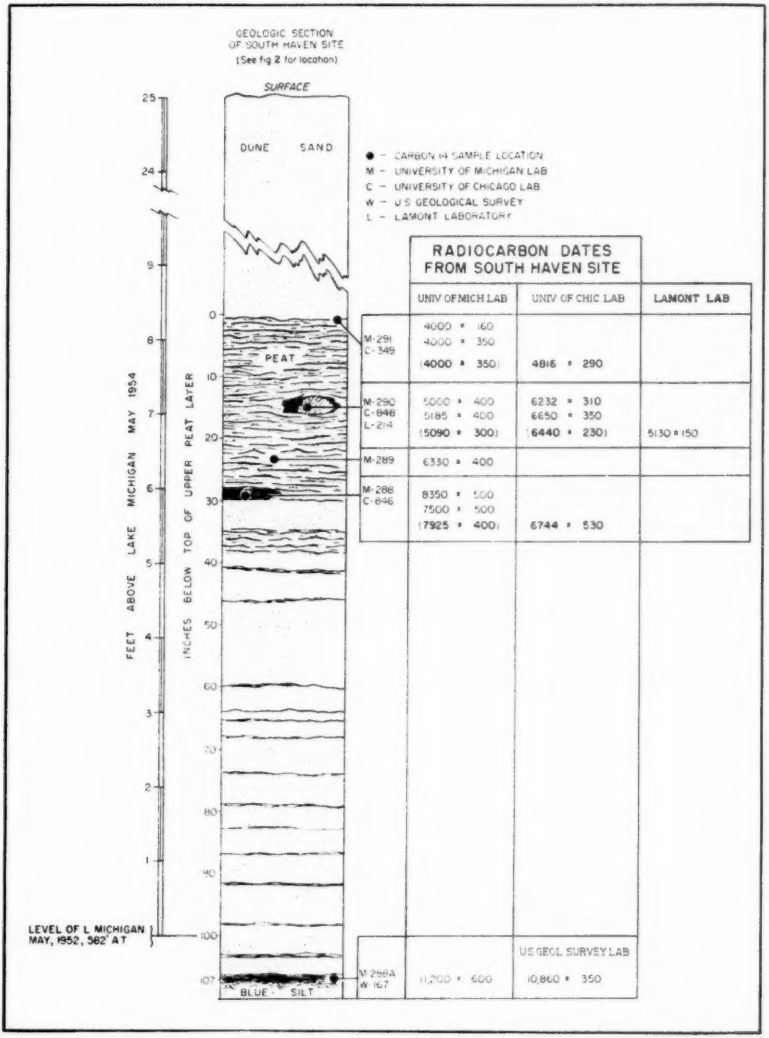

FIGURE 3.—CHART SHOWING GEOLOGIC SECTION AND RADIOCARBON DATES FROM THE SOUTH HAVEN SITE

Figures in brackets are averages where more than one run was made of the same sample.

detected in the sand beneath the B horizon for a depth of more than 10 feet, and it is questionable whether these sands were ever calcareous.

At B (Fig. 2), the buried soil grades laterally into a 30-inch layer of peat containing lenses of iron-stained sand, and wood fragments (Pl. 1, fig. 4). Pollen samples were taken from each inch of peat thickness, and larger samples were selected for radiocarbon determinations (Fig. 3). The peat layer constitutes the upper 30 inches of the South Haven pollen profile (Fig. 5).

The soil zone and peat layer are covered by dune sand containing several discontinuous bands of organic material (Fig. 2; Pl. 1, fig. 2). These bands are similar in gross appearance to the buried soil profile, but differ in that they are not continuous for a distance of more than 400 or 500 feet.

The stratigraphic relationships of the South Haven section provide the basis for the interpretation of geological events of late Wisconsin time.

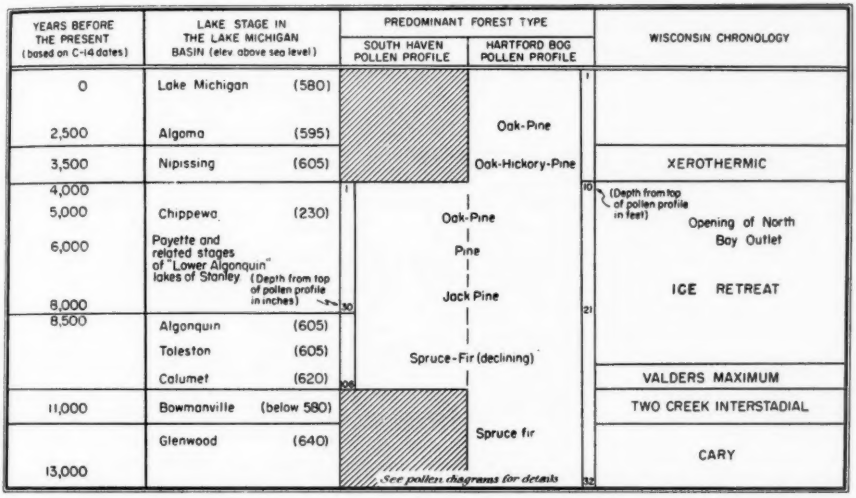

FIGURE 4.—CORRELATION CHART OF GEOLOGIC EVENTS WITH FOREST SUCCESSION

Geologic Interpretation

A cursory examination of Figure 2 reveals two major breaks or discontinuities in the sedimentation record. These are represented by the organic layer on top of the basal silt and the buried soil higher in the section. Both are typical unconformities and record emergence from beneath the water body in the Lake Michigan basin at some time in the past. Both stages required a water plane lower than the present level, and two such periods of low water have already been established in the Lake Michigan area.

If during the Glenwood stage of Glacial Lake Chicago lacustrine silts were deposited in this area, the basal blue-gray silt must be of Glenwood age. The present elevation of the top of these silts is about 580 feet A.T., and the level of the Glenwood water plane was 640 feet A.T.; so these silts accumulated in water 60–70 feet deep.

The contortions of the laminae are difficult to explain. Overriding by glacier ice is a possibility if, as Hough (1953, p. 96) suggested, the Lake Michigan lobe advanced to the position of the Lake Border moraine sometime during Glenwood time. Another possibility is that they represent periglacial involutions associated with the later exposure of the silts to subaerial conditions during the Bowmanville low-water stage. Of the two possible explanations, the former seems more plausible.

The Glenwood silts emerged when the water fell from the Glenwood stage to the Bowmanville low-water stage, thus ushering in Two Creeks time. The unconformity marking the upper limit of the Glenwood lacustrine silts is correlated with the Two Creeks interstadial, and the peat and wood associated with the unconformity must be equivalent in age to the peat at Two Creeks, Wisconsin (Libby, 1952, p. 88). A radiocarbon date of the wood collected at B (Fig. 2), resting on the silts, was reckoned at 11,200 ± 600 years by the University of Michigan Laboratory and 10,860 ± 350 years by the U. S. Geological Survey Laboratory (Fig. 3). This further corroborates the interpretation that the lowermost organic zone is a correlative of the Bowmanville low-water phase of Two Creeks time.

The rise of the waters from the Bowmanville low-water stage to the Calumet stage at 620 feet A.T. submerged the organic material and silts beneath shallow waters of Lake Chicago. Depo-

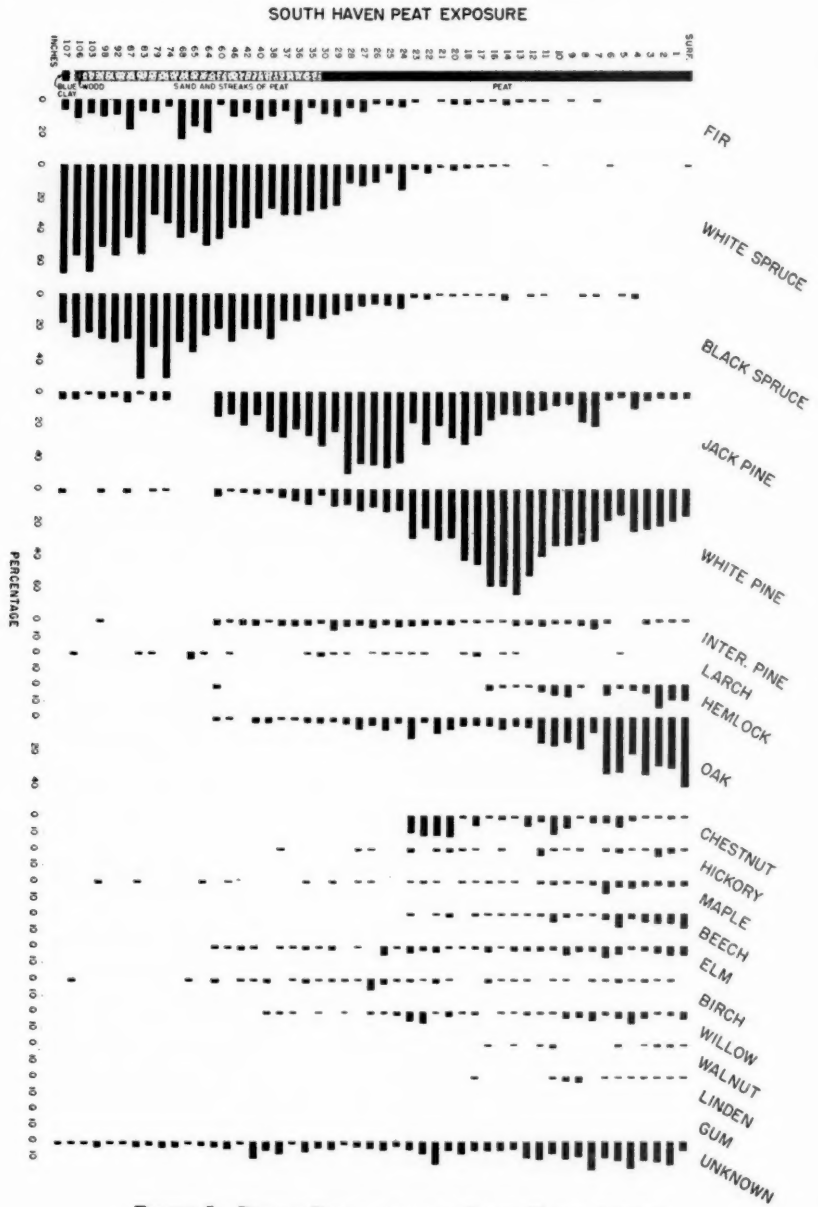

FIGURE 5.—POLLEN DIAGRAM OF THE SOUTH HAVEN SECTION

sition of littoral sands and a few lenses of fine gravel was initiated by this rise to the Calumet stage. At B (Fig. 2), about 6 feet of lacustrine sand accumulated above the basal silt. However, interbedded with the sand are several thin lenses or stringers of organic matter. These organic bands were sampled for pollen grains and represent the 106-inch to 31-inch section of the South Haven pollen profile (Fig. 5).

Deposition of the sand layers alternating

with thin organic layers requires an environment of minimum wave agitation; in this case a protected bay along the shore is most plausible. A spit or barrier beach must have existed lakeward from B (Fig. 2) in order that the sand and organic material could accumulate. The sand may have been inwash from waves breaking over the barrier, or it could have been blown into the protected waters by wind. At any rate, the bedded sands with thin organic layers at B (Fig. 2) represent continuous deposition with no significant breaks until the beginning of peat accumulation. The uniformity of the forest history as shown by the pollen profile (Fig. 5) for this part of the section also favors such an interpretation.

If the interpretation is correct, this part of the section includes all of Calumet, Toleston, and Algonquin time. Because much of the shore area has been eroded by post-Nipissing wave action, and because most of the lower part of the South Haven section is badly slumped, it is impossible to reconstruct the exact shore conditions at this locality during the three stages of lake history mentioned. The Calumet shore lies east of the present shore in the South Haven area, but probably both the Toleston and Algonquin shores once lay west of the present shore. The buried sand dune at D in Figure 2 required a source of sand west of the present shore line.

The waters of Lake Algonquin began to recede when eastern outlets were opened by further recession. Hough (1952; 1953, p. 71) presented clearly defined evidence from bottom cores in Lake Michigan for an extremely low-water stage in the Lake Michigan basin, 350 feet below modern lake level (230 feet A.T.). Hough named it Lake Chippewa, and his reconstruction (1955, p. 966) shows its eastern shore line about 20–25 miles west of South Haven.

Westward recession of the strand line from the South Haven area at the end of Algonquin time eventually stabilized dunes such as the one perched at D (Fig. 2). This stabilization, owing to removal of the source of sand, is indicated by the soil profile and the associated peat now exposed in the South Haven section. Radiocarbon dates from the top and bottom of the peat at B (Fig. 2) indicate a duration of about 4000 years for the peat bog (Fig. 3). This 4000 years includes all of Lake Chippewa time plus most of the time involved in the drop from Algonquin to Chippewa, through the "lower Algonquin" levels, and the rise from Chippewa to Nipissing levels.

Uplift of the North Bay outlet (Hough, 1953, p. 86) re-established the southern outlets and caused the waters to rise from the Chippewa level (230 feet A.T.) to the Nipissing stage (605 feet A.T.). The strand line was thus returned to the South Haven area, and eolian activity was renewed. Sand dunes began covering the soil and peat of the South Haven section before the Nipissing level was fully attained, and continued rise of the water eventually drowned the pre-Nipissing—post-Chippewa dunes. Shore erosion since Nipissing time has destroyed all evidence of the Nipissing beach at the South Haven site, but presumably it existed west of the present shore line.

Modern eolian activity in the area, restricted to the local formation of blowouts and the shifting of sand over dunes previously stabilized by vegetation, accounts for the discontinuous organic bands in the dunes above the buried soil. Lutz (1941) used a similar reasoning in studies of fine-textured material in sand dunes of Cape Cod and Glen Haven, Michigan. The local encroachment of wind-blown sand onto forested parts of near-by dunes is a common phenomenon today along the entire eastern shore of Lake Michigan.

Summary of Geologic Events as Indicated by the South Haven Section

The South Haven section indicates the following events:

(1) Withdrawal of the Lake Michigan lobe from the Valparaiso moraine and formation of basal silts in Lake Chicago during Glenwood time

(2) Possible overriding of the Glenwood silts by readvance of the ice

(3) An extensive retreat of the Lake Michigan lobe, resulting in Bowmanville low-water stage during Two Creeks time. Represented at South Haven by the lower unconformity locally containing wood and peat. Radiocarbon dates of 11,200 ± 600 years (M-288A) and 10,860 ± 350 years (W-167) verify this correlation.

(4) Rise to Calumet level owing to glacial readvance; Valders stage

(5) Continuous sand deposition behind barrier beach at the South Haven site during Calumet, Toleston, and Algonquin time; some dune activity

(6) Ice retreat, exposing eastern outlets and development of the "lower Algonquin" levels. Opening of North Bay outlet culminated in the drop to Lake Chippewa. Soil and peat formed at the South Haven site. Radiocarbon dates at top and bottom of the peat bog indicate a 4000-year time span between beginning of drop to Chippewa level and return to the Nipissing level. Eolian activity was resumed during post-Chippewa–pre-Nipissing interval. The difference in age between Lake Algonquin and Lake Nipissing is thus fixed at 4000 years.

(7) Post-Nipissing time has been one continuous lowering of the lake, but shore erosion during that time has destroyed all evidence of post-Nipissing levels. Dunes are now locally shifting owing to blowouts.

Radiocarbon Chronology

Previous Work

A recent attempt to establish an absolute chronology of late-Wisconsin history in North America (Flint, 1953) was based on radiocarbon dates from the University of Chicago laboratory (Libby, 1952). Strong disagreement with this basic outline skeleton of dates has been expressed by Antevs (1953; 1954; 1955) who builds a geochronology of the "Deglacial" and "Neothermal" ages based essentially on varve analyses correlated with recessional moraines. The chief reason for Antevs' disbelief in radiocarbon dates stems from his insistence that an ice cap disappears chiefly by retreat of the margin. Apparently, he does not consider widespread and almost complete stagnation and catastrophic disintegration *in situ* a valid possibility. For those who accept the radiocarbon dates as essentially correct, the concept of the rate of disappearance of the final shrunken ice sheet must be modified to include the possibility of rapid disintegration in place.

The chronology shown in Figure 4 differs from those proposed by Antevs (1953; 1954) and Flint (1953, Pl. 3). The major difference between the Antevs chronology and the one proposed here is the date of the Valders maximum. The C^{14} date of sample M-288a (Fig. 3) requires a date of slightly less than 11,000 years ago for the Valders maximum, whereas Antevs (1954, p. 520) considers the Valders maximum to have been reached about 19,000 years B.P. Another difference is that Antevs places the Xerothermic period (his Altithermal), which is the age of maximum warmth since retreat of the ice, at 7000–4500 years ago (Antevs, 1952, p. 204), whereas the writers conclude from the South Haven radiocarbon dates correlated with pollen studies that the Xerothermic was not reached until sometime after 4000 years ago and is, in fact, correlative in time with the Nipissing Great Lakes. Finally, for the date of the opening of the North Bay outlet (Mattawa Valley) Antevs (1954, p. 520) has proposed about 13,700 years B.P., but the writers place this event at about 5000–6000 years ago.

The writers' chronology is in disagreement with Flint (1953, Pl. 3) in the age of the Xerothermic. Flint considers the Xerothermic (his Thermal Maximum) to have reached a maximum about 5000 years ago. Under his interpretation, the Xerothermic antedates the Nipissing Great Lakes and had actually ended prior to the low-water stage in the Lake Michigan basin (Lake Chippewa) between Algonquin and Nipissing time (Flint, 1953, p. 911). According to the writers' interpretation the Xerothermic is a correlative of the Nipissing Great Lakes and therefore postdates Lake Chippewa. Table 1 is a comparison of some of the Antevs and Flint dates with the ones proposed by the writers.

Discussion of South Haven Radiocarbon Dates

Without the stratigraphic information necessary for reconstructing geologic history, C^{14} determinations are obviously meaningless. Furthermore, geologist must not depend upon C^{14} dates that are obviously anomalous.

The writers present in Figure 3 a comparison of several radiocarbon dates determined by three different laboratories. These are among the first dates published from the University of Michigan laboratory and represent the first instance in which a cross check on dates for such a large series of samples has been made. None of the three laboratories had knowledge of the dates determined by the others until after all

dates were completed. Each laboratory used a different method of age determination; Michigan and Lamont used carbon dioxide gas, Chicago used carbon black, and the Washington laboratory used acetylene.

The agreement in order of magnitude of the various dates as well as the consistency of results in terms of the geologic section is striking. In each case, a single sample was divided into equal portions and sent to the various laboratories. In the case of sample M-290 (C-848, L-214), a piece of buried log was split into several samples so that the radiocarbon dates shown in Figure 3 are all based on the *same piece of wood*. The writers had hoped for a three-way check on all samples, but, because the U. S. Geological Survey laboratory was not in operation during the early part of this study, and because all the laboratories were extremely busy with a tremendous back log of samples, only a two-way check for each sample was possible.

The writers believe that the objective approach to the radiocarbon dates as presented in this paper provides a sound basis for the evaluation of the process in general. Most geologists are not qualified to judge the methods and theories involved in the radiocarbon-dating procedure, but as geologists we can attest to the reasonableness of the dates insofar as they are in accordance with sound stratigraphic interpretation. The South Haven dates seem to fulfill this requirement.

Pollen Studies of the South Haven and Hartford Sites

Introduction

Pollen analysis has established itself as a valuable tool for the study of forest history with inferred climatic changes during late Pleistocene time. Most pollen data are collected from borings in peat bogs where there is little or no stratigraphic information that can be the basis for geologic interpretation. It was thus a rare opportunity to find a buried layer of peat (Fig. 2 B) exposed in cross section on a vertical cut, permitting easy and accurate sampling at inch intervals. The particular value of the South Haven pollen profile, however, is the fact that the South Haven peat could be related to the late Pleistocene history of the Lake Michigan basin. In addition, because of the excellent exposure, several samples of peat could be easily and accurately obtained for radiocarbon analyses.

As a check on the South Haven profile, which was truncated both at the top and bottom, a deep bog was bored 15 miles inland from the South Haven site near Hartford, Michigan (about 660 feet A.T.), well above levels of the water bodies formerly occupying the Lake Michigan basin.

Methods of Collecting and Preparing Samples for Pollen Analysis

A yard stick was placed vertically against the exposed peat; a pocket knife cut a clean surface and took samples at 1-inch intervals for the total depth of 30 inches. The samples were placed in waxed paper accurately marked for level and later transferred to small vials and securely stoppered. Samples were taken of organic streaks contained in sand beneath the peat for 75 inches, giving a total pollen profile of 106 inches (Fig. 5). A sample was also taken of the buried soil associated with the peat.

A deep bog on the farm of Mr. Clair Lamb, here called the Hartford bog, which probably represents the filling of a kettle lake in the Valparaiso ground morainic upland southeast of South Haven (Fig. 1), was sampled in April 1954. The boring was made with a Hiller borer to a depth of 32 feet. Samples were taken at 6-inch intervals and placed in stoppered glass vials. The bottom 8 feet of the boring was through rock flour. Further penetration of the rock flour was discontinued because of the danger of twisting off the sampler.

Because the peat from the South Haven and Hartford sites separated readily, the Geisler (1935) alcohol method was used to prepare the pollen slides. In a few instances the separation was in hot alcohol. Gentian violet stained the pollen grains which stood out prominently from the particles of other organic substances, and thus could be easily and accurately counted. Except for a few foot levels of the Hartford bog and some of the organic streaks in the sand underlying the South Haven peat where counts of 100 pollen grains were made, at least 150

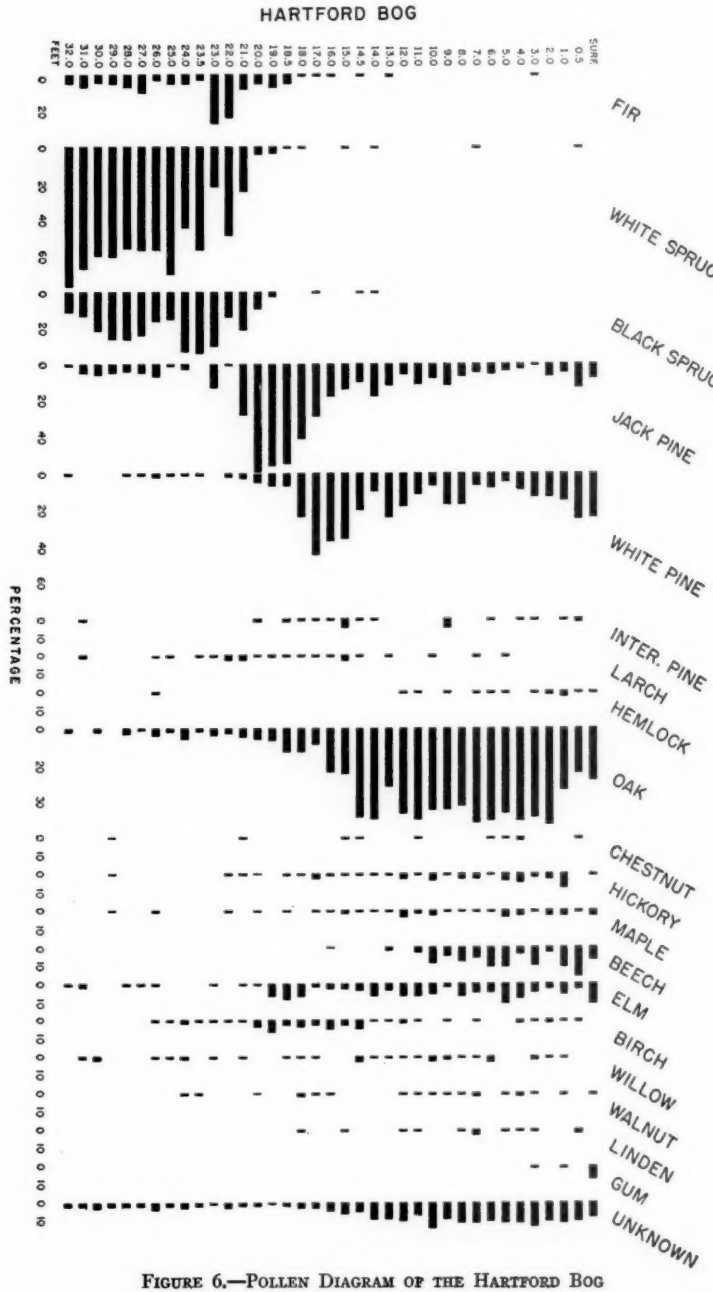

FIGURE 6.—POLLEN DIAGRAM OF THE HARTFORD BOG

pollens of trees were tabulated at each level. For the South Haven peat, a count of 200 was made at almost all the inch levels. The two pollen profiles are shown in Figures 5 and 6. Pollen representation of shrubs, herbaceous plants, and ferns at the two stations is shown in Tables 2 and 3.

Pollen Profiles

The lower 42 inches of sand of the South Haven profile (Fig. 5) was deposited during a decided spruce-fir period (up to 94 per cent). Between the lower 42 inches and the base of the peat (the 68-inch to 30-inch level) spruce-fir shows a steady decline, with a corresponding increase in jack pine.

The 30 inches of peat represent 4000 years according to C^{14} dates (Fig. 3) and record at least five or six major forest changes. Successions are from spruce-fir to jack pine to white-red pine to oak to oak-hemlock-broad-leaved forest. Spruce and fir almost disappeared during the pine period. No evidence of pronounced tundra is indicated in either profile. During the final stages of the growth of the South Haven peat, paludification expanded the bog area into an extensive wet meadow that can be correlated with the buried soil for a considerable distance along the exposure (Fig. 2). The pollen records of the soil horizon closely resemble those of the 2- to 3-inch levels of the South Haven profile.

Shrubs of greatest significance in the South Haven profile are alder (*Alnus*) and hazelnut (*Corylus*). Grasses have the highest representation from the 21-inch to the surface levels, and spores of ferns in places reached numbers equal to those of total tree pollens (Table 2).

The Hartford bog is completely enclosed (verlandet) and now has a dense growth of blueberries with scattered white pine and broad-leaved trees. The Hartford pollen profile (Fig. 6) no doubt records forest changes during much of post-Cary time. Although the forest succession at the Hartford bog is similar to the one indicated by the South Haven profile, hemlock is much less abundant in upper levels, and a prominent pine peak becomes evident in the closing foot levels. Apparently the South Haven peat layer (1-inch to 30-inch level) is the correlative of the 21-foot to 10-foot levels of the Hartford bog.

Radiocarbon dates of the South Haven peat (Fig. 3) permit the following correlation of forest change with time: close of the spruce-fir period (beginning of peat formation at South Haven), about 8000 years ago; jack pine period, about 7000 years ago; white-red pine period, 6000 years ago; oak-pine period, 5000 years ago; oak-hemlock, broad-leaved forest, 4000 years ago.

TABLE 1.—COMPARISON OF THE ANTEVS, FLINT, AND ZUMBERGE-POTZGER CHRONOLOGIES

All dates are in years before the present.

Event	Antevs (1953; 1954)	Flint (1953)	Zumberge-Potzger
Xerothermic	4500–7000	5000	3500–4000
Two Creeks	19,000	11,000	11,000

By correlating the truncated South Haven profile with the Hartford profile, it follows that the Xerothermic (climatic optimum) reached its maximum development after the cessation of peat deposition at the South Haven site, 4000 years ago. This is indicated by the 9- to 2-foot levels of the Hartford profile. Since the end of the Xerothermic, an increase in pine at the Hartford site (0- to 2-foot levels) suggests climatic deterioration.

Discussion

The physical features of the Hartford bog suggest continuous deposition since the time the meltwaters from near-by glaciers poured rock flour into the depression, while pioneer forests of spruce and some fir added pollen to the inorganic sediments. This early forest (lowermost 9 feet of the Hartford profile) must have been a strikingly simple association, because not even jack pine participated in the crown cover. In this respect the forest history differs greatly from that of lower Quebec, as described by Potzger (1953), and from that of the Laurentian highland regions of central Quebec as Potzger and Courtemanche (1954) found in a recent study. If jack pine is, indeed, so extremely overrepresented by pollen as it usually seems to be, then the Hartford moraines

TABLE 2.—POLLENS OF SHRUBS, TREES, AND HERBACEOUS PLANTS AND SPORES OF FERNS COUNTED AT SOUTH HAVEN

Depth in inches	No. of tree pollens	Alder	Dwarf birch	Hazelnut	Deciduous holly	Grasses	Sedges	Chenopods	Composites	Water lily	Cattail	Shield fern	Club mosses	Osmunda ferns	Sphagnum	Fern spores
Surface	185	2	..	2	2	10	..	..	..	..	..	..	..	..	..	..
1	200	1	..	..	3	14	4	..	4	4	2	..	..	1	..	7
2	175	..	..	..	1	8	1	1	6	7	6	2	..	1	..	3
3	200	..	..	1	3	12	..	1	5	8	7	5	..	1	..	15
4	150	..	..	1	1	30	2	..	5	17	8	10	..	90	..	24
5	200	..	1	..	1	28	2	1	4	..	4	6	..	1	..	8
6	200	..	..	3	3	17	7	..	4	13	5	4	..	4	..	15
7	150	1	..	..	..	33	..	..	4	1	..	22	..	17	..	47
8	150	3	..	1	..	14	..	2	4	2	..	8	..	4	..	31
9	195	..	..	..	2	25	3	..	5	2	5	11	..	7	..	60
10	150	4	1	1	6	13	1	..	1	1	2	19	..	..	..	26
11	200	1	..	..	3	21	2	..	2	..	3	16	..	6	..	43
12	200	..	..	..	..	17	1	..	4	..	..	23	..	4	..	102
13	200	4	..	..	..	19	..	3	..	1	..	127	..	2	..	23
14	200	4	..	..	..	22	1	1	1	..	..	15	..	8	..	1
16	150	2	..	..	..	11	1	..	1	..	1	11	..	5	..	19
17	200	4	..	..	..	10	1	..	1	1	..	20	..	..	..	13
18	150	2	..	1	..	4	1	..	1	..	..	19	1	..	..	10
20	200	5	1	1	..	10	..	..	1	..	..	14	..	..	..	13
21	200	7	..	2	..	16	1	..	4	1	..	20	..	1	..	5
22	200	5	..	1	..	9	..	..	1	..	2	11	..	1	..	6
23	200	1	..	1	1	4	..	..	2	..	4	13	..	..	..	11
24	200	4	1	..	..	3	..	..	..	1	2	..	..	..	..	..
25	200	10	..	4	..	9	..	..	..	..	..	31	..	..	..	3
26	200	11	..	2	..	4	1	1	2	..	1	..	1	..	..	..
27	200	2	..	..	..	4	..	1	..	1	..	..	..	..	..	1
28	200	1	..	1	..	7	..	..	..	..	1	..	..	..	..	..
29	200	3	..	1	..	14	1	..	2	1	..	..	..	..	..	..
30	200	2	..	..	..	13	..	..	3	1	..	..	..	..	..	..
35	150	..	..	..	..	12	..	..	2	..	..	..	..	..	..	2
36	200	3	1	1	..	6	2	1	..	2	..	1	..	..	..	2
37	150	2	..	1	..	4	..	2	..	..	..	..	..	..	..	..
38	150	..	..	1	..	16	2	..	1	..	..	..	..	..	..	..
40	150	2	..	3	..	24	1	1	3	1	..	..	..	..	..	1
42	150	1	..	..	..	7	3	..	1	..	..	..	1	..	..	..
46	200	..	..	1	..	10	1	1	3	..	..	..	..	..	..	1
60	150	4	..	1	..	5	1	..	..	..	..	1	..	..	..	..
64	150	1	..	..	..	3	..	..	..	..	..	..	..	..	..	..
74	100	1	..	..	..	4	..	..	..	..	..	1	..	..	..	..
79	125	..	..	..	..	4	1	..	..	..	..	..	..	..	..	..
82	150	..	..	1	..	4	..	..	..	..	..	..	..	..	..	..
98	150	..	..	..	..	4	1	..	1	..	..	..	..	..	..	..
107 (clay)	150	..	..	..	..	5	1	..	3	..	..	..	..	..	..	..
Soil horizon	150	5	1	2	..	60	1	..	8	..	..	14	..	..	1	14

TABLE 3.—POLLENS OF SHRUBS, TREES, AND HERBACEOUS PLANTS, AND SPORES OF FERNS, HARTFORD BOG

Depth in feet	No. of tree pollens	Alder	Dwarf birch	Hazelnut	Ericads	Deciduous holly	Grasses	Sedges	Chenopods	Composites	Water lily	Cattail	Shield fern	Club mosses	Osmudna ferns	Sphagnum	Spores
Surface	100	1	..	..	7	..	6	..	..	52	..	..	1	..	..	..	6
6-inch	150	1	..	..	8	2	27	..	1	..	..	..	7	..	..	18	1
1	150	1	..	1	19	..	23	..	1	..	..	..	1	..	..	16	2
2	150	..	..	1	24	..	2	..	..	2	..	..	..	..	..	79	..
3	150	..	..	..	12	1	9	..	..	2	..	..	..	..	..	21	1
4	150	..	..	1	53	..	20	1	..	5	..	2	..	2	..	64	3
5	150	3	..	3	..	..	16	1	..	7	..	1	2	..	..	99	4
6	150	2	1	..	2	1	5	1	..	5	..	..	..	..	..	7	4
7	150	1	..	..	1	..	8	1	1	7	..	..	1	..	1	..	1
8	150	1	..	2	7	..	17	3	1	3	1	..	11	..	1	..	12
9	150	..	..	..	2	..	9	2	..	4	..	..	19	..	1	2	3
10	150	2	..	..	1	..	15	..	1	1	..	..	7	..	..	4	3
11	175	3	2	2	..	..	26	..	..	4	..	1	1	..	2	2	1
12	150	2	..	1	..	..	12	1	1	5	..	1	13	..	..	2	4
13	150	..	1	..	3	..	10	..	..	1	..	1	1	1	1	11	4
14	150	..	..	..	2	..	8	..	..	..	..	..	..	..	..	..	..
14.5	150	..	..	..	2	..	4	..	..	3	..	..	..	..	..	..	..
15	150	..	..	..	5	..	5	..	..	..	..	..	4	..	..	..	..
16	200	..	..	..	3	..	4	..	..	..	..	..	..	..	..	..	..
17	150	..	..	..	..	..	10	..	..	..	..	..	..	..	..	..	..
18	150	4	..	..	..	..	4	..	..	..	..	..	..	..	..	..	..
18.5	150	1	..	..	..	..	3	..	..	..	..	..	..	..	..	..	..
19	150	3	..	..	..	..	4	..	..	..	..	..	..	..	..	..	..
20	200	2	..	..	..	..	5	..	..	..	..	..	..	..	..	..	..
21	150	2	..	..	..	..	3	..	..	..	..	..	..	..	..	..	..
22	150	..	..	..	..	..	2	..	..	..	..	..	..	..	..	..	..
23	150	..	..	..	..	..	3	..	..	..	..	..	..	..	..	..	..
23.5	150	..	..	..	..	..	2	..	..	..	..	..	..	..	..	..	..
24	150	..	..	..	..	..	8	..	..	..	..	..	..	..	..	..	..
25	150	..	..	..	..	..	2	..	..	..	..	..	..	..	..	..	..
26	125	..	..	..	..	..	6	..	..	..	..	..	..	..	..	..	..
27	150	..	..	..	..	..	1	..	..	..	..	..	..	..	..	..	..
28	150	..	..	..	..	..	8	..	..	..	..	..	..	..	..	..	..
29	140	..	..	..	..	..	1	..	..	..	..	..	..	..	..	..	..
30	140	..	..	..	..	..	5	..	..	..	..	..	..	..	..	..	..
31	150	..	..	..	..	..	3	..	..	..	..	..	..	..	..	..	..
32	150	..	..	..	..	..	2	..	..	..	..	..	..	..	..	..	..

must have had only a few scattered individual trees. Moreover, it is therefore even more striking that at the 20- to 18-foot levels of the Hartford profile, and at the 28- to 24-inch levels of the South Haven peat, jack pine indicates a decided control of the forest. In a recent airplane trip into the Quebec tundra, Potzger saw thousands of square miles where jack pine constituted at least 75 per cent of the forest cover. One might therefore readily assume that southwestern Michigan must have had a similar forest cover 7000 years ago.

The forest history gives no indication of great climatic fluctuations. Just what the climatic significance of the double peaks for chestnut-oak and the lesser two hemlock peaks in the South Haven profile is cannot be conclusively inferred. It is also questionable whether the decline of jack pine and the accompanying increase of fir at the 22-foot level in

the Hartford profile is significant in terms of climatic deterioration. Another possible indication of slight climatic deterioration can be read into the decline of oak and increase in pine for the upper 2 feet of the Hartford profile.

The location of the Hartford bog between the Valparaiso and Lake Border moraines (Leverett and Taylor, 1915, Pl. VII) makes it possible for deposition to have started in this basin after the ice retreated from the Valparaiso position. Indeed, it appears that the rock flour underlying the peat in the Hartford bog represents deposition while the ice front was not far away, perhaps at the Lake Border position. At any rate, it is safe to infer that pollen rain began in the Hartford bog sometime during the early retreat of Cary ice (Lake Michigan Lobe) and has continued ever since.

Therefore, the Hartford pollen profile readily indicates forest changes during deteriorating climate which theoretically ushered in Valders time. While there is a marked increase of fir and black spruce with decline of jack pine at the 23- to 22-foot levels, there is no replacement between coniferous and broad-leaved genera, nor is there replacement of pine by spruce-fir over several sampling levels. However, deteriorating climate can well be read into the forest change just referred to, for then as now in northern Quebec the forest belts must have been wide in latitudinal extent.

A similar situation is evident in pollen profiles from Tazewell and Cary regions in Indiana (Potzger, 1946). In bogs from areas where the surface drift is Tazewell, no replacement occurs between broad-leaved and coniferous genera to mark initiation of Cary time, nor is there anything in the profile to indicate a warming of the climate during the Tazewell-Cary interstadial. The profiles show one continuous prominent spruce-fir period, and this is consistently spread over more foot levels in the Tazewell than in Cary regions. This raises the question as to how far northward ice had retreated during interstadial periods. If the South Haven profile began in Valders or early post-Valders time and the Hartford bog in early post-Cary time, climate could not have moderated greatly during the Two Creeks interstadial as expressed by the high spruce-fir abundance in lower levels at both stations.

According to Suess (1954) radiocarbon dates from deposits in Steuben County, Indiana, interpreted as late Cary by W. J. Wayne of the Indiana Geological Survey, permit a late Cary date of 12,000–13,000 years before the present. This allows only 1000–2000 years for the ice margin to melt back and readvance to the Valders position (Fig. 4) and thus supports the idea that some of the glacial substages developed without causing pronounced changes in forest cover.

TABLE 4.—CLIMATIC CHANGE INFERRED FROM FOREST HISTORY IN SOUTHWESTERN MICHIGAN

Years before present	Forest cover	Climate
	Oak-pine	Deterioration
3500–4000	Expanding oak-hemlock-broadleaved forest	Warmest and driest since retreat of ice
5000	Decline of pine period and ascendency of oak and chestnut	Continued warming
6000	Pine maximum, near elimination of spruce and fir	Warming climate
8000	Decline of spruce-fir, increase of pine	Moderating climate
11000	Spruce-fir	Cool to cold, moist

Summary of Pollen Studies at South Haven and Hartford Bog

(1) The South Haven forest succession appears to have continued uninterruptedly from Bowmanville-Two Creeks time until deposition of peat was abruptly ended by eolian activity just before the beginning of Nipissing time. Seventy-five inches of sand within thin organic bands beneath the 30-inch peat layer accumulated during a prominent spruce-fir period. The sand represents lacustrine deposition in the shallow waters of the Calumet and Toleston stages of Lake Chicago, and in Lake Algonquin The 30-inch peat layer represents 4000 years of forest history beginning with the close of the spruce-fir period and ending with the beginning of the Climatic Optimum (Xerothermic), or oak-pine-broad-leaved forest.

(2) The correlation of geologic events with the forest changes in the South Haven latitude

is given in Figure 4. Inference of climatic changes from forest history correlated with time is shown in Table 4.

(3) The Hartford bog records continuous deposition since Cary ice retreated from the Valparaiso moraine in southwestern Michigan. The 32- to 22-foot levels show a spruce-fir maximum comparable to the 75 inches of sand (106- to 31-inch levels) in the South Haven profile. The slight decline of spruce with increase of jack pine at the 23-foot level of the Hartford profile, followed by a decided decrease of jack pine and increase of fir at the 22-foot level, may indicate initiation of Valders time, although this cannot be definitely stated. The 21- to 10-foot levels of the Hartford profile are correlated with the 30-inch peat layer at South Haven. The forest history is similar except that hemlock and chestnut are less important in the Hartford forest association. This could be due to local differences in soil factors.

(4) Development of the Xerothermic (climatic optimum) at the Hartford bog (9- to 2-foot levels), and later deterioration of climate (increase of pine) are events of the last 4000 years of this latitude.

References Cited

Alden, W. C., 1902, Description of the Chicago district: U. S. Geol. Survey Geol. Atlas, Chicago folio no. 81, 14 p.

—— 1906, Description of the Milwaukee quadrangle, Wisconsin: U. S. Geol. Survey Geol. Atlas, Milwaukee folio no. 140, 12 p.

—— 1918, The Quaternary geology of southeastern Wisconsin: U. S. Geol. Survey Prof. Paper 106, 356 p.

Antevs, Ernst, 1953, Geochronology of the deglacial and neothermal ages: Jour. Geology, v. 61, p. 195–230

—— 1954, Geochronology of the deglacial and neothermal ages: a reply: Jour. Geology, v. 62, p. 516–520

—— 1955, Varve and radiocarbon chronologies appraised by pollen data: Jour. Geology, v. 63, p. 495–499

Baker, F. C., 1910, Preliminary note on the life of Glacial Lake Chicago: Science, n. ser., v. 31, p. 715

Bretz, J H., 1951, The stages of Lake Chicago: their causes and correlation: Am. Jour. Sci., v. 249, p. 401–429.

Chamberlin, T. C., 1877, Geology of Wisconsin: Survey of 1873–77, v. 2, p. 219–228.

Chapman, L. J., 1953, Outlet of Lake Algonquin at Fossmill, Ontario, Canada (Abstract): Geol. Soc. America Bull., v. 64, p. 1407

Flint, R. F., 1953, Probable Wisconsin substages and late Wisconsin events in northeastern United States and southeastern Canada: Geol. Soc. America Bull., v. 64, p. 897–919

Geisler, Florence, 1935, A new method of separating fossil pollen from peat: Butler Univ. Bot. Studies, v. 3, p. 140–141

Goldthwait, J. W., 1906, Correlation of the raised beaches on the west side of Lake Michigan: Jour. Geology, v. 14, p. 411–424

—— 1907, The abandoned shorelines of eastern Wisconsin: Wis. Geol. Nat. History Survey, sci. ser., Bull. 17, 134 p.

—— 1908, A reconstruction of water planes of the extinct glacial lakes in the Michigan Basin: Jour. Geology, v. 16, p. 459–476

Hough, J. L., 1952, Postglacial low-water stage of Lake Michigan indicated by bottom sediments (Abstract): Geol. Soc. America Bull., v. 63, p. 1265.

—— 1953, Pleistocene chronology of the Great Lakes region: mimeographed report, Urbana, Illinois, Office of Naval Research, Contract No. NGori-07133, Project NR-018-122.

——1955, Lake Chippewa, a low stage of Lake Michigan indicated by bottom sediments: Geol. Soc. America Bull., v. 66, p. 957–968.

Leverett, Frank, 1897, The Pleistocene features and deposits of the Chicago area: Chicago Acad. Sci. Bull. 2, 86 p.

—— 1899, The Illinois glacial lobe: U. S. Geol. Survey Mon. 38, 817 p.

—— 1929, Moraines and shorelines of the Lake Superior region: U. S. Geol. Survey Prof. Paper 154, p. 1–72.

Leverett, Frank, and Taylor, F. B., 1915, The Pleistocene of Indiana and Michigan and the history of the Great Lakes: U. S. Geol. Survey Mon. 53, p. 316–518.

Libby, W. F., 1952, Radiocarbon dating: Chicago, Univ. Chicago Press, 124 p.

Lutz, H. J., 1941, The nature and origin of layers of fine-textured material in sand dunes: Jour. Sed. Petrology, v. 11, p. 105–123

Potzger, J. E., 1946, Phytosociology of the primeval forest in central-northern Wisconsin and upper Michigan, and a brief post-glacial history of the lake forest formation: Ecol. Mon., v. 16, p. 211–250

—— 1953, Nineteen bogs from southern Quebec: Canad. Jour. Botany, v. 31, p. 383–401

Potzger, J. E., and Courtemanche, Albert, 1954, Bog and lake studies on the Laurentian shield in Mont Tremblant Park, Quebec: Canad. Jour. Botany, v. 32, p. 549–560

Sharp, R. P., 1953, Shorelines of the glacial Great Lakes in Cook County, Minnesota: Am. Jour. Sci., v. 251, p. 109–139

Stanley, George, 1936, Lower Algonquin beaches of Penetanguishene Peninsula: Geol. Soc. Soc. America Bull., v. 47, p. 1933–1955.

—— 1937, Lower Algonquin beaches of Cape Rich, Georgian Bay: Geol. Soc. America Bull., v. 48, p. 1665–1686

—— 1938, The submerged valley through Mackinac Straits: Jour. Geology, v. 46, p. 966–974

Suess, H. F., 1954, U. S. Geological Survey radiocarbon dates I: Science, v. 120, p. 467–473

Tague, G. C., 1946, The post-glacial geology of the Grand Marais embayment in Berrien County, Michigan: *In* Occasional papers for 1946 on the geology of Michigan, Mich. Dept. Conservation, Pub. 45, Geol. ser. 38, p. 82

Taylor, Frank, 1894, A reconnaissance of the ancient

shorelines of Green Bay: Am. Geologist, v. 8, p. 315–327

Thwaites, F. T., 1943, Pleistocene of part of northeastern Wisconsin: Geol. Soc. America Bull., v. 54, p. 87–144

Wilson, L. R., 1932, The Two Creeks forest bed, Manitowoc County, Wisconsin: Wis. Acad. Sci. Trans., v. 27, p. 31–46

Wright, G. F., 1918, Explanation of the abandoned beaches about the south end of Lake Michigan: Geol. Soc. America Bull., v. 29, p. 235–244

Department of Geology, University of Michigan, Ann Arbor, Mich.

Manuscript Received by the Secretary of the Society, March 2, 1955

BULLETIN OF THE GEOLOGICAL SOCIETY OF AMERICA
VOL. 67, PP. 289-300, 10 FIGS. MARCH 1956

STRUCTURE OF LOPOLITHS

BY H. D. B. WILSON

ABSTRACT

Field studies of five large differentiated lopolithic intrusions show that they possess many similar features. The bottoms of the intrusions are not parallel to the layering but in general dip more steeply toward the center. The bottoms of the intrusions are irregular and may deepen or shallow abruptly as much as several thousand feet. Any particular section of a lopolith reveals only a portion of the layers so that the average composition cannot be determined from outcrops. Corresponding patterns may be found in the layering of the Sudbury, Bushveld, and Great Dyke intrusions.

The lopoliths are interpreted as funnel-shaped in cross section with the most basic rocks in the lower portion of the funnel. The upper portion of the lopoliths may be similar to some batholithic granites, and the overlying roof rocks display mountain-folded structures in contrast to the gently warped underlying formations.

CONTENTS

TEXT

	Page
Introduction	289
Acknowledgments	289
Insizwa intrusion	290
Bushveld complex	290
Kungwe Bay lopolith	292
Great Dyke	293
Sudbury intrusion	296
Sudbury lopolith and the Sudbury breccia	297
Sudbury breccia	298
Granite portion of lopoliths	299
References cited	300

ILLUSTRATIONS

Figure		Page
1.	Insizwa intrusion	290
2.	Bushveld igneous complex	291
3.	Columnar sections of the Bushveld complex	292
4.	Kungwe Bay lopolith, Tanganyika	293
5.	Geology of part of the Great Dyke, Southern Rhodesia	294
6.	Cross sections of the Great Dyke	295
7.	Composite section of the Great Dyke	295
8.	The Sudbury lopolith	296
9.	Columnar sections of the Sudbury lopolith	297
10.	Diagrammatic cross section of the Sudbury lopolith from Levack to Gertrude	297

INTRODUCTION

Field studies of the Insizwa intrusion and the Bushveld complex in South Africa, the Great Dyke in Southern Rhodesia, the Kungwe Bay intrusion in Tanganyika, and the Sudbury intrusion in Canada have shown that the intrusions have many similar characteristics that suggest a well-defined structural type. The intrusions are called lopoliths in this paper although they do not fit Grout's (1948, p. 518) definition exactly. They are all centrally depressed, and the upper surfaces and the layering are basinlike. However, the intrusions are more funnel-shaped than lenslike, and they are concordant only in some places.

The layered structure in many lopoliths such as the Bushveld and Insizwa intrusions is parallel to the bedding of the country rocks below. Other lopoliths such as the Great Dyke and the Sudbury lopoliths intrude Precambrian complexes, and the banding may form a shallow basin structure as in the Great Dyke, or a slightly steeper basin structure as at Sudbury. The lower contact of all these lopoliths, however, is not parallel to the layering of the intrusion, nor is it in all cases concordant with the bedding of the underlying country rocks.

ACKNOWLEDGMENTS

The author is indebted to Dr. G. H. Charlewood, chief geologist of the Manitoba Mines Branch, and Dr. G. M. Brownell of the Uni-

versity of Manitoba for critical reading of the manuscript.

Insizwa Intrusion

Along the southeast and eastern edge of the Insizwa intrusion the lower contact of the intrusion is between norite and hornfels at some places, and between picrite and hornfels at others. In some canyons (Fig. 1) the norite forms a layer above the picrite. The dip of the norite-picrite contact is similar to that of the sediments, but the base of the intrusion dips more steeply than the sediments. The actual contact of the base is rarely seen in surface outcrops because of overburden, although in limited exposures it appears vertical in some places and almost horizontal in others. The contact is well exposed in the mine workings at Waterfall gorge. Outward from the center the intrusion continually steps upward in the thinly bedded sedimentary series. Individual steps range from a few inches to 10 feet. The dip of the sediments and the banding of the intrusion near Waterfall gorge is from 5° to 10°. The average dip of the lower contact of the intrusion obtained from many observations in winzes is approximately 30°. This dip is confirmed by a deep drill hole farther up Waterfall gorge. This hole intersected the contact of the intrusion about 1000 feet vertically below the level of the mine openings.

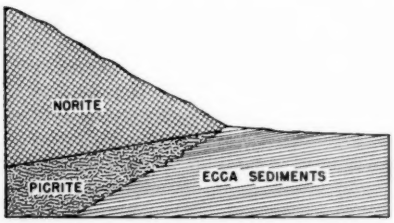

Figure 1.—Insizwa Intrusion
Diagrammatic section showing the relationship of the norite-picrite-Ecca sedimentary series; east side of Insizwa mountain, looking north

The lower contact of the intrusion, therefore, dips more steeply than both the layering and the enclosing sediments. The intrusion is not a sill, and the type of intrusive rock to be seen in contact with the foot-wall sedimentary rocks depends upon the depth to which the contact has been exposed by eorsion.

Bushveld Complex

Contact details are not so clear for the larger Bushveld complex because mine workings do not exist on the lower contact, and outcrops of the contact are rare. The Bushveld complex (Fig. 2) has the shape of an elongated basin which has been tilted downward to the east, so that the bottom of the basin is exposed at the west end of the intrusion, while the outcrop on the north and south sides, and to a lesser extent the east end, represents positions well up on the flanks of the basin.

Hall's (1932, p. 259) "norite" portion of the intrusion includes: (1) the massive, almost uniformly noritic and gabbroic basic rocks that occur in the Main and Upper zones between the Merensky horizon and the overlying granite, and (2) the banded or layered ultrabasic rocks of the Transition and Critical zones below the Merensky horizon. The Merensky horizon is not the actual boundary between the basic and ultrabasic portions, but it occurs near the top of the ultrabasic rocks and can be mapped as a consistent marker. Layered noritic and anorthositic rocks occur with the pyroxenites and peridotites of the ultrabasic zone, but all plagioclase feldspar in the ultrabasic zone is either anorthite or bytownite in contrast to the labradorite of the basic-zone norite.

Only ultrabasic rocks occur in the bottom of the trough of the basin (Fig. 2). Their thickness is very great; Hall (1932, p. 268) has estimated 15,100 feet from surface outcrops near Vlakfontein. A drill hole at Vlakfontein 3100 feet deep shows that the intrusion is actually much deeper than Hall calculated from the dip of the surface layering. With the dip of the surface layering used as a guide, the hole was expected to intersect the lower contact of the intrusion many hundred feet above the 3100-foot level. The hole not only failed to reach the bottom of the intrusion but did not even reach the chill zone which in this area is about 1000 feet thick. Obviously the lower contact dips considerably more steeply than the layering, and the ultrabasic section in the deeper parts of the basin is considerably thicker than Hall's estimate.

The isolated Marico portion of the complex is

a basin-shaped body composed of the ultrabasic group of rocks. All the upper horizons have been removed by erosion, and had no other sector of the intrusion been left, it might have been considered an ultrabasic lopolith.

intrusion. The flat Merensky horizon, the chromite horizons, and other adjacent horizons above the bulge are not affected by the downward bulge of the lower contact. Thus, where the intrusion becomes shallower by cutting

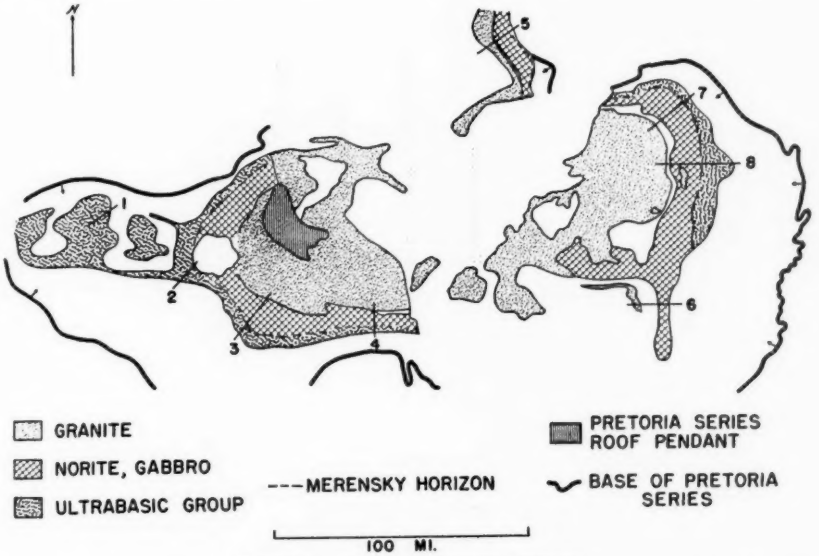

FIGURE 2.—BUSHVELD IGNEOUS COMPLEX

Compiled from maps published by the Geological Survey of the Union of South Africa and from observations by the author. The sections are as follows: 1. Marico, 2. Vlakfontein, 3. Rustenburg, 4. Pretoria, 5. Potgeitersrust (Zandsloot), 6. Dullstroom, 7. Northern Sekukuniland, 8. Steelpoort

Eastward from Vlakfontein toward Pretoria along the south flank of the intrusion the ultrabasic portion narrows and becomes less basic because high-olivine rocks form a much smaller proportion of the layers below the Merensky horizon. A magnetometer traverse north of Pretoria revealed only two narrow magnetic bands of the serpentinized peridotite, whereas at Vlakfontein the peridotite forms an important part of the ultrabasic series.

The east end of the intrusion shows many places where the intrusion becomes shallower by breaking sharply upward across the footwall formations, particularly toward the southeast flank. Where the intrusion shallows abruptly the lower layers are missing.

The deepest part of the intrusion on the east end is the Steelpoort bulge (Fig. 2, section 8), consisting of layered ultrabasic rocks, mainly stratified parallel to the regular layering of the across the footwall bedding, the deeper ultrabasic layers are terminated.

Farther up the flank of the lopolith toward the south in the Dullstroom sector the intrusion again abruptly shallows. This shallowing cuts out all the ultrabasic rocks including the Merensky and chromite horizons. Thus, farther south the lopolith consists only of the massive uniform norite and the overlying granite, granophyre, and felsite.

North of Potgeitersrust the Merensky horizon lies at, or only a few hundred feet above, the base of the intrusion, so the section is composed mainly of norite and granite with only a minimum of ultrabasic rock at the base.

Figure 3 compares the sections cropping out along the lopolith near Marico, Vlakfontein, Rustenburg, Pretoria, Zandsloot, Dullstroom, Northern Sekukuniland, and Steelpoort.

At Marico, Vlakfontein, and Steelpoort,

which represent the deep portion of the basin along the east-west axis, the layered ultrabasic section is well developed and approximately as thick as the Main Zone norite. However, farther out on the flanks of the basin the intrusion steps upward in the sedimentary series, the deeper ultrabasic layers are gradually cut out, and even the Main Zone norite phase thins. The intrusion is not sill-like, the bottom dips more steeply than the layering, and the ultrabasic rocks are concentrated at the bottom of the intrusion.

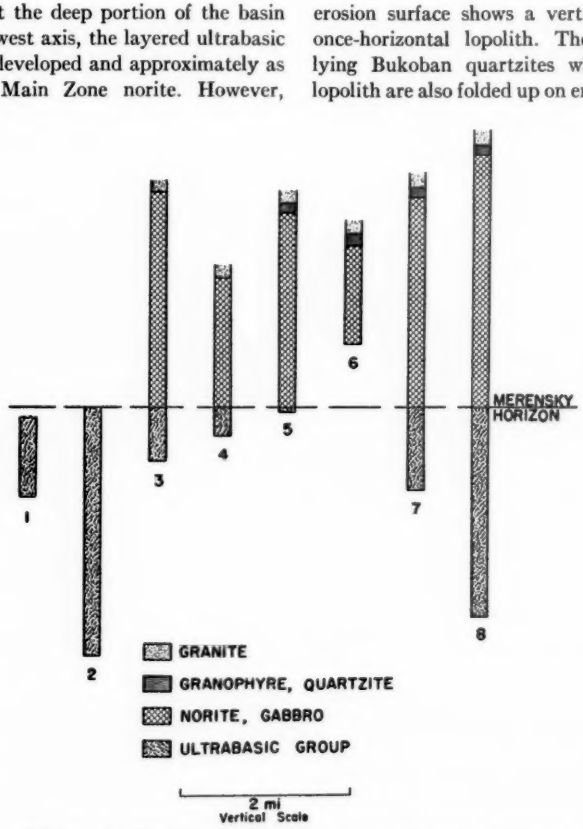

FIGURE 3.—COLUMNAR SECTIONS OF THE BUSHVELD COMPLEX
Thickness of section according to Hall (1932), p. 268. 1. Marico, 2. Vlakfontein, 3. Rustenburg, 4. Pretoria, 5. Potgeitersrust (Zandsloot), 6. Dullstroom, 7. Northern Sekukuniland, 8. Steelpoort

KUNGWE BAY LOPOLITH

The Kungwe Bay lopolith in Tanganyika (Fig. 4) reveals a section of a lopolith that is rarely seen. This lopolith has been turned up on end by the folding and faulting connected with the Western Rift Valley, so that the present erosion surface shows a vertical section of a once-horizontal lopolith. The typically flat-lying Bukoban quartzites which overlie the lopolith are also folded up on end in the immediate vicinity of the lopolith, so the nature of the structure is evident. The greater part of the intrusion is well exposed, although a small portion at the southeast end is covered by mantle.

This lopolith, like other lopoliths, has an arcuate section. It also has two deep lower lobes. Serpentinized peridotite occurs at the base of the intrusion but only in the lower lobes. Relatively uniform picrite forms the next important layer overlying the discontinuous peridotite. This picrite layer extends almost the whole length of the intrusion but narrows toward the north end and terminates abruptly where the intrusion shallows and pinches out. Many layers of norite, anorthosite, and gabbro overlie the picrite layer. Unlike the Bushveld,

this smaller lopolith is layered strongly to the top. The uppermost layers exposed consist of gabbros and diorites with much interstitial granophyre.

The Great Dyke (Fig. 5), 300 miles long and 4–7 miles wide, has the surface form of a huge dike and the same trend as the large dolerite dikes near by. Unlike most dikes, however, the

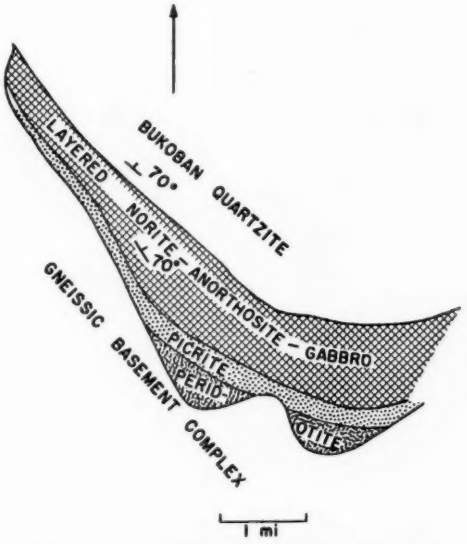

FIGURE 4.—KUNGWE BAY LOPOLITH, TANGANYIKA

The basal contact of this lopolith again is not parallel to the layering of the intrusion because the intrusion has a flat funnel shape with ultrabasic rocks concentrated in the bottom of the funnel.

GREAT DYKE

The structure of the Great Dyke and of the Sudbury lopolith is less clear than that of the lopoliths already discussed. The Great Dyke has a dikelike outcrop but is a layered intrusion with the layers in the shape of a shallow, elongated basin. The Sudbury intrusion is layered but has generally been considered a folded sill. Field study of the Great Dyke and the Sudbury intrusion shows that each bears remarkable similarities to sections of the Bushveld complex. The structures of both intrusions may, therefore, be similar to that of the whole Bushveld complex, but the present erosion surfaces exhibit an incomplete or nonrepresentative section.

Great Dyke is almost horizontally layered. The rocks of the Great Dyke are divided into a strongly layered ultrabasic group at the bottom overlain by a very thick, almost massive, uniform, basic member.

The ultrabasic group are strongly layered pyroxenites and peridotites with chromite bands similar to those of the Bushveld comple, although in general less feldspathic. Within a few feet of the top of the ultrabasic section, the Great Dyke contains a very uniform, persistent horizon, enriched in copper and nickel sulphides and platinum, corresponding to the Merensky horizon of the Bushveld complex. The Great Dyke basic rock overlying the ultrabasic layers is a massive, uniform, unlayered norite composed of labradorite and pyroxene similar to the massive uniform Main Zone of the Bushveld complex. The norite now forms the uppermost layer of the Great Dyke owing to erosion; the norite and the platinum horizon have been removed from two-thirds of the length of the intrusion.

The layering of the Great Dyke is horizontal at the center as seen in mine workings such as those at Wedza and in outcrops of some chromite and other distinctive layers. In cross section, the layering gradually rises from the center of the intrusion toward the edges to give the layering a shallow synclinal shape, except within a few hundred feet of the outer edge where the layers steepen sharply to dips of 30° or more as shown distinctly by the chromite horizons. At either end the Great Dyke rounds off with gentle dips indicating the very elongated basin structure of the layering.

The outer contacts of the Great Dyke are almost entirely covered by mantle. Only two or three poor exposures are known. In these exposures the contact dips approximately 45° inward toward the center of the intrusion. Only a few feet of contact is exposed, however, so, while an inward dip is suggested, evidence is too scanty to be conclusive.

Distribution of the basic and ultrabasic por-

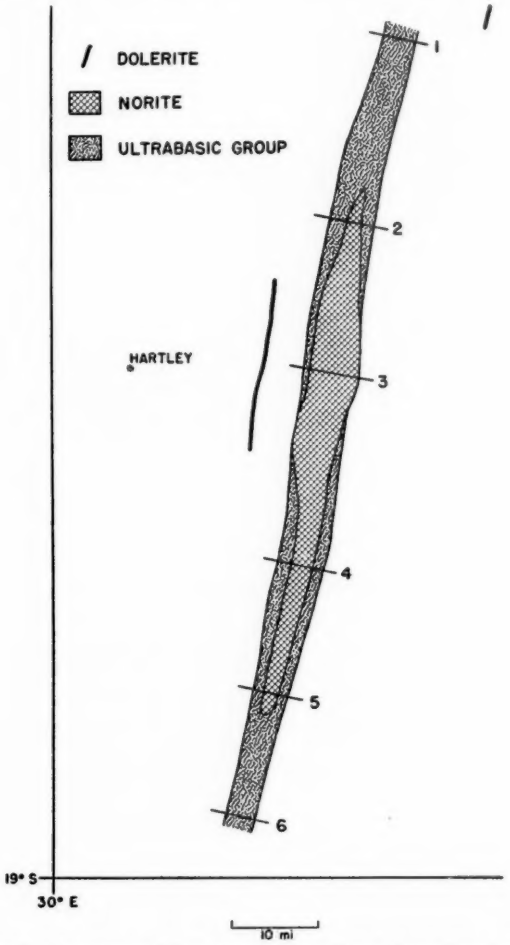

FIGURE 5.—GEOLOGY OF PART OF THE GREAT DYKE, SOUTHERN RHODESIA
Drawn from the Provisional Geological Map of Southern Rhodesia, 1946, Geological Survey of Southern Rhodesia

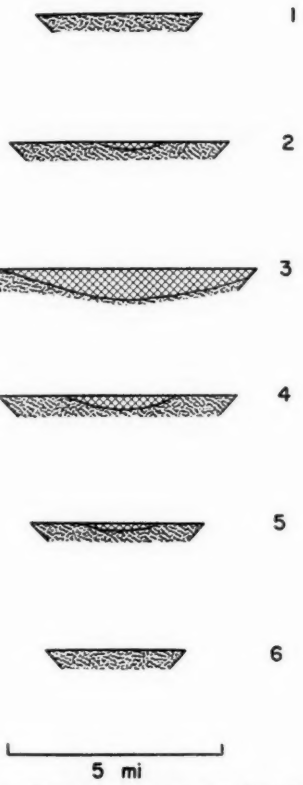

FIGURE 6.—CROSS SECTIONS OF THE GREAT DYKE
Sections correspond to the numbered sections in Figure 5; norite—cross-hatched, peridotite—granular pattern

tions of the Great Dyke shows that the contacts of the intrusion dip inward. The largest portion of the intrusion having a norite layer is shown in Figure 5. The intrusion is wider where the upper layer of norite is present and narrower in the deeper portions where it is missing. The upper portion of the dike is therefore wider than the lower portion, and the lower contacts must dip inward. The norite overlaps the ultrabasic rocks and forms the outer contact of the intrusion in the upper part, so that, like the intrusions already described, the layering is not parallel to the dip of the lower contact.

Sections located on Figure 5 are shown in cross section in Figure 6. Again the relation between the width of the intrusion and the distribution of the layers is apparent, and a funnel shape is indicated (Fig. 7). The inward dip of the walls must be of the order of 35° to make the sections fit when the width of the dike and the dip of the layering are considered. Where accurate dips and elevations are available it should be possible to approximate the dip of the contacts.

The upper part of the Great Dyke has been removed by erosion, but the similarity of the Great Dyke and the lower part of the Bushveld complex suggests that a large granophyre or granite phase once existed at the top of the Great Dyke. If the Great Dyke magma had the composition of the dolerite dikes parallel to it, the great volume of ultrabasic material must be balanced by a large volume of acid rocks even

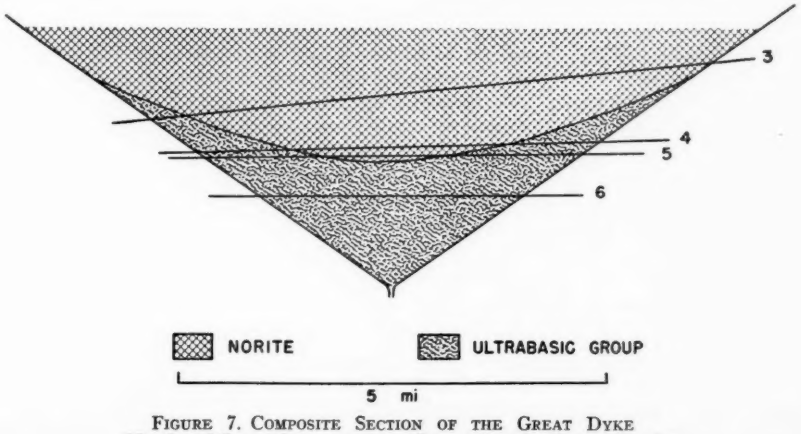

FIGURE 7. COMPOSITE SECTION OF THE GREAT DYKE
Numbered lines refer to corresponding sections in Figures 5 and 6

if no reaction took place between the magma and the granite wall rocks.

Sudbury Intrusion

The Sudbury intrusion (Fig. 8) is similar to the upper part of the Bushveld complex or to the sectors which contain only the Main Zone norite and the granite or granophyre. The Sudbury norite is a massive, uniform norite composed mainly of pyroxene or uralite and labradorite with only a faint suggestion of layering, just like the Bushveld norite in the Main Zone. Both intrusions have a magnetite layer near the top of the norite although in the Bushveld complex the magnetite occurs as massive magnetite layers whereas at Sudbury the magnetite in the magnetite zone is disseminated in the silicates in a broad but well-defined layer. Both intrusions have a thick layer of massive granitic rocks overlying the basic layers. The Sudbury intrusion is so similar to the upper part of the Bushveld intrusion that the probability arises that, like other lopoliths, the deeper levels of the Sudbury intrusion are composed of ultramafic members.

Relative proportions of norite and micropegmatite are greatly different on the north and south ranges of the Sudbury lopolith (Fig. 8). The ratio of micropegmatite to norite on the north range is approximately 3 to 1, on the south range it is 1 to 1. So, like other lopoliths, the banding and bottom must not be parallel, and the proportions of the rock types depend upon the section taken.

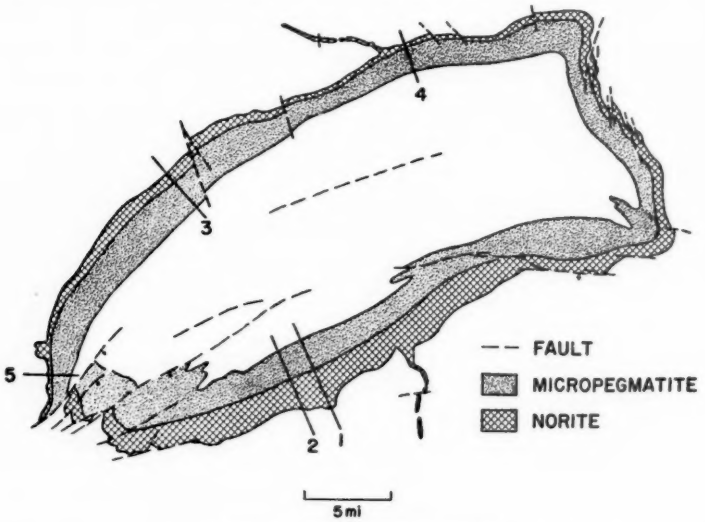

Figure 8.—The Sudbury Lopolith
Sections: 1. Creighton, 2. Gertrude, 3. Levack, 4. Nelson Lake, 5. Trill

The south range represents a considerably deeper section of the intrusion than the north range because it has been thrust upward on the order of 2–4 miles along the large thrust faults which cross the center of the basin.

The Sudbury lopolith, like other lopoliths, is characterized by sudden deepenings or shallowings of the bottom of the intrusion. The Creighton embayment (Fig. 8, section 1) is the best example of this deepening, but many other examples exist. At Sudbury the embayments are partly controlled by fracture systems in the preexisting rocks. The embayments in the bottom of the intrusion are not reflected in the roof nor in the upper layers such as the norite-micropegmatite contact, so that the deep portions merely contain more basic material. This type of structure at Sudbury is similar to that of the Steelpoort embayment of the Bushveld complex.

The sections of the Sudbury intrusion indi-

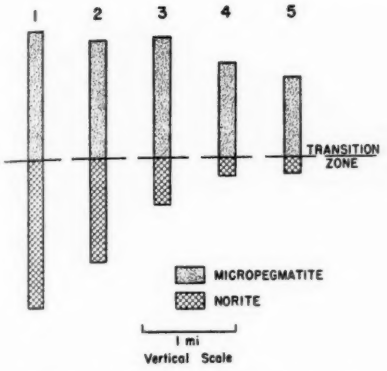

FIGURE 9.—COLUMNAR SECTIONS OF THE SUDBURY LOPOLITH

1. Creighton, 2. Gertrude, 3. Levack, 4. Nelson Lake, 5. Trill

be expected. These valleys and ridges may have characteristic plunges if they are controlled by fracture systems in the pre-existing footwall rocks. A new section of the Sudbury lopolith as shown in Figure 10 presents the structure as a funnel-shaped lopolith with layering not parallel to the lower contact. The bottom of the intrusion is composed of ultrabasic rocks, probably highly layered and possibly serpentinized.

Seismic studies of the Sudbury basin have been considered but have been rejected because tests showed that the norite is probably too similar to the granite basement rocks to show the contact seismically. This conclusion was based on the assumption of a norite bottom. If, however, the bottom of the lopolith is layered ultrabasic rocks, the possibilities of seismic studies of the lopolith should be reconsidered.

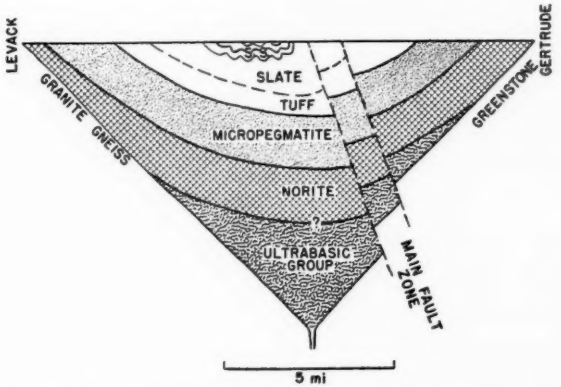

FIGURE 10.—DIAGRAMMATIC CROSS SECTION OF THE SUDBURY LOPOLITH FROM LEVACK TO GERTRUDE

cated in Figure 8 are shown graphically in Figure 9. The sections chosen are those which are least complicated by faulting. It is again apparent that the proportion of the rock types depends upon the location of the section—that is, the erosion level—and the structure of the bottom of the intrusion.

Because the Sudbury intrusion has the characteristics of other large lopoliths, it is suggested that it is not a folded sill but is a typical funnel-shaped lopolith probably with a feeder at the bottom.

The average 40- to 45-degree dip of the lower contact on the north and south ranges is likely to be maintained, but abrupt deepenings and shallowings resulting in valleys and ridges may

SUDBURY LOPOLITH AND THE SUDBURY BRECCIA

Figure 10 shows a problem of room since the footwall rocks must have been pushed aside to make way for the magma. More gently dipping lopoliths which are intruded into gently dipping sediments do not have such a serious room problem because much adjustment may take place along the sedimentary layers and by simple lifting of the overlying sediments. The Sudbury intrusion, however, is pictured as a steeply dipping funnel-shaped body intruded into massive Archean rocks. This intrusion could not take place without great adjustments which were the cause of the Sudbury breccia.

Sudbury Breccia

A small area of the Sudbury breccia, also called the "Frood breccia," has been described by Fairbairn and Robson (1942) who consider it a structural breccia. The breccia is characterized by rounded and subrounded fragments in a fine-grained matrix. The term "crush conglomerate" is often used as it is more descriptive of the physical appearance of the unit. The fragments may be derived from adjacent rocks, but many fragments are foreign to the enclosing rocks and must have been transported many thousands of feet during the brecciation. The matrix, like the fragments, typically reflects the composition of the enclosing rocks but in some places the matrix, too, is obviously foreign. The breccia may occur within a bed or flow, or between two formations, or it may involve whole formations or groups of formations. It may also occur in dikelike bands crosscutting granite or other formations, so it is obvious that the muddy matrix allowed the material to flow. The breccia units range from tiny stringers to large bands several hundred feet wide and several miles long. Bands may be straight and dikelike, or the breccia may occur in irregularly shaped areas.

The breccia is one of the major mapping units in the Sudbury district. It occurs in the footwall rocks on the north, south, east, and west ranges and may be found several miles from the intrusion although it has an apparent spacial relation to the intrusion. This type of breccia does not occur within the lopolith itself nor in the Whitewater tuffs and sediments above the intrusion, but all footwall rocks except those related to the intrusion and the late dikes are brecciated. Every major contact between the formations on the south range as far east as the Mississagi quartzite is a breccia contact except the contact of the norite itself.

The time sequence of the brecciation is of prime importance in establishing its origin. Recent field mapping has indicated that a much closer age relationship exists between the intrusion and the brecciation than was postulated previously. The age relations affect theories of ore deposition as well as of the origin of the breccia.

Fairbairn and Robson (1942, p. 30) suggested that the breccia might be related to late faulting in the district, but it is now known that the brecciation preceded the faulting. Breccia zones have been offset as much as other formations by the late faults such as the Creighton fault.

Several localities are now known where the quartz diorite offsets of the intrusion are chilled against the breccia and crosscut the breccia zones, showing that the brecciation took place before intrusion of the offsets, and hence also before the late faulting because the offsets are pre-faulting. When the strong brecciation of all adjoining formations is considered, it seems remarkable that the main mass of norite and its contacts were not brecciated unless the norite, too, is mainly post-breccia.

The Creighton granite, which is not related to the Sudbury lopolith, is brecciated. Recent remapping of the whole granite body and its relation to the norite, and microscopic study of many granite specimens agree with Collins' (1936) mapping and the interpretation that the Creighton granite is pre-norite, rather than with Yate's (1938, p. 165–168) interpretation that it is post-norite. Collins (1936) gave an excellent summary of the overall evidence, and this along with later evidence seems conclusive. The norite is chilled in many places along the main norite-granite contact. The granite is recrystallized and thermally metamorphosed along the norite cotact whereas the norite is fresh and unaltered. The gneissose structure of the granite is truncated by the norite in lots 3 and 4, Concession IV, Snider township. Composite, metamorphosed Creighton granite inclusions occur in the fresh norite, and previously mapped "norite" inclusions of the granite are older metamorphic rocks of the Sudburite type. The Copper Cliff offset, which is an integral part of the norite, cuts across the granite. Furthermore, detailed mapping in the norite at the west side of the Copper Cliff offset in lot 4, Concession IV, Snider township, shows that the reported (Yates, 1938, p. 165) long granite dike in this area does not exist. In compiling and publishing Collins map of the Chelmsford sheet (Map 871) the Geological Survey of Canada inserted such a dike without re-examining the area although Collins' Figure 2, (1936, p. 40) shows no dike at the locality.

The small, rare, irregular masses of Creighton granite which project a few feet into the norite

seem best interpreted as small quantities of granitic material mobilized by the hot norite, because a microscopic study of all the "dikes" located shows that the matrix of the porphyritic granite in the bulges has become granophyric and the phenocrysts are recrystallized so the microscopic texture is not similar to that of the fresh granite although the megascopic texture is relatively unchanged.

The correct sequence of events seems to be Creighton granite intrusion, brecciation, solidification of the lopolith, and offsets. The position of the Murray granite is the only doubtful factor in the time sequence because its age relationships are not yet fully understood, unless it is related in time to the intrusion of the lopolith.

The observed sequence of events takes the formation of the Sudbury breccia very close to the time of intrusion of the magma that consolidated to form the lopolith and its related offset dikes. Thus, because of the time and space relationship, the Sudbury breccia has probably resulted from the magma forcing the country rocks aside to make room for its funnel-shaped chamber. It also seems reasonable that the tapering, star-shaped arrangement of the offset dykes is the result of a radiating system of tensional fractures caused by the intrusion because this fracture pattern does not resemble any other fracture system of the area.

Granite Portion of Lopoliths

The question "if granite batholiths are derived from basaltic magmas, why do we never find a granite batholith with a basic bottom?" is often asked. A study of the great lopoliths may in part answer this question.

The occurrence of granitic phases at the top of differentiated sills, sheets, laccoliths, and lopoliths is well known. Daly (1933, p. 334–337) lists 12 examples where the upper layer is composed of micropegmatite, granophyre, or graphic granite. Many others are listed in which the upper parts consist of ordinary granite or alkaline phases. Seven other intrusions in the list have an upper layer of diabase, dolerite, norite, or gabbro enriched in micropegmatite or granophyre. In these seven intrusions the granitic portion is the last material to crystallize but it is not a separate granitic rock. The basic portions of intrusions with a separate granitic phase may also contain interstitial granitic minerals and micropegmatite. The Sudbury norite, for example, contains interstitial quartz, alkali feldspar, and micropegmatite almost everywhere.

The amount of granitic material that can be differentiated from a basaltic magma has been variously estimated at 5–10 per cent. If lopolithic intrusions are in general funnel-shaped, large portions of the most basic part of the intrusion may not be visible so the granitic phase may appear to form a larger proportion of the lopolith than it actually does.

A basaltic magma may also add to the 5–10 per cent of original granitic material by dissolving or reacting with pre-existing granites and other siliceous rocks. The basaltic magma is undersaturated with respect to granitic constituents, and in a closed system of basic magma and granitic fragments the heat of crystallization of the basic constituents could more than supply the heat of solution of a corresponding amount of acid fragments.

The nature of the lower contact of the lopoliths and the great number of inclusions found in some lopoliths show the strong fragmentation that goes on in the walls during intrusion. A study of the multitude of inclusions along the north range of the Sudbury intrusion gives some evidence of the disappearance of the granitic inclusions. On the north range, the lopolith intrudes a complex of older granite containing many basic fragments and dikes. Most of the complex is composed of granitic rocks, yet granite inclusions in the lopolith are extremely rare, and the few that do occur show marked evidence of corrosion. The shattered granite inclusions must have been dissolved because the inclusions in the thick inclusion zone at the base of the norite are almost entirely basic, and no trace of floated granite fragments has been found either within or at the top of the intrusion. The amount of granite dissolved and assimilated to leave all these basic inclusions must have been very great.

The granitic layers of the Bushveld and Sudbury intrusions cover an area of several hundred square miles so are of batholithic area, and these granites undoubtedly form a top layer as shown by drilling at Sudbury and by the valleys that cut through the Bushveld granite and

expose the underlying norite. Figure 2 shows the great volume of granite involved in the Bushveld intrusion. The granites have been separated into three principal masses by erosion, faulting, and deposition of later sediments. The largest mass, however, covers 2360 square miles (Hall, 1932, p. 370), a considerable batholith in itself. But this is only a small portion of the great granite mass that must have existed above the basic parts of the intrusion which extend east-west for a distance of 250 miles and north-south nearly 100 miles. The Bushveld granite, like other batholithic granites, has variations in composition and contains large areas of granitized rocks.

The Great Dyke is now composed only of basic and ultrabasic members but it most probably had an upper layer of granite, probably in a body 300 miles long, perhaps 10 or 20 miles wide, and many thousand feet thick. This would have been a major batholith with a basic bottom, just like the Bushveld intrusion.

The structure of roof rocks of lopoliths is also of interest, especially when compared with the structure of footwall formations. The floor of the Bushveld complex is composed of gently warped Pretoria series sediments, whereas the roof rocks are composed of large blocky areas of intricately folded and faulted sediments. An airborne magnetometer map of the roof pendant indicated in Figure 2 shows large tight folds in the iron formation, which illustrates that the roof sediments have undergone a severe mountain-building epoch which has not affected the earlier sediments below the lopolith. The lopolith must be the direct cause of the mountain building.

Granite bodies of batholithic area with basic bottoms do exist, then, as the top layer of great lopoliths. These granites possess all the attributes of normal batholiths, and the intrusions have caused mountain-building orogenies. The granitic portions may be in orogenic areas while the deeper basic portions are in nonorogenic areas. It is not implied that all batholiths originate in this manner, but, when the different compositions at different levels are considered, some batholiths composed only of granite at the surface level may well be the top of a lopolith with the deeper basic layers overlapped.

References Cited

Collins, W. H., 1936, Life history of the Sudbury nickel irruptive. Part 3; Environment: Royal Soc. Canada Trans., sec. IV, v. 30, p. 29–54

Daly, R. A., 1933, Igneous rocks and the depths of the earth: N. Y., McGraw-Hill, p. 334–337

Fairbairn, H. W., and Robson, G. M., 1942, Breccia at Sudbury, Ontario: Jour. Geology, v. 50, p. 1–33

Grout, F. F., 1918, The lopolith, an igneous form exemplified by the Duluth gabbro: Am. Jour. Sci., ser. 4, v. 46, p. 516–522

Hall, A. L., 1932, The Bushveld igneous complex of the Central Transvaal: Union of South Africa Geol. Survey Mem. 28, 560 p.

Yates, A. B., 1938, The Sudbury intrusive: Royal Soc. Canada Trans., sec. IV, v. 32, p. 151–172

Department of Geology, University of Manitoba, Winnipeg, Canada

Manuscript Received by the Secretary of the Society, April 1, 1955

BULLETIN OF THE GEOLOGICAL SOCIETY OF AMERICA
VOL. 67, PP. 301-316, 9 FIGS. MARCH 1956

PALEOMAGNETIC SURVEY IN ARIZONA AND UTAH: PRELIMINARY RESULTS

BY S. K. RUNCORN

ABSTRACT

Measurements of the remanent magnetization of sediments from the Colorado Plateau, ranging in age from the Algonkian to the Cretaceous, are reported. In some cases the stability of the magnetizations is clear, but in other cases instability is present to a degree for which corrections can be made. The original magnetizations are presumed to have been along the geomagnetic field at the time of deposition. Thus the position of the mean magnetic pole for five epochs is determined and compared with the pole positions calculated on the basis of measurements of strata in Great Britain. The agreement is sufficiently close to give strong support to the hypothesis of polar wandering.

CONTENTS

TEXT

	Page
Introduction	301
Acknowledgments	303
Collection and measurement of specimens	304
Magnetic stability	305
Summary of paleomagnetic directions	308
General statement	308
Precambrian formation	309
Upper Paleozoic formations	309
Mesozoic formations	311
Discussion of results	315
References cited	316

ILLUSTRATIONS

Figure	Page
1—Direction of magnetization of Hakati shale (Precambrian)	302
2—Direction of magnetization of Naco sandstone (Carboniferous-Pennsylvanian)	303
3—Directions of magnetization of Supai formation (Permian)	304
4—Direction of magnetization of Cutler formation (Permian)	305
5—Direction of magnetization of the Organ Rock tongue of the Cutler Formation (Permian)	309
6—Direction of magnetization of Moenkopi formation (Lower Triassic)	311
7—Direction of magnetization of Springdale sandstone (Triassic)	312
8—Direction of magnetization of Dakota sandstone (Cretaceous)	313
9—Migration of pole since Precambrian time	314

INTRODUCTION

Creer, Irving, and Runcorn (1954) and Runcorn (1955a) have suggested, mainly from consideration of paleomagnetic measurements in Great Britain, that the geographical pole has migrated slowly over the earth's surface throughout geological time. This study was based on rocks in which the natural remanent magnetization could be presumed to be the original magnetization. Thus rocks with considerable magnetic stability were used, and, where possible, the hypothesis that their magnetizations were acquired early in their history was tested. For such a study it is necessary to exclude rocks which have been subjected to circumstances that might appreciably change the magnetization, either through heating on deep burial or by diagenesis. Apart from random effects, it is reasonable to suppose that the original remanent magnetization of lavas and fine-grained red sandstones is in the same direction as that of the geomagnetic field at the time of cooling or deposition, respectively, when a correction is made for any subsequently acquired geological dip. Such rocks are found to have directions of magnetization, the mean of which in any one geological epoch has a direction characteristic of that epoch and in general different from ad-

jacent epochs. Within many such series of rocks, however, the direction shows frequent sharp reversals of sign. It is probable that this is accounted for by reversals of the polarity of the geomagnetic field. Between oppositely magnetized strata are often found thin zones of intermediate magnetization which presumably correspond to the relatively short periods during which the geomagnetic field is undergoing reversal of polarity.

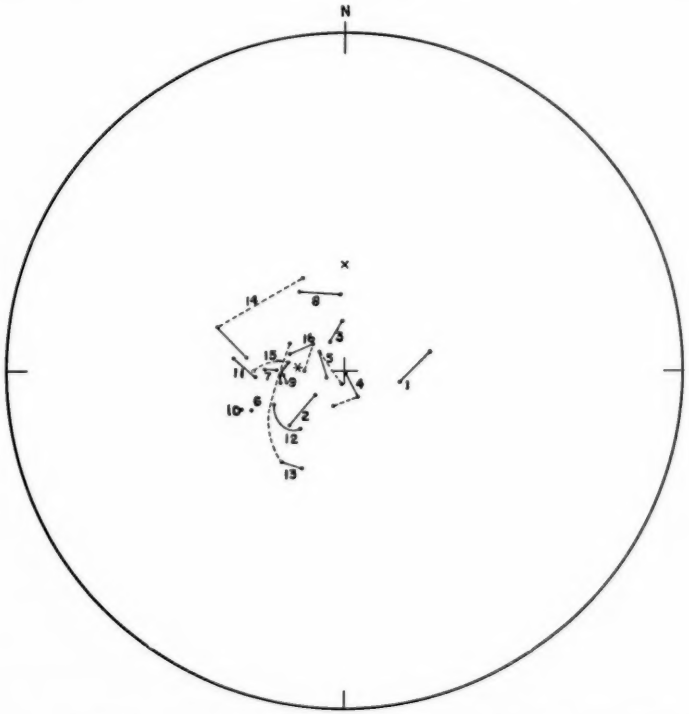

FIGURE 1.—DIRECTION OF MAGNETIZATION OF HAKATAI SHALE (PRECAMBRIAN)

Now the direction of magnetization of a single hand specimen is acquired usually within an interval *short* on the time scale of the geomagnetic secular change. The latter causes the field at any time to be substantially different from the mean dipole field with appreciable nondipole components. Thus a number of specimens, well spaced stratigraphically, will have directions of magnetizations with a random scatter not only from imperfect alignment of the magnetization along the field and from experimental errors but also from the effect of the geomagnetic secular variation.

But the mean direction should be that of the mean dipole of the epoch. In Tertiary time, as has clearly been shown by Hospers (1955), the mean field direction, inferred from measurements in Europe, is that of a geocentric dipole with its axis along the axis of the Earth's rotation. In pre-Tertiary times this is not so; therefore, unless relative movements of the continents are postulated, paleomagnetic results show that the mean dipole axis has varied with time. Creer, Irving, and Runcorn (1954) accordingly have calculated positions of the dipole axis, or mean magnetic poles, for different geological periods. It seems certain (Runcorn, 1955a) that these poles will be the same as the pole of rotation for the corresponding epoch.

A necessary stage in the test of this hy-

pothesis consists of the study of paleomagnetic directions throughout the geological column in some other area of the globe to examine how closely the positions of the pole inferred from these measurements agree with those inferred from the European measurements. Measurements of rocks from the Southwestern United States are particularly valuable for this purpose as this area lies about 90° along a great circle from Great Britain. In the summer of 1954 the writer collected specimens of various ages from the Grand Canyon and Colorado plateau, and the results of this preliminary survey are described in this paper.

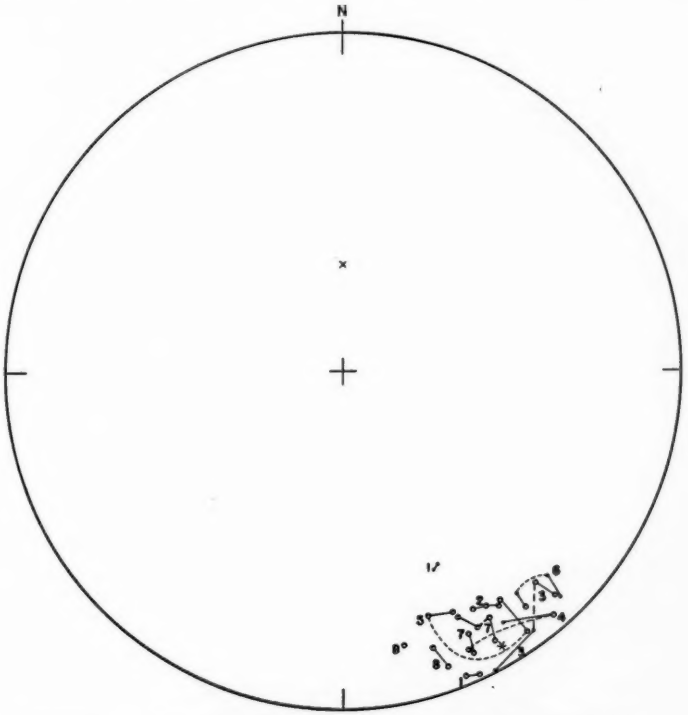

FIGURE 2.—DIRECTION OF MAGNETIZATION OF NACO SANDSTONE (CARBONIFEROUS-PENNSYLVANIAN)

ACKNOWLEDGMENTS

The author was enabled to visit the U.S.A. in the summer of 1954 by an invitation to participate in a Conference on Rock Magnetism held under the auspices of the National Science Foundation and the Institute of Geophysics of the University of California.

The collection of specimens was made possible by generous support from the Penrose Bequest of The Geological Society of America and by the invitation of the Director of the Museum of Northern Arizona, Flagstaff, to use the facilities there. The writer is grateful for much helpful advice from Dr. Henry R. Aldrich, from Mr. J. R. Balsley of the U. S. Geological Survey, and from Mr. L. F. Brady and Dr. J. F. Lance of the Museum of Northern Arizona. He is indebted to the Superintendents of the Grand Canyon and Zion and Bryce national parks for permission to collect specimens. Mr. R. R. Dorsey gave great help in the field work. Mr. J. C. Belshé made a preliminary compilation of the results presented in this paper. The writer is especially grateful to Mr. G.

Turnbull for carrying out most efficiently the measurements and much of the computation of the results described.

The present orientation was determined with a Brunton compass and marked on the upper surface as strike and dip marks. From each

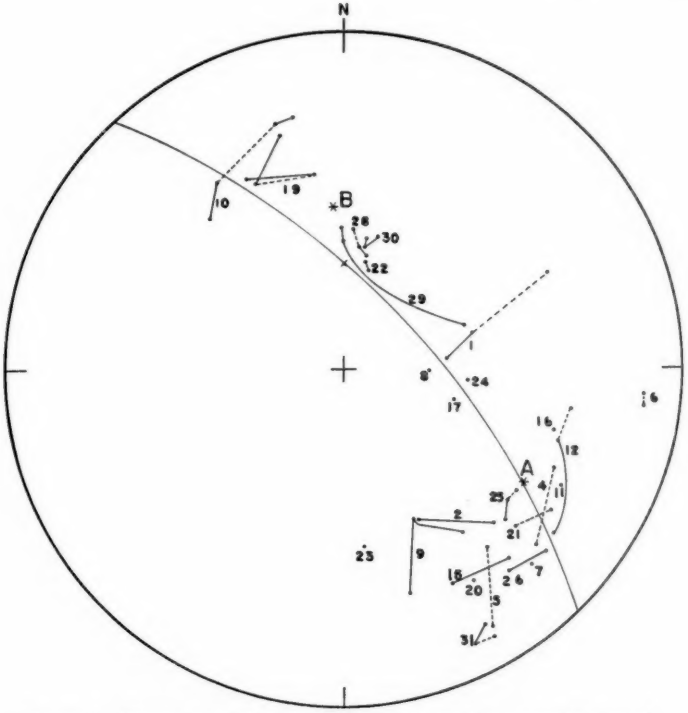

FIGURE 3.—DIRECTION OF MAGNETIZATION OF SUPAI FORMATION (PERMIAN)

COLLECTION AND MEASUREMENT OF SPECIMENS

Collection was limited to fine-grained red sandstones, siltstones, and shales. Previous work on the paleomagnetism of sediments has demonstrated (Runcorn, 1955a) that red sandstones are usually magnetized fairly strongly and have considerable magnetic stability, presumably because of the presence of hematite. Normally it is only fairly fine-grained well-bedded sandstones within one formation that are magnetized in a reasonably uniform direction. The settling of coarser material apparently occurs faster and in more turbulent water, so that mechanical forces have considerable influence in the orientation of the iron-oxide mineral grains. Sampling was limited to rocks whose original orientation can be determined. specimen one, or more commonly two, 3.5-cm diameter cores were cut with the axes perpendicular to the bedding plane. The cores were sliced into discs (usually two) about 1 cm thick.

The directions of magnetization of the discs were measured on the Cambridge astatic magnetometer following the procedure of Collinson, Creer, Irving, and Runcorn. The declination (relative to the present geographical north) and the inclination of the magnetic vector of the sample were measured relative to the original horizontal. The measurements are essentially observations of the angular deflections of a horizontal magnet suspended by a fine fiber when the rock specimen is raised beneath it. The high sensitivity required is obtained by removing the control of

the geomagnetic field on the suspended magnet. With the axis of the disc vertical and coincident with the magnet, the deflections obtained in various azimuths determine the declination.

nonuniformity of intensity of magnetization in addition to purely observational errors.

The instrument's limit of sensitivity through the period covering these measurements is

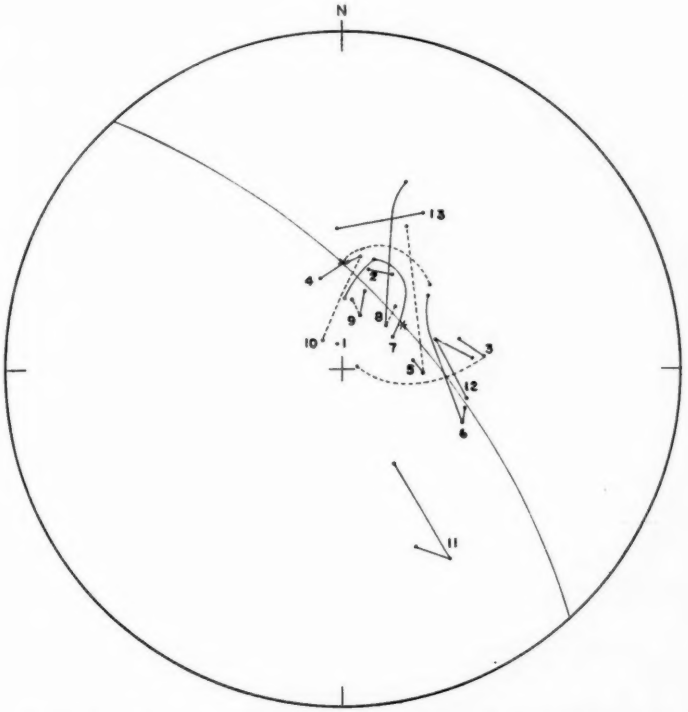

FIGURE 4.—DIRECTION OF MAGNETIZATION OF CUTLER FORMATION (PERMIAN)

In the present experiments the determination of the vertical component of magnetization was made by taking two series of measurements with the geometric center of the disc displaced 0.25 cm on one side of the vertical through the magnet for the first series of measurements of the deflection of the suspended system and the same distance on the other side for the second.

The observations yield more information than would be needed to determine the direction of magnetization on the assumption that this was adequately represented by a dipole at the center of the disc. Thus the reported directions of magnetizations are mean values calculated from a set of observations. This procedure therefore reduces errors arising from

estimated to be such as to give an average of 7.5×10^{-7} cgs e.m.u./cm^3 for the limit of detectable magnetization.

MAGNETIC STABILITY

The directions of magnetization of magnetically stable specimens from one formation will be scattered randomly, and this scatter will therefore nearly be eliminated in the mean direction. The directions may be represented by a number of unit vectors directed from a point or by their poles on the unit sphere. The mean direction is obtained by adding vectorially the number N of the unit vectors. The direc-

TABLE 1.—DIRECTIONS OF MAGNETIZATION, HAKATAI SHALE

Specimen and Core No.	Distance along trail (Feet)	Disc 1		Disc 2	
		Declination	Inclination	Declination	Inclination
1	0	N 77 E	60.8	S 78.3 E	70.8
2	20	S 45.0 W	64.4	S 48. W	77.4
3	70	N 25 W	79.5	N 1.5 W	73.5
4-a	140	S 61 E	89.4	S 31 W	79.9
4-b		S 15 W	77.4		
5-a	180	S 8 W	85.4		
5-b		N 52 W	79.3	S 68 W	84.4
6	1000	S 67 W	57.0		
7	1090	N 89 W	67.6	N 89 W	63.7
8	2070	N 2 W	64.6	N 39 W	60.0
9	2220	S 79 W	70.6	S 86.5 W	70.0
10	2270	S 69 W	54.2		
11	2650	S 96 W	60.7	N 83.5 W	53.8
12	3520	S 64.6 W	64.3	S 37 W	66.1
13-a	3520	N 62 W	70.2		
13-b		S 34 W	54.2	S 23 W	55.1
14-a	3520	N 24 W	57.2		
14-b		N 83 W	57.9	N 71 W	47.3
15-a	3520	N 81 W	71.6	S 78.5 W	69.0
15-b		S 89 W	60.4		
16-a	3520	N 90 W	77.6		
16-b		N 48 W	77.0	N 73 W	71.3

TABLE 2.—DIRECTIONS OF MAGNETIZATION, NACO SANDSTONE

Specimen and Core No.	Disc 1		Disc 2		Disc 3	
	Declination	Inclination	Declination	Inclination	Declination	Inclination
1-a	S 22.4 E	−1.7	S 24.1 E	−0.9		
1-b	S 26.1 E	25.0	S 22.8 E	24.3		
2	S 28.9 E	−12.8	S 31.5 E	−12.1	S 33.8 E	−10.5
3-a	S 42.3 E	−9.8	S 43.8 E	−5.3		
3-b	S 36.6 E	2.9	S 26.9 E	0.2		
4-a	S 24.7 E	−5.8				
4-b	S 40.8 E	−3.0	S 32.5 E	7.3		
5-a	S 24.8 E	−14.3	S 19.4 E	−15.3		
5-b	S 35.6 E	−3.3	S 34.2 E	−11.5		
6-a	S 44.1 E	4.7	S 45.5 E	9.3		
6-b	S 38.1 E	10.2	S 37.9 E	−7.1		
7-a	S 29.8 E	−5.2	S 31.0 E	−9.6		
7-b	S 25.7 E	−8.7	S 24.7 E	−5.3		
7-b*	S 25.5 E	−12.9	S 29.7 E	−9.5		
8	S 18.1 E	−8.4	S 19.9 E	−4.1		
8*	S 12.7 E	−10.4				

* Repeat measurements after two months' interval

tion of this resultant vector (of length R) is that of the mean. About this mean pole on the unit sphere may be described the circle of confidence subtending the half angle α, calculated from N and R (Fisher, 1953). This circle encloses the true direction with a probability of 95 per cent. The dispersion K, a measure of the scatter, may also be calculated. The examples

TABLE 3.—DIRECTIONS OF MAGNETIZATION, SUPAI FORMATION

Specimen and Core No.	Distance down Kabaib Trail	Disc 1		Disc 2		Disc 3	
		Declination	Inclination	Declination	Inclination	Declination	Inclination
1-a	200	N 74.5 E	47.1	N 84.2 E	55.9		
1-b		N 64.4 E	22.8				
2	280	S 44.0 E	25.1	S 26.1 E	37.2		
4-a	770	S 47.0 E	14.9				
4-b				S 64.2 E	20.7		
5-a	940	S 29.8 E	7.3				
5-b		S 38.6 E	21.8				
6-a	1370	S 82.7 E	6.7				
6-b		S 84.9 E	6.9				
7	1800	S 43.5 E	12.7				
8	2000	S 88.2 E	61.2				
9-a	2150	S 36.0 E	28.0	S 25.0 E	37.6	S 16.4 E	20.4
10-a	2620	N 41.8 W	28.5	N 34.4 W	22.7		
10-b		N 11.3 W	15.5	N 15.4 W	16.0		
11	2720	S 61.8 E	17.9				
12-a	2990	S 51.4 E	13.8	S 71.3 E	22.3		
12-b		S 79.8 E	21.0				
15-a	4000	S 37.8 E	16.6	S 26.5 E	19.1		
16-a	4520	S 73.6 E	24.0				
17	4960	S 74.6 E	52.5				
19-a	5800	N 25.4 W	27.6	N 15.0 W	18.8		
19-b		N 8.6 W	29.4	N 2.7 W	25.1		
20	6000	S 31.3 E	17.3				
21-a	6500	S 55.5 E	16.8				
21-b		S 47.0 E	20.6				
22	6990	N 14.2 E	56.4	N 11.3 E	54.7		
23		S 6.3 E	34.0				
24-a		S 84.7 E	49.9				
25-a		S 46.4 E	23.6	S 51.5 E	26.1		
25-b		S 54.2 E	25.6				
26-a		S 47.1 E	12.1	S 39.2 E	14.8		
28-a		N 11.4 E	52.2	N 7.5 E	50.2		
28-b		N 3.8 E	45.4				
29		N 0.8 W	44.8	N 9.0	48.6	N 7.0 E	48.5
30		N 14.3 E	46.3	N 9.4 E	49.9	N 10.1 E	47.8
31-a	S	S 29.4 E	6.0				
31-b		S 25.4 E	6.1	S 29.0 E	8.2		

The following specimens are omitted because they possessed magnetizations too small for accurate measurements: 3, 4-a, 4-b, 7, 8, 9-b, 13, 14, 15-b, 16-b, 17, 18, 24-b, 27-a, 27-b.

of Figures 1 and 2 show cases in which this simple analysis of the results is appropriate.

In Figures 3, 4, and 7, however, the magnetizations in one series of rocks are distributed near a plane rather than about a point, and clearly a mean direction is unlikely to have a simple significance. At ordinary temperatures, through exposure to fields of the order of that of the earth, rocks can acquire an isothermal remanent magnetization (I.R.M.) in addition to their original stable magnetization. The theory of I.R.M. has been worked out by Néel (1949; 1955); the intensity rises as the logarithm of the time of exposure to the field. Although such I.R.M. may, in certain cases, obscure the stable magnetization after quite short exposures to the field, in general a substantially long build-up time is necessary before I.R.M. becomes of comparable importance to the original magnetization. Thus

the I.R.M. acquired by a rock in nature will be directed parallel to the field of a geocentric dipole along the present geographical axis, which we will call the present axial dipole field. Thus it may be expected that the directions of the magnetizations of specimens from one series of rocks, neglecting scatter, will lie near a plane containing this latter direction and the stable magnetization. The directions will lie between these limits clustering toward the one or other depending on the relative importance of the I.R.M. in different samples. Thus in such cases the directions as plotted on a stereographic projection should be scattered along a great circle passing through the mean direction of all the specimens and the present axial dipole field direction at that locality. It is with this principle that we proceed to interpret the measured directions of magnetization where the calculation of a simple mean is clearly inappropriate.

TABLE 4.—DIRECTIONS OF MAGNETIZATION, CUTLER FORMATION

Specimen and Core No.	Disc 1		Disc 2		Disc 3	
	Declination	Inclination	Declination	Inclination	Declination	Inclination
1	N 9.7 W	81.7	(Not measured)			
2-a	(Not measured)		N 71.7 E	54.5		
2-b	N 15.3 E	56.1	N 28.1 E	55.0		
3-a	N 78.3 E	84.8				
3-b	N 84.7 E	44.1	N 75.5 E	50.7		
4-a	N 13.4 W	59.9	N 1.9 E	55.3		
4-b	N 46.4 E	50.7				
5-a	N 82.6 E	66.0	S 86.3 E	62.8		
5-b	N 24.6 E	40.2				
6	N 50.0 E	53.2	S 65.6 E	4.8	S 72.0 E	48.2
7	N 57.9 E	70.0	N 16.7 E	53.4	N 2.7 E	66.8
8-a	N 19.1 E	29.6	N 45.7 E	69.3	N 40.2 E	62.3
8-b	N 40.2 E	62.3				
9-a	N 8.4 E	67.1				
9-b	N 19.2 E	71.2	N 16.3 E	63.1		
10-a	N 3.2 E	54.6	N 9.7 E	53.4		
10-b	N 34.7 W	78.8				
11	S 28.5 E	54.7	S 29.7 E	24.1	S 22.4 E	30.6
12	N 85.2 E	47.8	S 72.0 E	57.5	S 76.5 E	48.1
13	N 1.9 W	45.3	N 27.6 E	35.4		

TABLE 5.—DIRECTIONS OF MAGNETIZATION, ORGAN ROCK TONGUE OF CUTLER FORMATION

Specimen and Core No.	Disc 1		Disc 2	
	Declination	Inclination	Declination	Inclination
65-a	S 63.5 E	66.6	S 83.1 E	59.7
65-b			S 19.3 E	73.4
66-a	N 79.5 E	53.9	N 70.0 E	57.5
66-b			N 41.0 E	69.2

A single specimen may have a direction of magnetization quite different from the rest of its group. Such will be ignored in this discussion. Quite apart from the chance of mistakes in the process of orientation in the field or laboratory, very local disturbed conditions during or after deposition, which upset the process of magnetization, are always possible.

SUMMARY OF PALEOMAGNETIC DIRECTIONS

General Statement

The stereographic projection is used throughout this paper to plot the directions of magnetizations. Solid dots represent projections on the lower hemisphere—*i.e.*, positive inclinations (north-seeking pole downward); open circles represent the upper hemisphere—*i.e.*, negative inclinations (north-seeking pole upward). Directions of magnetization of discs

from the same core are joined by solid lines, measurements on cores from the same rock specimen by broken lines. The small cross represents the direction of the present axial dipole field in Arizona. Stars represent mean directions of all, or some, of the measurements on each formation.

In Figure 1 the directions are shown: Specimens 12–16 were collected a few feet above each other, but their scatter is no less than the scatter of the whole group.

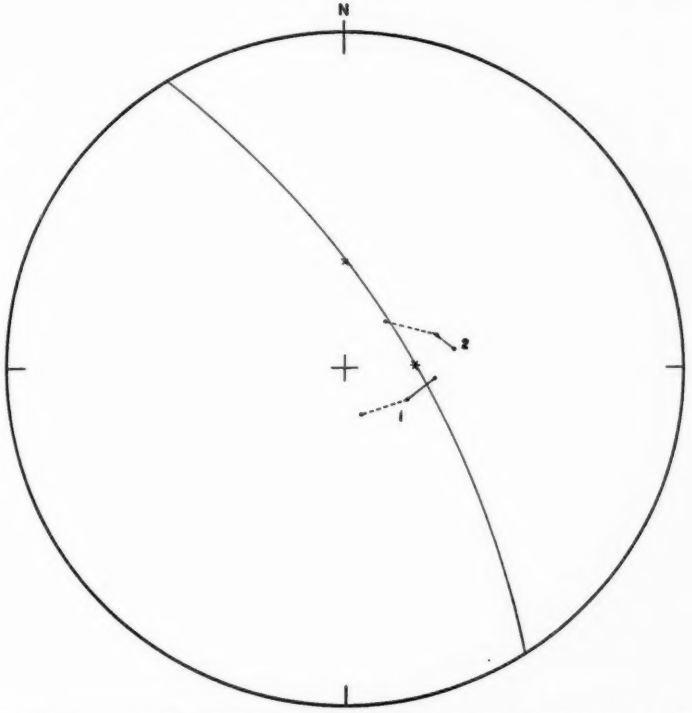

FIGURE 5.—DIRECTION OF MAGNETIZATION OF THE ORGAN ROCK TONGUE OF THE CUTLER FORMATION (PERMIAN)

Precambrian Formation

HAKATAI SHALE (Algonkian or late Precambrian): Sixteen specimens of the Hakatai shale were collected along the Kaibab trail in the Grand Canyon (Table 1). The first specimen was collected 264 feet farther down the Trail, from where the Kaibab fault crosses it. Omitting specimen 1 as being spurious, the statistics were calculated to be as follows:

Mean declination S. 87.7° W. } denoted by * on
Mean inclination +72.8° } Fig. 1
$N = 34$ $R =$ 32.475 $K = 21.6$
Circle of confidence $\alpha =$ 5.4°

Upper Paleozoic Formations

NACO SANDSTONE (Carboniferous-Pennsylvanian): Eight specimens (1–8) of the Naco sandstone spanning a thickness of about 200 feet were collected a quarter of a mile north of Carizzo Creek Bridge, Arizona, on the west bank on a road cut. Figure 2 and Table 2 show the direction of magnetization, and the following statistics were calculated:

Mean declination S. 30.3° E. } denoted by * on
Mean inclination −3.4° } Fig. 2
$N = 31$ $R = 30.25$ $K = 40.0$
Circle of confidence $\alpha =$ 4.1°

SUPAI FORMATION (Permian): Twenty-two specimens (1–22) were collected from the Supai formation in the Grand Canyon along

TABLE 6.—DIRECTIONS OF MAGNETIZATION, MOENKOPI FORMATION

Specimen and Core No.	Disc 1		Disc 2		Disc 3	
	Declination	Inclination	Declination	Inclination	Declination	Inclination
1-a	N 35.3 W	29.3	N 44 W	21.1		
1-b	N 40.7 W	17.3				
2-a	N 44.7 W	27.7				
2-b	N 39.6 W	22.3	N 50.8 W	23.1		
3-a	N 10.9 W	31.9	N 2.8 W	39.2		
3-b	N 26.3 W	47.8				
4-a	N 24.4 W	41.4	N 13.3 E	55.2		
4-b	N 25.9 W	43.6				
5-a	S 3.0 W	57.2	S 4.0 W	55.0		
5-b	S 4.0 E	49.8				
6-a	N 12.3 W	33.9	N 8.4 W	39.4		
6-b	N 9.7 W	40.8				
7-a	N 22.5 E	24.7				
7-b	N 50.3 E	44.9				
8-a	N 4.7 W	47.3				
8-b	N 54.7 E	48.6				
9-a	N 31.2 E	22.6	N 31.0 E	16.3		
9-b	N 30.0 E	20.6				
10-a	S 55.3 E	18.0	S 36.4 E	28.5		
10-b	S 46.3 E	19.8				
11-a	N 32.4 E	21.0	N 37.7 E	31.8		
11-b	N 51.8 E	18.0	N 54.2 E	25.4		
12-a	N 29.2 W	11.0				
12-b	N 17.4 W	14.5	N 15.9 W	22.1		
13-a	N 2.0 W	9.4	N 2.8 W	11.7		
13-b	N 2.8 W	17.3				
14-a	N 9.1 W	11.3	N 14.3 W	11.1		
14-b	N 4.4 W	14.9	N 5.7 W	14.0		
15			N 32.9 E	−1.9	N 33.4 E	5.2
16-a	N 15.3 W	19.3	N 13.8 E	18.6		
16-b	N 4.3 E	34.5	N 14.5 E	37.6		
17	N 6.1 E	42.6	N 16.3 E	32.5	N 0. E	26.6
18-a	N 8.4 W	7.7	N 2.3 E	7.9		
18-b	N 4.3 E	9.8	N 1.7 E	7.0		

the Kaibab Trail; 5 specimens (23–27) were collected in a road cut south of Midgley Bridge, on U. S. Highway 88, 32.1 miles south of the Research center of the Museum of Northern Arizona, Flagstaff; 3 (28–30) from a quarry near Flagstaff; and 1 (31) from a quarter of a mile above Pendley's Bridge. Table 3 and Figure 3 show the results. In Table 3 the position at which the samples were collected is shown as measured from the 1.5 mile marker down the Kaibab Trail. The main group of specimens have southeast declinations. Omitting specimens 10, 19, 22, 28, 29, and 30, the following statistics were calculated:

Mean declination S. 47.3° E.
Mean inclination +22.9°
} denoted by the point A in the quadrant in Fig. 3.

$N = 34$ $R = 31.9$ $K = 15.7$
Circle of confidence $\alpha = 7.5°$

A small group (22, 28, 29, 30) center on the present direction of the earth's field, and another group (1, 8, 17, 24) lies near the great circle between this direction and the prevalent direction, shown on Figure 3. Clearly the former group is completely unstable, and the latter partially unstable. Considering specimens 10, 19, 22, 29, and 30 the following mean

direction (denoted by the point *B* toward the north of Fig. 3) was found: declination N. 4.0° W., inclination + 39.7°. The point *A* will be regarded as the paleomagnetic direction, although it is likely to be slightly in error, the true one lying farther southeast along the great circle.

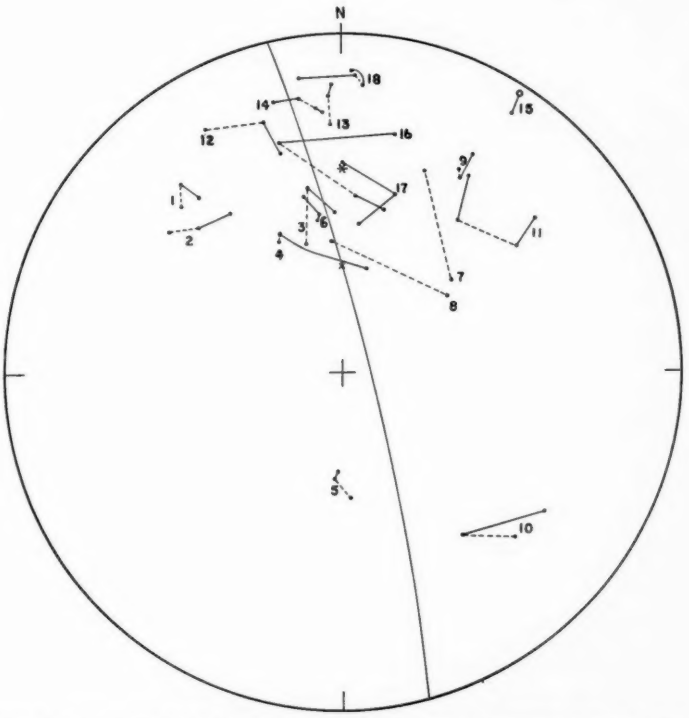

FIGURE 6.—DIRECTION OF MAGNETIZATION OF MOENKOPI FORMATION (LOWER TRIASSIC)

CUTLER FORMATION (Permian): Thirteen specimens (1–13) were collected from the Cutler formation in Monument Valley spanning a thickness of about 100 feet. Figure 4 and Table 4 show the results. The magnetizations lie along a great circle through the present dipole field direction and their mean direction. This great circle is nearly the same as that for the Supai formation in Figure 3. These rocks are therefore inferred to be partially unstable. The mean declination is N. 54.5° E., and mean inclination is +65.0°.

ORGAN ROCK TONGUE OF THE CUTLER FORMATION (Permian): Two specimens were collected 6 miles south of Gouldings on the west side of the road 30–40 feet below the de Chelly formation. Table 5 and Figure 5 give the results. Again the great circle through the mean value and the present dipole field is similar to those of Figures 3 and 4, and we infer that these samples are partially unstable.

These three Permian formations show varying degrees of instability, but the great circles are in good agreement. This is consistent with their having the same original magnetization. Consequently the mean value *A* of the magnetization of the Supai is best taken to be the paleomagnetic direction for Permian time.

Mesozoic Formations

MOENKOPI (Lower Triassic): Two specimens (1, 2) were collected 60 feet below the Shinarump formation in Zion National Park, just west of Springerville, Utah; 4 (3–6) from a road

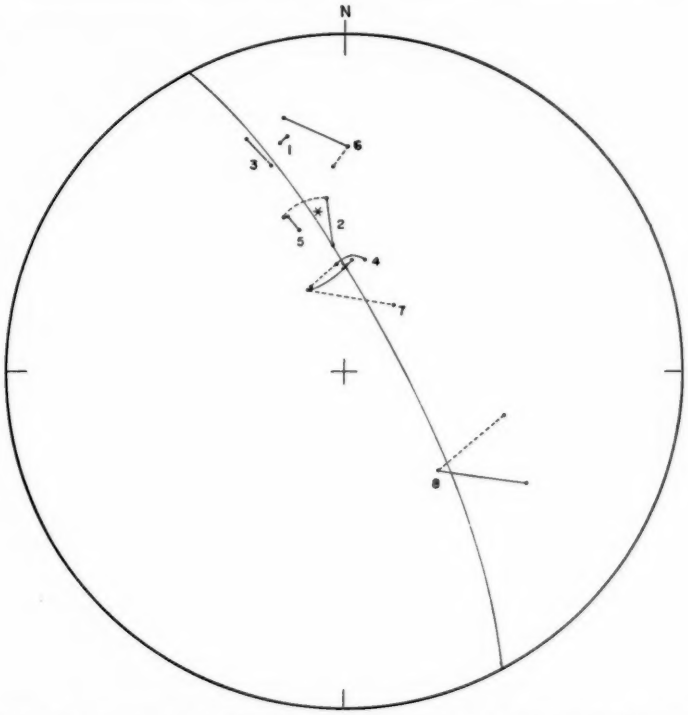

FIGURE 7.—DIRECTION OF MAGNETIZATION OF SPRINGDALE SANDSTONE (TRIASSIC)

TABLE 7.—DIRECTIONS OF MAGNETIZATION, SPRINGDALE SANDSTONE

Specimen and Core No.	Disc 1		Disc 2	
	Declination	Inclination	Declination	Inclination
1	N 13.8 W	18.4	N 15.6 W	19.6
2-c	N 21.3 W	37.1		
2-b	N 6.2 W	35.0	N 5.2 W	48.3
3	N 19.6 W	24.0	N 22.9 W	16.5
4-a	N 10. E	52.5	N 4.3 W	54.3
4-b	N 21.5 W	59.3		
5	N 17.9 W	42.3	N 20.2 W	37.1
6-a	N 13.4 W	14.8	N 0.9 E	22.5
6-b	N 3.1 W	27.2		
8-a	N 36.1 E	62.7		
8-b	N 23.3 W	59.9	N 3.4 E	53.1
7-a	S 58.9 E	25.8	S 43.8 E	46.6
7-b	S 74.8 E	38.2		

cut a mile from the east city limit sign in Flagstaff; 8 (7–14) from a road cut 2.8–3.8 miles south of Cameron; and 4 (15–18) 5 miles from Holbrook on the east bank of a road cut. Table 6 and Figure 6 give the results. Omitting specimens 5 and 10, the mean declination is N. 0.2° E., and the mean inclination is +27.4°, denoted by the star on Figure 6. The scatter is somewhat great. This may be connected with the fact that these rocks are often nonuniform in composition. Inclusions of gypsum are common. If specimens 1, 2, 9, 11, and 15 are omitted because they lie away from the main cluster of points and specimens 7, 8, and 16 are omitted because their internal magnetization seems unusually scattered, the great circle would lie as shown rather than through the mean point.

SPRINGDALE SANDSTONE (Triassic): Eight specimens (1–8) were collected in Zion National Park. Figure 7 and Table 7 show the results. Their directions lie near the great circle which has been drawn on Figure 7 through the mean direction. It may therefore be inferred that the

TABLE 8.—DIRECTIONS OF MAGNETIZATION, DAKOTA SANDSTONE

Specimen and Core No.	Disc 1		Disc 2		Disc 3	
	Declination	Inclination	Declination	Inclination	Declination	Inclination
1-a	S 2.3 W	−65.5	S 2.2 W	−67.5		
1-a*	S 0.8 E	−68.7				
1-b	S 9.6 W	−65.3	S 5.7 W	−63.7		
2-a	S 35.6 E	−50.6				
2-b	S 24.3 E	−54.1	S 32.8 E	−51.1		
3-a	S 35.2 E	−62.7				
3-b	S 24.7 E	−60.4				
4-a	N 15.5 W	+61.8	N 30.4 W	+64.1		
4-b	N 7.5 W	+63.5	N 9.3 W	+65.8		
4-a*	N 4.6 E	+58.9	N 4.7 E	+62.8		
5-a	N 10.5 E	+39.1	N 15.5 E	+37.8		
5-b	N 2.7 E	+35.9	N 0.3 W	+36.7		
6	S 49.7 E	+7.9	S 47.8 E	−4.3	S 39.0 E	11.9

* Repeat measurements after two months' interval

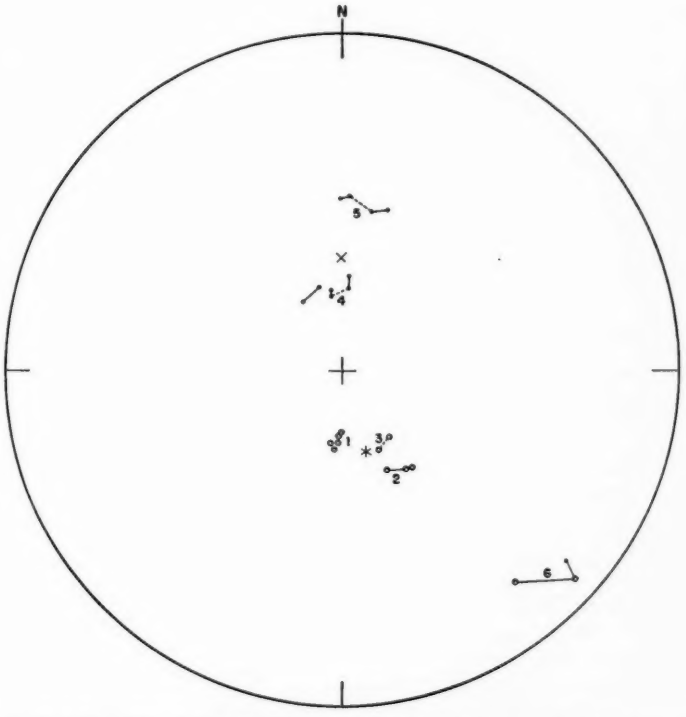

FIGURE 8.—DIRECTION OF MAGNETIZATION OF DAKOTA SANDSTONE (CRETACEOUS)

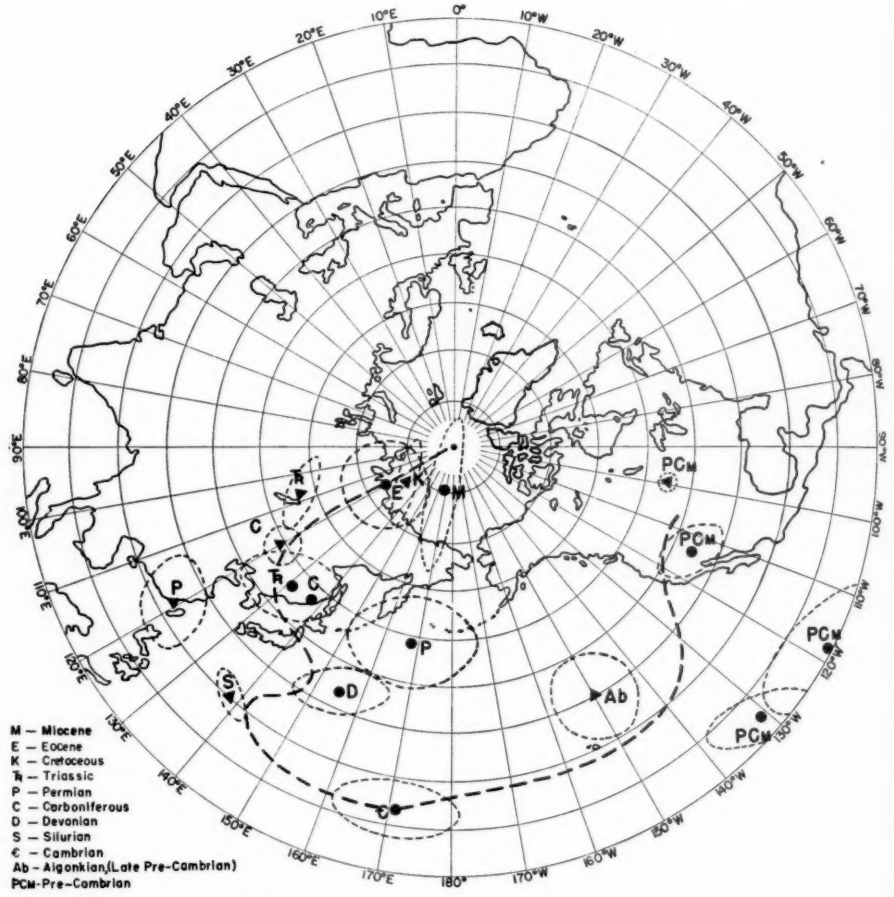

FIGURE 9.—MIGRATION OF POLE SINCE PRECAMBRIAN TIME
Based on paleomagnetic measurements in Europe and North America

rock is partially unstable. If 8 is omitted from the statistics we obtain

Mean declination N. 9.75° W. } shown by star
Mean inclination +38.8° } on Fig. 7
$N = 18$ $R = 17.0$ $K = 17$
Circle of confidence $\alpha = 8.7°$

These two Triassic formations do not therefore give unambiguous results, but in comparing them it seems reasonable to believe that the true paleomagnetic direction for this period has a smaller dip than that of the present field and a declination just west of north. Therefore a point on the great circle on Figure 7 farther north than the mean point is taken as more probably the true one rather than the mean value of the measurements quoted above. A mean declination of N. 22° W. and a mean inclination of +16° are taken, but the possibility of considerable error must be borne in mind.

DAKOTA SANDSTONES (Cretaceous): Six specimens were collected, 1–3, 3 miles west of Showlow on the south of the U. S. Highway and 4–6, 4 miles south of Showlow on the west bank of a road cut. The results are shown in Figure 8 and Table 8. There is no obvious evidence

that specimens 4 and 5 are stable, and but 1, 2, 3 clearly are. Whatever interpretation is put on this reversed magnetization, these results show that the Cretaceous pole cannot have been far from the present one. Specimens 1, 2, and 3 give a mean declination of S. 16° E. and a mean inclination of −62°.

TABLE 9.—DIRECTIONS OF MAGNETIZATION OF ROCKS FROM ARIZONA AND UTAH AND INFERRED POLE POSITIONS

Age	Formation	Declination	Inclination	Magnetic Lat.	Sign of field	Position of North Pole Lat.	Long.
Cretaceous	Dakota sandstones	S 16°E	−62°	43°N	−	76.5°N	127°E
Triassic	Springdale and Moenkopi	N 22°W	+16°		+	54.9°N	107°E
Permian	Supai	S 47.3°E	+22.9°	11.9°N	+	26.0°N	119°E
Carboniferous-Pennsylvanian	Maco sandstones	S 30.3°E	−3.4°	1.7°S	+	48.7°N	120°E
Pre-Cambrian	Hakatai shales	S 87.7°W	+72.8°	58.2°N	−	30.7°N	148°W

TABLE 10.—SEMI-AXES OF OVALS OF CONFIDENCE OF POLE POSITIONS

	β	α
EUROPEAN ROCKS		
Precambrian (Lower Torridonian)	8°	4.6°
Precambrian (Longmyndian)	13.2°	6.8°
Precambrian (Upper Torridonian)	7.8°	5.1°
Cambrian	9.6°	5.8°
Devonian	10.0°	5.0°
Triassic	13.0°	7.0°
Tertiary Eocene	12.1°	9.1°
Tertiary Miocene	17.6°	15.5°
AMERICAN ROCKS		
Precambrian (Michigan)	2°	2°
Algonkian	9.7°	8.7°
Silurian	3.6°	2.2°
Pennsylvanian	4.1°	4.1°
Permian	8.0°	6.4°
Triassic	8.7°	4.3°
Cretaceous	11.0°	8.5°

DISCUSSION OF RESULTS

From the true paleomagnetic directions for each of the geological epochs, the direction of the mean magnetic, and therefore the geographical, axis for that epoch may be calculated. It is not possible, because of the reversals of polarity, to distinguish between the north and the south geographical poles. However, by assuming that the axis of rotation travels slowly on a fairly smooth path, Creer, Irving, and Runcorn (1954) have traced the motion of the north geographical pole backward in time from its present position, and they find it seems not to have migrated outside the present northern hemisphere since Precambrian time. It is convenient to call the field of a geomagnetic dipole oriented with its south pole pointing to the geographical north (or the pole star on the celestial sphere) negative and a field with opposite polarity positive. Thus the present geomagnetic field has a negative sign. It is then possible with the above assumption about the motion of the axis of rotation to determine the sign of the field corresponding to each paleomagnetic direction. Irving (1954, Thesis, Cambridge Univ.) finds frequent reversals in the Torridonian (upper Precambrian) sandstones of northwest Scotland, as do Clegg, Almond, and Stubbs (1954) in the Keuper marls (Triassic) of England. However, reversals in Paleozoic time seem rather rare; Creer (1955, Thesis, Cambridge Univ.) finds from somewhat extensive sampling, positive fields in Cambrian through Devonian time and again in Permian time. Quite possibly in certain periods reversals of the geomagnetic field were very frequent and in other periods quite rare. The results described in this paper show that positive fields existed in Pennsylvanian and Permian time and negative

fields in Algonkian and Triassic time, though in no cases is the sampling extensive enough to prove that fields of the other polarity did not occur in these epochs.

In Figure 9 the position of the north geographical pole for various epochs, inferred by Creer, Irving, and Runcorn (1954) from European data, is plotted by solid circles on the aximuthal equidistant projection of the northern hemisphere. The triangles denote the pole positions obtained by measurements of North American rocks including those from Arizona and two, the Silurian and mid-American Precambrian poles, deduced by Creer (1955, Thesis, Cambridge Univ.) from some measurements by Graham. The pole in the late Precambrian, inferred from the results on the upper Torridonian (Aultbea and Applecross groups) and Longmyndian formations or from the Hakatai shales, was in the east Pacific in low latitudes. Earlier in Precambrian time it had been in Arizona as inferred from the direction of magnetization of the Diabaig group of the Torridonian. In early Paleozoic time the pole was in the western Pacific near the tropics. In Late Paleozoic and Mesozoic time it was near the Asiatic mainland in higher latitudes.

The positions of the poles shown are surrounded by closed curves computed from the circles of confidence of the respective formations so that the true pole lies within these curves with a probability of 95 per cent. The semi-axes of these curves, α and β, along the great circle joining the pole position and the locality and the great circle orthogonal to it, respectively, are given in Table 10. This estimate of accuracy will be misleading if few samples were taken close to each other; the Permian pole deduced from British measurements and that of the Silurian and Precambrian measurements of Graham are likely to have artificially high accuracies for this reason.

Runcorn (1955b) considered that the agreement between the European and American results is sufficiently good to conclude that no appreciable continental drift of the amount postulated by Wegener and du Toit—*i.e.*, 60° of longitude—could have taken place, at least since Precambrian time. Only the Permian poles are displaced by this amount, and this is probably the result of inadequate sampling. Consequently if the coincidence of the mean magnetic axis with the geographical axis is accepted, these measurements must be regarded as giving considerable support to the reality of polar wandering.

References Cited

Clegg, J. A., Almond, M., and Stubbs, P. H. S., 1954, The remanent magnetization of some sedimentary rocks in Britain: Philos. Mag., v. 45, p. 583–598

Creer, K. M., Irving, E., and Runcorn, S. K., 1954, The direction of the geomagnetic field in remote epochs in Great Britain: Jour. Geomag. and Geoelect., v. 6, p. 163–168

Fisher, R. A., 1953, Dispersion on a sphere: Royal Soc. A Pr., v. 217, p. 295–305

Hospers, J., 1955, Rock magnetism and polar wandering: Jour. Geology, v. 63, p. 59–74

Néel, L., 1949, Theorie du trainage magnetique des ferromagnetiques en grains fins avec applications aux terras cuites: Ann. Geophysics, v. 5, p. 99–136

—— 1955, Some theoretical aspects of rock magnetism: Adv. in Physics, v. 4, p. 191–243

Runcorn, S. K., 1955a, Rock magnetism—geophysical aspects: Adv. in Physics, v. 4, p. 244–291

—— 1955b, Palaeomagnetism of sediments from the Colorado Plateau: Nature, v. 176, p. 505

Museum of Northern Arizona, Flagstaff, Ariz., and Dept. of Geodesy and Geophysics, Cambridge University, Cambridge, England

Manuscript Received by the Secretary of the Society, June 24, 1955

Project Grant 659-54

BULLETIN OF THE GEOLOGICAL SOCIETY OF AMERICA
VOL. 67, PP. 317-390, 19 FIGS., 6 PLS. MARCH 1956

MINERALOGY AND PETROLOGY OF THE SITTAMPUNDI COMPLEX, SALEM DISTRICT, MADRAS STATE, INDIA

BY A. P. SUBRAMANIAM

ABSTRACT

The mineralogy and petrology of a thoroughly metamorphosed and reconstituted layered complex of anorthositic rocks with associated gabbroic and chromitic facies from Peninsular India are described in detail. This is one of the few known occurrences of highly metamorphosed anorthositic rocks, and the mineral associations are unique. New chemical analyses and optical studies are presented for two plagioclases, three amphiboles, three garnets, and one each of clinozoisite, cordierite, and chromite together with eight chemical analyses of the rocks. Of special interest are the very calcic plagioclases (An_{80-100}) in the anorthosites. Chemical analyses in duplicate of a calcic plagioclase, found to be An_{100} by optical methods, indicated it to be An_{98}, perhaps the nearest approach in nature to synthetic anorthite. The complex consists of a layered sequence of meta-anorthositic gneisses and eclogite-gabbros, with the former containing layers of chromitite and perknite; by analogy with other described occurrences of stratiform sheets, this is interpreted as a metamorphosed gravity-stratified sheet. A plot of available chemical analyses of garnetiferous metagabbros and eclogites and their associated garnets is given, and the possibility of a compositional field for most true eclogites as distinguished from garnetiferous metagabbros is pointed out. Deformation and mineral reconstitution during two periods of Archean orogeny, following primary crystallization from a basic magma, modified the paragenesis and mineralogy of these rocks with the development of new minerals such as hornblende, anthophyllite, pyralmandite, epidote-clinozoisite, grossularite garnet, porphyroblastic corundum (in part with calcite rims), and chromite with unmixed rutile. It is proposed to call this stratiform sheet "Sittampundi complex" after the village near its type exposure.

CONTENTS

TEXT

	Page
Introduction	319
Location	319
Acknowledgments	319
Previous investigations	320
Recent work	321
Present study	321
Geological setting of anorthosite-eclogite-gabbro complex	322
Principal rock units	322
Structure	324
Mineralogy	324
Introduction	324
Methods	325
Separations	325
Indices of refraction	325
Modes	325
Twinning in plagioclases	325
Garnets	325
General	325
Garnet C.12 from anorthite-clinozoisite-corundum-garnet assemblage	325
Garnets C.41 from eclogite-gabbro and C.60 from bronzitic pyropite	329
Plagioclase feldspars	329
Optical properties of calcic plagioclases	334
General	334
Twinning	336
Compositional variations	338
Summary of observations on plagioclases	339
Clinozoisite	341
Cordierite	342
Anthophyllite	343
Clino-amphiboles	350
Chromite	352
General	352
Mineralogy	352
Pyroxenes	355
Clinopyroxenes	355
Orthopyroxenes	355
Minor minerals	355
Scapolite	355
Corundum	356
Sillimanite	356
Rutile	356
Sphene	357
Petrography	357
General	357
Anorthosite series	357

	Page
General	357
Anorthite-edenite gneiss: C.33	359
Anorthite-clinozoisite-garnet rock: C.50	359
Anorthite - anthophyllite - edenite rock: C.69	360
Bytownite - clinozoisite - edenite gneiss: C.128	360
Schistose edenite gneiss: C.15	361
Chromitites	361
Cordierite - corundum - sillimanite - anthophyllite - anorthite - bytownite rock: C.71	362
Eclogite-gabbro series	363
General	363
Bronzitic pyropite (pyroxene-garnet rock) C.60	364
Bronzitic eclogite	364
Hornblende eclogite	364
Plagioclase eclogite (garnet-hornblende-plagioclase rock): C.41	365
Retrograde characters of eclogitic rocks	365
Pyroxenite	366
General	366
Websterite pegmatite	366
Websterite	366
Amphibolite	367
Chemical petrology and metamorphism	367
Introduction	367
Origin of minerals	367
Garnets	367
Epidote-plagioclase equilibrium	370
Clinozoisite	371
Cordierite	372
Corundum	373
Anorthosite series	373
General and metamorphic facies	373
Cordierite - corundum - sillimanite - anthophyllite-anorthite-bytownite rock	374
Problem of the eclogites	374
Introduction	374
Eclogites of Sittampundi complex	376
(FeO + MnO), MgO, CaO molecular diagram	376
Origin of the eclogites	380
Origin of chromitite	380
Equivalent unmetamorphosed rocks	381
Origin of banding and lineation	382
Banding	382
Preferred orientation of minerals	382
Comparison with stratiform sheets and evidence for igneous origin	384
Summary	384
Mineralogy	384
Petrology	385
References cited	386

ILLUSTRATIONS

Figure	Page
1. Geological sketch map of India showing location of Sittampundi complex	320
2. Diagrammatic interpretation of form and structure of the complex	323
3. Micrograph of garnet replacing anorthite	328
4. Micrographs of garnet coronas in eclogite	332
5. Micrograph of a garnet corona in eclogite	332
6. Curve correlating indices of refraction and An content of calcic plagioclases	337
7. Micrograph of clinozoisite in anorthite gneiss	343
8. Micrograph of well-developed clinozoisite crystal in anorthite gneiss	343
9. Curve showing relation between optic axial angle and (K_2O + Na_2O)—CaO for cordierite	346
10. Micrograph of anthophyllite in anorthosite	346
11. Micrograph showing skeletal crystals of diopside in anorthosite	356
12. Micrograph showing corundum replacing anorthite	357
13. Micrograph of bronzitic eclogite	364
14. Micrograph of garnet corona in eclogite	364
15. Micrograph of garnet corona in eclogite	365
16. A C F diagram for amphibolite facies	375
17. A C F diagram for sanidinite facies	375
18. (FeO + MnO), MgO, CaO molecular diagram	377
19. Sketch showing corundum crystals in meta-anorthosite	382

Plate	Facing page
1. Petrological map of the Sittampundi anorthosite-eclogite-gabbro complex	317
2. Banded anorthosites	322

	Following page
3. Anorthosite and chromitite exposures	363
4. Photomicrographs of Sittampundi minerals	363
5. Photomicrographs of Sittampundi rocks	363
6. Layered Sittampundi rocks	363

TABLES

Table	Page
1. Chemical composition with physical and optical properties of some minerals from the Sittampundi complex, Salem, India	326, 327
2. Composition and physical properties of garnet C.12	328
3. Properties of garnets	329
4. Composition and physical properties of garnet C.41	330
5. Composition and physical properties of garnet C.60	330
6. Chemical composition and physical properties of eclogite garnets	331
7. Properties of anorthites	333
8. Chemical composition and physical and optical properties of some anorthites	334
9. Anorthite content of plagioclases in Sittampundi rocks as determined by various methods	336
10. Twinning laws of plagioclase feldspars in the Sittampundi rocks	338
11. Analyses of clinozoisites from anorthite-corundum rocks of Sittampundi	339
12. Composition of clinozoisite C.39	340
13. Properties of clinozoisite C.39	341
14. Chemical composition and physical and optical properties of some clinozoisites	342
15. Composition of cordierite C.71	344
16. Composition and physical and optical properties of some magnesian cordierites	345
17. Composition and optical properties of cordierite C.71	346

Table	Page
18. Composition of anthophyllite C.58	347
19. Composition of amphibole C.34	348
20. Composition of amphibole C.70	349
21. Composition of amphibole from rock C.33	350
22. Composition of amphibole C.33	351
23. Structural account of analyzed amphiboles	352
24. Optical and physical properties of analyzed amphiboles	353
25. Optical properties of some amphiboles	353
26. Composition of chromite from chromitite C.101	354
27. Calculation of atoms per unit cell of chromite C.101	354
28. Chemical composition of some chromites from stratiform sheets	356
29. Approximate modes of rocks from the Sittampundi complex (weight per cent)	358
30. Chemical composition with normative and modal mineralogical composition of rocks from the Sittampundi complex	368, 369
31. Chemical composition of Sittampundi anorthosites and comparable analyses	371
32. Chemical composition of Sittampundi eclogites C.41 and C.60 with comparable analyses	372
33. (FeO + MnO), MgO, CaO molecular ratios of gabbroic and eclogitic rocks and garnets in them	378, 379
34. Comparative vertical sequence in some gravity-stratified sheet complexes	383

Introduction

This report embodies the results of petrological and mineralogical studies on a group of calcic and mafic rocks from the Archean complex of southern India. The field studies were carried out between 1944 and 1949, during the course of the writer's official duties with the Geological Survey of India. Laboratory studies based on field investigations, were carried out in the Geology Department of Princeton University, during the academic years 1949–1950 and 1950–1951. This paper is abridged from a Ph.D. dissertation accepted by the Department of Geology, Princeton University.

Location

These rocks occur in the Namakkal and Tiruchengodu taluks[1] of the Salem district in the Madras State of the Indian Union; the area is represented in portions of Survey of India topographic sheets 58 I/3, I/4, E/15, and E/16 on the scale of 1 inch to a mile. The precise location of the area is between Lat. 11°10′ and 11°25′N. and Long. 77°50′ and 78°05′E. (Fig. 1).

Acknowledgments

The writer is grateful for support from the Higgins Fund allotted to Princeton University for financing the laboratory work including cost of 19 chemical analyses of rocks and minerals, 100 thin sections, and the illustrations in this report.

The writer is most grateful to Professors A. F. Buddington and H. H. Hess, under whose direction this investigation was carried out, for stimulating discussions of the problem and helpful criticisms of the manuscript. Professor E. Sampson helped the writer in studying the chromitites and later visited the Sittampundi area. It is a pleasure to thank Dr. J. R. Smith who determined the cell size of the analyzed garnets and made a statistical analysis of a zoned plagioclase. Mr. R. Witter made a point counter with which the modal analyses were carried out.

Dr. N. L. Bowen of the Geophysical Laboratory kindly examined some of the calcic plagioclases and determined their compositions, for which the writer thanks him. Dr. J. R. Goldsmith of the University of Chicago determined the melting point of the analyzed specimen of anorthite, and his colleague Mr. O. Joensuu, spectroscopist, made spectroscopic analyses of 12 specimens of calcic plagioclase; for these the writer is deeply indebted. Professor Hisashi Kuno of the Tokyo University kindly placed at the disposal of the writer a specimen and an unpublished analysis of anorthite from an allivallite ejected from Hakone volcano.

Dr. T. P. Thayer of the U. S. Geological Survey critically read the manuscript and made several useful suggestions much appreciated by the writer. To Dr. M. S. Krishnan, Director of the Geological Survey of India, the writer owes a deep debt of gratitude for his keen interest and help during field studies, and for permission to publish this report. It is a pleasure to thank Shri: Shanmuga Gownder of Sittampundi Village, who helped the writer in many ways during field studies.

[1] Taluk means county.

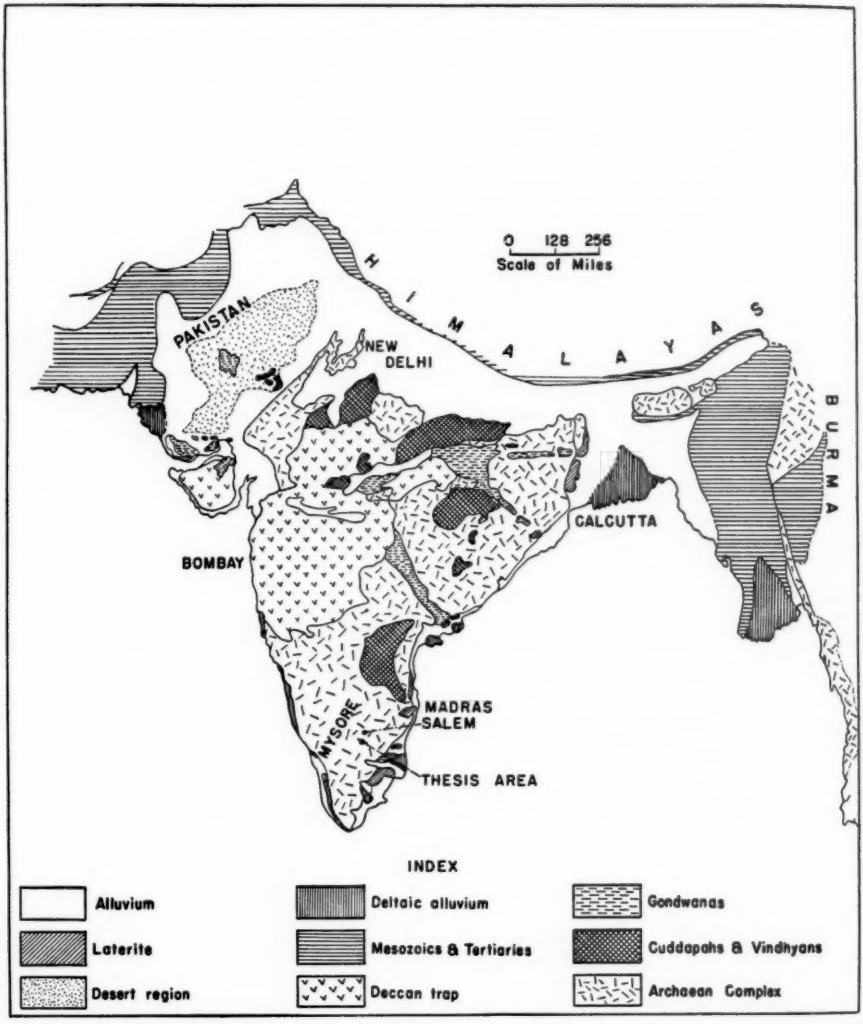

FIGURE 1.—GEOLOGICAL SKETCH MAP OF INDIA SHOWING LOCATION OF SITTAMPUNDI COMPLEX

PREVIOUS INVESTIGATIONS

Rocks of this area were referred to in scientific literature nearly 150 years ago in a classic paper by Count de Bournon (1802), who later proposed the name *Indianite* for the calcic plagioclase forming the matrix of the corundum rocks. It is unfortunate that the law of priority did not apply to the name proposed by Count de Bournon, thereby denying this savant the credit of discovering and describing a most significant rock-forming mineral.

The first scientific report on these rocks by Count de Bournon and Richard Chenevix appeared in the Philosophical Transactions of the Royal Society of London in 1802. They described the corundum-bearing rock and determined that the clear matrix had a specific gravity of 2.742. They also refer to a calcareous incrustation that commonly covers or par-

tially covers many fragments of imperfect corundum.

Count de Bournon (1817) named the main mineral of the matrix *Indianite* in honor of the country from which it came. It may be of interest to mention in this connection that a specimen of rock bearing this calcic feldspar reached the United States a century ago and was described by Silliman (1849), with a chemical analysis by Brush.

The earliest description of this area in Salem district is by Captain Newbold (1843), who described the abundant occurrence of corundum in gneiss and grayish earth, on a low hill near the village of Sholasigamany, in Tiruchengodu taluk. In 1892 Warth of the Geological Survey of India visited the area and made a report to the Government of Madras, but the first published geological description of this area is by Middlemiss (1896), who described the corundum occurrences of the Salem and Coimbatore districts.

The most important contribution to the petrography and mineralogy of these rocks is a monograph entitled *Contributions à l'etude des gneiss à pyroxene et des roches à wernerite* (Lacroix, 1889), relevant sections of which have been translated by Mallet (1891). This monograph by Lacroix details his petrographic and mineralogic studies of several collections of rocks from India and Ceylon, including those of Count de Bournon, preserved in the French Museum of Natural History. The scientific value of this excellent paper has been somewhat diminished owing to the lack of precise locations of the rocks described, probably because of poor cataloging of the original collections on which he based his work. Lacroix' paper contains a wealth of optical data on several minerals, detailed petrographic descriptions of many rocks, and chemical analyses of *indianite* and *thallite* (clinozoisite). He considered Bournon's thallite a new mineral and named it *fouqueite*.

In 1933, Iyer of the Geological Survey of India presented a brief paper on these rocks at the Indian Science Congress. This has not, however, been published in full. According to Iyer, these rocks resulted by the "differentiation fractionation of a basic magma, which has given rise to the large exposure of anorthite gneiss, in which the ultrabasic fraction consisting of chromite-pyroxene rock, and basic garnet-plagioclase-pyroxene rock, is intrusive." He considered the pegmatites and quartz veins in the area the acid fraction of the same magma. He also postulated an oversaturation in alumina of the anorthosite fraction of the magma, which subsequently crystallized out as corundum.

Recent Work

During World War II the increasing demand for corundum resulted in a revival of mining and prospecting activity in the Sittampundi area. In 1944 the writer and N. K. N. Aiyengar of the Geological Survey of India re-examined the Sittampundi corundum area to assess the prospects of corundum production. A few traverses in the area resulted in the discovery of layers of chromitite within the corundum anorthosites, extending over several miles, and indicated that the true extent of this complex of rocks had not been realized. About 2 weeks was spent in mapping the chromitite-rich horizons, but chemical analyses of samples of chromite ores and concentrates indicated they were of inferior grade, and work was discontinued. Aiyengar traced the eastern and northeastern extension of this belt of rocks during areal mapping of the region in 1945. The writer made a brief petrographic study of these rocks and, realizing their uniqueness, revisited the area to make a detailed field study, carefully revising the original geological map of the area and collecting rock types from critical horizons. About 5 weeks was spent in field study.

Present Study

The present investigation concerns the mineralogy and petrography of these rocks, probable mechanism of their emplacement, the history of their metamorphic and mineralogical transformations, and the origin of the chromite and corundum. The interpretations in this report are based on petrographic studies of more than 600 thin sections of these rocks and the chemical analyses of 8 rocks and 11 minerals.

Geological Setting of Anorthosite-Eclogite-Gabbro Complex

Principal Rock Units

The Salem district forms one of Fermor's (1936–1940) type subdivisions of the iron-ore province of the charnockitic region; the following general sequence was established by the writer for the Sittampundi area.

Stratigraphic Position	*Rocks of the Area*
Closepet or Arcot granite	Pink granites and pegmatites
	Pyroxenite-websterite
Peninsular gneiss	Biotite gneiss and migmatites
Dharwar Group	Anorthosite-eclogite-gabbro complex
	Ultrabasics: peridotites, saxonites, and dunites; banded magnetite, quartzite, crystalline limestone, amphibolites, and hornblende schists

The anorthosite-eclogite-gabbro complex consists of an assemblage of meta-anorthosites and eclogite-gabbros; the anorthosites carry layers of chromitite, perknite, and eclogite, and occur as an arcuate belt among the Peninsular gneisses, with a lateral extent of more than 20 miles and a maximum width of nearly 6000 feet.

At its western end the belt strikes nearly east-west and dips more than 70°S. To the east the rocks veer to an east-southeasterly trend and straighten out again in about 5 miles. The complex is widest south of Sittampundi from where the belt thins, gradually veering to an east-northeasterly trend, straightening out again about 5 miles farther east near Karungalpatti, with uniformly steep southerly dips of foliation. From Karungalpatti this belt takes a sharp northerly trend in the form of an arc, ending 7 miles to the north near Suryapatti. Between Karungalpatti and Suryapatti the anorthositic rocks form individual bands of varying thickness making a number of small ridges and hillocks. In this section the foliation dips range from 25° to 60°.

The major rock types of the area recognizable in the field are: (1) anorthositic gneisses and their variants, (2) conformable chromitite layers within the anorthosites, (3) eclogite-gabbros consisting of pyroxene-garnet rocks and garnet-hornblende-plagioclase rocks, (4) peridotites, (5) pyroxenites, (6) amphibolites, (7) biotite gneiss and migmatites, and (8) pink granites and related pegmatites; the first three types represent genetic units of the basic complex. The general distribution of these rocks is shown in Plate 1.

The anorthosite, which is well foliated (Pl. 3, fig. 1), attains a maximum width of about 6000 feet. It includes within it several layers of chromitite which range in thickness from a few inches up to as much as 10 feet (Pl. 3, fig. 2), with individual layers traceable along the strike for more than 4 miles. These chromitites occur as regular layers and not as lenses and do not display any transgressive relationship to the enclosing anorthosites. Several layers of bronzitic pyropite and eclogite-gabbro, ranging in thickness from 5 to 50 feet and extending laterally up to 1000 feet or more, are also found within the anorthosites. The major eclogite-gabbro layers outside the anorthosite horizon are nearly 600 feet and narrow down laterally. The proportion of anorthosite to mafic rocks over the whole complex would be roughly 4 to 1, and at its widest exposed section south of Sittampundi 3 to 1.

The eclogitic rocks occur as discontinuous layers within the anorthosites and as fairly consistent bands outside them. They resist weathering and form low ridges and small knolls. These eclogite bands are structurally conformable to the anorthosites, as they maintain the same strike and dip of foliation as the adjacent anorthosites. Peridotites presumably related genetically to the larger masses of peridotites in the district occur 1 mile south of the main anorthosite band, as a series of lenticular masses in the gneisses. They are mainly dunites and hornblende peridotites, and have been altered in many places to

Plate 2.—Banded Anorthosites

Figure 1.—Banded anorthosite near Sayakkadupudur. Note mafic layers at an angle to foliation. The layers are largely composed of hornblende.

Figure 2.—Anorthosite with mafic layers near Molasi. Note perfect layering, and offsetting of some layers because of folding.

FIGURE 1

FIGURE 2

BANDED ANORTHOSITES

magnesite which forms a network of economically workable veins. Small intrusive masses of pyroxenite (websterite) which appear to margin, and in the southern margin of the complex they grade into biotite gneisses. These amphibolites are possibly members of the meta-

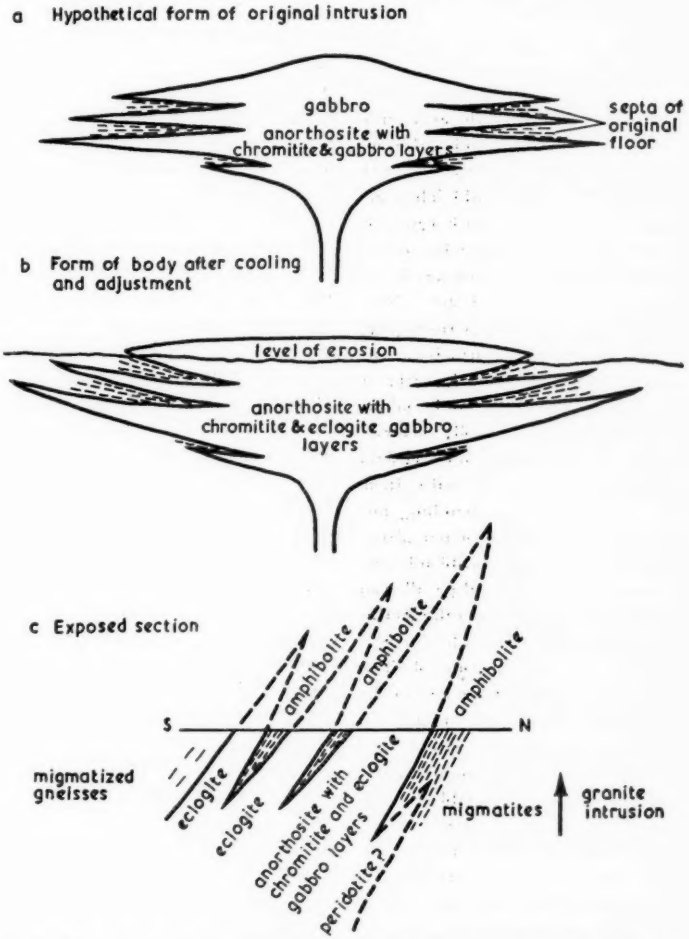

FIGURE 2.—DIAGRAMMATIC INTERPRETATION OF FORM AND STRUCTURE OF THE COMPLEX

a. Hypothetical form of original intrusion
b. Form of body after cooling and adjustment
c. Exposed section

cut the anorthosite complex occur at four places. Their freshness and lack of mineralogical and textural transformation comparable in magnitude with those of the anorthosite complex also point to their being later.

Amphibolites form a definite zone conformable with the anorthosites along the northern sedimentary group of rocks into which the basic complex was intruded, but they may be igneous and perhaps genetically related to the complex. The southern portion of the area is predominantly gneissic, consisting of migmatized biotite gneisses with interlayered crystalline limestone and calciphyre. Later intrusions

have transformed some of the older gneisses into injection gneisses. Pink granite with related pegmatites is conspicuously developed on the northern portion of the area and has forcefully domed the entire region.

Structure

The close association of anorthosites with included layers of chromitite and gabbroic rocks is very similar to that in several layered complexes in other parts of the world. The conformity of structure among the rock types of the complex, and the layered character of the anorthosites and associated chromitites indicate the complex is a gravity-stratified sheet. Further evidence based on the petrography, mineralogy, and chemistry supports this concept. The anorthosites, in general, carry a variable proportion of hornblende and contain several mafic layers composed wholly of hornblende (Pl. 2, fig. 2). The hornblende crystals in the anorthosites are aligned with their longer axes in the plane of the banding, imparting a megascopically visible planar structure. The prismatic crystals of hornblende display a fairly consistent dimensional parallelism in the plane of foliation and a generally south-southwest plunge of the lineation. The epidote-clinozoisite group of minerals in some of these rocks also displays a parallelism similar to the hornblendes, but the corundum crystals in them, insofar as noticeable, grow with their *c* axes across the lineation. The chromitites also display a linear structure conformable to that in the anorthosites, and the lineation in the rocks of the basic complex as a whole is conformable to the lineation in the adjacent amphibolites. The eclogite-gabbros also display primary layering, particularly where they are in contact with the anorthosites. Occasionally the layering is at an angle to the prevalent foliation, both in the anorthosites and eclogites, probably a result of folding and deformation (Pl. 2, fig. 1).

A system of vertical and horizontal joints occurs in the complex, particularly in the chromitites and anorthosites, and to a lesser degree in the eclogitic gabbros. Toward the northeastern end of the complex, the anorthosites contain several mafic layers which simulate flow banding or schlieren banding, and at one place these layers show a boudinage structure.

The anorthosites and eclogite-gabbros form an arc with steep southerly or easterly dips according to the prevailing strike. It is difficult to interpret the relative position of these two types, particularly in view of their metamorphic transformations. However, by general comparison with other gravity-stratified sheets, the anorthosites, with included layers of chromitite and the eclogitic gabbros, may be considered as the lower section of a gravity-stratified sheet. What is exposed now may be only a section of the sheet, the remaining sections being either concealed or eroded. On this assumption a probable sequence of events with regard to this complex may be reconstructed. It is postulated that a basaltic magma was emplaced as a sheet in gently folded Dharwarian metasediments (Fig. 2a); after cooling and adjustment it assumes a more general form (Fig. 2b). The uniform distribution and the lateral extent of the chromitite layers within the anorthosites indicate quiescence during emplacement. After a long time, during which crystallization and settling of the crystals must have been accomplished, the level of erosion reached the complex, and the top sections of the complex were eroded. The complex was then folded and intensely deformed into an anticlinal structure with concomitant development of a lineation about parallel to the fold axis and plunging generally south-southwest. Forceful intrusion of the pink granite followed. Further erosion revealed part of the fold as now exposed (Fig. 2c). In the region 20 miles south of the complex, the foliation of the older metasediments trends north-northeast or north, and there is a series of anticlines and synclines. This area has been little affected by granite intrusion. The Sittampundi complex is merely a remnant in the southern part of a large granite massif. The above interpretation has been adopted as a working hypothesis and will be discussed in the light of petrographic, mineralogic, and chemical data.

Mineralogy

Introduction

The mineralogy of the rocks constituting the anorthosite-gabbro complex is significant in

interpretations of its genetic and metamorphic history, and some of the following minerals have been studied in detail, chemically and optically (Table 1).

Oxides

Type A_2X_2 ..... Corundum
Type AX_2 ..... Rutile
Type AB_2X_4 ..... Chromite, spinel

Silicates

Group	Manner of linkage of silicon-oxygen tetrahedra	Minerals
Neosilicates	Separate (SiO_4) groups which do not share any oxygen with the neighboring SiO_4 tetrahedra	Garnets, sphene
Sorosilicate	Rings of six tetrahedra	Cordierite
Inosilicates	Chains or double chains of SiO_4 tetrahedra	Epidote clinozoisite Amphiboles Pyroxenes Sillimanite
Tectosilicates	Continuous frameworks of linked tetrahedra, sharing all four oxygen atoms with neighboring tetrahedra	Plagioclases

Methods

Separations.—To ensure purity of the mineral specimens used for chemical analyses, careful separations were made, using the Frantz Isodynamic Magnetic Separator, heavy liquids, and the centifruge.

Indices of refraction.—The principal indices of refraction of the minerals were determined by immersion methods using closely spaced and calibrated liquids, and using a temperature-controlled cell in the case of analyzed material. The determinations have been made in sodium light, and the accuracy of the determinations made with a temperature-controlled cell are thought to be ±.0005, while others are certainly better than ±.002.

Modes.—All the modes expressed in this paper are weight percentages, obtained by multiplying volume percentages by densities. The modal measurements have been made by the point-count method described by Chayes (1949). A clicker mechanism was installed on a Spencer mechanical stage giving spacings of a third of a millimeter, and a Clay-Adams blood-cell counter was used for tabulating the counts. This method of modal analysis is much less tedious than the usual methods and has none of the disadvantages of the various types of integrating stages. For the analyzed rocks, 10,000 points have been counted to obtain a close approximation to the actual volumetric composition.

Twinning in plagioclases.—The determination of twin laws of plagioclase feldspars has been very popular, and several refinements have been made on the original methods of Berek, Reinhard, and Duparc, particularly by Emmons (1943) and Turner (1947). The writer believes that many twin laws of plagioclase feldspar can be recognized by observations under the ordinary microscope, and in this connection a recent paper by Gorai (1950b) is significant. Of the universal-stage methods, the five-axis method of Emmons is perhaps the easiest and most practicable, as the older methods of Reinhard and the recent refinement of the same by Turner, using a four-axis stage, involve considerable amount of plotting, transfers, etc., which to say the least are time consuming. Nearly 100 determinations have been made using the method of Emmons, and the writer's belief that many of the common twinning laws can be deduced by observations under the microscope is based on this experience.

Garnets

General.—Garnet is an essential constituent of the eclogitic rocks and occasionally occurs in the anorthositic rocks. Chemical analyses of garnets from these rocks show them to be magnesia rich in the eclogites and lime rich in anorthosites.

Garnet C.12[2] *from anorthite-clinozoisite-corundum-garnet assemblage.*—The chemical composition and physical properties of this garnet

[2] The numbered specimens described in this paper are deposited in the Department of Geology, Princeton University, and are available for examination there.

TABLE 1.—CHEMICAL COMPOSITION WITH PHYSICAL AND OPTICAL PROPERTIES OF SOME MINERALS FROM THE SITTAMPUNDI COMPLEX, SALEM, INDIA

Constituent	1	2	3	4	5	6	7	8	9a	9b	10	11
SiO_2	38.69	40.71	41.50	45.50	42.32	44.96	38.64	49.54	43.74	43.88	54.90	0.34
TiO_2	0.55	0.08	0.08	0.23	0.27	0.23	0.14	0.03	....	0.00	0.01	0.36
Al_2O_3	18.17	22.31	22.35	17.64	15.62	14.90	27.69	33.42	36.40	36.18	28.72	24.12
Fe_2O_3	5.70	1.31	0.95	2.16	4.22	1.51	7.57	0.14	0.10	0.08	0.08	
Cr_2O_3	.....	.....	.....	.....	0.06	1.92	.....	.....	....	....	.....	36.88
FeO	3.78	16.49	14.56	9.04	6.78	4.05	0.14	3.75	0.00	0.00	.....	29.40
MnO	0.64	0.33	0.29	0.16	0.15	0.09	0.04	0.09	0.00	0.00	.....	0.68
MgO	0.76	12.03	14.82	20.51	13.68	16.05	0.11	11.34	0.00	0.00	0.08	7.22
CaO	31.76	6.77	5.36	0.87	11.78	11.92	23.79	0.10	19.38	19.37	11.07	0.77
Na_2O	.....	.....	.....	1.73	2.41	1.51	.....	0.32	0.24	0.22	.....	5.24
K_2O	.....	.....	.....	0.00	0.34	0.12	.....	0.01	0.04	0.00	0.02	....
P_2O_5	.....	.....	.....	.....	.....	.....	.....	.....	....	....	.....	....
H_2O+	0.13	0.23	0.36	2.12	2.13	2.26	1.84	1.32	0.37	0.28	0.04	....
H_2O-	0.06	0.09	0.09	0.09	0.11	0.15	0.00	0.03	0.04	0.08	0.00	....
CO_2	.....	.....	.....	.....	.....	.....	.....	.....	....	....	.....	....
Cl	.....	.....	.....	0.05	0.03	0.05	0.07	0.00	....	....	.....	....
F	.....	.....	.....	0.02	0.02	0.02	.....	0.01	....	....	.....	....
										SrO 0.01		
Less 0 for Cl + F	.....	.....	.....	0.02	0.02	0.02	0.02	.....	....	....	.....	....
Total...	100.24	100.35	100.36	100.10	99.90	99.72	100.01	100.10	100.31	100.10	100.16	99.77
N =	1.7692 ± 0005	1.7615 ± 0005	1.7542 ± 0005	N_X = 1.6415 ± 0005	1.6506 ± 0005	1.6402 ± 0005	1.7154–1.7202	1.5392 ± 0005	1.5754 ± 0004		1.5545 ± 0004	....
Density =	3.688 gm/cm³ at 29/4°C	3.835 gm/cm³ at 27/4°C	3.786 gm/cm³ at 25/4°C	N_Y = 1.6494 ± 0005	1.6611 ± 0005	1.6473 ± 0005	1.7158–1.7299	1.5438 ± 0005	1.5833 + 0004		.....	....
	.....	.....	.....	N_Z = 1.6578 ± 0005	1.6688 ± 0005	1.6565 ± 0005	1.7196–1.7329	1.5462 ± 0005	1.5885 ± 0004		1.5618 ± 0004	....
	.....	.....	.....	$2V$ = +88 ± 2°	−83½ ± 2°	+85½ ± 2°	−85° to +85°	−66 ± 2°	−77.2°		+78 ± 1°	....

$Z \wedge c$	.....	.....	.....	.....	16 ± 1°	19 ± 1	0–36°	.....	.....	.....	.....	....
D =	.....	.....	.....	3.164 gm/cm³ at 26/4°C	3.167 gm/cm³ at 26/4°C	3.117 gm/cm³ at 26/4°C	3.390 gm/cm³ at 28/4°C	2.591 gm/cm³ at 27/4°C	2.753 gm/cm³ at 26.5/4°C	2.749 gm/cm³ at 26.5/4°C	2.690 gm/cm³ at 23/4°C	....

C.12 (1) Garnet from anorthite gneiss, corundum quarries south of Sittampundi, Salem district, Madras, India. Analyst: Eileen K. Oslund, Minnesota

C.41 (2) Garnet from plagioclase eclogite band west-southwest of Sittampundi, Salem district, Madras, India. Analyst: Eileen K. Oslund, Minnesota

C.60 (3) Garnet from bronzitic pyropite (eclogite) east-northeast of Vadugupalaiyam, Salem district, Madras, India. Analyst: Eileen K. Oslund, Minnesota

C.58 (4) Anthophyllite from coarse anorthite-anthophyllite-edenite rock, quarry east-northeast of Tottiyanattam, Salem district, Madras, India. Analyst: S. S. Goldich, Minnesota

C.34 (5) Clinoamphibole (edenite) from anorthite-edenite gneiss a mile southwest of Sittampundi, Salem district, Madras, India. Analyst: Eileen K. Oslund, Minnesota

C.70 (6) Clinoamphibole (pargasite) from chromitite, quarries three-quarters of a mile west of Karungalpatti, Salem district, Madras, India. Analyst: Eileen K. Oslund, Minnesota

C.39 (7) Clinozoisite from anorthite-clinozoisite rock, corundum quarries 1½ miles southwest of Sittampundi, Salem district, Madras, India. Analyst: Eileen K. Oslund

C.71 (8) Cordierite from cordierite-corundum-sillimanite-anthophyllite-bytownite rock, three-quarters of a mile west of Karungalpatti, Salem district, Madras, India. Analyst: Eileen K. Oslund, Minnesota

C.50 (9a and 9b) Anorthite from anorthite-clinozoisite-garnet rock, old corundum workings 2 miles south of Konasamudram, Salem district, Madras, India. Analysts: S. S. Goldich and Eileen K. Oslund, Minnesota

C.41 (10) Plagioclase feldspar from plagioclase eclogite, band west-southwest of Sittampundi, Salem district, Madras, India. Analyst: Eileen K. Oslund, Minnesota

C.101 (11) Chromite from chromitite, old quarries east of Chettiyampalaiyam, Salem district, Madras, India. Analyst: W. H. Herdsman, Glasgow

Note: All halogen determinations by Mr. P. K. Kuroda of the Rock analysis Laboratory, Minnesota. All density determinations by Rock analysis Laboratory, Minnesota.

TABLE 2.—COMPOSITION AND PHYSICAL PROPERTIES OF GARNET C.12

Weight	Per cent	Ions	Metal ratio		Metal atoms	Ratio
SiO	38.69	Si^{4+}	645		2.973	
TiO_2	0.55	Ti	7	652	0.032	3.005
Al_2O_3	18.17	Al^{3+}	356		1.641	
Fe_2O_3	5.70	Fe	72	428	0.331	1.972
FeO	3.78	Fe^{2+}	53		0.244	
MnO	0.64	Mn	9		0.041	
MgO	0.76	Mg	19		0.091	
CaO	31.76	Ca	567	648	2.631	3.007
H_2O^+	0.13					
H_2O^-	0.06					
	100.24					

"Molecular" weight: 463.5

Analyst: Eileen K. Oslund

Formula:

$$(Ca_{37.5}Fe_3Mg_3Mn_{1.5})_3(Al_{33}Fe_{17})_2(Si_3O_{12})_{100}$$

Garnet "molecules" recalculated to 100 per cent from above analysis

Grossularite	68.90
Andradite	18.29
Almandite	8.94
Pyrope	2.40
Spessartite	1.47
	100.00

Determined density at 29/4°C
= 3.688 gm/cm³

Calculated density based on values for end members
= 3.702

Calculated density based on molecular weight from chemical analysis and on a_o as measured, using formula $G = 1.65\ WZ/a_o^3$, where $Z = 8$ mols/cell
= 3.724

Measured value a_o for edge of unit cell
= 11.844 ± .005 Å

Calculated value of a_o based on values for end members
= 11.855 Å

Refractive index N in sodium light
= 1.7692 ± .0005

Refractive index calculated from values of N for end members
= 1.7731

Color: brownish red in hand specimen; reddish brown at 80 mesh; pale brownish red in thin section

are shown in Table 2. This garnet, $GR_{69}AN_{18}AL_9PY_{2.5}SP_{1.5}$, is unusual in having a fair amount of almandite and a little pyrope. The exhaustive list of analyses of garnets tabulated by Wright (1938) contains one similar analysis,

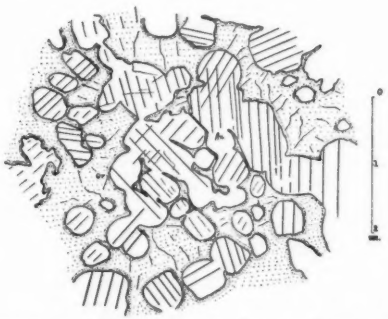

FIGURE 3.—MICROGRAPH OF GARNET REPLACING ANORTHITE

Note garnet selectively replacing anorthite resulting in "atolls" of garnet. The rock is anorthite-garnet-clinozoisite gneiss. An, Anorthite; Gr, Garnet.

$GR_{63.5}AN_{25}AL_1\ PY_0SP_{1.5}$, though it does not carry any pyrope. Heritsch (1926) reports this garnet from a serpentine contact, and hence it differs in paragenetic relations from garnet C.12. The following assemblages have been observed in the anorthositic series:

(1) anorthite, garnet, clinozoisite, corundum;

(2) anorthite, garnet, clinozoisite, corundum, hornblende;

(3) anorthite, garnet, vesuvianite (?).

In hand specimens the mineral is pale brownish red and occurs as disseminated grains with clinozoisite and corundum; occasionally it forms aggregates simulating augen. In thin section the mineral is mostly rounded and replaces anorthite resulting in a peculiar sieve texture (Fig. 3). It is difficult to distinguish this garnet from clinozoisite in plain light owing to their similarity in color, refringence, and replacement relationship with anorthite.

In some thin sections, the garnets are enveloped by a mineral showing anomalous birefringence and almost the same refringence and color as the garnet and clinozoisite. Duncan McConnell (1939, p. 63) has drawn attention to the chemical and structural similarity of vesuvianite (idocrase) and grossularite, and the

possibility of the presence of vesuvianite in the present assemblage cannot be ruled out, especially in view of the fact that volatiles have played an important role in the evolution of typical eclogite garnets. They are essential constituents of the eclogitic rocks, making up 25–50 per cent, and in an exceptional type up to 80 per cent, by weight of the rock. In thin

TABLE 3.—PHYSICAL PROPERTIES OF GARNETS

Name	*A* 2^+ ion	*B* 3^+ ion	*N*	*G*	a_o in Å	Mol. Weight
Pyrope (PY)	Mg	Al	1.705	3.554	11.463	403.1
Almandite (AL)	Fe	Al	1.830	4.325	11.518	497.6
Spessartite (SP)	Mn	Al	1.800	4.196	11.613	494.9
Grossularite (GR)	Ca	Al	1.735	3.582	11.863	450.4
Andradite (AN)	Ca	Fe	1.895	3.838	12.068	508.1

Refractive Indices of Some Garnets With Estimated Composition, and the Compositions of Associated Plagioclase and Orthopyroxene

Rock type	*N* of garnet ±0.0005	Composition of garnet	En % in ortho-pyroxene	An % of Plag.	Remarks
C.12 Anorthosite	1.7692	.....	....	90	Garnet analyzed
C.40 Anorthosite	1.7658	.....	....	90	.....
C.19 Eclogite	1.7530	$Mg_{55}Fe_{30}Ca_{15}$	84	....	.....
C.36 Eclogite	1.7568	$Mg_{51}Fe_{34}Ca_{15}$	86	55	.....
C.41 Eclogite	1.7615	$Mg_{46}Fe_{35}Ca_{19}$	84.5	50	Rock and garnet analyzed
C.48 Eclogite	1.7568	$Mg_{51}Fe_{34}Ca_{15}$	....	....	.....
C.60 Eclogite	1.7542	$Mg_{55}Fe_{31}Ca_{14}$	84	....	Rock and garnet analyzed
C.77 Eclogite	1.7542	$Mg_{55}Fe_{31}Ca_{14}$	....	73	.....
C.122 Eclogite	1.7658	$Mg_{45}Fe_{40}Ca_{15}$	85	55	.....
C.130 Eclogite	1.7580	$Mg_{50}Fe_{35}Ca_{15}$	....	45	.....

Note: Composition of garnets has been estimated from the values for N following Eskola (1921), except in the case of analyzed specimens.

these minerals. The anomalous biaxial character of vesuvianite, and its other optical similarities to clinozoisite, renders precise identification of the mineral difficult.

Garnets C.41 from hornblende-garnet-plagioclase rock (eclogite gabbro), and C.60 from pyroxene-garnet rock (bronzitic pyropite).—These garnets are chemically similar and are different from those in the anorthositic rocks (Table 3). They are pyralmandites with a small proportion of grossularite, andradite, and spessartite. The chemical composition and physical properties of these two garnets are tabulated in Tables 4 and 5, and Table 6 shows the chemical composition and physical properties of eclogite garnets. The two garnets analyzed appear to be

section they are distributed as rounded crystals 1–4 mm in diameter in a matrix of kelyphite or pyroxenes. The rocks display remarkable corona structures and plagioclase-diopside-hornblende symplectites around the garnets (Figs. 4, 5).

Plagioclase Feldspars

The most abundant silicate mineral in the rocks of this complex is plagioclase feldspar, which ranges from An_{75-100} in the anorthosites to An_{50-70} in the eclogite-gabbros. The feldspar in the anorthosite was described by Count de Bournon in 1802 and identified by him as a new mineral, *indianite*, in 1817. Three more chemical analyses of this feldspar were pub-

TABLE 4.—COMPOSITION AND PHYSICAL PROPERTIES OF GARNET C.41

Weight	Per cent	Ions	Metal ratio		Metal atoms	Ratio
SiO_2	40.71	Si^{4+}	678		3.003	
TiO_2	0.08	Ti	1	679	0.004	3.007
Al_2O_3	22.31	Al^{3+}	438		1.940	
Fe_2O_3	1.31	Fe	16	454	0.070	2.010
FeO	16.49	Fe^{2+}	229		1.014	
MnO	0.33	Mn	5		0.022	
MgO	12.03	Mg	301		1.333	
CaO	6.77	Ca	121	656	0.536	2.905
H_2O^+	0.23					
H_2O^-	0.09					
	100.35					

"Molecular" weight: 464.3
Analyst: Eileen K. Oslund
Formula:
$(Mg_{45.9}Fe_{35}Ca_{18.4}Mn_{0.7})_3(Al_{96.6}Fe_{3.6})_2(Si_3O_{12})_{100}$

Garnet "molecules" recalculated to 100 per cent from above analysis

Pyrope	41.57
Almandite	38.44
Grossularite	14.97
Andradite	4.17
Spessartite	0.85
	100.00

Determined density at 27/4°C
= 3.835 gm/cm³
Calculated density based on values for end members
= 3.871
Calculated density based on molecular weight from chemical analysis and on a_o as measured, using formula $G = 1.65\ WZ/a_o^3$, where $Z = 8$ mols/cell
= 3.971
Measured value a_o for edge of unit cell
= 11.556 ± .005 Å
Calculated value of a_o based on values for end members
= 11.569
Refractive index N in sodium light
= 1.7615 ± .0005
Refractive index calculated from values of N for end members
= 1.7662
Color: pinkish red in hand specimen; pink at 80 mesh; and pale pink in thin section; acicular inclusions seen occasionally

TABLE 5.—COMPOSITION AND PHYSICAL PROPERTIES OF GARNET C.60

Weight	Per cent	Ions	Metal ratio		Metal atoms	Ratio
SiO_2	41.50	Si^{4+}	692		3.010	
TiO_2	0.08	Ti	1	693	0.004	3.014
Al_2O_3	22.35	Al^{3+}	438		1.905	
Fe_2O_3	0.95	Fe	12	450	0.052	1.957
FeO	14.56	Fe^{2+}	202		0.878	
MnO	0.29	Mn	4		0.017	
MgO	14.82	Mg	371		1.613	
CaO	5.36	Ca	96	673	0.417	2.925
H_2O^+	0.36					
H_2O^-	0.09					
	100.36					

"Molecular" weight: 436.0
Analyst: Eileen K. Oslund
Formula:
$(Mg_{55.1}Fe_{30.1}Ca_{14.2}Mn_{0.6})_3(Al_{97}Fe_3)_2(Si_3O_{12})_{100}$

Garnet "molecules" recalculated to 100 per cent from above analysis

Pyrope	50.47
Almandite	33.92
Grossularite	11.85
Andradite	3.08
Spessartite	0.68
	100.00

Determined density at 25/4°C
= 3.786 gm/cm³
Calculated density based on values for end members
= 3.831
Calculated density based on molecular weight from chemical analysis and on a as measured, using formula $G = 1.65\ WZ/a_o^3$, where $Z = 8$ mols/cell
= 3.742
Measured value a_o for edge of unit cell
= 11.543 ± .005 Å
Calculated value of a_o based on values for end members
= 11.568 Å
Refractive index N in sodium light
= 1.7542 ± .0005
Refractive index calculated from values of N for end members
= 1.7574
Color: pinkish red in hand specimen; pink at 80 mesh; pale pink in thin section; acicular inclusions seen occasionally

TABLE 6.—CHEMICAL COMPOSITION AND PHYSICAL PROPERTIES OF ECLOGITE GARNETS

	SiO_2	TiO_2	Al_2O_3	Fe_2O_3	Cr_2O_3	FeO	MnO	MgO	CaO	H_2O+	H_2O-	Total	RO	R_2O_3	SiO_2	Formula	N	G	Rock
1	41.52	Tr	23.01	1.22	0.22	12.86	0.33	16.64	4.71	{0.	16}	100.67	2.92	1.00	2.95	$(Fe_{26}Mn_1Mg_{61}Ca_{12})_3(Al_{97}Fe_3)_2$	1.7498	3.782	Eclogite
2	41.50	0.08	22.35	0.95	..	14.56	0.29	14.82	5.36	0.36	0.09	100.36	3.014	0.979	2.92	$(Fe_{30.1}Mn_{0.6}Mg_{55.1}Ca_{14.2})_3(Al_{97}Fe_3)_2$	1.7542	3.786	Bronzitic pyropite
3	40.20	Tr	22.88	1.74	..	16.00	0.14	13.60	5.33	..	..	99.89	2.80	1.00	2.85	$(Fe_{34}Mn_{0.3}Mg_{51}Ca_{14.7})_3(Al_{95.5}Fe_{4.5})_2$	1.755	3.730	Garnet-pyroxenite
4	37.97	0.00	21.79	6.02	..	12.87	0.13	13.34	7.65	0.18	0.08	100.32	2.58	1.00	2.51	$(Fe_{27.6}Mn_{0.3}Mg_{51}Ca_{21})_3(Al_{85}Fe_{15})_2$	1.772	3.754	Eclogite
									$Na_2O + K_2O = 0.29$										
5	39.39	Tr	24.75	2.55	..	12.65	Tr	12.54	7.71	..	..	100.19	2.75	1.14	2.92	$(Fe_{28}Mg_{50}Ca_{22})_3(Al_{96}Fe_4)_2$	1.7610	3.758	Kyanite eclogite
6	39.64	0.26	24.19	1.15	..	13.63	0.33	12.90	7.98	{0.	08}	100.16	2.93	1.08	2.97	$(Fe_{28.7}Mn_{0.7}Mg_{48.9}Ca_{21.7})_3(Al_{97}Fe_3)_2$	1.756	3.760	Kyanite eclogite
7	40.71	0.08	22.31	1.31	..	16.49	0.33	12.03	6.77	0.23	0.09	100.35	3.00	1.05	2.90	$(Fe_{35}Mn_{0.7}Mg_{45.9}Ca_{18.4})_3(Al_{96.5}Fe_{3.5})_2$	1.7615	3.835	Plagioclase- eclogite
8	40.17	Tr	22.07	1.19	..	17.26	0.55	11.61	6.82	..	..	99.67	2.93	1.00	2.97	$(Fe_{37}Mn_1Mg_{44}Ca_{18})_3(Al_{94}Fe_6)_2$	1.7658	3.83	Eclogite in labradorite rock
9	40.30	Tr	21.86	2.16	..	19.08	0.69	11.28	5.22	..	..	100.59	2.83	1.00	2.93	$(Fe_{40}Mn_2Mg_{43}Ca_{15})_3(Al_{94}Fe_6)_2$	1.7660	3.882	Eclogite
10	40.30	Tr	21.60	1.30	..	18.00	0.70	11.20	7.20	..	..	100.30	3.02	0.985	3.01	$(Fe_{37.4}Mn_{1.5}Mg_{41.8}Ca_{19.8})_3(Al_{96.4}Fe_{3.6})_2$	1.756	3.74	Eclogite

(1) Garnet from eclogite, Rodhaugen, Almklovdalen, Sondmore (Eskola, 1921, p. 28). Analyst: P. Eskola.

(2) Garnet from pyroxene-garnet rock (bronzitic pyropite, C.60), Sittampundi complex, Salem, India. Analyst: Eileen K. Oslund.

(3) Garnet from garnet pyroxenite, Anorthosittkomplex i Hedal (Gjelsvik, 1947, p. 25). Analyst: Gjelsvik.

(4) Garnet from eclogite, Greenland (Sahlstein, 1935, p. 16). Analyst: Th. G. Sahlstein.

(5) Garnet from kyanite eclogite, Silberbach, Fichtelgebirge (Dull, 1903, p. 148). Analyst: E. Dull.

(6) Garnet from eclogite, Weissenstein, Bavaria (Tilley, 1936, p. 425). Analyst: Hilda Bennet.

(7) Garnet from plagioclase eclogite C.41, Sittampundi complex, Salem, India. Analyst: Eileen K. Oslund.

(8) Garnet from eclogite inclusion in labradorite rock from Indre Sogn (Eskola, 1921, p. 84). Analyst: P. Eskola.

(9) Garnet from the eclogite from Silden, Nordford (Eskola, 1921, p. 38). Analyst: P. Eskola.

(10) Garnet from eclogite, half a mile northeast of Bienn a' Chapuill (Alderman, 1936, p. 498). Analyst: W. Pollard.

lished before Lacroix (1889) presented the optical properties and chemical analysis of this anorthite. Petrographic examination of these

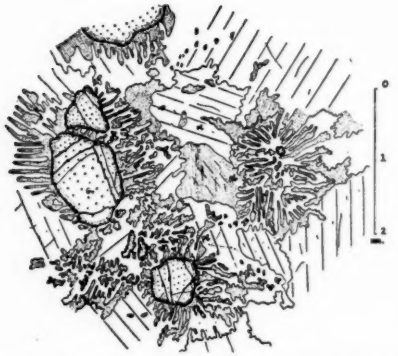

FIGURE 4.—MICROGRAPH OF GARNET CORONAS IN ECLOGITE

Note symplectite of hornblende and plagioclase around garnet forming a corona. Gr, Garnet; Pl, Plagioclase; Hb, Hornblende.

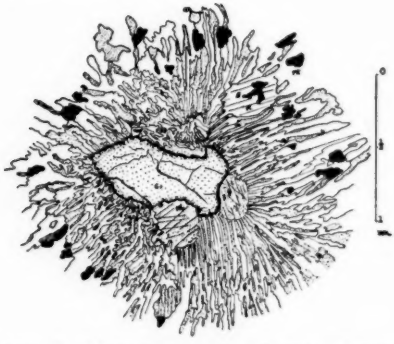

FIGURE 5.—MICROGRAPH OF A GARNET CORONA IN ECLOGITE

Note hornblende-plagioclase symplectite forming corona around garnet crystal and the zonal distribution of ores around the corona. Gr, Garnet; Hb, Hornblende; Mt, Magnetite. In Figure 2 of Plate 5 this corona can be seen.

rocks by the writer indicated that the composition of the calcic feldspar was very variable, thereby showing that the older analyses did not necessarily represent those of the most calcic feldspars. A pure sample of this feldspar (Pl. 4, fig. 1) was separated from rock C.50 and chemically analyzed. As a check on this analysis, the same sample was refined further and analyzed again. These analyses together with the older analyses are presented in Table 7.

Mr. Joensuu, Spectroscopist at the Geology Laboratory of Chicago University, made spectroscopic determinations on 12 specimens of calcic feldspar from these rocks. He devised a new technique for these analyses using the continuous-arc method, with Li as an interval standard for Na, and Sr as an interval standard for Ca. As absolute standards for comparison, glasses of the composition of pure anorthite, and Ab_1 An_8 were used by him as well as an analyzed albite supplied by the Bureau of Standards. These determinations (Table 7) are stated to have an accuracy within ±10 per cent.

A review of the literature showed that only 87 analyses of anorthite have been published, 20 of them before 1850, 46 between 1850 and 1900, and 21 since then. Most of these analyses do not conform to present-day standards of accuracy, and in many of them several constituents have not been determined. In Table 8, five analyses of anorthites from the literature and their physical properties, and three new analyses of anorthites are presented. Two are of sample C.50, while the third is a new analysis of anorthite occurring in allivallite ejected from Hakone volcano, Japan (reproduced here through the courtesy of Dr. Hisashi Kuno). As may be seen from the tabular statement, most known anorthites are from high-temperature rocks, and the most calcic feldspar recorded in a plutonic rock is $An_{93.3}$ in a hornblende-olivine-anorthite gabbro, described by Miller (1935). Sample C.50 with An_{98} is without doubt from a rock formed at temperatures of plutonic conditions, which has subsequently undergone chemical transformations and recrystallization.

N. L. Bowen, who has investigated high- and low-temperature plagioclases by means of x-rays, kindly examined some of these anorthites and indicated a value of $An_{99\text{-}100}$ for sample C.50. J. R. Goldsmith determined the minimum melting temperature of sample C.50 to be 1548°C. only 5° below the accepted melting point of pure synthetic anorthite.

Lacroix (1889, p. 323–326) made an excellent optical study of this feldspar and established

TABLE 7.—CHEMICAL COMPOSITION OF ANORTHITES OF SITTAMPUNDI COMPLEX

	1	2	3	4	5	6	7
SiO_2	42.50	42.00	43.00	42.09	42.80	43.74	43.88
Al_2O_3	37.50	34.00	34.50	38.89	38.06	36.40	36.18
Fe_2O_3	3.00	3.20	1.00		....	0.10	0.08
							SrO
CaO	15.00	15.00	15.60	15.78	19.31	19.38	19.37 + 0.01
Na_2O	.....	3.35	2.60	4.08	Tr	0.24	0.22
K_2O	.....	.....	.....			0.04	0.00
H_2O^+	2.00	1.00	1.00	.....	....	0.37	0.28
H_2O^-						0.04	0.08
Total.....	100.00	98.55	97.70	100.84	100.17	100.30	100.10
An %.....	89	83	87	81	96	97.5	98

Partial Spectroscopic Analyses of Some Anorthites

Sample No.	Na_2O	CaO	An	Ab
C.6	1.72	17.6	85.3	14.7
C.14	1.20	18.3	90.0	10.0
C.28	0.50	20.0	95.7	4.3
C.33	1.17	18.8	89.8	10.2
C.40	1.12	19.0	90.3	9.7
C.50	0.17	19.7	98.6	1.4
C.52	1.40	18.1	87.5	12.5
C.69	0.95	18.0	91.3	8.7
C.82	1.60	18.1	86.1	13.9
C.86	2.45	15.0	77.2	22.8
C.96	0.10	20.0	99.1	0.9
C.128	1.80	17.7	84.4	15.6

Analyst: Mr. Oiva Joensuu, Department of Geology, University of Chicago
(1) Chenevix (1802, p. 334)
(2, 3) Lacroix (1889)
(4) Silliman (1849, p. 391)
(5) Lacroix (1889)
(6, 7) New analyses of C.50. FeO, TiO_2, MgO, and MnO totally absent

its identity with anorthite. His description translated by Mallet (1891) follows:

"Microscopic sections show the anorthite in the form of rounded grains, the contact lines between which are often rectilinear. Twinning occurs on the carlsbad, albite and pericline types, but untwinned crystals are not uncommon. The form of the hemitrope plates on the albite type is most varied: sometimes a patch is composed of two or three large bands; sometimes on the other hand, there is a very large number of more or less narrow ones, but always very regular and not presenting any trace of dynamic phenomena. Very often carlsbad twinning is superposed on that of albite.

"The hemitrope-lamellae on the pericline type are only observed as a rule, in the midst of some of the bands belonging to the albite twinning.

"Extinctions in parallel light take place in the zone perpendicular (010) at very large angles—as much as 45°.

"Extinction on a plate parallel to the principal cleavage (001) occurs at 39° from the edge of (001) and (010) faces. Owing to the small thickness of such plates, I have not been able to obtain any parallel to the second cleavage (010).

"During the examination of a great number of sections, I succeeded in finding some sufficiently nearly perpendicular to the three principal axes of the ellipsoid of the indices, and in measuring their

TABLE 8.—CHEMICAL COMPOSITION AND OPTICAL PROPERTIES OF SOME ANORTHITES

Number	1	2*	3	4*	5*	6*	7	8
Author	F. S. Miller	S. Kozu	J. Kratzert	Z. Harada	S. Tsuboi	H. Kuno	A. P. Subramaniam	
Country	U.S.A.	Japan	Italy	Japan	Japan	Japan	India	
SiO_2	43.77	44.49	43.34	43.91	43.54	44.24	43.74	43.88
TiO_2	.....	.....	.....	.....	Tr	.....	.....	0.00
Al_2O_3	36.11	36.00	35.31	35.98	35.66	35.75	36.40	36.18
Fe_2O_3	0.09	0.08	0.65	0.15	0.58	0.64	0.10	0.08
FeO	.....	.....	.....	0.18	0.00	.....	0.00	.....
MnO	.....	.....	.....	.....	Tr	.....	0.00	.....
MgO	0.07	0.04	0.17	0.14	0.06	.....	0.00	0.00
CaO	18.73	19.29	19.93	19.58	19.53	18.88	19.38	19.37
Na_2O	0.67	0.59	0.39	0.48	0.26	0.16	0.24	0.22
K_2O	0.11	0.03	0.36	0.03	Tr	0.04	0.04	0.00
P_2O_5	.....	.....	.....	.....	Tr	.....	.....	SrO 0.01
H_2O+	0.40	.....	0.21	0.20	0.20	.....	0.37	0.28
H_2O-	.....	.....	.....	0.18	0.10	.....	0.04	0.08
Total	99.95	100.72	100.36	100.83	99.93	99.71	100.31	100.10
Analyst:	F. A. Gonyer	H. S. Washington	J. Kratzert	T. Nemoto	S. Tanaka	Ind. Chem. Lab. Tokyo	S. S. Goldich and E. K. Oslund	
Density	2.759	.....	2.760	.....	.....	.....	2.753	2.749
Anorthite %	93.3	94.6	95.0	95.6	97.6	98.3	97.5	98.0
Albite %	6.0	5.1	3.3	4.2	2.4	1.5	2.2	2.0
Orthoclase %	0.7	0.3	1.7	0.2	?	0.2	0.3	0.0
N_X	1.574	1.5747	1.5751	.....	1.576	1.5752 ± .0004†	1.5754 ± .0004	
N_Y	1.582	1.5827	1.5830	.....	1.584	1.5828 ± .0004	1.5833 ± .0004	
N_Z	1.586	1.5880	1.5882	.....	1.588	1.5882 ± .0004	1.5885 ± .0004	
$2V$	−79°	−77°.16′	−77°.10′	.....	−78°	−79°	76.8 to 77.7	
Dispersion	weak $r < v$	.....	.....	.....	very weak $r < v$	.....	$r < v$ weak	
Year published	1935	1914	1921	1933	1935	.....	.....	

* High-temperature anorthites from effusive rocks.

† Determined by A.P.S.

difference by means of Michel Levy's comparateur we have

$$N_Z - N_X = 0.013$$

$$N_Z - N_Y = 0.007$$

$$N_Y - N_X = 0.008$$

"The bisectrix is negative X. In the section perpendicular to the bisectrix, the trace of the plane of the optic axis makes an angle of 41° with the trace of the twinning of the albite type.

$$2E = \text{about } 130°.\text{"}$$

Optical Properties of Calcic Plagioclases

General.—The principal indices of refraction N_X and N_Z were measured on cleavage fragments by the immersion method, using a temperature cell and closely spaced calibrated oils. For the analyzed specimen the values N_X, N_Y, and N_Z were measured several times to ensure accuracy. The value N_Y was determined on the universal stage with great precision by

the following method. A grain of the feldspar showing low birefringence was removed from a thin section and mounted on the universal stage, using as mounting medium a liquid with a slightly higher index of refraction than N_Y of the feldspar. After allowing the setting to attain room temperature, the plate of plagioclase was oriented with N_X vertical and N_Z and N_Y in a plane parallel to the microscopic stage. The N_Y of the plagioclase was lower than that of the liquid for the above orientation. The microscope stage was then rotated until the index of the liquid was the same as that of the crystal for a particular direction, and the angle of rotation recorded. Having previously determined the birefringence and optic axial angle of the plagioclase, the partial birefringence ($N_Z - N_Y$) could be calculated. With this figure, and the number of degrees of rotation on the microscope stage from N_Y toward N_Z, the amount to be subtracted from the index of the liquid to obtain N_Y (or added to obtain N_Z) could be determined using Emmons' chart (1943, Pl. 10). This method may be adopted for measurement of indices of certain minerals under the ordinary microscope, if they have a cleavage or parting parallel to one of the principal optic indicatrix planes.

The birefringence of this anorthite was determined by Professor Hess, following his own technique (1949). The optic axial angle was measured on several grains which showed emergence of both the optic axes and the dispersion of optic angle recorded by use of filters. The physical and optical properties of anorthite C.50, together with some of the properties of synthetic anorthite, are shown below:

	Optical and physical properties of anorthite C.50	*Optical and physical properties of synthetic anorthite*
N_X*	= 1.5754 ± .0004	1.5760 ± .0004
N_Y*	= 1.5833 ± .0004	1.5838 ± .0004
N_Z*	= 1.5885 ± .0004	1.5895 ± .0004
Birefringence†		
$N_Z - N_X$	= 0.0131	0.0133
$2V_X$*	= −76.8, 76.9, 77.6, 77.7 Average value = 77.2°	−75.2°†
Dispersion*	= $r < v$ weak	—
Cleavages	001 and 010 well developed	—
Twinning	Albite, Baveno, Acline, Carlsbad, Pericline, Albite-Ala, Carlsbad-albite and Manebach Ala	—
Density	= 2.749 to 2.753 gm/cm³†††	2.765 gm/cm³***
Minimum melting temperature	= 1548°C.**	1553°C.††
Color	Snow-white, transparent crystals	White
Alteration	Incipient, occasionally to calcite and scapolite, easily attacked by strong HCl.	
Note	Extinction and cleavage angles were measured on the Universal Stage, but it will require several hundreds of determinations to arrive at precise values.	

* Measured by writer
† Measured by H. H. Hess
** Value determined by J. R. Goldsmith
†† Melting point of pure anorthite (synthetic)
*** Value determined by Geophysical Laboratory
††† Value determined by Rock Analysis Laboratory, Minneapolis

The principal indices of refraction, optic axial angles, and anorthite contents of some calcic feldspars are presented in Table 9. The An contents have been read from Hess's curve (unpublished), correlating the An content-refractive indices, and 2V of plagioclases for the

TABLE 9.—ANORTHITE CONTENT OF PLAGIOCLASES IN SITTAMPUNDI ROCKS AS DETERMINED BY VARIOUS METHODS

No.	$2V \pm 1°$	An per cent[1]	$N_X \pm .0008$	An[1] per cent	$N_Z \pm .0008$	An[1] per cent	An per cent by Universal Stage[2]	An per cent from spectroscopic data[3]
C.4	−79,−80,−81	85,88,90	1.5726	89.0	1.5826	87.5	.....	....
C.6	−81,−82	84,85	1.5694	84.5	1.5796	82.0	.....	85.3
C.11	.....	.....	1.5634	71.5	1.5715	68.0	.....	....
C.14	−80,−81,−82	84,85,88	1.5688	84.0	1.5812	85.0	.....	90.0
C.27	.....	.....	1.5686	84.0	1.5783	80.0	.....	....
C.28	−77.5,−78,−79	91,94,96	1.5738	94.5	1.5864	94.5	.....	95.7
C.33	−78,−79,−80	87,91,94	1.5724	89.0	1.5824	87.5	90,92,95, 98,99	89.8
C.34	−78,−79,−80	87,91,94	1.5686	87.0	1.5816	85.5	.....	....
C.35	.....	.....	1.5640	70.0	1.5736	71.5	.....	....
C.39	−78,−79,−80	87,91,94	1.5718	88.0	1.5824	87.5	.....	....
C.40	.....	.....	1.5724	91.0	1.5822	87.5	.....	90.3
C.41	+77,+78,+79	55,56,58	1.5545	50.0	1.5618	50.0	54,56,58	52.0
C.50	−77,−77.5,−78,−79	91,94,96,100	1.5754	98.0	1.5885	98.0	92,94,96, 98,99,100	98.0[4]
C.52	−80,−81	85,87	1.5708	87.0	1.5816	85.5	.....	87.5
C.53	.....	.....	1.5696	85.0	1.5816	85.5	.....	....
C.54	.....	.....	1.5662	77.0	1.5772	78.0	.....	....
C.58	−80	85	1.5686	84.0	1.5806	84.0	.....	....
C.66	.....	.....	1.5686	84.0	1.5806	84.0	.....	....
C.69	−78,−79,−80	87,91,94	1.5735	92.5	1.5864	94.5	90,92,94	91.3
C.71	−79,−81,+84	67,84,94	1.5642	72.5	1.5737	72.0	60,66,70	
			1.5718	90.0	1.5838	90.0	88,92,95	....
C.77	.....	.....	1.5636	71.5	1.5742	72.5	.....	....
C.82	−80,−81,−82	84,85,87	1.5705	87.0	1.5808	84.5	.....	86.1
C.86	−86	77	1.5655	76.0	1.5770	77.5	.....	77.2
C.88	.....	.....	1.5672	80.0	1.5754	75.0	.....	....
C.96	−76,−76.5,−77	100	1.5758	100.0	1.5888	99.0	100	99.1
C.117	.....	.....	1.5681	81.5	1.5781	79.5	.....	....
C.119	.....	.....	1.5706	87.0	1.5807	84.0	.....	....
C.120	.....	.....	1.5706	87.0	1.5812	85.0	.....	....
C.122	+78,+80	55,60	1.5527	48.0	1.5607	48.0	58,61	....
C.128	−83	82	1.5692	84.0	1.5788	81.0	.....	84.4

Note (1) An% deduced from optical data using a new set of curves by Professor Hess
(2) An% on 'U' Stage by Emmons, five-axis method
(3) Spectroscopic data by Mr. Joensuu of Chicago
(4) An% for samples C.50 and C.41 from chemical analysis.

range An_{65} to An_{100}. The anorthite contents of 12 specimens calculated from spectroscopic data are also included in the tabular statement. In Figure 6 these values have been plotted, together with Professor Hess's curves for N_X and N_Z. Most of the determined values for N_X fall very close to the N_X curve, while values of N_Z tend to lie below the curve between An_{80} and An_{90}. This is in conformity with Tsuboi's (1923) observation that N_X would be almost the same irrespective of the nature of the cleavage flakes.

Twinning.—Twinning laws in plagioclase feldspars have received recent attention from mineralogists, and the most significant contributions on the subject are those of Gorai (1950a; 1950b; 1950c; 1951) and Turner (1951), who arrived at almost identical conclusions independently. Gorai, after statistical analyses of thousands of plagioclase twins in

common igneous and metamorphic rocks, classified the twins into types *A* and *C*. The *A* type includes the albite, pericline, and acline twinning as complex as that of igneous plagioclase. The twinned condition and crystal habit of such plagioclases are considered by him rel-

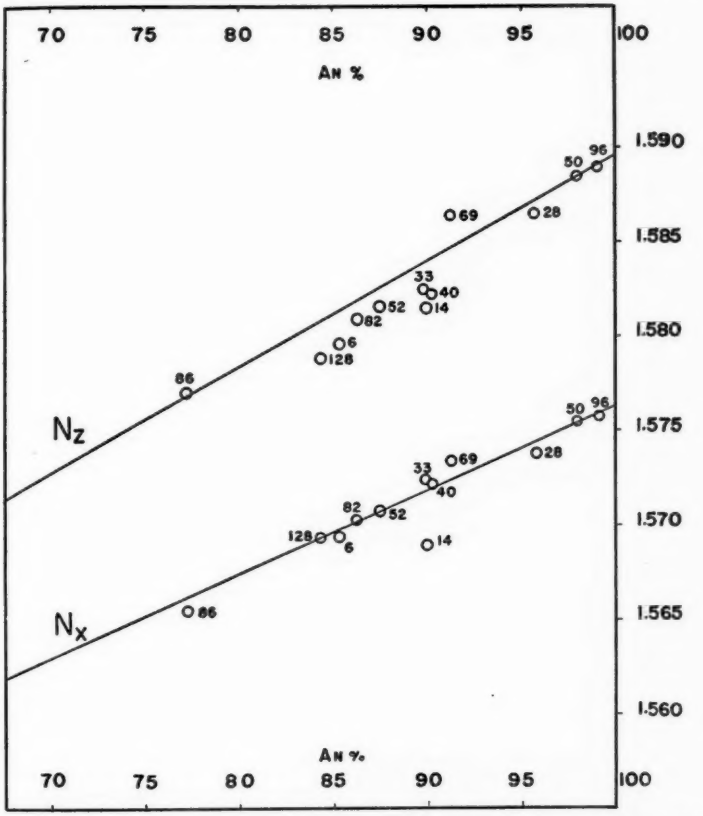

FIGURE 6.—CURVE CORRELATING INDICES OF REFRACTION AND AN CONTENT OF CALCIC PLAGIOCLASES

N_X and N_Z of Sittampundi plagioclases plotted against composition fixed from spectroscopic data and chemical analysis of C.50. Heavy lines indicate new curves of H. H. Hess for calcic plagioclase. Numbers along curve represent rocks from which feldspars were isolated for study.

twins, and the *C* type the Carlsbad, Carlsbad-albite, Baveno, Ala, Manebach Ala, and Albite-Ala twins. Gorai considers the *C* type to be characteristic of plagioclases in rocks crystallized from a melt, and the *A* type characteristic of metamorphic and metasomatic rocks. On the basis of his own observations and those in the literature, Turner has analyzed the question of twinning of plagioclase in rocks and reached similar conclusions. Turner (1951, p. 583) points out that, in amphibolites of igneous origin, coarse plagioclase may show ict and indicative of the igneous parentage of the amphibolite in which they occur.

The plagioclases in the Sittampundi rocks consist of an equal proportion of twinned and untwinned individuals. Results of twin determinations carried out on the plagioclases of these rocks following Emmons (1943) are presented in Table 10. Following Gorai, there are 56 *A* twins and 34 *C* twins in a total of 90 determinations. While in general these plagioclases exhibit twinning tendencies indicative of metamorphic rocks, the presence of a fair pro-

portion of *C* type twins indicates an igneous parentage for these rocks. It is believed that much of the twinning of the plagioclases in these rocks was obliterated during deformation and recrystallization of the complex. Polysynthetic twins of labradorite in the eclogite gabbros display bent twin lamellae, which in some cases disappear from portions of a crystal, supporting Turner's conclusion that in plagioclases in tectonites, resulting from deformation proceeding simultaneously with crystallization, lamellar twinning is on the whole much less well developed. Emmons and Gates (1943, p. 292–293) consider twinning in plagioclases a secondary phenomenon as a result of forces external to the crystal, while Donnay (1943, p. 1651) considers it a function of crystal growth controlled by the geometry of the space lattice. Observations on the twinning in Sittampundi rocks support Donnay's view. If twinning is an external phenomenon and essentially secondary as contended by Emmons, one would expect an abundance of twins in slightly deformed recrystallized rocks, in which there is mutual interference of grains and other factors considered to favor twinning.

TABLE 10.—TWINNING LAWS OF PLAGIOCLASE FELDSPARS IN THE SITTAMPUNDI ROCKS

Type of twin	C.33	C.41	C.50	C.69	C.71	C.122	C.128
Normal Twins							
Albite	4	3	8	2	2	1	3
Baveno	1	..	1	..	1	..	..
Manebach	3	..	..	2	2	..	1
Parallel Twins							
Acline	4	..	2	1	1	..	1
Ala	..	1	..	..	..	2	..
Carlsbad	1	2	1	..	..	2	..
Pericline	6	1	6	3	3	1	4
Complex Twins							
Albite-Ala	2	..	2	2	1	..	..
Carlsbad-Albite	1	1	1	1	..	1	..
Manebach-Ala	..	..	1	..	..	..	..
Manebach-Acline	..	..	..	1	..	..	..
Total	22	8	22	12	10	7	9

A Twins (Albite, Acline, and Pericline)—56
C Twins (Manebach, Ala, Baveno, Carlsbad Albite-Ala, Carlsbad-Albite, Manebach-Ala, and Manebach-Acline)—34

C.33, C.50, C.69, and C.128—Rocks of the anorthosite series

C.41 and C.122—Rocks of the eclogite-gabbro series

C.71 Cordierite-corundum-sillimanite-anthophyllite-anorthite rock

Compositional variations.—In general a compositional variation of 2 per cent An, and occasionally as much as 3 per cent, is indicated by the plagioclases of most of the rocks. This was apparent during index determinations when a statistical basis was adopted to avoid inconsistencies. It is believed that chemical transformations during metamorphism have contributed to the formation of feldspars of varying composition in the same rock.

The plagioclase feldspars in the eclogite gabbros range from An_{50} to An_{72}. They show their igneous parentage by displaying a fair proportion of *C* twins. Some of the larger crystals contain bands of regularly arranged inclusions, which have lower indices of refraction than the host feldspar, showing them to be liquid or gas inclusions. Professor Hess (Personal communication) noticed similar inclusions in the groundmass feldspar of stony meteorites, and such inclusions in the plagioclases of these eclogites may well indicate their original igneous character.

Chemical analysis of plagioclases from rock C.41

SiO_2	54.90
TiO_2	0.01
Al_2O_3	28.72
Fe_2O_3	0.08
MgO	0.08
CaO	11.07
Na_2O	5.24
K_2O	0.02
H_2O+	0.04
H_2O-	0.00
	100.16

G.....2.690 gm/cm³ at 23/4°C.
Average composition.....$An_{53.6}$
Calcic rims.....12 per cent An_{80}
Core.....88 per cent An_{40}

The plagioclases of the analyzed eclogite C.41 have thin, calcic rims with a core of An_{50}. As very few feldspars in this compositional range have been analyzed, the feldspar was carefully separated from the rock and chemically analyzed. Statistical analysis of the chemically analyzed material by Dr. J. R. Smith showed about 12 per cent calcic rims with composition An_{80}, which indicates the core to have a composition An_{50}, since the chemical analysis calculates to an average composition of $An_{53.6}$.

Barth (1952, p. 96) states that zoned plagioclases of metamorphic rocks generally show inverse order, with a sodic core and calcic shell. Hills (1936, p. 55) considers sudden release of pressure during crystallization as a potent factor in the production of reversed zoning of plagioclases. Probably the inverse zoning in the plagioclase of the eclogites may have resulted during diaphthoresis accompanying sudden release of pressure; and consequent chemical readjustment of the mineral phases present.

Summary of observations on plagioclases.—The plagioclases in the anorthosite series are very calcic and fall between An_{75} and An_{100}. They are generally 1–2 mm long, but occasionally crystals up to 5 cms occur in pegmatitic rocks. In thin sections of rocks they have subhedral boundaries, imparting a mosaic texture. They are exceptionally fresh and devoid of inclusions and secondary alteration products, though scapolitization is noticed occasionally. They also exhibit replacement by clinozoisite, garnet, and corundum.

The following conclusions have been reached on the basis of the above study.

(1) The anorthositic rocks of this complex contain calcic plagioclase exceptionally rich in the anorthite molecule, as indicated by the chemical analysis of one specimen, spectroscopic analyses of 12 others, and optical study of more than 40 specimens. Plagioclases, separated from rocks C.96 and C.50, have anorthite contents of 99.1 per cent and 98 per cent, indicated by spectroscopic and chemical analyses respectively, and these represent the purest specimens of natural anorthite known.

(2) Several accepted optical methods were tried to deduce the composition of these feldspars, and the indices of refraction on cleavage flakes proved most reliable indicators of the composition because they showed perceptible changes for small variations in composition.

TABLE 11.—ANALYSES OF CLINOZOISITES FROM ANORTHITE-CORUNDUM ROCKS OF SITTAMPUNDI

	1	2	3	4	5
SiO_2	45.0	40.0	42.0	38.6	38.3
Al_2O_3	28.0	25.0	25.5	32.5	31.9
Fe_2O_3	11.0	11.5	14.0	..	...
FeO	...	...	...	1.9	4.4
CaO	15.0	21.5	16.0	23.9	23.5
Loss of ignition	1.0	2.0	2.5	2.7	2.7
Total	100.0	100.0	100.0	99.6	100.8

(1) Thallite in crystals with a rough surface. Analyst: R. Chenevix (1802 p. 335)

(2) Thallite in prisms like tourmaline. Analyst: R. Chenevix (1802)

(3) Thallite in fragments, transparent yellow. Analyst: R. Chenevix (1802)

(4) White Fouqueite. Analyst: A. Lacroix (1889)

(5) Yellow Fouqueite. Analyst: A. Lacroix (1889)

Value of N_X measured on grains was better suited for fixing the composition as it was nearly the same for cleavage fragments on both (001) and (010).

(3) A statistical analysis of the twinning laws of plagioclases in these rocks indicated igneous parentage. The fact that deformation and recrystallization have obliterated some original twinning directly contradicts the concept of Emmons and Gates (1943, p. 292–293), who believe that twinning is accentuated by external factors. It appears that twinning is a function of crystal growth controlled by the geometry of the space lattice, as proposed by Donnay. The fact that more complex types of twins are encountered in magmatic rocks is consistent with this concept.

(4) The calcic feldspars show frequent compositional variations of ± 2 per cent within a single thin section. Larger compositional variations may be attributed to chemical transformations during metamorphism and recrystallization.

(5) If in the future it is found desirable to restrict the names albite and anorthite to the

TABLE 12.—COMPOSITION OF CLINOZOISITE C.39

	Weight per cent	Mol ratio	Ratio O, OH, Cl	Ratio metals	Metal atoms	
SiO_2	38.64	644	1288	644	6.021	6.030
TiO_2	0.14	1	2	1	0.009	
Al_2O_3	27.69	272	816	544	5.090	5.980
Fe_2O_3	7.57	47	141	94	0.890	
FeO	0.14	2	2	2	0.019	4.011
MnO	0.04	.....	.....	.....	...	
MgO	0.11	3	3	3	0.028	
CaO	23.79	424	424	424	3.964	
H_2O^+	1.84	102	102	204	1.907	1.935
H_2O^-	.....	.....	.....	.....	...	
Cl	0.07	3	3	3	0.028	
	100.03		2781			
O for Cl	0.02		2			
	100.01		2779			

Analyst: Eileen K. Oslund

As the unit cell of epidote-clinozoisite series contains 26 (O, OH) atoms, the multiplication factor necessary to bring the oxygen ratios up to this sum would be $\frac{26}{2.779} = 9.35$

Structural Account *Structure Type:* $X_2A_4B_6C_6Y_{26}$

Ionic ratio		X	A	B	C	Y	Electrical charges (+)	Electrical charges (−)
Ca^{2+}	3.964	....	3.964	.....	.....	.....	7.928	.....
Fe	0.019	....	0.008	0.011	.....	.....	0.038	.....
Mg	0.028	....	0.028	.....	.....	.....	0.056	.....
Fe^{3+}	0.890	....	.....	0.890	.....	.....	2.670	.....
Al	5.090	....	.....	5.090	.....	.....	15.270	.....
Ti^{4+}	0.009	....	.....	0.009	.....	.....	0.036	.....
Si	6.021	....	.....	.....	6.021	.....	24.084	.....
	24.065	....	.....	.....	.....	24.065	.....	48.130
O^{2-}	1.907	....	.....	.....	.....	1.907	.....	1.907
OH^{1-}	0.028	....	.....	.....	.....	0.028	.....	0.028
Cl^{1-}		....	.....	.....	.....	.....	.....	.....
		....	4.00	6.00	6.021	26.00	50.082	50.065

end components alone, it is suggested that the name indianite be revived and used for all natural feldspars with compositions An_{90} to An_{100}, restricting the name anorthite to the theoretical end molecule hitherto unrecorded in nature. This would be consistent with the

accepted law of nomenclature and would acknowledge Bournon's contribution to mineralogy.

Clinozoisite

The rocks of the anorthositic series contain varying proportions of the epidote-clinozoisite group of minerals, and the following assemblages occur frequently: (1) anorthite, corundum, clinozoisite; (2) anorthite, clinozoisite, garnet (grossularitic); and (3) anorthite, clinozoisite, hornblende. While more mafic anorthite rocks are relatively free from this mineral, the felsic anorthosites carry a fair proportion.

Lacroix (1889) on the basis of his optical and chemical study considered this mineral a dimorphic form of zoisite and called it Fouqueite, a name which has become obsolete in mineralogical nomenclature. The chemical analyses of the mineral made by Lacroix in 1889 and Chenevix in 1802 are tabulated in Table 11, and Tables 12, 13, and 14 show the chemical composition and physical properties of clinozoisite separated from rock C.39, and similar clinozoisites from elsewhere. The ratios of metal atoms calculated from the analysis agree very well with the accepted empirical formula for the epidote-clinozoisite series, $H_2O \cdot 4CaO \cdot 3(AlFe)_2O_3 \cdot 6SiO_2$.

In thin section the mineral occurs as rounded grains and as anhedral and euhedral crystals, ranging in size from a fifth of a millimeter to as much as 5 mm with occasional development of large crystals (Figs. 7, 8). Polysynthetic twinning, zoning, and anomalous birefringence are common. Johnstone (1949) and Orlov (1926) noticed changes in the dispersion of optic axes, and the former indicated a relationship between the extinction angle and optic angle. In the present instance, the changes in dispersion of the optic axes, and wide variations in the optic and extinction angles have been noticed.

Changes in composition within a single specimen of the mineral isolated from a rock are indicated by the variations in refractive indices for different magnetic fractions (Table 13). Index determinations indicate 5–30 per cent epidote molecule for the clinozoisites from the anorthosites. Occasionally a few grains with extinction angles larger than 45° have been noticed; according to Orlov (1926), these should be pure clinozoisite. Johnstone (1949) has stated that, when the iron content is low, temperatures and pressures prevailing during the period of crystallization may influence the optics of clinozoisite. The wide variation in optical properties of the clinozoisites under study warrants concurrence with Johnstone's view.

TABLE 13.—PHYSICAL AND OPTICAL PROPERTIES OF CLINOZOISITE C.39

	R_2O_3	RO (CaO + FeO + MgO)	SiO_2
Fe_2O_3	47	63	94
Al_2O_3	272	361	544
Calculated:	319	428.5	638
Actual:	319	429.0	644

14.8% of H $Ca_2Fe_3Si_3O_{13}$
85.2% of H $Ca_2Al_3Si_3O_{13}$
} $H_2O \cdot 4(CaO + FeO + MgO) \cdot 3(Al, Fe)_2O_3 \cdot 6SiO_2$

REFRACTIVE INDICES OF DIFFERENT MAGNETIC FRACTIONS OF C.39

Field strength (Amperes)	N_X	N_Y	N_Z
0.60	1.7202 ± 001	1.7299 ± 001	1.7329 ± 001
0.65	1.7178 ± 001	1.7288 ± 001	1.7324 ± 001
0.70	1.7160 ± 001	1.7210 ± 001	1.7288 ± 001
1.00	1.7154 ± 001	1.7158 ± 001	1.7196 ± 001

Optical axial angle $2V_X$ = 85° to 95° (variable; sometimes 0°)
Extinction angle $X \wedge c$ = 0°–36° (variable)
Dispersion of optic axes: variable; weak to strong
Dispersion of optic angle: $r > v$ to $r < v$
Orientation: Optic plane = {001}
Elongation parallel to b axis
Determined density at 28/4°C = 3.390 gm/cm³
Color: In hand specimens lemon yellow to pinkish brown: in thin sections pale yellow to colorless with faint pleochroism

TABLE 14.—CHEMICAL COMPOSITION AND OPTICAL PROPERTIES OF SOME CLINOZOISITES

	1	2	3	4	5
SiO_2	37.57	39.02	38.54	38.64	37.80
TiO_2	0.18	tr	.....	0.14	0.10
Al_2O_3	28.20	28.64	28.39	27.69	27.63
Fe_2O_3	6.61	6.81	6.89	7.57	7.62
FeO	1.87	0.34	0.50	0.14	0.19
MnO	0.12	tr	.....	0.04	0.04
MgO	.....	tr	tr	0.11	0.29
CaO	23.56	23.73	24.12	23.79	24.56
Na_2O	0.08	.....	.....	.....	.....
K_2O	0.01	.....	.....	.....	.....
H_2O^+	1.93	1.76	2.26	1.84	1.83
H_2O^-	.....	.....	.....	.....	.....
Cl	.....	.....	.....	0.07 Less O for Cl: 0.02	.....
Total:	100.13	100.30	100.70	100.01	100.06
Author:	H. Heritsch, 1931	H. H. Thomas, 1905	F. W. Clarke, 1894	A.P.S.	H. G. Tempel, 1938
% Total iron as Fe_2O_3	8.67	7.18	7.43	7.72	7.83
X	.....	1.714	.....	(1.7154–1.7202) 1.7173	1.712
Y	.....	1.7196	.....	(1.7158–1.7299) 1.7239	1.723
Z	.....	1.725	.....	(1.7196–1.7329) 1.7284	1.735
$2V$	.....	90°25′	.....	85–95°	.....
$X \wedge c$	.....	1°	.....	0–36°	.....
Density	.....	3.37	.....	3.390	3.324

Cordierite

Cordierite occurs in a peculiar assemblage composed of anorthite-bytownite, corundum, cordierite, anthophyllite, and sillimanite, and occurring as inclusions in the anorthositic rocks.

The mineral, which occurs as grains of varying size in a matrix of corundum and anorthite, is readily identified in hand specimens by its blue color and greasy luster. In thin section the mineral is distinguished from untwinned anorthite by its lower indices of refraction and by the presence of aggregates of acicular sillimanite and inclusions of anthophyllite, which range in size from acicular crystals to dusty particles and impart a cloudy appearance to the mineral in thin section. It is devoid of pleochroic haloes, and alteration to pinite is rare. Pleochroism is not noticeable, indicating it is an iron-poor, magnesia-rich variety. Occasionally the mineral displays lamellar twinning of a pseudo-Baveno type, simulating plagioclase feldspar. The pole of the composition plane, when plotted on a stereogram and transposed on the composition curves for plagioclase feldspars, falls on the "Baveno" curve, a feature recorded in cordierites from South Africa by Willemse (1938) and Brink (1950).

The chemical composition of this cordierite is shown in Table 15, and the composition and physical properties of some magnesian cordierites are shown in Table 16. The calculation of the molecular formula of the mineral after the method of Winchell (1937) and its physical and optical properties are shown in Table 17.

The optical properties of cordierite have been

investigated by several workers all over the world. Krishnan (1924), Pehrman (1932), Shibata (1936), Winchell (1937), Thiele (1940), and Folinsbee (1941) have attempted to relate its anomalous characters to the chemical

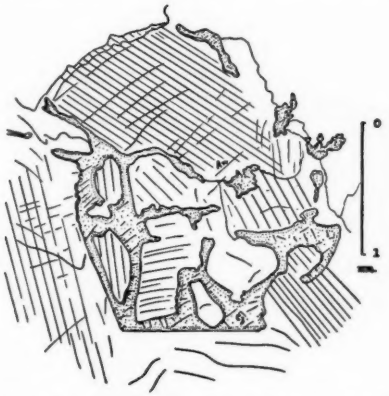

FIGURE 7.—MICROGRAPH OF CLINOZOISITE IN ANORTHITE GNEISS

Note clinozoisite replacing anorthite and tending to develop crystal form. Cz, Clinozoisite; An, Anorthite

composition. Folinsbee suggested that alkalis and lime play an important role in determining the size of the optic angle and the sign of the mineral, and he considered the size of the optic angle of cordierite to be a function of effective alkali content [$(K_2O + Na_2O) - CaO$]. Four analyses of cordierite published since then, and the present one, do not support this concept, nor do some of the older analyses of Oppenheimer (1914) and Pehrman (1932). Table 16 shows that positive cordierites do not differ chemically from negative ones. Folinsbee's curve relating the size of optic angle to the percentage of effective alkali content in cordierites is shown in Figure 9, with the plots of some analyses of cordierites. Thiele (1940) discussed the effects of water content and isomorphous substitution of Si and Mg for Al on the optical properties of cordierite, and the writer attempted to correlate the chemistry and optics of cordierites found in literature. Nothing satisfactory could be evolved owing to the paucity of precise data. While agreeing with Stewart (1942) and Heald (1950) that sufficient data are not available to establish specific relationships between the chemical and optical characters of cordierite, available information in the literature suggests that these optical anomalies may be due to peculiarities in the distribution of the ions in the cordierite

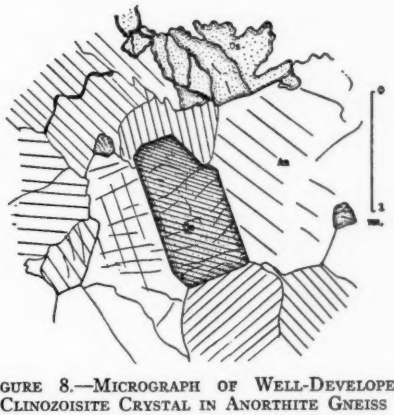

FIGURE 8.—MICROGRAPH OF WELL-DEVELOPED CLINOZOISITE CRYSTAL IN ANORTHITE GNEISS

Note how the crystal of clinozoisite has developed by replacing several anorthite plates. An, Anorthite; Cz, Clinozoisite

structure. Statistical x-ray analyses of positive and negative cordierites are necessary in evaluating the merits of this suggestion. The thermal history probably has nothing to do with the anomalous optical peculiarities of cordierites found in metamorphic assemblages.

Anthophyllite

Anthophyllite occurs with monoclinic amphiboles in some anorthositic rocks and in most chromitites, as honey-brown prismatic crystals, ranging from 1 mm to as much as 10 cm long (Fig. 10; Pl. 4, fig. 2). In some chromitites the bladed crystals display an unusual play of colors caused by microscopic inclusions of chrome spinel, noticeable in thin sections.

The chemical composition of the mineral and the distribution of the various ions are presented in Table 18. The analyzed anthophyllite is exceptionally rich in alumina and magnesia and is similar to anthophyllite from Mason's Creek, described by Henderson (1931). This, according to Rabbitt (1948), is an aluminian anthophyllite, or according to Berman (1937), Winchell (1938), Tilley (1939), Sundius (1944),

TABLE 15.—COMPOSITION OF CORDIERITE C.71

	Weight per cent	Mol ratio	Ratio O, OH	Ratio metals	Metal atoms
SiO_2	49.54	825	1650	825	4.859
TiO_2	0.03	.....	.....	.....	.....
Al_2O_3	33.42	328	984	656	3.863
Fe_2O_3	0.14	1	3	2	0.012
FeO	3.75	52	52	52	0.306
MnO	0.09	1	1	1	0.006
MgO	11.34	281	281	281	1.655
CaO	0.10	2	2	2	0.012
Na_2O	0.32	10	10	20	0.120
K_2O	0.01	.....	.....	.....	.....
H_2O^+	1.32	73	73	146	0.860
H_2O^-	0.03	.....	.....	.....	.....
F	0.01	.....	.....	.....	.....
Cl	0.01	.....	.....	.....	.....
	100.10		3056		

Analyst: Eileen K. Oslund

The unit cell of cordierite contains 18 (O, OH) atoms, and the multiplication factor necessary to bring the oxygen ratios up to this would be: $\frac{18}{3.056} = 5.89$

Structural Account *Structure Type*—$X_0A_2B_4C_5Y_{18}$

Ionic ratio		*X*	*A*	*B*	*C*	*Y*	Electrical charges (+)	Electrical charges (−)
K^{1+}		....	.....	.....	.....	.....	.....	.....
Na	0.120	....	.....	0.120	.....	.....	0.120	.....
Ca^{2+}	0.012	....	0.012	.....	.....	.....	0.024	.....
Mn	0.006	....	0.006	.....	.....	.....	0.012	.....
Fe	0.306	....	0.306	.....	.....	.....	0.612	.....
Mg	1.655	....	1.655	.....	.....	.....	3.310	.....
Fe^{3+}	0.012	....	.....	0.012	.....	.....	0.036	.....
Al	3.863	....	.....	3.863	.....	.....	11.589	.....
Ti^{4+}	....	....	.....	.....	.....	.....	.....	.....
Si	4.859	....	.....	.....	4.859	.....	19.436	.....
O^{2-}	17.14	....	.....	.....	.....	17.14	.....	34.28
OH^{1-}	0.86	....	.....	.....	.....	0.86	.....	0.86
		....	1.979	3.995	4.859	18.00	35.139	35.14

and Eskola (1950) a gedrite. Rabbitt (1948) has proposed, without any specific reasons, that the name gedrite be dropped. It appears to the writer more reasonable to retain the name gedrite since, according to Sundius (1944), anthophyllite-gedrite represents one of several isomorphic series in the amphibole group. Rabbitt presented a curve, expressing relationship between N_Z and the weight percentage of (FeO + Fe_2O_3 + MnO + TiO_2). The refractive index N_Z of the analyzed anthophyllite does not fit Rabbitt's curve. This may be attributed to the high alumina content of the analyzed mineral, as the more aluminian anthophyllites used by Rabbitt generally show points for N_Z above the curve. This distinctive optical character of the aluminian variety warrants retention of the name gedrite.

TABLE 16.—CHEMICAL COMPOSITION AND OPTICAL PROPERTIES OF SOME MAGNESIAN CORDIERITES

Number:	1	2	3	4	5	6	7
Author:	Pehrman	Tilley	Subramaniam	Oppenheimer	Thiele	Oppenheimer	Thiele
Locality:	Attu	Antarctica	India	Twedestrand	Twedestrand	Bodenmais	Orijarvi
SiO_2	50.15	47.96	49.54	49.18	48.05	48.58	49.60
TiO_2	0.38	0.00	0.03	.....	.....	.....	.....
Al_2O_3	33.07	31.56	33.42	32.28	33.37	31.47	31.19
Fe_2O_3	1.52	1.03	0.14	0.08	0.09	1.85	1.19
FeO	2.22	3.24	3.75	4.05	4.01	4.90	4.10
MnO	0.12	1.09	0.09	.....	tr	.....	.....
MgO	11.01	12.16	11.34	11.25	11.11	10.68	11.13
CaO	0.29	0.00	0.10	.....	0.05	tr	0.23
Na_2O	0.14	0.33	0.32	0.65	0.26	0.35	0.21
K_2O	0.08	tr	0.01	.....	0.39	.....	0.06
H_2O+	1.37	2.80	1.32	2.04	2.75	1.82	2.33
H_2O-	0.09	n.d.	0.03	0.27	.....	0.14	0.08
F	.....	.....	0.01	.....	.....	.....	.....
Total	100.44	100.17	100.10	99.80	100.08	99.79	100.12
Percentage of $Mg_2Al_4Si_5O_{18}$	84.3	84.2	83.6	83.0	82.9	81.6	79.5
Analyst:	Pehrman	A. P. White	E. K. Oslund	Dittrich	Thiele	Dittrich	Thiele
Density	2.588	.....	2.591	2.581	2.581	2.603	2.598
N_X	1.527	1.534	1.5392	1.5358	1.536	1.5400	1.541
N_Y	1.532	.....	1.5438	1.5406	.....	1.5460	1.545
N_Z	1.538	1.543	1.5462	1.5428	1.543	1.5486	1.547
$2V$	88°	76°	66 ± 2°	69°26′	65°36′	65°36′	78°12′
Optic sign	+	+	−	−	−	−	−
Parent rock	Anthopyllite gneiss	Gneiss	Cordierite Corundum-Sillimanite Anthophyllite bytownite rock	Gneiss	Gneiss	Gneiss	Gneiss

The following general formula has been proposed for the anthophyllite series by Rabbitt:

$$X_7\ Y_8\ O_{22}\ (OH, F, Cl)_2$$

where X is mainly Mg, Fe^{2+}, Al, and in minor

TABLE 17.—COMPOSITION AND OPTICAL PROPERTIES OF CORDIERITE C.71

	RO	Al_2O_3	SiO_2
MgO	140.5	281	702.5
FeO	26	52	130
MnO	0.5	1	2.5
Fe_2O_3	1	2	5.0
Calculated	168	336	840.0
Actual	168	328	825.0

83.6% $Mg_2Al_4Si_5O_{18}$
16.4% $(Fe, Mn)_2Al_4Si_5O_{18}$

Determined density at 27/4°C: 2.591 gm/cm³
Refractive indices in sodium light:
N_X 1.5392 ± .0005
N_Y 1.5438 ± .0005
N_Z 1.5462 ± .0005
Optic axial angle 2V in sodium light: 64°, 64.5°, 65°, 66°, 67°, 68°, 69°, 70°
General value: 66 ± 2°
Dispersion of optic angle: $r < v$ weak
Inclusions of sillimanite and anthophyllite noticed in abundance in thin sections
Color: in fragments grayish blue to dark blue; in translucent chips pale blue; in 80 mesh lilac blue; in thin sections very pale blue to colorless and nonpleochroic

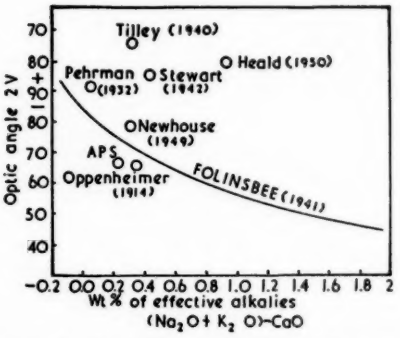

FIGURE 9.—CURVE SHOWING RELATION BETWEEN OPTIC AXIAL ANGLE AND $(K_2O + Na_2O)$—CaO FOR CORDIERITE

Curve of Folinsbee (1941). New analyses since Folinsbee's study and some older analyses shown by small circles

part Mn, Ti, Fe^{3+}, Ca, Na, and K; and *Y* mostly Si with part replacement by Al.

Berman (1937) proposed the following formula for gedrite: $(Mg \cdot Fe \cdot Al)_7(Al \cdot Si)_8O_{22}(OH)_2$. In the present instance the following formula is indicated by the chemical analysis: $X_{7.36}Y_8O_{22}(OH, F, Cl)_{1.98}$ or

$$[(Na_{0.47}Ca_{0.12}Mn_{0.02}Mg_{4.24}Fe_{1.05}Fe^{3+}_{0.22} \cdot Al^{3+}_{1.22}Ti_{0.045}][Si_{6.33}Al_{1.67}][OH, F, Cl]_{1.91}$$

which are in accord with those proposed by Berman and Rabbitt. The physical properties of the analyzed specimen are:

$N_X = 1.6415 \pm .0005$
$N_Y = 1.6494 \pm .0005$
$N_Z = 1.6578 \pm .0005$

Birefringence, $N_Z - N_X = 0.0163$
Optic axial angle $2V = +88° \pm 2°$
Orientation $= Z = c, Y = b$
Elongation = Positive
Absorption $= X = Y < Z$

X = Pale tan gray
Y = Pale tan gray
Z = Tan gray to clove brown

Dispersion = Weak
Density at 26/4°C = 3.164 gm/cm³

The anthophyllite from some chromities has lower values for N_Z, as shown below, which may be due to their being more magnesian.

C.94 $N_Z = 1.6372 \pm .0005$
C.72 $N_Z = 1.6436 \pm .0005$

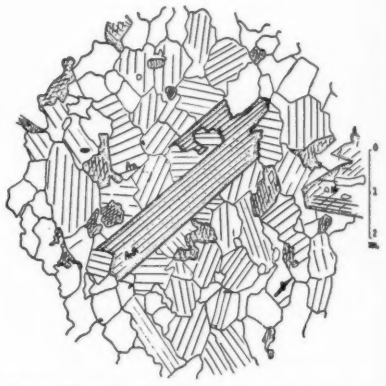

FIGURE 10.—MICROGRAPH OF ANTHOPHYLLITE IN ANORTHOSITE

Note bladed crystal of anthophyllite and smaller crystals of hornblende (edenite). Note mosaic texture of rock due to subhedral anorthite crystals. An, Anorthite; Anth, Anthophyllite; Hb, Hornblende

TABLE 18.—COMPOSITION OF ANTHOPHYLLITE C.58

	Weight per cent	Mol. ratio	Ratio O, OH, F, Cl	Ratio metals	Metal atoms
SiO_2	45.50	757	1514	757	6.330
TiO_2	0.23	3	6	3	0.025
Al_2O_3	17.64	173	519	346	2.890
Fe_2O_3	2.16	13.5	41	27	0.220
FeO	9.04	126	126	126	1.050
MnO	0.16	2	2	2	0.017
MgO	20.51	508	508	508	4.240
CaO	0.87	15	15	15	0.120
Na_2O	1.73	28	28	56	0.470
K_2O	0.00	.....	.....	.....	.....
H_2O^+	2.12	117	117	234	1.95
H_2O^-	0.09	.....	.....	.....	.....
Cl	0.05	2	2	2	0.017
F	0.02	1	1	1	0.008
	100.12		2879		
O for Cl and F	0.02		2		
	100.10		2877		

Analyst: S. S. Goldich

Multiplication factor to build 24 (O, OH) atoms in unit cell = $\frac{24}{2.877} = 8.35$

Structural Account *Structure Type:* $(X+A+B)_7C_8Y_{24}$

Ionic ratio		X	A	B	C	Y	Electrical charges (+)	Electrical charges (−)
K^{1+}	0.00	....	.....	.....	.....	.....	.....	.....
Na	0.47	0.47	.....	.....	.....	.....	0.47	.....
Ca^{2+}	0.12	....	0.12	.....	.....	.....	0.24	.....
Mn	0.017	....	0.017	.....	.....	.....	0.034	.....
Fe	1.05	....	1.05	.....	.....	.....	2.10	.....
Mg	4.24	....	.....	4.24	.....	.....	8.48	.....
Fe^{3+}	0.22	....	.....	0.22	.....	.....	0.22	.....
Al	2.890	....	.....	1.22	1.67	.....	8.67	.....
Ti^{4+}	0.025	....	.....	0.025	.....	.....	0.100	.....
Si	6.330	....	.....	.....	6.33	.....	25.320	.....
O^{2-}	22.025	....	.....	.....	.....	22.025	.....	44.050
OH^{1-}	1.950	....	.....	.....	.....	1.950	.....	1.950
Cl^{1-}	0.017	....	.....	.....	.....	0.017	.....	0.017
F^{1-}	0.008	....	.....	.....	.....	0.008	.....	0.008
		0.47	1.187	5.705	8.00	24.00	46.074	46.025

TABLE 19.—COMPOSITION OF AMPHIBOLE C.34

	Weight per cent	Mol. ratio	Ratio O, OH, F, Cl	Ratio metals	Metal atoms
SiO_2	42.32	705	1410	705	6.330
TiO_2	0.27	4	8	4	0.035
Al_2O_3	15.62	153	459	306	2.662
Fe_2O_3	4.22	26	78	52	0.452
Cr_2O_3	0.06	.....	.....	.....	.....
FeO	6.78	94	94	94	0.818
MnO	0.15	2	2	2	0.017
MgO	13.68	339	339	339	2.950
CaO	11.78	210	210	210	1.830
Na_2O	2.41	39	39	78	0.678
K_2O	0.34	3	3	6	0.052
H_2O^+	2.13	118	118	236	2.053
H_2O^-	0.11	.....	.....	.....	.....
Cl	0.03	1	1	1	0.008
F	0.02	1	1	1	0.008
	99.92	.....	2762	.....	.....
O for Cl & F	0.02	.....	1	.....	.....
	99.90	.....	2761	.....	.....

Analyst: Eileen K. Oslund; Halogens by P. K. Kuroda

Multiplication factor to build 24 (O, OH) atoms in unit cell = $\frac{24}{2.761} = 8.70$

Structural Account *Structure Type:* $X_{0\text{-}1}A_2B_5C_8Y_{24}$

Ionic Ratio		*X*	*A*	*B*	*C*	*Y*	Electrical charges (+)	Electrical charges (−)
K^{1+}	0.052	0.052	.....	.....	.....	.....	0.052	.....
Na	0.678	0.678	.....	.....	.....	.....	0.678	.....
Ca^{2+}	1.830	0.094	1.736	.....	.....	.....	3.660	.....
Mn	0.017	.....	0.017	.....	.....	.....	0.034	.....
Fe	0.818	.....	0.247	0.571	.....	.....	1.636	.....
Mg	2.950	.....	.....	2.950	.....	.....	5.900	.....
Fe^{3+}	0.452	.....	.....	0.452	.....	.....	1.356	.....
Al	2.662	.....	.....	0.992	1.670	.....	7.986	.....
Cr	...	.....	.....	.....	.....	.....	.....	.....
Ti^{4+}	0.035	.....	.....	0.035	.....	.....	0.140	.....
Si	6.330	.....	.....	.....	6.330	.....	25.320	.....
O^{2-}	21.931	.....	.....	.....	.....	21.931	.....	43.862
OH^{1-}	2.053	.....	.....	.....	.....	2.053	.....	2.053
Cl^{1-}	0.008	.....	.....	.....	.....	0.008	.....	0.008
F^{1-}	0.008	.....	.....	.....	.....	0.008	.....	0.008
		0.824	2.00	5.00	8.00	24.00	46.762	45.931

TABLE 20.—COMPOSITION OF AMPHIBOLE C.70

	Weight per cent	Mol. ratio	Ratio O, OH, F, Cl	Ratio metals	Metal atoms
SiO_2	44.96	749	1498	749	6.381
TiO_2	0.23	3	6	3	0.025
Al_2O_3	14.90	146	438	292	2.487
Fe_2O_3	1.51	9.5	28	19	0.162
Cr_2O_3	1.92	12.5	38	25	0.213
FeO	4.05	56	56	56	0.477
MnO	0.09	1	1	1	0.008
MgO	16.05	398	398	398	3.391
CaO	11.92	212	212	212	1.806
Na_2O	1.51	24	24	48	0.409
K_2O	0.12	1	1	2	0.017
H_2O^+	2.26	126	126	252	2.147
H_2O^-	0.15	.....	.....	.....	.....
Cl	0.05	2	2	2	0.017
F	0.02	1	1	1	0.008
	99.74	.....	2829	.....	.....
O for Cl & F	0.02	.....	2	.....	.....
	99.72	.....	2827	.....	.....

Analyst: Eileen K. Oslund; Halogens by P. K. Kuroda

Multiplication factor to build 24 (O, OH) in unit cell $= \frac{24}{2.827} = 8.52$

Structural Account *Structure Type:* $X_{0\text{-}1}A_2B_5C_8Y_{24}$

Ionic Ratio		X	A	B	C	Y	Electrical charges (+)	Electrical charges (−)
K^{1+}	0.017	0.017	.....	.....	.....	.....	0.017	.....
Na	0.409	0.409	.....	.....	.....	.....	0.409	.....
Ca^{2+}	1.806	.....	1.806	.....	.....	.....	3.612	.....
Mn	0.008	.....	0.008	.....	.....	.....	0.016	.....
Fe	0.447	.....	0.186	0.291	.....	.....	0.954	.....
Mg	3.391	.....	.....	3.391	.....	.....	6.782	.....
Fe^{3+}	0.162	.....	.....	0.162	.....	.....	0.486	.....
Al	2.487	.....	.....	0.868	1.619	.....	7.461	.....
Cr	0.213	.....	.....	0.213	.....	.....	0.639	.....
Ti^{4+}	0.025	.....	.....	0.025	.....	.....	0.100	.....
Si	6.381	.....	.....	.....	6.381	.....	25.524	.....
O^{2-}	21.828	.....	.....	.....	.....	21.828	.....	43.656
OH^{1-}	2.147	.....	.....	.....	.....	2.147	.....	2.147
Cl^{1-}	0.017	.....	.....	.....	.....	0.017	.....	0.017
F^{1-}	0.008	.....	.....	.....	.....	0.008	.....	0.008
		0.426	2.00	4.950	8.00	24.00	46.00	45.828

Clino-Amphiboles

Monoclinic amphibole is the prevalent mafic mineral in the anorthositic rocks and chromitites. The eclogitic gabbros also contain monoclinic amphibole, commonly replacing pyroxene. The amphibole in the anorthositic rocks occurs as prismatic and acicular crystals ranging in length from 0.2 mm to 15 mm, with their longer axes parallel and imparting a lineation to the rocks. These rocks contain 5–90 per cent amphiboles; the more mafic concentrations occur as layers within the anorthosites. The amphibole in the chromitites is bright green and ranges in length from 0.2 to 15 mm; it constitutes 20–90 per cent of the rock depending on the chromite content. These amphiboles also occur as prismatic and acicular crystals, imparting a lineation to the rocks by their preferred orientation. These two varieties of amphibole were separated from the parent rocks and chemically analyzed, in view of their differing optical characters. The analyses and the probable distribution of ions in the amphiboles are presented in Tables 19 and 20. Tables 21 and 22 show the chemical composition of an amphibole as recalculated from the rock analysis. According to Sundius (1946), the distribution of the ions in the above three analyses indicates their affinities to edenite and pargasite (Table 23). The physical and optical properties of the analyzed specimens and the optical properties of others from the various rocks are tabulated in Tables 24 and 25.

TABLE 21.—COMPOSITION OF AMPHIBOLE FROM ROCK C.33

	Weight % in rock	Weight % in 79% of plagioclase An_{90}	Weight % in rock after deducting feldspar	Composition of amphibole recalculated
SiO_2	44.58	36.14	8.44	40.19
TiO_2	0.06	..	0.06	0.28
Al_2O_3	30.81	27.63	3.18	15.14
Fe_2O_3	0.94	..	0.94	4.47
Cr_2O_3	0.02	..	0.02	0.09
FeO	1.77	..	1.77	8.41
MnO	0.04	..	0.04	0.18
MgO	2.72	..	2.72	12.95
CaO	17.05	14.21	2.84	13.50
Na_2O	1.35	0.93	0.42	2.00
K_2O	0.07	..	0.07	0.33
H_2O^+	0.58	0.14*	0.44	2.09
H_2O^-	0.06	..	0.06	0.28
Cl	0.01	..	0.01	0.04
F	0.01	..	0.01	0.04
Less O for Cl & F	0.01	..	..	0.02
Total.....	100.06	..	..	99.97

* Analysis of feldspar from similar rocks indicated combined H_2O in them, and hence a proportionate amount has been allotted.

Important discussions have appeared in recent years on the chemical and optical properties of monoclinic amphiboles (Hallimond, 1943; Winchell, 1945; Foslie, 1945; Sundius, 1946). The most important contribution is by Sundius who presented a classification of the monoclinic amphiboles on the basis of their chemistry. According to him the Si content in the calciferous amphiboles is always less than 8, with characteristic substitutions of NaAl for Si and AlAl for MgSi. The type formulas arising from such substitutions are $Na \cdot Ca_2 \cdot Mg_5 \cdot Al \cdot Si_7 \cdot O_{22}(OH)_2$ = edenite, $Na \cdot Ca_2 \cdot Mg_4 \cdot Al_3 \cdot Si_6 \cdot O_{22}$ $(OH)_2$ = pargasite, and $Ca_2 \cdot Mg_3 \cdot Al_1 \cdot Si_6 \cdot O_{22}(OH)_2$ = tschermakite.

Berman (1937) gives the following structural formula for edenite and pargasite:

$Ca_4 \cdot Na_2 \cdot Mg_{10} \cdot Al_2 \cdot Si_{14} \cdot O_{44}(OH, F)_4$ = Edenite

$Ca_4 \cdot Na_2 \cdot Mg_9 \cdot Al_4 \cdot Si_{13} \cdot O_{44}(OH, F)_4$ = Pargasite.

The formulae indicated by the analyzed amphiboles are:

$$C.34 = Ca_{3.6}(Na + K)_{1.4} \cdot (Mg + Mn + Fe + Ti + Al^{3+} + Fe^{3+})_{10.6} \cdot Al_2Si_{14} \cdot O_{44}(OH, Cl, F)_4$$

$$C.70 = Ca_{3.6}(Na + K)_{0.85} \cdot (Mg + Mn + Fe + Ti + Al^{3+} + Fe^{3+})_9 \cdot Al_4 \cdot Si_{12.8}O_{44}(OH, Cl, F)_4.$$

Berman's formula for pargasite differs from that of Sundius in containing more magnesia and less alumina. However, the present analyses support Berman's formula, except for deficiency in lime and alkalis. The chemical compositions of the analyzed amphiboles approach edenite and pargasite respectively. The optical

TABLE 22.—COMPOSITION OF AMPHIBOLE C.33

	Weight per cent	Mol. ratio	Ratio O, OH, F, Cl	Ratio metals	Metal atoms
SiO_2	40.19	669	1338	669	5.920
TiO_2	0.28	4	8	4	0.036
Al_2O_3	15.14	148	444	296	2.619
Fe_2O_3	4.47	28	84	56	0.495
Cr_2O_3	0.09	1	3	2	0.018
FeO	8.41	117	117	117	1.035
MnO	0.18	3	3	3	0.027
MgO	12.95	321	321	321	2.841
CaO	13.50	241	241	241	2.132
Na_2O	2.00	32	32	64	0.566
K_2O	0.33	3	3	6	0.054
H_2O^+	2.09	116	116	232	2.053
H_2O^-	0.28	.....	.....	.....	.....
Cl	0.04	2	2	2	0.018
F	0.04	2	2	2	0.018
	99.71	.....	2714	.....	.....
O for Cl & F	0.02	.....	2	.....	.....
	99.69	.....	2712	.....	.....

Analyst: Eileen K. Oslund

Multiplication factor to build 24 (O, OH) atoms in unit cell $= \frac{24}{2.712} = 8.85$

Structural Account *Structure Type:* $X_{0\text{-}1}A_2B_5C_8Y_{24}$

Ionic Ratio		X	A	B	C	Y	Electrical charges (+)	Electrical charges (−)
K^{1+}	0.054	0.054	....	.....	.....	.....	0.054	.....
Na	0.566	0.566	....	.....	.....	.....	0.566	.....
Ca^{2+}	2.132	0.123	2.00	0.009	.....	.....	4.264	.....
Mn	0.027	.....	....	0.027	.....	.....	0.054	.....
Fe	1.035	.....	....	1.035	.....	.....	2.070	.....
Mg	2.841	.....	....	2.841	.....	.....	5.682	.....
Fe^{3+}	0.495	.....	....	0.495	.....	.....	1.485	.....
Al	2.619	.....	....	0.539	2.080	.....	7.857	.....
Cr	0.018	.....	....	0.018	.....	.....	0.054	.....
Ti^{4+}	0.036	.....	....	0.036	.....	.....	0.144	.....
Si	5.920	.....	....	.....	5.920	.....	23.680	.....
O^{2-}	21.911	.....	....	.....	.....	21.911	.....	43.822
OH^{1-}	2.053	.....	....	.....	.....	2.053	.....	2.053
Cl^{1-}	0.018	.....	....	.....	.....	0.018	.....	0.018
F^{1-}	0.018	.....	....	.....	.....	0.018	.....	0.018
		0.743	2.00	5.00	8.00	24.00	46.054	45.911

properties of some of these amphiboles are variable within a single thin section, particularly the optic and extinction angles.

Probably the rocks that were originally assemblages containing calcic feldspar, olivine, or bronzite and diopside were transformed during metamorphism to amphibole-rich varieties. The formation of amphibole may be attributed to the absorption of lime from the calcic feldspar (An_{90}) and of olivine or bronzite and diopside; the small amount of alkalis also enter the amphibole structure. Chemical analyses indicate the amphiboles have a general composition $H_2 \cdot Ca_2 \cdot Mg_4 \cdot Al_2 \cdot Si_7 \cdot O_{24}$, with a small amount of alkalis. The following reactions indicate the trends of chemical transformations resulting in the formation of these amphiboles:

TABLE 23.—STRUCTURAL ACCOUNT OF ANALYZED AMPHIBOLES

Ions	Amphibole C.34			Amphibole C.33 (calculated)			Amphibole C.70		
	Distribution of ions after Sundius (1946)		Type formula for edenite	Distribution of ions after Sundius (1946)			Distribution of ions after Sundius (1946)		Type formula for pargasite
Si	6.330	7	7	7	5.920		6.381	6.381	6
	0.670				1.080				
Al	2.662	1.00	1	1	1.00	2.619	2.487	2	2
	0.992				0.539		.487		
Fe^3	0.452				0.495		0.162	.649	1
Ti^2	0.035				0.036		0.025		
Fe	0.818	5.264	5	4.973	1.035		0.477	3.901	4
Mg	2.950				2.841		3.391		
Mn	0.017				0.027		0.008		
Ca	1.830	1.830	2	2.132	2.132		1.806	1.806	2
Na	0.678	0.730	1	0.620	0.566		0.409	0.426	1
K	0.052				0.054		0.017		
OH	2.053				2.053		2.147		
Cl	0.008	2.069	2	2.089	0.018		0.017	2.172	2
F	0.008				0.018		0.008		

$$Ca \cdot Al_2 \cdot Si_2 \cdot O_8 + Mg_2 \cdot SiO_4 + 2Ca \cdot Mg \cdot Si_2O_6 + CO_2 + H_2O \rightarrow H_2 \cdot Ca_2 \cdot Mg_4 \cdot Al_2 \cdot Si_7O_{24} + Ca \cdot CO_3$$
anorthite + olivine + diopside → amphibole + calcite

$$Ca \cdot Al_2 \cdot Si_2 \cdot O_8 + Ca \cdot Mg \cdot Si_2O_6 + 3Mg \cdot SiO_3 + H_2O \rightarrow H_2 \cdot Ca_2 \cdot Mg_4 \cdot Al_2 \cdot Si_7 \cdot O_{24}$$
anorthite + diopside + enstatite → amphibole

$$2Ca \cdot Al_2 \cdot Si_2 \cdot O_8 + 4Mg \cdot SiO_3 + H_2O \rightarrow H_2Ca_2 \cdot Mg_4 \cdot Al_2 \cdot Si_7 \cdot O_{24} + Al_2O_3 + SiO_2$$
anorthite + enstatite → amphibole + corundum + quartz

Chromite

General.—The only significant metallic mineral in the complex is chromite which occurs in varying quantities in the steeply dipping layers of chromitite in the anorthosite horizon. The chromite grains are fairly conspicuous in these greenish-black chromitites because of their metallic luster. The proportion of chromite in the chromitites is variable as shown by electromagnetic separations of several specimens, and the chromite appears to be more magnetic than normal chromites, perhaps because of the high tenor of iron present.

Mineralogy.—Chromite occurs as granular aggregates in close association with amphiboles, in these chromitites. The mineral is black and

generally opaque, though in thin sections the translucent edges are pale coffee brown. Fisher (1929a) states that these varieties have a low chromic-oxide content, which is true in this instance. The grain size ranges from 0.2 mm to 2.0 mm, but occasionally grains are up to 4 mm.

Table 24.—Optical and Physical Properties of Analyzed Amphiboles

	C.34	C.70
N_X	1.6506 ± .0005	1.6402 ± .0005
N_Y	1.6611 ± .0005	1.6473 ± .0005
N_Z	1.6688 ± .0005	1.6565 ± .0005
$Z \wedge c$	16° ± 1°	19° ± 1°
$2V$	−83.5° ± 2°	+85.5° ± 2°
Dispersion of optic angle	$r < v$	$r > v$
Dispersion	weak	weak
Absorption	$X < Y < Z$	$X = Y < Z$
X	Pale yellowish green	Pale green
Y	Pale green	Pale green
Z	Bluish green	Emerald green
Orientation	Optic plane ∥ {010}	Optic plane ∥ {010}
Elongation	Positive	Positive
Cleavage	Well developed (110)	Well developed (110)
Parting	Distinct (010)	Distinct (010)
Twinning	Rare	Rare
Habit	Long prismatic and acicular crystals	Long prismatic and acicular crystals
Size	1 mm to 5 cm	1 mm to 5 cm
Color in hand specimens	Greenish black to black	Emerald green to dark green
Density at 26/4°C	3.167 gm/cm³	3.117 gm/cm³

Polished sections show subhedral and anhedral crystals of rutile in the chromitites, both in and outside the chromite grains (Pl. 4, fig. 3). The rutile is recognized by its extreme birefringence in thin sections, marked internal reflection, and white color in polished sections. The only other instance of chromite containing inclusions of rutile was recorded in Turkey by Wijkerslooth (1947). Professor Sampson (Personal communication), on the basis of new chemical analyses of pure chromite concentrates from different localities, believes that TiO_2 is invariably present in the chromite structure and that, in the older analyses of chromite, TiO_2 has gone undetermined. In 52 analyses of chromite presented by Stevens (1944), TiO_2 is invariably present, ranging from 0.06 to 3.00 per cent.

Table 25.—Optical Properties of Some Amphiboles in Sittampundi Anorthosites*

	C.33	C.128
N_X	1.6517 ± .0005	1.6572 ± .0005
N_Y	1.6614 ± .0005	1.6695 ± .0005
N_Z	1.6694 ± .0005	1.6792 ± .0005
$2V$	−84° ± 1°	−79.5° ± 1°
$Z \wedge c$	17° ± 1°	18° ± 1°
Dispersion of optic angle	$r < v$	$r < v$
Dispersion	Weak	Weak
Absorption	$X < Y < Z$	$X < Y < Z$
X	Yellowish green	Yellowish green
Y	Pale green	Pale green
Z	Bluish green	Bluish green

No.	N_X	N_Y	N_Z	$2V$	Absorption
C.47	1.639	1.647	1.657	+85	$X = Y < Z$
C.94	1.639	1.648	1.658	+85	$X = Y < Z$
C.101	1.639	1.648	1.658	+86	$X = Y < Z$
C.4	1.649	1.658	1.667	−82	$X < Y < Z$
C.15	1.651	1.661	1.669	−83	$X < Y < Z$
C.84	1.651	1.661	1.669	−83	$X < Y < Z$
C.53	1.653	1.663	1.671	−81	$X < Y < Z$
C.69	1.649	1.659	1.667	−84	$X < Y < Z$
C.96	1.651	1.660	1.668	−82	$X < Y < Z$
C.120	1.650	1.658	1.668	−82	$X < Y < Z$

* All index measurements ±.002, and 2 V measurements ±1°

The rutile present in the chromite may represent the original TiO_2 in the chromite structure expelled during the metamorphism. This explanation must be accepted with reservations until more data are available on the chemical composition of chromites which have suffered intense metamorphism. It is estimated that about 2–3 per cent of rutile is present in the chromitites, indicating the original chromite was rich in titanium. High-titania chromites containing up to 3 per cent TiO_2, occur at Casper Mountain, Wyoming.

Some grains of chromite, under high magnification, reveal the presence of fine plates of white anisotropic mineral (Pl. 4, fig. 4) with marked internal reflection. Its hardness is

about the same as chromite, and it is negative to etching reagents. These plates show a micaceous habit, and their internal reflection is unlike that of rutile in the section. The identity of this mineral is uncertain, but its disposition within the chromite is considered due to exsolution, consequent on unmixing during the cooling of the chromite. Ramdhor (1931) noticed such plates in the accessory chromites of the Bushveld norite and identified them as hematite, but in a later paper (1940) he described them as ilmenite. Brownell (1943) also recorded such inclusions in chromite from the Bird River sill of Manitoba, identifying them as hematite. In the present instance the optical properties of the mineral plates do not suggest ilmenite or hematite, and they are thought to be plates of rutile with a different orientation. Baker (1952) reported micrographic intergrowths of magnetite-rutile-ilmenite and magnetite-rutile-ilmenite-hematite from gabbroic rocks in the basement complex of New Guinea. It is not unlikely therefore that the fine plates in the chromite represent exsolved rutile.

Tables 26 and 27 give the chemical analysis of this chromite with calculations of the spinel molecules after the methods of Thayer (1946) and Stevens (1944). Comparable analyses of chromites from stratiform complexes are presented in Table 28.

The composition of the chromite indicates that it is related to chromohercynite (Fisher, 1929a). The ionic ratios when plotted on the triangular diagram of Stevens (1944) fall at the boundary between aluminian chromite and chromian spinel. The molecular formula calculated from the analysis indicates nearly 45 per cent spinel molecule, proving the impossibility of mechanically beneficiating the ore to a higher grade.

TABLE 26.—COMPOSITION OF CHROMITE FROM CHROMITITE C.101

	Weight per cent	Molecular ratio	3^+	2^+
Cr_2O_3	36.88	485	485	.....
Al_2O_3	24.12	473	473	.....
FeO	29.40	409*	86	319
MgO	7.22	179	....	179
MnO	0.68	10	....	10
CaO	0.77	14	....	14
TiO_2	0.36	4*	....	.....
SiO_2	0.34	6	....	.....
.....	99.77	....	1044	522

Formula according to Thayer's method:

$Cr_{47}Al_{45}Fe_8(Mg_{34}Fe_{61}Ca_3Mn_2)$

or

$Cr_{47}Al_{45}(Mg_{34})$, (Fe^{3+} and Fe^{2+} obtained by difference)

Norm

Chromite (Mg, Fe) Cr_2O_4	46.45
Spinel (Mg, Fe) Al_2O_4	45.31
Magnetite $Fe \cdot Fe_2O_4$	8.24
	100.00

* 4 mols of Fe^{2+} may have combined with 4 mols of Ti^{4+} forming ilmenite presumed to be in solid solution in the chromite.

TABLE 27.—CALCULATION OF ATOMS PER UNIT CELL OF CHROMITE C.101

	Weight per cent	Molecular ratios		Atoms per unit cell
Cr_2O_3	36.88	.2425	Cr	7.43
Al_2O_3	24.12	.2365	Al	7.25
Fe_2O_3	6.80	.0430	Fe^{3+}	1.32
		.5220		16.00
FeO	23.20	.3230 − .0040* = .3190	Fe^{2+}	5.00
MgO	7.22	.1790 − .0120† = .1670	Mg	3.00
MnO	0.68	.0100	Mn	
CaO	0.77	.0140	Ca	
		.5260 − .0160 = .5100		8.00
TiO_2	0.36	.0040		
SiO_2	0.34	.0060		

* Subtracting .0040 for ilmenite

$RO/R_2O_3 = .5100/.5220 = 0.996$

† Subtracting .0120 for olivine

The above analysis when plotted in triangular diagram of Stevens (1944, p. 31, Fig. 5) falls at the boundary between aluminian chromite and chromian spinel.

Pyroxenes

Clinopyroxene.—Pyroxene is rare in the rocks of this complex, possibly because of its transformation to amphibole during metamorphism. In the anorthositic rocks a few thin sections showed skeletal crystals of clinopyroxene altering to amphibole (Fig. 11). The mineral is pale green with a fairly distinct cleavage and the following optical properties:

C.53 $2V = +59° \pm 1°$, $Z \wedge c$ $43° \pm 1°$

C.128 $2V = +60° \pm 1°$, $Z \wedge c$ $42° \pm 1°$

These optical properties place them in the diopside-hedenbergite series according to the recent curves of Hess (1949).

The eclogites and websterites contain clinopyroxenes with the following optical properties:

No.	N_X	N_Z	$2V$	$Z \wedge c$	Rock
C.19	—	—	$+57 \pm 1°$	$38 \pm 1°$	Bronzitic pyropite
C.20	1.681 ± 002	$1.709 + 002$	$+56 + 1°$	$42 + 1°$	Websterite pegmatite
C.41	1.681 ± 002	1.708 ± 002	$+58 \pm 1°$	$43 \pm 1°$	Eclogite
C.43	1.670 ± 002	1.699 ± 002	$+60 \pm 1°$	—	Websterite
C.60	1.680 ± 002	1.709 ± 002	$+59 \pm 1°$	$44 \pm 1°$	Bronzitic pyropite
C.122	—	—	$+58 \pm 1°$	—	Eclogite

These properties place them in the diopside-salite range of the diopside-hedenbergite series.

The above monoclinic pyroxenes have diallagic structure owing to well-developed 100 parting. Uralitization of these clinopyroxenes has resulted in an abundance of green amphibole.

Orthopyroxene.—The eclogites and websterites contain orthorhombic pyroxene, and the optical properties of some of them are:

No.	N_Z	Per cent enstatite	Rock
C.19	1.685 ± 002	84.0	Bronzitic pyropite
C.20	1.689 ± 002	79.5	Websterite pegmatite
C.36	1.682 ± 002	86.0	Eclogite
C.41	1.683 ± 002	84.5	Eclogite
C.43	1.695 ± 002	77.0	Websterite
C.60	1.685 ± 002	84.0	Bronzitic pyropite
C.122	1.684 ± 002	85.0	Eclogite

The above characters conform to those of bronzite and hypersthene, and the enstatite percentages shown are from the curve of Hess and Phillips (1940). These orthopyroxenes have well-developed lamellae, characteristic of slow cooling, as in many gabbros in stratiform complexes. The orthopyroxene is bronzite in the eclogites and hypersthene in the websterites.

Minor Minerals

Scapolite.—Many anorthositic rocks contain scapolite as an alteration product of the calcic plagioclase. It is readily distinguished from the accompanying plagioclase by its lower refringence and higher birefringence. Fragments of the mineral were removed from thin sections for index determinations; the values and the anorthite content of the related plagioclase are:

	N_E	N_O	Per cent of meionite (after Winchell)	Per cent An in plagioclase
C.50	1.552	1.582	70	98
C.71	1.548	1.576	65	91
C.82	1.548	1.576	65	86

Thus the composition of the scapolite is closely related to the anorthite content of the plagioclase from which it is derived, affording an example of a regular relationship in the chemical composition of associated phases, during metamorphic transformation. The following reaction shows the trend of transformation of anorthite to scapolite:

$$4Ca \cdot Al_2 \cdot Si_2O_8 + CO_2 \rightarrow Ca_4 \cdot CO_3 \cdot Si_6 \cdot Al_6 \cdot O_{24} + Al_2O_3 + 2SiO_2 \text{ (leached out)}$$

anorthite → meionite + corundum

Corundum.—Corundum is sparsely distributed in the anorthosites and chromitites. The mineral occurs as euhedral and subhedral prismatic crystals, ranging in length from a fraction of a centimeter to nearly 15 cm. Well-developed crystals showing combinations of hexagonal prism, base, and rhombohedron occasionally occur in the anorthositic rocks. Corundum in the chromitites is ruby red, which may be attributed to traces of chromic oxide, and is grayish white to pale green in the anorthosites. Occasionally, the corundum crystals occurring as porphyroblasts in the anorthosites have a thin shell of calcite.

In thin section, corundum is distinguished by its high relief and low birefringence and occasionally replaces anorthite (Fig. 12). In thick sections the pink corundum found in the chromitites is pleochroic in shades of ruby red. The densities of the two types of corundum determined on small fragments are:

(1) White corundum from anorthite gneiss 3.943 gm/cm³ at 26.0°C.

(2) Pink corundum from chromitite 3.913 gm/cm³ at 26.0°C.

Sillimanite.—Sillimanite occurs as acicular crystals and aggregates in cordierite and calcic plagioclase, in a cordierite-corundum-anthophyllite-bytownite assemblage. The identity of the mineral is established by its low optic axial angle, form, and general occurrence in cordierite.

Rutile.—In several thin sections of chromi-

TABLE 28.—CHEMICAL COMPOSITION OF SOME CHROMITES FROM STRATIFORM SHEETS

	1	2	3	4	5	6	7	8
Cr_2O_3	36.88	46.09	42.76	38.91	38.51	32.46	37.66	43.50
Al_2O_3	24.12	23.81	23.85	25.29	24.57	22.70	27.30	17.23
							Fe^{3+}	8.16
FeO	29.40	24.05	21.51	21.93	22.17	24.16	19.01	20.86
MgO	7.22	5.43	10.36	10.77	10.06	11.33	8.66	8.70
CaO	0.77	.....	.....	.....	.....	2.06	1.66	0.10
MnO	0.68	.....	.....	.....	.....	.....	.....	0.23
NiO	.....	.....	.....	.....	.....	.....	.....	0.02
TiO_2	0.36	.....	.....	.....	.....	0.84	.....	0.39
SiO_2	0.34	1.02	1.68	3.50	3.68	6.00	5.80	0.30
H_2O	.....	.....	.....	.....	.....	.....	.....	0.90
	99.77	100.40	100.16	100.40	98.99	99.55	100.09	100.39

(1) Chromite concentrate from chromitite C.101 occurring as a layer in anorthosite, Sittampundi complex

(2) Chromite from Benbow property, Stillwater complex, Montana, quoted from Peoples and Howland (1941, p. 389)

(3) Chromite from lower group, eastern belt, Bushveld igneous complex, South Africa, quoted from Kupferburger *et al.* (1937, p. 25)

(4–7) Chromites from middle and upper groups of Bushveld igneous complex, South Africa, quoted from Kupferburger *et al.* (1937, p. 27)

(8) Chromite from Bird River sill complex, Manitoba, Canada, quoted from Bateman (1945, p. 598)

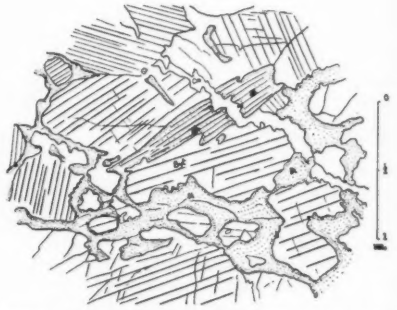

FIGURE 11.—MICROGRAPH SHOWING SKELETAL CRYSTALS OF DIOPSIDE IN ANORTHOSITE
Note paramorphic alteration of diopside to hornblende (edenite) Byt, Bytownite; Di, Diopside, Hb, Hornblende (edenite)

tites, a mineral with extreme birefringence and very high relief was noticed. Optically it is unaxial and positive. Polished sections of some chromitites showed the mineral in abundance.

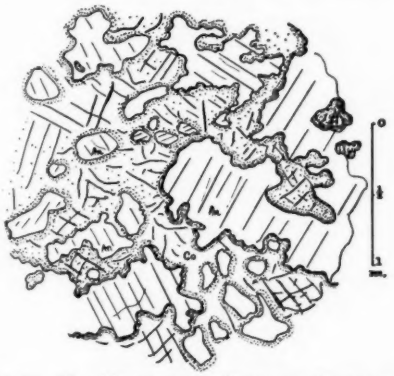

FIGURE 12.—MICROGRAPH SHOWING CORUNDUM REPLACING ANORTHITE

Note corundum replacing anorthite; small insets of plagioclase within the corundum. An, Anorthite; Co, Corundum

It is brilliant white with marked internal reflection. These properties indicate the mineral to be rutile. Fine plates of rutile, probably exsolved, are also encountered in some grains of chromite. A sample of crushed chromite when passed through the electromagnet at high field strength yielded a small amount of nonmagnetic concentrate composed of brilliant-red prismatic crystals, with adamantine luster. It was confirmed as rutile by x-ray examination. The mineral probably represents titania released from the chromite structure during metamorphism.

Sphene.—This is a rare constituent in the rocks of the complex. In one specimen of anorthositic rock a fair aggregate of sphene developed around a core of rutile. The mineral was recognized by its high relief, strong birefringence, strong dispersion, and biaxial positive nature. It is likely the mineral developed during metamorphism through reaction between calcic plagioclase and ilmenite.

Secondary chlorite and talc are found in some chromitites, developed at the expense of the ortho- and clino-amphiboles. Spinel, calcite, apatite, and ores (magnetite and ilmenite) are rare accessory minerals in the rocks of the complex.

PETROGRAPHY

General

The rocks of this complex can be divided into two main series, the anorthosite series and the eclogite-gabbro series, based on paragenesis and petrographic characters. The anorthosite series is composed of a group of felsic rocks characterized by a high proportion of calcic plagioclase and variable amounts of edenite, clinozoisite, garnet, and corundum. Johannsen (1937, vol. III, p. 196) has defined anorthosites as rocks practically free from dark minerals, and their calciclase equivalents—anorthitite. However, the term anorthosite has been extended to rocks containing up to 10 per cent mafic minerals (Buddington, 1939, p. 19); the more mafic varieties are described as noritic and gabbroic anorthosites. The anorthositic rocks of the Sittampundi complex have a variable proportion of mafic minerals and represent what were originally different facies of true anorthosites. The term anorthosite series in this report designates a group of gneissic, meta-anorthositic rocks made up essentially of calcic plagioclase (An_{80-100}), with minor amounts of edenite (hornblende), epidote-clinozoisite, garnet (grossularitic), and corundum. The eclogite-gabbro series is composed of a group of pyroxene and hornblende-garnet rocks, varying from bimineralic to polymineralic assemblages. There are also several layers of chromitites and perknites within the anorthosite belt and a few small bodies of websterite (pyroxenite) within the limits of the complex.

Anorthosite Series

General.—Rocks of the anorthosite series constitute a large part of the complex, and the following assemblages frequently occur:

(1) Bytownite, anorthite, edenite, (2) Anorthite, corundum, edehite, (3) Anorthite, clinozoisite, garnet, (4) Anorthite, garnet, clinozoisite, corundum, (5) Bytownite, clinozoisite, edenite, (6) Anorthite, anthophyllite, edenite.

In the field, the anorthosite series are characterized by a regular alternation of felsic and mafic bands. The felsic bands are rich in clinozoisite, corundum, and garnet, while the

TABLE 29.—APPROXIMATE MODES OF ROCKS FROM THE SITTAMPUNDI COMPLEX

Minerals	1	2*	3	4	5*	6	7	8*	9	10*	11	12	13*	14	15*	16	17	18*	19	20
Quartz	...	...	...	...	...	...	...	...	...	...	...	...	...	...	1.5	...	...	...	...	...
Plagioclase	93.0	89.2	87.1	81.0	79.1	78.2	74.3	69.7	68.0	66.1	65.6	12.6	30.2	22.4	19.3	17.5	7.5	1.4	...	...
Clino-amphibole	0.5	5.3	10.3	7.0	20.9	1.3	23.2	21.8	18.4	...	0.2	83.0	...	25.3	12.0	16.3	24.3	2.2	32.2	27.0
Ortho-amphibole	...	...	...	...	...	...	...	8.2	9.7	...	...	...	4.0	...	...	...	...	...	10.0	8.8
Clinopyroxene	1.8	2.4	...	2.8	...	...	0.5	...	...	...	...	...	...	4.4	7.0	7.1	14.1	5.8	...	...
Orthopyroxene	...	...	...	...	...	...	...	...	...	...	...	...	...	3.9	7.2	6.4	8.3	7.2	...	...
Clinozoisite	3.7	3.1	2.2	4.8	...	8.7	...	...	...	21.1	20.4	2.0	1.4	...	...	...	...	...	...	...
Corundum	...	...	0.4	1.4	...	5.3	1.4	...	...	...	6.0	...	21.2	...	...	...	...	...	...	1.0
Garnet	...	...	...	...	...	4.4	...	...	...	7.2	3.8	...	...	31.2	32.3	39.8	29.4	72.4	...	...
Scapolite	0.7	...	...	2.0	...	1.3	0.6	...	2.4	4.2	3.2	1.7	4.4	1.7	...	...	...	...	...	...
Sillimanite	...	...	...	...	...	...	...	...	...	...	...	...	5.0	...	...	...	...	...	...	...
Cordierite	...	...	...	...	...	...	...	...	...	...	...	...	30.8	...	...	...	...	...	...	...
Calcite	...	...	...	0.4	...	0.8	...	...	1.0	1.4	0.8	0.7	2.0	...	...	...	...	...	...	...
Chromite	...	...	...	...	...	...	...	...	...	...	...	...	...	...	...	...	...	...	54.8	59.2
Ores	0.3	...	...	0.6	...	...	...	...	0.5	...	...	...	0.5	1.2	1.5	1.6	2.3	1.2	...	...
Spinel	...	...	...	...	...	...	...	0.3	...	...	...	...	0.5	0.7	...	0.4	...	...	...	...
Rutile	...	...	...	...	...	...	...	...	...	...	...	...	...	...	...	...	...	...	2.5	0.5
Talc	...	...	...	...	...	...	...	...	...	...	...	...	...	...	...	...	...	...	0.5	3.5
Kelyphite	...	...	...	...	...	...	...	...	...	...	...	...	...	9.2	19.2	10.9	14.1	9.8	...	...

* Analyzed specimens C.128, C.33, C.69, C.50, C.71, C.41, and C.60

All modes are expressed as weight percentages

(1–11) Anorthositic rocks

(12) Mafic band in anorthosite

(13) Cordierite-corundum-anthophyllite rock

(14–18) Eclogite gabbros (18 is bronzitic pyropite)

(19, 20) Chromitites

mafic bands contain variable proportions of edenite. The leucocratic rocks have a saccharoidal texture and are megascopically similar to typical marbles. The more mafic types are even-grained, with pronounced gneissic texture accentuated by the preferred orientation of the edenite crystals in the plane of foliation; some of these may be called amphibolites. Hadley (1949) has described the bytownite-edenite gneisses of North Carolina under the name edenite amphibolite.

Hand specimens of anorthositic rocks are pale gray to white, depending on the percentage of mafic minerals present, with occasional porphyroblasts of corundum and discernible linear and planar structures. The density of these rocks ranges from 2.75 to 2.93 gm/cm³.

The rocks contain the following minerals in order of abundance: (1) calcic plagioclase (An_{80-100}), (2) edenite, (3) epidote-clinozoisite, (4) anthophyllite, (5) diopside, (6) corundum, (7) garnet, (8) scapolite, (9) calcite, (10) sphene, (11) rutile, and (12) apatite; the last three are relatively rare. The modal compositions of some these rocks are presented in Table 29.

In thin section these rocks display an equigranular interlocking texture with the plagioclase forming a mosaic of polygonal crystals, in which the other minerals are scattered, some with a preferred orientation. The dimensional orientation of plagioclases is apparent under crossed nicols with the gypsum plate. Sohnge (1946, p. 51–52) noticed similar preferred orientation of feldspar grains parallel to the banded structure in the anorthosite gneisses of Messina. He attributed this to the recrystallization of the rocks, according to Riecke's principle whereby crystals become elongate in the direction of least pressure, as solution takes place more readily at the points of greater stress.

Planar structure is imperceptible in thin sections, though marked in some mafic anorthosites. Edenite, and in some rocks anthophyllite, occurs as acicular and bladed crystals with their longer axes oriented in the plane of layering, to produce a distinct lineation. Clinozoisite occurs in these rocks as oriented euhedral and subhedral crystals, displaying preferred orientation. Occasionally skeletal crystals of diopside, undergoing paramorphic alteration to edenite, are encountered. Garnet occurs occasionally, replacing anorthite. Porphyroblasts of corundum are scattered in these rocks, generally with a thin rim of calcite. The other minerals mentioned occur in minor amounts.

Anorthite-edenite (hornblende) gneiss: C.33.—Hand specimens show planar and linear structures, owing to the platy parallelism of the plagioclase crystals and dimensional orientation of edenite prisms. In appearance they simulate dark-gray feldspathic amphibolites. The density of this type is 2.825 gm/cm³. Thin sections indicate this type to be essentially bimineralic with a trace of ores in some thin sections. The measured modal composition in weight per cent is:

Anorthite (An_{90-96})	79.1
Edenite	20.9

Thin sections show a mosaic of polygonal plagioclase crystals in which dimensionally oriented idioblasts of edenite prisms are scattered. Preferred orientation of the plagioclase is brought out under crossed nicols, with a gypsum plate.

The plagioclase is anorthite (An_{90-96}) displaying an equal proportion of twinned and untwinned crystals, while a few crystals show complex twin laws. Edenite occurs as pale-green prismatic crystals with the following optical properties: $N_X = 1.652$, $N_Y = 1.661$, $N_Z = 1.669$; $2V = -84 \pm 1°$; $Z \wedge c = 17 \pm 1°$; $r < v$; $X < Y < Z$ in yellowish to bluish green. The plagioclase grains are 0.6–1 mm long, and the edenite prisms 1–3 mm. Occasionally this rock carries porphyroblasts of corundum with a shall of calcite.

Anorthite-clinozoisite-garnet rock: C.50.—This rock is conspicuous by the absence of amphibole and abundance of clinozoisite. Hand specimens closely resemble a marble in texture and general appearance. The density is 2.934 gm/cm³. Thin sections display a coarse, crystalloblastic texture, and the grain sizes of the various minerals measured along the longest dimension are: plagioclase 0.8–2.5 mm, clinozoisite 0.5–5 mm, garnet 0.5–1.5 mm, and scapolite 1–2 mm. The modal mineralogical composition of this type in weight per cent is:

Anorthite (An_{98})	66.1
Clinozoisite	21.1
Garnet	7.2
Scapolite	4.2
Calcite	1.4

The plagioclase in this type is remarkably fresh and is almost pure anorthite. More than a dozen thin sections were examined on the five-axis stage; the plagioclase crystals exhibit several twin laws, including complex types. The clinozoisite is very low in epidote molecule as indicated by the refractive indices: N_X = 1.715, N_Y = 1.716, N_Z = 1.718. The garnet is grossularitic with N = 1.768. Another mineral closely resembling this garnet and clinozoisite is present in some anorthosites of this type and may be vesuvianite. Scapolite, secondary after anorthite, is present, and the indices of refraction for these grains, N_E = 1.552 and N_O = 1.582, indicate nearly 70 per cent meionite molecule in the mineral. Corundum occurs as porphyroblastic crystals in fair abundance, while clinozoisite and garnet replace anorthite.

Anorthite-anthophyllite-edenite rock: C.69.—This unusual rock has a limited distribution; it is interpreted as a pegmatitic phase of the anorthosite. Megascopically it resembles the feather amphibolite of the Grenville terrane (Adams and Barlow, 1910). Hand specimens consist of granular anorthite, in which dimensionally oriented edenite prisms with a marked lineation, and large prismatic crystals of anthophyllite are embedded; the longer axes of the anthophyllite are parallel to the plane of banding, but in all azimuths within that plane. The density of this type is 2.833 gm/cm^3.

Thin sections display a mosaic texture, composed of polygonal crystals of anorthite, with prismatic crystals of edenite and anthophyllite aligned in a matrix of anorthite. Occasionally large blades of edenite show a diablastic relationship and enclose small grains of pure anorthite (An_{98}). The grain sizes of the various minerals measured in their direction of maximum elongation are: plagioclase 0.6–1.5 mm; anthophyllite 3–14 mm, occasionally up to 10 cm; edenite 1–3 mm, occasionally up to 5 cm. The approximate modal mineralogical composition in weight per cent is:

Plagioclase An_{90-92}	69.70
Anthophyllite	8.20
Edenite	21.80
Spinel	0.30

The feldspar is anorthite (An_{90-92}), with incipient scapolitization. Anthophyllite is obviously an aluminian variety with N_Z = 1.659, nearly the same as that of an analyzed specimen of the mineral from a similar rock. The mineral is distinguished from edenite by its straight extinction and characteristic absorption in shades of tan and clove brown. The edenite in this rock has the following optical characters: N_X = 1.649, N_Y = 1.659, N_Z = 1.667; $2V$ = −84°; $r < v$; $X < Y < Z$ in yellowish and bluish green. These optical properties indicate a composition close to that of the analyzed edenite C.34. Small grains of green spinel are scattered in the groundmass feldspar and may have resulted during formation of amphibole from the primary pyroxenes.

Bytownite-clinozoisite-edenite gneiss: C.128.—This rock is characterized by a fine-grained texture, with a smaller grain size. Clinozoisite and edenite show a dimensional orientation, and the rock as a whole is pearl gray with a density of 2.751 gm/cm^3. Thin sections display an inequigranular xenoblastic texture, with marked mutual interference of grains. The plagioclase feldspars range in length from 0.1 to 1.2 mm, the edenite prisms from 0.5 to 1.0 mm, clinozoisite from 0.4 to 7.0 mm, and the diopside skeletal crystals are 0.2 mm wide and 1.5–3.0 mm long. The modal composition of this type is:

Plagioclase (An_{84-88})	89.2
Clinopyroxene	2.4
Edenite	5.3
Clinozoisite	3.1

The plagioclase in this rock is bytownite (An_{84-88}) forming a mosaic of polygonal grains, most of which are untwinned (Pl. 5, fig. 4). Skeletal crystals of diopside undergoing paramorphic alteration to edenite occur interstitially in the plagioclase mosaic. The optical properties of this clinopyroxene ($2V$ = +60°; $Z \wedge c$ = 43) indicate it is in the diopside-hedenbergite group. The edenite has the following optical characters: N_X = 1.657, N_Y = 1.669,

$N_Z = 1.679$; $2V = 79.5°$; $Z \wedge c = 18°$; $r < v$; $X < Y < Z$, yellowish to bluish green. In comparison with the analyzed edenite this appears to be an iron-rich variety. The clinozoisite is intensely zoned and indicates two distinct compositions, as may be seen from the values for the indices of refraction $N_X = 1.718$ and 1.730, $N_Z = 1.729$ and 1.766; the higher values indicate a higher proportion of epidote molecule. Corundum is infrequent. This type is fairly conspicuous in the anorthosite belt, forming low hills.

Schistose edenite gneiss: C.15.—Within the anorthosites there are several mafic layers composed mainly of monoclinic amphibole. In hand specimen these perknites are dark green with a density of 3.0 gm/cm³ and have a schistose texture because of the platy parallelism of the amphibole crystals. The approximate modal composition is:

Edenite	83.0
Plagioclase	12.6
Clinozoisite	2.0
Scapolite	1.7
Calcite	0.7

Thin sections have a schistose texture. Scapolite and calcite form at the expense of the plagioclase. The edenite crystals are 0.8–8 mm long and have the following optical characters: $N_X = 1.651$, $N_Y = 1.661$, $N_Z = 1.669$; $2V = -83°$; $X < Y < Z$ in yellowish and bluish green.

The above general description of some of the principal types adequately summarizes the petrographic characters of the anorthosite series. Besides those described, there are types with a variable assemblage of the minerals described, but the general textural and paragenetic relaionships remain the same. The petrography of these rocks indicates a remarkable homogeneity in the composition of the minerals, and the variations noted are quite normal. The distribution of corundum appears to be controlled by the composition of the associated plagioclase and does not depend on the mineral composition of the rock.

Chromitites.—The chromitites occur as steeply dipping layers in the anorthosite horizon. These chromitite layers are parallel to the general layering, and the ore bodies run for more than 10 miles in this horizon of the complex. The chromitites are composed of clinoamphibole and varying proportions of chromite, with rutile and corundum as rarer constituents. While the chromitites are essentially made up of amphiboles and chromite, the rocks of the chromitite horizon are mostly anorthite-hornblende gneisses. This is an exceptional feature, as in other investigated stratiform sheet complexes the mineralogy of the chromitites is similar to that of the entire ore horizon, except for the high proportion of ore. This peculiarity must be attributed to the metamorphic transformations undergone by these rocks, resulting in two distinct assemblages.

Chromitite has been defined by Johannsen (1937, vol. 4, p. 466) as a rock composed essentially of chromite. If pyribole exceeds 50 per cent it is prefixed by the corresponding appropriate name. The chromitites under consideration contain 55–75 per cent chromite; the rest is largely monoclinic and orthorhombic amphiboles identified as pargasite and gedrite. Hence, by definition, these rocks should be regarded as amphibole chromitites. The term chromitite is, however, adopted here to indicate such rocks.

In hand specimen these rocks are greenish black, and the chromite grains display a metallic luster. The amphiboles show a preferred orientation comformable to that in the anorthosites. The proportion of ore in these rocks ranges from 50–85 per cent, but the average is about 60 per cent. The chromite is distributed as granular aggregates in the groundmass of amphiboles. In thin section these chromitites show a schistose texture displaying the preferred orientation of the amphiboles. The rocks have pseudo-porphyritic poikilitic texture with the chromite grains distributed in a groundmass of monoclinic and orthorhombic amphiboles. The chromite grains are euhedral to subhedral with coffee-brown semitranslucent, thin edges. They range from 0.02 to 2 mm in diameter with some grains carrying small insets of rutile. The monoclinic amphibole present has the following optical characters: $N_X = 1.640$, $N_Y = 1.647$, $N_Z = 1.656$; $Z \wedge c = 19°$; $2V = +85.5°$; $r > v$; $X = Y < Z$, pale green to emerald green. Chemical analysis of

this type of amphibole indicates affinities with pargasite. The orthorhombic amphibole in these chromitites has an unusual play of colors, attributable to chadacrysts of chromite and spinel. The refractive index N_Z for the orthorhombic amphibole is 1.637 and 1.643 for different specimens, the low values indicating a more magnesian composition, as compared with the anthophyllites in the anorthosites. Green spinel, corundum, and talc are present in minor amounts.

Cordierite - corundum - sillimanite - anthophyllite-bytownite rock: C.71.—This rock occurs in an old corundum quarry within the anorthosite belt. In view of its peculiar mineral assemblage and restricted occurrence, it has been interpreted as a xenolith. The rock is a fine-grained aggregate of anorthite-bytownite with several large crystals of cordierite, anthophyllite, pinkish corundum, and knots of sillimanite developed in the feldspathic matrix. The density of the rock is 2.90 gm/cm^3, and the modal composition is:

Plagioclase (An_{73-91})	30.2
Cordierite	30.8
Anthophyllite	4.0
Corundum	21.2
Clinozoisite	1.4
Scapolite	4.4
Calcite	2.0
Spinel	0.5
Sillimanite	5.0
Ores	0.5

The grain sizes of the minerals are: feldspar 0.5–2 mm, cordierite 1.4–6 mm, corundum 1.8–10 mm, sillimanite 0.2–4 mm, and anthophyllite 0.2–3 mm.

Thin sections show crystalloblastic texture with a mosaic of calcic plagioclase in which larger grains of cordierite and corundum are embedded with apparent replacement relationship. Anthophyllite occurs as prismatic crystals within and outside the cordierites; aggregates of acicular sillimanite are distributed within larger cordierite and plagioclase crystals. Scapolite and calcite are secondary after the feldspar. A few grains of clinozoisite are scattered over the matrix; green spinel (pleonaste?) is intergrown with plagioclase. Plagioclase of two compositions occurs in this rock; grains in contact with corundum and occurring as insets in the corundum are An_{91}, while the larger grains of feldspar away from the corundum are An_{73}. Feldspars of two compositions are recorded in a corundum-sillimanite xenolith from the Bushveld complex (Hall and Nel, 1926, p. 8). Both simple and complex twins of plagioclase occur, the former in greater profusion. The scapolite secondary after the feldspar has 65 per cent meionite, as indicated by values for $N_E = 1.548$ and $N_O = 1.576$. Chemical analysis of the cordierite shows it to be a magnesium variety. It exhibits lamellar twinning and though fresh carries abundant sillimanite needles and other dusty particles.

The optical properties of the cordierite are: $N_X = 1.539$, $N_Y = 1.544$, $N_Z = 1.546$; $2V = -66°$. The anthophyllite is an aluminian variety as indicated by the value for $N_Z = 1.658$ which is close to that of the analyzed anthophyllite. Sillimanite is identified by its fibrous habit and small optic angle.

PLATE 3.—ANORTHOSITE AND CHROMITITE EXPOSURES

FIGURE 1.—Typical exposure of anorthosite south of Sittampundi. Note perfect foliation which coincides with layering, and the steep dips of layers.

FIGURE 2.—Chromitite layer in corundum quarry near Karungalpatti. The chromitite layer is dipping steeply and is over 10 feet thick. Note the layering of chromitite to the left of view.

PLATE 4.—PHOTOMICROGRAPHS OF SITTAMPUNDI MINERALS

FIGURE 1.—Twinned anorthite crystal in rock C.50, being replaced by clinozoisite. Magnification × 22, crossed nicols.

FIGURE 2.—Bladed anthophyllite in anorthosite C.58. Magnification × 9, plain polarized light.

FIGURE 3.—Polished section of chromitite C.101 showing chromite with unmixed rutile. The white area represents rutile, while the gray portion is chromite. Magnification × 180, plain reflected light.

FIGURE 4.—Polished surface of chromite C.101 showing exsolved plates of rutile (white) within chromite (gray). Note geometric orientation of plates. Magnification × 400, plain reflected light.

FIGURE 1

FIGURE 2

ANORTHOSITE AND CHROMITITE EXPOSURES

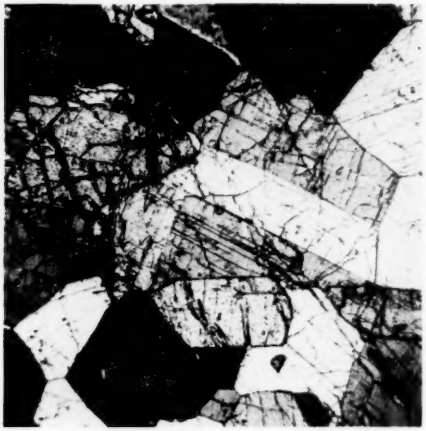

FIGURE 1

FIGURE 2

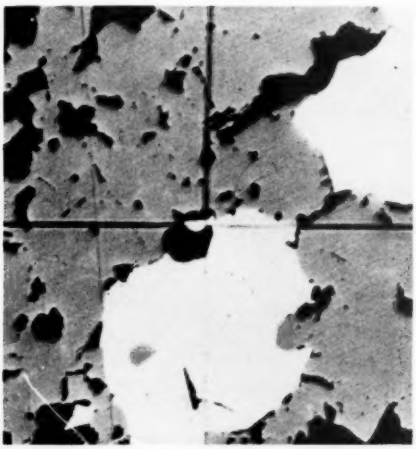

FIGURE 3

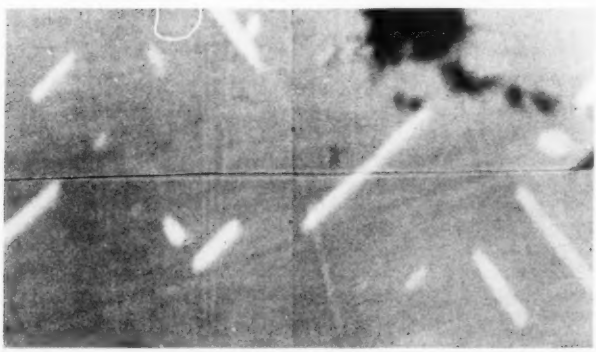

FIGURE 4

PHOTOMICROGRAPHS OF SITTAMPUNDI MINERALS

FIGURE 1

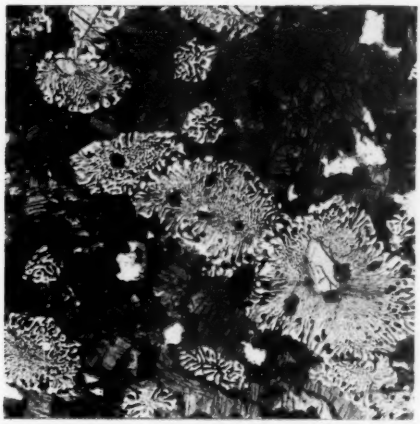

FIGURE 2

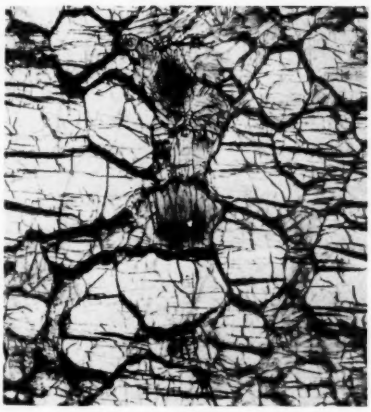

FIGURE 3

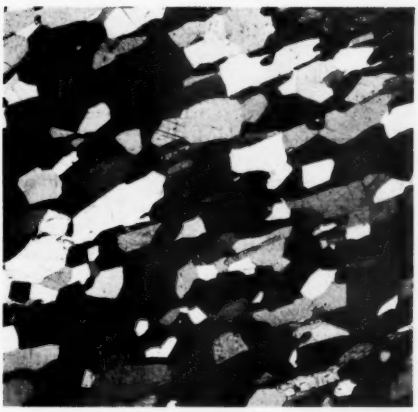

FIGURE 4

PHOTOMICROGRAPHS OF SITTAMPUNDI ROCKS

FIGURE 1

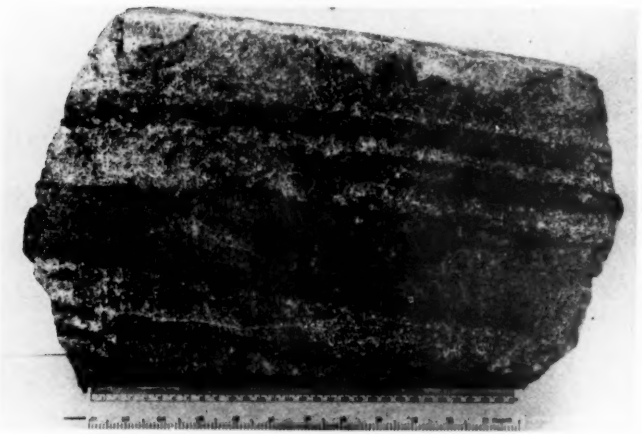

FIGURE 2

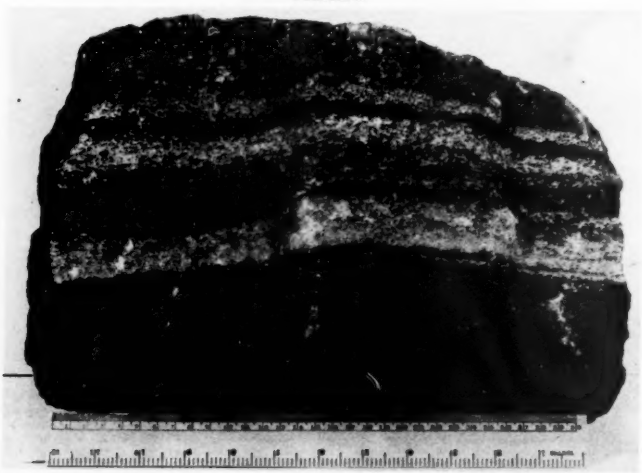

FIGURE 3

LAYERED SITTAMPUNDI ROCKS

Eclogite-Gabbro Series

General.—Eclogitic rocks occur as layers within the anorthosites and also as conspicuous bands on the southern margins of the complex. The term eclogite-gabbro series has been adopted as suitable for this assemblage of rocks, consisting of the following types: (1) eclogite-bronzitic pyropite (Bronzitic pyralmanditite), (2) bronzitic eclogite, (3) hornblende eclogite, and (4) plagioclase eclogite.

Eclogite was defined by Johannsen (1937, vol. 4, p. 462) as a rock composed of the grass-green pyroxene omphacite and pink garnets, probably metamorphic. This definition, originally made in 1822 by Hauy, has been considerably modified since then, following studies on eclogites by Briere, Eskola, Hezner, Tilley, and others. From strictly bimineralic assemblages of pyroxene and garnet, the name has been extended to polymineralic assemblages, with plagioclase, amphiboles, kyanite, and other minerals. Many authorities have considered omphacite a critical mineral for establishing a rock as an eclogite. This, to the writer, appears inadequate because the precise status of omphacite among clinopyroxenes, and distinct properties to distinguish it from green diopside, are undetermined. In this connection Davidson's (1943, p. 99–100) remarks on omphacite from eclogites of Rodil district are pertinent:

"The following physical properties of the pyroxene have been determined: $N_X = 1.680$, $N_Y = 1.687$, $N_Z = 1.704$, $N_Z - N_X = .024$, $Z \wedge c = 43°$ (+) $2V = 64° - 65°$, Sp. Gr. = 3.32.

No chemical analysis has been made, but two points are worthy of notice. Firstly, the alkalies of the eclogites are low, and the omphacite cannot therefore contain more than a small amount of the jadeite molecule. Secondly the very low silica percentage of these rocks (40.78%, 42.66%) is not greatly in excess of that of the garnet (38.72%), and the omphacite may, therefore, be presumed to be much poorer in silica than the pyroxenes from eclogites listed by Alderman (1936, pp. 495; 54.21–55.56% SiO_2). It appears probable that the greater part of the alumina in the pyroxene is present as Tschermak's silicate $[(MgFe)(AlFe)_2SiO_6]$ rather than as jadeite $[(NaK)(AlFe)Si_2O_6$ or lime jadeite $[(CaMg)(AlFe)_2Si_4O_{12}]$. In this the mineral is similar to the pyroxenes of the Saxon pyroxene granulites described by von Philipsborn (1930).

It may be noted that while in general composed dominantly of diopside + jadeite, the eclogite pyroxene recorded in petrographic literature have a wide range of composition. Eskola (1922) remarks that most of them contain an excess of alumina in addition to the alumina combined with the soda in the jadeite molecule and that they also show great variation in their CaO: (MgFe) O ratio, and also in the amount of silica. In all cases their composition may be expressed in terms of $Ca(MgFe)\ Si_2O_6$, $(MgFe)\ SiO_3$, $CaSiO_3$ $(NaK)\ (AlFe)\ Si_2O_6$, $(CaMgFe)\ (AlFe)_2\ Si_4O_{12}$, and $(CaMgFe)\ (AlFe)\ SiO_6$. In the most basic rocks the proportion of jadeite and lime jadeite is almost always small; while chromic oxide also enters into varieties associated with chromiferous peridotites. It is questionable whether any special purpose is served by

---

PLATE 5.—PHOTOMICROGRAPHS OF SITTAMPUNDI ROCKS

FIGURE 1.—Bronzitic eclogite showing incipient coronas around garnets. Note distribution of bronzite, diopside, plagioclase, and garnet. Magnification × 9, plain polarized light.

FIGURE 2.—Plagioclase eclogite C.41, showing coronas of hornblende-plagioclase symplectite around garnets. Note zonal distribution of ores around garnets. Figures 5 and 15 are micrographs of garnet coronas from the same thin section. Magnification × 10, plain polarized light.

FIGURE 3.—Bronzitic pyropite C.60 composed mainly of garnet and bronzite. Note horizontal fracturing of the garnets. Magnification × 15, plain polarized light.

FIGURE 4.—Bytownite edenite clinozoisite gneiss C.128. Note abundance of untwinned plagioclase. Magnification × 7, crossed nicols.

PLATE 6.—LAYERED SITTAMPUNDI ROCKS

FIGURE 1.—Chromitite layers in anorthosite. Note several layers at the top of specimen and the thick layer in the middle. The thin discontinuous layers below the central chromitite layer are segregations of hornblende in anorthosite.

FIGURE 2.—Layered bronzitic pyropite (eclogite). Darker layers consist of garnet and orthopyroxene; lighter layers are composed essentially of bronzite with a little garnet and secondary amphibole. The layers seem to reflect primary compositional layering.

FIGURE 3.—Chromitite layers in anorthosite. The thick layer at the bottom of specimen is chromitite. Note the absence of mafic minerals in the zone immediately below the chromitite layer. The layers at the top are mainly composed of hornblende.

maintaining the name omphacite for a species of considerable range in composition."

Eclogites are generally regarded to carry a garnet rich in pyrope and almandite molecules; no critical range has been fixed for its composition, though suggestions have been made by Eskola (1921), Heritsch (1926), and Wright (1938).

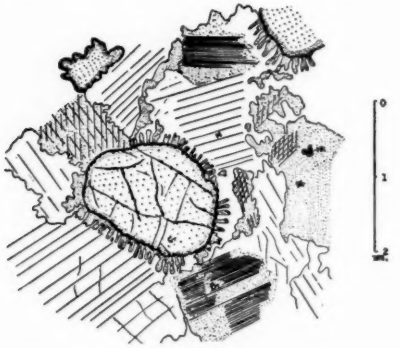

FIGURE 13.—MICROGRAPH OF BRONZITIC ECLOGITE

Note incipient development of coronas around the garnets. Gr, Garnet; Br, Bronzite; Pl, Plagioclase; Hb, Hornblende; Mt, Magnetite

A review of the literature by the writer has shown that garnets in true eclogites are more pyropic than those in gabbros and granulites. The writer believes that many rocks carrying almandite garnets and described as eclogites may be only granulites or high-grade amphibolites.

Bronzitic pyropite.—Hand specimens are green, studded with pinkish-red grains of garnet, and have a density of 3.35 gm/cm³. Weathered specimens are studded with garnets, owing to differential weathering, giving the impression that the rocks are composed wholly of garnet. Hand specimens have a holocrystalline texture without foliation.

Thin sections show rounded grains of garnet with very thin kelyphitic rims and interstitial clino- and orthopyroxenes. The garnets are 0.8–4 mm in diameter and characterized by a system of horizontal cracks (Pl. 5, fig. 3). The optical properties of the minerals and their inferred compositions are shown in the tabulation of modes.

Similar rocks with higher proportions of garnet have been observed, and in view of the preponderance of pyralmanditic garnet and the presence of bronzite the name bronzitic pyropite is suggested for this unique petrographic type. For euphony the suffix pyropite is used here instead of pyralmanditite.

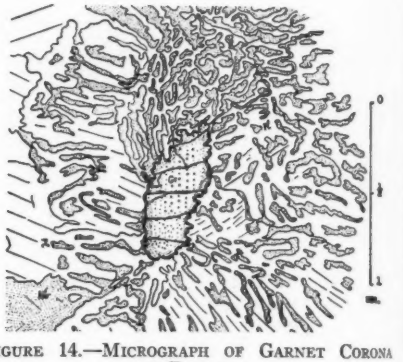

FIGURE 14.—MICROGRAPH OF GARNET CORONA IN ECLOGITE

Note profuse development of vermicular intergrowth of hornblende and plagioclase due to breaking up of garnet. Gr, Garnet; Hb, Hornblende; Pl, Plagioclase

Bronzitic eclogite.—This type is characterized by a lower proportion of garnet and the appearance of plagioclase and monoclinic amphibole (Fig. 13). This variety is fine-grained, and its garnets are less conspicuous than in the bronzitic pyropite. The density is 3.24 gm/cm³.

Thin sections display a granoblastic texture with rounded grains of garnet with kelyphitic coronas (Pl. 5, fig. 1). The pyroxenes show paramorphic alteration to a greenish amphibole. The garnets are 0.5–2 mm in diameter, while the other minerals have an average grain size of 0.5–2 mm. The optical properties of the minerals and their composition are indicated in the tabulation of modes.

Hornblende eclogite.—This type is similar to bronzitic eclogite, with a marked increase in plagioclase and amphibole and a commensurate decrease in pyroxenes and garnet. The development of plagioclase-hornblende symplectite around the garnets, which was incipient in the type described before, is conspicuous (Fig. 14). Texture and mineral associations are similar to the bronzitic eclogite, but the plagioclase shows alteration to scapolite. The optical properties of the minerals and their estimated compositions are tabulated.

Plagioclase eclogite (Garnet-hornblende-plagioclase rock) C.41.—This is perhaps the most prevalent type of eclogite in the complex and differs from the type described above in carrying a smaller proportion of amphibole. Weathered hand specimens show an incipient foliation with conspicuous rounded grains of garnet. Thin sections display a crystalloblastic texture, with garnets embedded in a matrix of pyriboles and plagioclase. Progressive development of plagioclase symplectites from garnets is noticed in thin sections of this type.

FIGURE 15.—MICROGRAPH OF GARNET CORONA IN ECLOGITE

The garnet has been completely broken down with consequent development of hornblende plagioclase symplectite, and liberation of iron in the form of ores, which are zonally distributed.

The first stage in the paramorphic alteration of the garnet is the development of incipient kelyphitic rims, which gradually give way to wisps of green hornblende. The next stage is the development of radial hornblende crystals all around the garnet in a matrix of turbid plagioclase. In the final stage garnet is completely replaced by a vermicular intergrowth of plagioclase and hornblende.

The grain sizes of the minerals are: garnet 0.2–3.5 mm, plagioclase 0.5–2 mm, orthopyroxene 0.5–2 mm, clinopyroxene 0.5–2 mm, and hornblende 0.2–2 mm. The density of the rock is 3.14 gm/cm³. The optical properties of the minerals and their estimated compositions are shown in the table of modes. The pyroxenes display peripheral alteration to amphibole, and in some cases the transformation is complete. The plagioclases display strained extinction and inverse zoning with a thin more calcic rim. Similar inverse zoning has been recorded in the plagioclases of eclogites of Norway by Eskola (1921) and in the basic charnockitic rocks of Jeypore by Ghosh (1941, p. 12). Dr. J. R. Smith estimated that the calcic rim constitutes 12 per cent of the total feldspar. Oriented liquid or gas inclusions are present in some feldspar plates. The only minor accessory mineral is magnetite which has a zonal distribution around the garnets (Figs. 5, 15; Pl. 5, fig. 2) and probably represents iron released from garnets during the formation of the symplectite.

The modal mineralogical composition of these types and the composition of the principal minerals in them are:

Minerals present	Bronzitic* pyropite	Bronzitic eclogite	Hornblende eclogite	Plagioclase* eclogite
Quartz	.....	...	...	1.5
Plagioclase	1.4	17.5	22.4	19.3
Clinoamphibole	2.2	16.3	25.3	12.0
Clinopyroxene	5.8	7.1	4.4	7.0
Orthopyroxene	7.2	6.4	3.9	7.2
Garnet	72.4	39.8	31.2	32.3
Ores	1.2	1.6	1.2	1.5
Spinel	.....	0.4	0.7	...
Scapolite	.....	...	1.7	...
Kelyphite (Plag + Pyrx) + Amp.	9.8	10.9	9.2	19.2
Orthopyroxene En per cent	84	86	86	84.5
Plagioclase An per cent	—	48–58	40–45	48–58
Mg per cent of garnet	55	51†	50†	46
Clinopyroxene	diopside-salite			
Density gm/cm³	3.35	3.24	3.18	3.14

* These rocks have been analyzed and will be discussed in a later section.

† Expressed as ratio of MgO molecules according to Eskola (1921) and estimated from value N.

Retrograde characters of eclogitic rocks.—Alderman (1936) and Davidson (1943) have deciphered the retrograde changes in eclogites by detailed petrographic examination. Some of their observations find a parallel in the eclogites of the Sittampundi complex. The retrograde features, incipient in the bronzitic pyropites, become marked in the bronzitic eclogites and pronounced in the hornblende and plagioclase eclogites.

The first stage in diaphthoresis is the paramorphic alteration of clinopyroxene to amphibole. In the bronzitic pyropites, kelyphitic rims composed of a mesostasis of plagioclase, clinopyroxene, and amphibole represent this stage. The next stage is the development of green hornblende as wisps and vermicular intergrowths in plagioclase around the garnets marking the destruction of the garnet. This is discernible in thin sections of bronzitic eclogite. In some cases the plagioclase-clinopyroxene stage is not discernible; Davidson (1943, p. 101) believes this is due to the low alkali content and basic composition of the rock and to the presence of hypersthene molecule in the clinopyroxene.

The garnets in the retrograde eclogites have exceptional symplectite rims consisting of wisps of green hornblende radially arranged around the garnets in a groundmass of plagioclase An_{50}, surrounded by a zone of granular ore. Davidson (1943, p. 101) recorded the presence of iron ore in some eclogites from Rodil district and considered them as released during the amphibolization of pyroxene. He also stated that soda and lime released during the amphibolization of the pyroxene might have reacted with the garnet to form kelyphite accompanied by considerable separation of magnetite. These observations and inferences hold good in the case of the Sittampundi eclogites (Fig. 15).

Holland (1896, p. 29) regarded the reaction rim around garnets as representing a stage in the formation of garnet from the primary mafic minerals. Fermor (1912) believed that kelyphitic rims or reaction borders are formed by the destruction of garnet owing to gradual lowering of pressure accompanied by rapid reduction of temperature. Eskola (1920, p. 176), discussing such structures in Norwegian eclogites, states:

> "In the igneous Norwegian eclogites the development often has been the following: When the crystallization of the garnet was completed and liquid magma was still present, the conditions of the amphibole facies set in, and now hornblende and plagioclase crystallized directly from the magma around the garnet. The latter may thus be an unstable relic, if its field of stability does not continue into lower temperatures than that of pyroxene."

This interpretation is based on the doubtful assumption that garnet crystallizes out of a magma. Buddington (1939, p. 297), discussing corona structures in the Adirondack metagabbros, interpreted them as having formed during the closing stages of deformation associated with regional dynamothermal metamorphism. Shand (1945, p. 264) proposed a theory which fits observed petrographic details. He believed that the corona formed during thermal metamorphism, when iron and magnesium ions liberated from an iron-rich olivine reacted with anorthite of the plagioclase forming garnet or amphibole, and spinel; the albite molecule left in the feldspar redistributed itself in the feldspar framework. Though this explanation maintains for the formation of primary garnet with a kelyphitic rim from an ultramafic plutonic rock, the formation of symplectites around garnets appears to be related directly to changes in temperature and pressure conditions.

Pyroxenite

General.—Two types of pyroxenites occur within the complex and are later intrusions. They can be considered websterites as they are composed of equal proportions of monoclinic and orthorhombic pyroxenes. The two types are: an even-grained websterite occurring as small masses and a coarse pegmatitic websterite occurring as narrow lenticular bodies within the anorthosites.

Websterite pegmatite.—This is bimineralic and composed of coarse crystals of hypersthene and diopside; the average grain size exceeds 3 cm. The orthopyroxene is faintly pleochroic with $N_Z = 1.689$, indicating a composition of 79.5 per cent enstatite. The clinopyroxene is a diallagic diopside with $N_X = 1.681$, $N_Z = 1.709$, $2V = +56°$, $Z \wedge c = 42°$.

Websterite.—This is an even-grained greenish rock composed of fresh pyroxenes. Thin sections show a typical granulitic texture; the ortho- and clinopyroxenes form a matrix of interlocking grains in which occasional grains of chromite are scattered. The orthopyroxene is hypersthene with 77 per cent enstatite as indicated by $N_Z = 1.695$. The clinopyroxene is deduced to fall in the diopside-salite range, on the basis of the following optical properties:

$N_X = 1.670, N_Z = 1.699, 2V = +60°, Z \wedge c = 42°$. The average grain size of the rock is 1.5–5 mm.

Amphibolite

Amphibolitic rocks at several points along the margins of the complex are interpreted as remnants of the metasedimentary country rock. Hand specimens are melanocratic and show preferred orientation of the amphiboles. The density of this type is 2.996 gm/cm³. Thin sections display fine-grained granoblastic texture, with an average grain size of 0.2 mm. Amphibole constitutes more than 50 per cent of the rock and forms layers in a groundmass of mortarized plagioclase. The mode of a chemically analyzed specimen of amphibolite is:

Plagioclase An_{42-45}	22.6
Orthoclase	1.5
Clinopyroxene	18.6
Clino-amphiboles	55.5
Calcite	0.9
Sphene	0.1
Ores	0.8

The plagioclase constituting the groundmass has a grain size of 0.2–0.5 mm. The principal indices of refraction on cleavage fragments $N_X = 1.552$ and $N_Z = 1.559$ indicate a composition of An_{42-45}. Undulatory extinction because of strain and turbid alterations of the crystals is noticeable. In a few specimens of amphibolite examined, the feldspar ranged from An_{30} to An_{50}. The amphiboles are pleochroic in olive greens and appear to be mostly derived from clinopyroxene. The amphibole has $N_X = 1.656, N_Y = 1.666, N_Z = 1.676$, and is negative with large optic angle. The clinopyroxene is identified as diopside from its optic angle of +60°. Calcite seems to be secondary and forms granular aggregates, while a few lozenge-shaped grains of sphene occur in some amphibolites. The bulk chemical composition of the amphibolites is substantially different from the composition of the other rocks of the complex and consistent with the concept of their being genetically unrelated to the complex. The presence of calcite, sphene, and apatite, with diopside and calciferous amphibole, differentiate the amphibolite from members of the complex.

Chemical Petrology and Metamorphism

Introduction

The chemical composition of some of the significant minerals from rocks of this complex, and their bearing on the chemistry of these rocks, have been discussed in an earlier section. An attempt will be made here to discuss the chemistry of the rocks and interpret their probable metamorphic transformations.

The chemical composition and the normative and modal mineralogical composition of the analyzed rocks of the complex are presented in Table 30. In Table 31, the analyses of the anorthositic rocks from the complex are compared with analyses of anorthosites from South Africa and Sweden. In Table 32 the analyses of eclogites from this complex and comparable analyses of similar rocks from other parts of the world are presented.

Origin of Minerals

Garnets.—The following reactions suggest the paragenesis of the garnet and related minerals in anorthositic rocks:

(1) $3CaAl_2Si_2O_8 + H_2O \rightarrow Ca_3Al_2Si_3O_{12} + 2Al_2O_3 + 3SiO_2 + H_2O$
anorthite — garnet + corundum + quartz in solution

(2) $7CaAl_2Si_2O_8 + H_2O \rightarrow 2Ca_2Al_3(SiO_4)_3(OH) + Ca_3Al_2Si_3O_{12} + 2Al_2O_3 + 5SiO_2$
anorthite — clinozoisite — garnet — corundum + quartz

(3) $2(MgFe)SiO_3 + CaAl_2Si_2O_8 + H_2O \rightarrow Ca(MgFe)_2Al_2Si_3O_{12} + SiO_2 + H_2O.$
hypersthene — anorthite — garnet — quartz in solution

These reactions merely indicate the possible trends in the evolution of the garnet from an anorthositic rock. Minerals such as augite must have partaken in these reactions to produce a grossularitic garnet with andradite and small

TABLE 30.—CHEMICAL COMPOSITION WITH NORMATIVE AND MODAL MINERALOGICAL COMPOSITION OF SOME ROCKS FROM THE SITTAMPUNDI COMPLEX

Constituent	1	2	3	4	5	6	7	8
SiO_2	44.58	41.61	44.89	46.86	37.63	46.93	44.21	48.50
TiO_2	0.06	0.06	0.05	0.03	0.00	0.12	0.24	0.63
Al_2O_3	30.81	33.17	31.53	33.05	47.50	19.42	17.86	14.15
Fe_2O_3	0.94	1.78	0.38	0.46	0.14	0.44	3.42	2.62
Cr_2O_3	0.02	...	...	...	0.01	0.04	...	0.09
FeO	1.77	0.22	2.66	0.48	1.15	8.24	7.89	6.36
MnO	0.04	0.02	0.05	0.01	0.03	0.15	0.16	0.29
MgO	2.72	0.23	3.68	0.42	2.48	10.08	14.76	9.18
CaO	17.05	20.96	14.88	16.53	9.05	12.43	10.94	12.95
Na_2O	1.35	0.32	1.35	1.99	1.12	1.61	0.30	2.43
K_2O	0.07	0.05	0.03	0.04	0.03	0.04	0.00	0.29
P_2O_5	0.00	0.01	0.01	0.01	0.01	0.00	0.01	0.02
H_2O+	0.58	0.97	0.68	0.30	0.66	0.74	0.35	1.27
H_2O-	0.06	0.20	0.11	0.04	0.07	0.12	0.05	0.13
CO_2	...	0.51	...	...	..	.....	...	0.95
Cl	0.01	0.00	0.00	...	0.01	0.02	...	..
F	0.01	0.01	0.01	...	0.00	0.01	...	..
Less O for Cl + F	0.01	...	...	...	..	0.01	...	..
Total	100.06	100.12	100.31	100.22	99.89	100.38	100.19	99.86
C.I.P.W. Norms								
Quartz	...	...	...	...	7.08	.....	...	..
Orthoclase	...	...	...	...	..	.....	...	1.67
Albite	7.60	...	11.53	15.98	9.43	13.62	2.62	20.44
Anorthite	77.84	88.96	73.95	80.90	45.04	45.04	47.26	26.69
Nepheline	2.13	1.42	...	0.43	..	.....	...	..
Corundum	...	...	2.14	...	29.10	.....	...	..
Wollastonite	...	3.36	...	...	..	.....	...	..
Calcium Orthosilicate	...	0.86	...	...	..	.....	...	..
Diopside								
Wo	2.90	0.58	...	0.46	..	6.84	2.90	13.22
En	1.95	0.50	...	0.30	..	4.10	2.10	8.70
Fs	0.72	...	...	0.13	..	2.38	0.53	3.56
Hypersthene								
En	...	...	3.10	...	6.20	4.50	16.04	6.60
Fs	...	...	1.45	...	1.98	2.51	5.02	2.77
Olivine								
Fo	3.36	...	4.27	0.49	..	11.62	12.88	2.24
Fa	1.57	...	2.34	0.31	..	7.55	4.69	5.32
Magnetite	1.39	0.70	...	0.70	0.23	0.70	4.87	3.71
Ilmenite	...	...	...	...	..	0.15	0.46	1.06
Hematite	...	1.28	...	...	..	.....	...	..
Chromite	...	...	...	...	..	.....	...	0.25
Calcite	...	1.10	...	...	..	.....	...	2.10
Normative plagioclase								
Anorthite per cent	90	100	88	83.5	82.5	79	94.5	57
Albite per cent	10	0	12	16.5	17.5	21	5.5	43

TABLE 30 (Cont.)

Constituent	1	2	3	4	5	6	7	8
Modes expressed as weight percentages on the basis of point-count analyses of 10000 points								
Quartz	...	...	...	...	..	1.5	...	..
Plagioclase	79.1	66.1	69.7	89.2	30.2	19.3	1.4	22.6
Orthoclase	...	...	...	...	..	.....	...	1.5
Cordierite	...	...	...	...	30.8	.....	...	..
Clinopyroxene	...	...	...	2.4	..	7.0	5.8	18.6
Orthopyroxene	...	...	...	...	..	7.2	7.2	..
Orthoamphibole	...	...	8.2	...	4.0	.....	...	..
Clinoamphibole	20.9	...	21.8	5.3	..	12.0	2.2	55.5
Garnet	...	7.2	...	...	..	32.3	72.4	..
Corundum	...	...	...	...	21.2	.....	...	..
Clinozoisite Epidote	...	21.1	...	3.1	1.4	.....	...	..
Scapolite	...	4.2	...	...	4.4	.....	...	..
Calcite	...	1.4	...	...	2.0	.....	...	0.9
Spinel	...	...	0.3	...	0.5	.....	...	..
Ores	Tr	...	...	...	0.5	1.5	1.2	0.8
Sphene	...	...	...	...	..	.....	...	0.1
Sillimanite	...	...	...	...	5.0	.....	...	..
Kelyphite plagioclase+ clinoamphibole+ clinopyroxene	...	...	...	...	..	19.2	9.8	..
Modal plagioclase								
Anorthite per cent	90–96	98–100	90–92	84–88	73–91	50 and 80		42–45
Albite per cent	4–10	0–2	8–10	12–16	9–27	20 and 50		55–58
Density	2.825	2.934	2.833	2.751	2.904	3.139	3.350	2.996

C.33 (1) Anorthite-edenite gneiss, from old corundum quarries 1 mile southwest of Sittampundi, Salem district, Madras, India. Analyst: Eileen K. Oslund, Minnesota

C.50 (2) Anorthite-clinozoisite-garnet rock, from old corundum workings 2 miles S of Konasamudram, Salem district, Madras, India. Analyst: Eileen K. Oslund, Minnesota

C.69 (3) Anorthite-anthophyllite-edenite rock simulating feather amphibolite, three-quarters of a mile west of Karungalpatti, Salem district, Madras, India. Analyst: Eileen K. Oslund, Minnesota

C.128 (4) Bytownite-clinozoisite-edenite gneiss, from summit of small temple hill north of Kattipalaiyam, Salem district, Madras, India. Analyst: Eileen K. Oslund, Minnesota

C.71 (5) Cordierite-corundum-sillimanite-anthophyllite-bytownite rock, three-quarters of a mile west of Karungalpatti, Salem district, Madras, India. Analyst: Eileen K. Oslund, Minnesota

C.41 (6) Garnet-hornblende-plagioclase rock (plagioclase eclogite) from band west-southwest of Sittampundi, Salem district, Madras, India. Analyst: Eileen K. Oslund, Minnesota

C.60 (7) Pyroxene garnet rock (bronzitic pyropite) east-northeast of Vadugupalaiyam, Salem district, Madras, India. Analyst: Eileen K. Oslund, Minnesota

C.45 (8) Amphibolite, from outcrop on northern margin of complex, three-quarters of a mile south of Konasamudram, Salem district, Madras, India. Analyst: J. A. Maxwell, Minnesota

amounts of almandite and pyrope. The close association of corundum, clinozoisite, and garnet in anorthitic rocks support this suggestion. The several massive quartz veins within the anorthositic belt may represent the SiO_2 released during the formation of the above minerals.

The paragenesis of garnets in gabbroic and eclogitic rocks has been discussed by several petrologists. Among others, Ghosh (1941, p.

15, 20, 25) and Davidson (1943, p. 103) suggested several equations indicating prograde reactions. While these reactions oversimplify the problem of the evolution of garnets, they indicate numerous chemical reactions operative in their formation. The paragenetic relationship of the ferromagnesian minerals, plagioclase, and garnet suggest some of these reactions:

$$2Ca(Mg\cdot Fe)Si_2O_6 + CaAl_2Si_2O_8 \rightarrow Ca_3Al_2Si_3O_{12} + 2(Mg\cdot Fe)SiO_3 + SiO_2$$
diopside + anorthite — garnet + hypersthene + quartz

$$2Ca(Mg\cdot Fe)Si_2O_6 + \left\{\begin{matrix}NaAlSi_2O_8\\CaAl_2Si_2O_8\end{matrix}\right\} \rightarrow Ca_3Al_2Si_3O_{12} + 2(Mg\cdot Fe)SiO_3 + NaAlSi_3O_8 + SiO_2$$
diopside + labradorite — garnet + hypersthene — albite + quartz

$$2MgSiO_3 + MgOAl_2O_3 + SiO_2 \rightarrow Mg_3Al_2Si_3O_{12}$$
enstatite + spinel + quartz — pyrope

$$\underbrace{3CaAl_2Si_2O_8 + 2NaAlSi_3O_8}_{\text{labradorite}} + 3Mg_2SiO_4 + nCaMg(SiO_3)_2 \rightarrow 3CaMg_2Al_2(SiO_4)_3$$
labradorite + olivine 2 + diopside — garnet

$$+ \underbrace{2NaAl(SiO_3)_2 + nCaMg(SiO_3)_2}_{\text{omphacite}} + 2SiO_2$$
omphacite + quartz

$$5CaAl_2Si_2O_8 + 5(Mg\cdot Fe)_2SiO_4 + 4(Mg\cdot Fe)SiO_3 \rightarrow \underbrace{5[Ca_{0.6}(Mg\cdot Fe)_{2.4}]Al_2Si_3O_{12}}_{\text{5 garnet}} + 2Ca(MgFe)Si_2O_6$$
5 anorthite + 5 olivine + 4 hypersthene — 5 garnet + 2 diospide

$$3MgSiO_3 + Al_2O_3 \rightarrow Mg_3Al_2Si_3O_{12}$$
enstatite + corundum — pyrope

$$Mg\cdot CaSi_2O_6 + CaAl_2Si_2O_8 \rightarrow MgCa_2Al_2Si_3O_{12} + SiO_2$$
diopside + anorthite — garnet + quartz

$$2(Mg\cdot Fe)SiO_3 + CaAl_2Si_2O_8 \rightarrow Ca(Mg\cdot Fe)_2Al_2Si_3O_{12} + SiO_2$$
hypersthene + anorthite — garnet — quartz

$$(Mg\cdot Fe)_2SiO_4 + CaAl_2Si_2O_8 \rightarrow Ca(Mg\cdot Fe)_2Al_2Si_3O_{12}.$$
olivine + anorthite — garnet

Eskola (1921), Heritsch (1926), and Wright (1938) suggested compositional ranges for eclogite garnets; these are tabulated, together with the compositional range for true eclogite garnets deduced by the writer from analysis of the literature.

Composition of eclogite garnet (per cent)

End member	Heritsch	Eskola	Wright	Subramaniam
Grossularite	9–42	9–20	5–41	12–22
Andradite	0–21	2–11	4–20	3–15
Almandite	33–57	26–61	6–66	25–40
Pyrope	19–37	16–61	10–81	42–61
Spessartite	0–3	1–2	1–12	0–2

Epidote-plagioclase equilibrium.—Ramberg (1944, p. 52) stated that under conditions of regional metamorphism temperature influences the equilibrium more than pressure, resulting in progressive enrichment in anothrite by increasing metamorphic grade. He further stated (p. 52):

". . . .but because of the small difference in the chemical composition of anorthite and zoisite the equilibrium: plagioclase-zoisite is not only dependent on *P-T*-conditions. The average composition of the paragenesis plays a role. In super-silicified and H_2O-saturated rocks only the ratio Ca/Al affects the equilibrium at constant *P* and *T*. Since the Ca/Al ratio is greater in zoisite than in anorthite, Ca-rich environments in the pore liquid will displace the equilibrium towards zoisite and albitic plagioclase. Al-rich environments, on the other hand, will displace it towards anorthitic plagioclase.

"Petrographic experience seems to prove that the difference in the Ca/Al ratios of the common minerals: Garnet, hornblende, biotite and diopsidic pyroxene has no important effect on the equilibrium plagioclase $\rightleftarrows$ zoisite. That is to say, that the composition of the plagioclase which is in stable equilibrium with zoisite in common rocks is principally determined by the *PT* conditions."

TABLE 31.—CHEMICAL COMPOSITION OF SITTAMPUNDI ANORTHOSITES AND COMPARABLE ANALYSES

	1*	2	3	4†	5	6	7	8**	9	10	11
SiO_2	48.90	48.25	47.48	48.62	41.61	46.86	44.58	48.85	43.49	48.19	44.89
TiO_2	tr	0.05	tr	0.40	0.06	0.03	0.06	0.10	0.19	0.42	0.05
Al_2O_3	30.00	30.60	32.34	28.77	33.17	33.05	30.81	26.45	29.27	26.54	31.53
Fe_2O_3	0.50	0.90	0.70	1.27	1.78	0.46	0.94	0.45	0.79	0.99	0.38
Cr_2O_3	..	..	..	0.00	..	.....	0.02	..	.....	0.18	..
FeO	1.30	0.95	0.38	1.44	0.22	0.48	1.77	2.15	2.61	3.22	2.66
MnO	0.00	0.00	0.19	0.06	0.02	0.01	0.04	..	0.03	0.06	0.05
MgO	0.55	0.65	0.38	1.42	0.23	0.42	2.72	4.25	4.50	2.59	3.68
CaO	16.90	17.75	16.00	14.10	20.96	16.53	17.05	14.05	15.06	13.99	14.88
Na_2O	1.95	0.60	1.92	2.64	0.32	1.99	1.35	2.10	1.24	2.50	1.35
K_2O	0.15	0.10	0.43	0.27	0.05	0.04	0.07	tr	1.09	0.35	0.03
P_2O_5	tr	0.25	0.20	0.02	0.01	0.01	..	0.05	0.25	0.20	0.01
CO_2	tr	..	0.04	0.65	0.51	.....	..	tr	.....	0.05	..
H_2O^+	0.10	0.25	0.23	0.40	0.97	0.30	0.58	0.15	1.37	0.71	0.68
H_2O^-	0.10	0.15	0.04		0.20	0.04	0.06	0.10	0.13	..	0.11
Cl	..	..	..	..	0.00	.....	0.01	..	S = 0.05	..	0.00
F	..	..	..	..	0.01	.....	0.01	..	.....	..	0.01
(Ni, CO)O	..	..	0.02	..	..	less 'O' for F + Cl	0.01	..	.....	..	..
	100.90	100.50	100.35	100.18	100.12	100.22	100.06	100.70	100.07	99.99	100.31
Density	2.79	2.737	2.728	..	2.934	2.751	2.825	..	2.75	..	2.833
Modal plagioclase	An_{83}	An_{90}	An_{80}	An_{80}	An_{98}	An_{86}	An_{90}	An_{78}	An_{80}	..	An_{91}
Approximate % of plagioclase	96	96	98	82	66	89	79	85	82	..	70

(1, 2, 3) Anorthosite, from critical zone of Bushveld complex, quoted from Hall (1932, p. 334)
(4) Anorthosite, Soutpansberg, quoted from Van Zyl (1950, p. 75)
(5, 6, 7) Anorthosite C.50, C.128, C.33 from Sittampundi complex
(8) Anorthositic norite, main zone, Bushveld complex, quoted from Hall (1932, p. 334)
(9) Anorthite gabbro north west of Edsvik Sweden, quoted from Johannsen (1937, p. 342)
(10) Anorthosite gabbro, Messina, quoted from Van Zyl (1950, p. 75)
(11) Anorthosite C.69 Sittampundi complex
* Summation = 100.45
† Summation = 100.06
** Summation = 98.70

In this instance the group of rocks is extremely rich in alumina, indicated by the corundum - anorthite - clinozoisite paragenesis, which supports Ramberg's hypothesis that the plagioclase-zoisite equilibrium will tend toward anorthitic plagioclase under Al-rich environment.

Ramberg (1943, p. 167) considers that the epidote minerals have a wide stability range and that the plagioclases associated with them become increasingly basic at elevated temperatures. He also considers that stable associations of plagioclase and epidote minerals are governed by equality in their pressures, which in turn is governed by pressure and temperature conditions.

Ramberg (1943, p. 166) also considers that grossularite, rich in pyrope and almandite, indicates high pressure, and vesuvianite, high-temperature environments, during metamorphism.

If Ramberg's assumptions are correct, the paragenesis of the anorthositic rocks in this complex indicates a facies formed at elevated temperatures and pressures.

Clinozoisite.—The following equations sug-

TABLE 32.—CHEMICAL COMPOSITION OF SITTAMPUNDI ECLOGITES AND COMPARABLE ANALYSES

	1	2	3	4	5	6	7	8	9	10
SiO_2	46.93	47.35	47.50	47.00	50.75	52.05	48.02	46.49	48.16	44.21
TiO_2	0.12	0.21	1.03	1.00	0.12	0.21	0.23	1.17	0.76	0.24
Al_2O_3	19.42	16.72	17.14	17.61	20.02	17.24	20.01	17.73	19.66	17.86
Fe_2O_3	0.44	0.34	2.00	2.25	0.42	0.65	1.13	3.66	1.53	3.42
Cr_2O_3	0.04	..	..	..	...	...	0.03	..	.....	..
FeO	8.24	6.91	6.04	6.78	3.87	6.65	7.29	6.17	5.06	7.89
MnO	0.15	..	..	..	0.05	0.13	0.18	0.17	0.14	0.16
MgO	10.08	12.42	10.37	8.78	9.34	8.98	10.05	8.86	7.59	14.76
CaO	12.43	14.09	13.61	14.90	13.07	11.37	11.42	11.48	13.46	10.94
Na_2O	1.61	1.42	1.42	1.14	1.14	1.83	0.51	2.16	1.88	0.30
K_2O	0.04	0.20	0.23	0.21	0.15	0.40	0.05	0.78	0.31	0.00
P_2O_5	0.00	0.01	0.14	0.40	tr	0.12	tr	0.29	0.11	0.01
H_2O^+	0.74	0.22	0.19		0.70	0.52	0.57	1.04	1.48	0.35
H_2O^-	0.12	..	0.02	0.40	0.50	0.11	0.10	..	.....	0.05
Cl	0.02	..	..	..	...	...	CO_2 = 0.25	..	S = 0.08	..
							S = 0.02			
F	0.01	..	..	..	..	...	NiO = 0.01	..	.....	..
							V_2O_3 = 0.02			
Less O Cl + F	0.01	..	..	..	...	...	.....	..	.....	..
	100.38	99.89	99.69	100.47	100.13	100.26	99.89	100.00	100.22	100.19
Density	3.139	3.383	3.36	3.01	3.386	2.965	2.98	..	.....	3.35

(1) Plagioclase eclogite, C.41, Sittampundi complex
(2) Plagioclase eclogite quoted from Marchet (1924, p. 313)
(3, 4) Kyanite eclogite and garnet amphibolite quoted from Briere (1920) p. 127 & 168
(5) Kyanite eclogite, quoted from Tilley (1937), p. 430
(6) Common Norite of the Bushveld, quoted from Hall (1932), p. 350
(7) Norite from Maryland quoted from Johannsen (1937) p. 220
(8) Daly's average of 17 olivine gabbros, Johannsen (1937) p. 222
(9) Noritic hornblende gabbro quoted from Miller (1937) p. 1412
(10) Bronzitic pyropite, C.60 Sittampundi complex.

gested by Turner (1948, p. 121–122) indicate the general trend of chemical reactions leading to the formation of this mineral:

$$\underset{\text{anorthite}}{8CaAl_2Si_2O_8} + 4CaO + 2SiO_2 + Al_2O_3 + 3H_2O \rightarrow \underset{\text{clinozoisite}}{6Ca_2Al_3(SiO_4)_3(OH)}$$

$$\underset{\text{anorthite}}{12CaAl_2Si_2O_8} + 2Na_2O + 6SiO_2 + 3H_2O \rightarrow \underset{\text{clinozoisite}}{6Ca_2Al_3(SiO_4)_3(OH)} + \underset{\text{albite}}{4NaAlSi_3O_8} + \underset{\text{corundum}}{Al_2O_3}$$

$$\underset{\text{anorthite}}{4CaAl_2Si_2O_8} + H_2O \rightarrow \underset{\text{clinozoisite}}{2Ca_2Al_3(SiO_4)_3(OH)} + 2SiO_2 + \underset{\text{corundum}}{Al_2O_3}$$
$$\qquad\qquad\qquad\qquad\qquad\qquad\qquad\qquad\qquad\qquad + \text{quartz} +$$

255) attributed the formation of cordierite in the xenoliths of Mull to their relative enrichment in magnesia and alkalis, with concomitant separation of corundum, spinel, and acid plagioclase. Bugge (1943, p. 92) advocated a metasomatic origin for cordierite suggesting the equations:

Cordierite.—This mineral makes up nearly 30 per cent of a xenolithic rock composed of calcic plagioclase, corundum, cordierite, anthophyllite, sillimanite, and spinel. Thomas (1922, p.

$$4NaAlSi_3O_8 + 2MgO \rightarrow \underset{\text{cordierite}}{Mg_2Al_4Si_5O_{18}} + 7SiO_2 + Na_2O$$
albite

$$2CaAl_2Si_2O_8 + 2MgO + SiO_2 \rightarrow \underset{\text{cordierite}}{Mg_2Al_4Si_5O_{18}} + 2CaO$$

The following modification of Bugge's second equation may have been operative in the present instance:

$$\underset{\text{anorthite}}{2CaAl_2Si_2O_8} + \underset{\text{olivine}}{Mg_2SiO_4} + 2CO_2 \rightarrow \underset{\text{cordierite}}{Mg_2Al_4Si_5O_{18}} + \underset{\text{calcite}}{2CaCO_3}$$

The presence of calcite and scapolite in the cordierite rock suggests a reaction similar to that shown in simplified form above.

Corundum.—The anorthositic rocks of the complex, which are extremely alumnious in bulk composition, contain corundum in varying proportions. The more mafic anorthosites carry little corundum, while the felsic varieties composed essentially of anorthite invariably contain 2–3 per cent corundum scattered as small basal plates and large porphyroblastic hexagonal crystals (Fig. 19). The corundum crystals range in diameter from 2 mm to 10 cm. A pinkish corundum is found in the pargasite-chromitite layers, generally as granular crystals.

The following equations show further possible origins of corundum:

$$\underset{\text{anorthite}}{2Ca\cdot Al_2\cdot Si_2O_8} + 4Mg\cdot SiO_3 + H_2O \rightarrow \underset{\text{amphibole}}{H_2Ca_2Mg_4Al_2Si_7O_{24}} + \underset{\text{corundum}}{Al_2O_3} + \underset{\text{quartz}}{SiO_2}$$

$$\underset{\text{anorthite}}{4Ca\cdot Al_2Si_2O_8} + CO_2 \rightarrow \underset{\text{meionite}}{Ca_4CO_3Si_6Al_6O_{24}} + \underset{\text{corundum}}{Al_2O_3} + \underset{\text{quartz}}{2SiO_2}.$$

The frequent presence of calcite rims around corundum indicates the reaction:

$$\underset{\text{anorthite}}{Ca\cdot Al_2Si_2O_8} + CO_2 \rightarrow \underset{\text{corundum}}{Al_2O_3} + \underset{\text{calcite}}{Ca\cdot CO_3} + \underset{\text{quartz}}{2SiO_2}.$$

Anorthosite Series

General and metamorphic facies.—The rocks of the anorthosite series are undersaturated and extremely rich in alumina, as shown by the presence in them of corundum, calcic plagioclase, and normative nepheline. While impoverishment in silica may be attributed to removal during metamorphism, it is difficult to explain the high alumina content, except by assuming that the primary magma was rich in alumina. Kolderup (1940) described corundum anorthosite facies from the Bergen Arc of Norway which supports the concept of an alumina rich magma. Van Zyl (1950) refers to a corundum-rich zone in the anorthosite gneisses of Soutpansberg in Transvaal, S. Africa, without giving petrographic details. Presumably the occurrence is similar to that in the Sittampundi rocks.

Mineralogy of these rocks show them to be rich in 'OH' molecule, and several chemical reactions have been indicated to derive an 'OH' rich paragenesis. The writer suggests that these rocks were subject to chemical readjustment during regional metamorphism, accentuated during the intrusion of a later granite which supplied adequate amounts of mineralizers. The volatiles moved along the intergranular spaces of the anorthositic rocks, actuating chemical reactions, resulting in the formation of corundum, clinozoisite, edenite and other minerals.

It is possible to infer two periods of chemical transformations in these rocks on the basis of their paragenesis. The first stage resulted in the formation of amphiboles from the primary pyroxenes and olivine, with some of the albite molecule of the plagioclase entering the amphibole framework, indicated by the composition of the amphiboles. Recrystallization and foliation were induced at this stage. These changes took place during Archean regional metamorphism characterized by intense migmatization and formation of Peninsular gneiss. This interpretation is based on the fact that corundum, clinozoisite, and garnet are definitely later,

as proved by their replacement relationship with anorthite and, sometimes, the amphibole. Skeletal diopside crystals interstitial among the feldspars and showing paramorphic alteration to amphibole are thought to be relic.

The second stage in the transformation of these rocks correlates with the intrusion of the younger granites containing mineralizers. It is thought that these changes probably took place under a limited supply of H_2O and CO_2, as otherwise the transformations would have been complete, resulting in essentially clinozoisite-corundum assemblages.

An *A-C-F* diagram of Eskola (1939, p. 352) for amphibolite facies with excess of alumina is shown in Figure 16, with the plots of analyzed anorthositic rocks amphiboles and an amphibolite from the complex. The values used in the plot are:

Rocks	*A*	*C*	*F*	
C.33	41.8	44.6	13.6	anorthositic rocks
C.50	46.4	52.5	1.1	
C.69	42.3	38.8	18.9	
C.128	48.4	48.7	2.9	
C.45	17.5	32.5	50.0	amphibolite
Amphiboles				
C.33	17.1	29.4	53.5	From anorthosite
C.34	17.4	26.9	55.7	From anorthosite
C.70	16.2	26.7	57.1	From chromitite

The hornblendes fall in the field defined by Eskola (1939, p. 352). The anorthositic rocks lie in the anorthite-cordierite-anthophyllite and anorthite-wollastonite-anthophyllite fields. Eskola (1915, p. 134) stated that anthophyllite-plagioclase paragenesis is of rare occurrence and that anothophyllite is often associated with the commingtonite-anorthite paragenesis. We have instead in the anorthositic rocks of the Sittampundi Complex, anorthite-anthophyllite-edenite paragenesis. As may be seen from the plot, Rock C.50 falls in the vacant field indicated by Turner (1948, p. 78) for the cordierite-anthophyllite subfacies.

Cordierite - corundum - sillimanite - anthophyllite-anorthite-bytownite rock.—This peculiar assemblage found within the anorthosites is interpreted as a xenolith of aluminous sediment. Thomas (1922, p. 240), described a similar paragenesis in xenoliths of the Tertiary intrusions of Mull. He (p. 255) considered them modifications of pure alumious sediments by reaction with the magma and particularly by diffusion of lime, ferrous iron, and magnesia. Hall and Nel (1926, p. 15) have reported the occurrence of corundum-sillimanite rock in the Bushveld Complex which they interpret as an aluminous sediment caught up in the noritic magma and subjected to intense metamorphism accompanied by interaction with magmatic material. According to them the consolidation of the magma prevented the normal course of completion of these reactions, resulting in a rock with unusual paragenesis.

Figure 17 shows the *A C F* diagram of Eskola (1939, p. 348) for the sanidinite facies with the plot of the above rock whose values are: $A = 65.1$, $C = 23.5$, and $F = 11.4$. The rock falls in the anorthite-sillimanite-cordierite field. Thomas (1922, p. 256) fixed the temperature of metamorphism at 1250–1400°C by comparison with the known stability ranges of similar phases in investigated systems. Turner (1948, p. 64) considered this excessive, because basaltic magmas are not known to attain such temperatures. Hall and Nel (1926, p. 11) state that high temperature is not necessary since the presence of several components in the melt would allow solid alumina to separate at an appreciably lower temperature. They further state that according to Morozewicz-Law corundum-spinel and sillimanite will separate when alumina is present in excess of certain ratio of the bases. They conclude that the high alumina content reflected in abundant sillimanite and corundum also strongly suggests that the original material was argillaceous and sedimentary.

The writer believes that the cordierite-corundum rock in this complex represents an aluminous or argillaceous sediment caught up in the original magma, modified by interaction with magmatic material.

Problem of the Eclogites

Introduction.—A brief summary of the present status of the eclogite problem is pertinent before entering into a discussion on the eclogites of the Sittampundi Complex. The significance of the original definition of eclogite

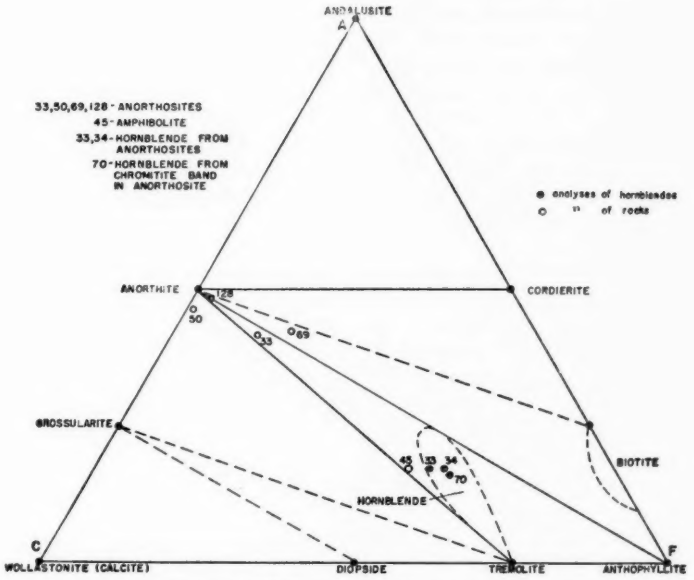

FIGURE 16.—A C F DIAGRAM FOR AMPHIBOLITE FACIES
With excess of alumina (Eskola, 1939, p. 352)

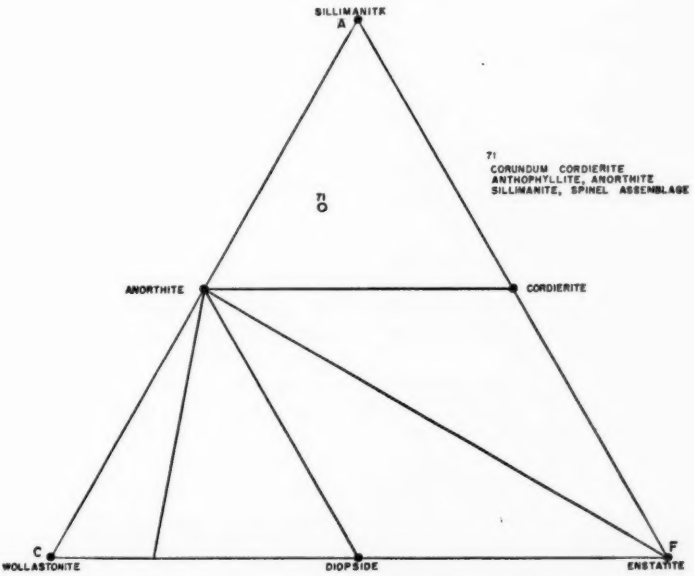

FIGURE 17.— A C F DIAGRAM FOR SANIDINITE FACIES (Eskola, 1939, p. 348)

has undergone modifications in the light of work by Briere, Hezner, Eskola, Tilley, and others. The green clinopyroxene omphacite, considered a critical mineral in eclogites, was shown by Davidson (1943, p. 99–100) to have an extensive compositional range. Yoder (1950, p. 247–248) stated that the small amount of soda commonly found in eclogite pyroxene does not justify the assignment of special extreme conditions for its formation.

Yoder (1950, p. 242–248) presented an admirable summary of the observations of several authorities on the eclogite problem, and some of the major trends of thought are presented here to help in a proper appreciation of the problem. Eskola (1921; 1939, p. 366, 367) classified the eclogites into four types, according to their mode of occurrence:

(1) Inclusions in kimberlites, basalts, basalt breccias, and garnet-bearing ultramafic rocks, with a paragenesis indicative of deep-seated igneous or metamorphic origin.

(2) Streaks and bands in dunites and related rocks, passing into garnetiferous granulites.

(3) Lenticular bands in migmatized gneisses, interpreted as fragments from deep-seated masses, moved upward into geosynclines by intrusive granites. These eclogites show retrograde metamorphism induced by the granite and consequent migmatization.

(4) Bands in rocks of a lower facies in highly folded tectonic zones.

Yoder (1950, p. 243) outlined six schools of thought on the genesis of eclogites: (1) direct crystallization from a magma under high hydrostatic pressure, (2) high-grade metamorphism of igneous or sedimentary rocks, (3) metasomatism of sedimentary or igneous rocks, (4) dynamic metamorphism of pre-existing rocks, (5) hydrothermal contact metamorphism, and (6) migmatization or diatectic metamorphism.

Eclogites of the Sittampundi complex.—The main types of eclogites in the Sittampundi area have been described earlier and are: (1) hornblende eclogite, (2) plagioclase eclogite, (3) bronzitic eclogite, and (4) bronzitic pyropite. Types (1) and (2) form conspicuous bands in the southern portion of the complex, becoming increasingly hornblendic towards their contacts with migmatized gneisses and amphibolites. Types (3) and (4) occur within the anorthosites forming irregular bands and lenticular bodies ranging in length from 15 to 100 yards, and in width from 5 to 20 yards. Peripheral transformation to types (1) and (2) are noticeable in some of these bands. The field relations of these eclogites are similar to those of the Rodil district described by Davidson (1943, p. 97). Foliation is noticeable in types (1) and (2) conforming to the prevalent foliation of the complex, perhaps consequent on development of retrograde hornblende as suggested by Davidson for the Rodil garnet amphibolites (p. 97). Types (3) and (4) show at some places compositional layering (Pl. 6, fig. 2), and generally have a system of joints conformable to those in the anorthosites and related chromitites. Field relations suggest that these eclogitic rocks are comagmatic with the anorthosites.

The *A C F* values for two analyzed eclogites and their garnets are:

	A	*C*	*F*
Rock C.41	21.8	29.4	48.8
Rock C.60	22.1	22.6	55.3
Garnet C.41	25.7	13.7	60.6
Garnet C.60	25.1	10.7	64.2

These values plotted in the *A C F* diagram of Eskola (1939, p. 364) for the eclogite facies, fall in a zone characteristic of eclogites.

(FeO + MnO), MgO, CaO molecular diagram.—The compositions of eclogites, garnetiferous gabbros and amphibolites together with the compositions of their garnets are plotted in a ternary diagram (Fig. 18) in which the molecular per cent ratios (FeO + MnO), MgO and CaO are represented at the corners. Fifteen paired analyses of rocks and their garnets, and 60 analyses of rocks, from the literature, together with two paired analyses of eclogites and their garents from the Sittampundi Complex are plotted in the diagram (data given in Table 33). Following Buddington (1952, p. 54) the plots of the compositions of garnets have been connected by tie lines to the compositions of corresponding parent rocks. Buddington (1952, p. 54) has shown that the ratio FeO/MgO is uniformly much greater in the garnet than in the host rock, for the Adirondack gabbroic rocks. This relationship has been found true for

most gabbroic and granulitic rocks described in the literature. In the case of eclogites a converse relationship was found; the FeO/MgO ratios of the garnets being uniformly lower than those of the host rocks. This contrasted relationship in eclogites and gabbroic rocks is clearly brought out in the diagram where the tie lines for the two types trend in different directions. The diagram also shows a probable compositional field, for eclogites based on the plots of several analyses. The eclogites from the Sittampundi Complex are indicated by plots 32 and 77, while 33 and 63 represent eclogitic rocks from Mysore and Uganda, described as basic charnockites. All these rocks fall well within the eclogite boundary fixed by the writer. Tie lines 20 and 31 for two typical eclogites are paralleled by tie lines 32 and 77 representing eclogites from Sittampundi Complex. The tie lines of rocks 13, 15, and 25 described as eclogites in the literature show trends characteristic of gabbroic rocks. Tie line 13 represents an eclogite and its garnet described by Davidson (1943), and parallels the tie lines of garnet gabbros from the Adirondacks and Norway. The almanditic garnet also suggests the host rock being a metagabbro of the Adirondack type. Tie line 15 represents an amphibolized eclogite and related garnet from Glenelg described by Alderman (1936). The analysis of the garnet used for the plot does not appear of high quality, and the tie line follows the trend for garnet gabbros. Plots 13 and 15 for the rocks also fall outside the probable eclogite field indicated in the diagram. Tie line 25 represents an eclogite from Greenland described by Sahlstein (1935). The description suggested the rock to be a garnetiferous amphibolite and the tie line follows the trend for garnet gabbros.

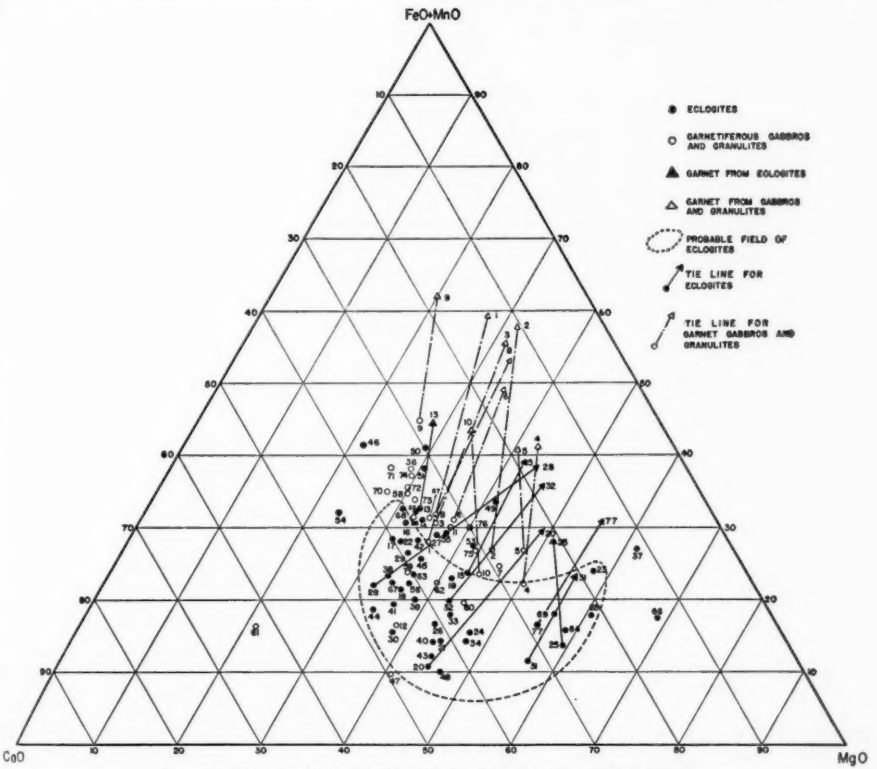

FIGURE 18.—(FeO + MnO), MgO, CaO MOLECULAR DIAGRAM

While generalizations are unwarranted in the

TABLE 33.—(FeO + MnO), CaO, and MgO MOLECULAR RATIOS OF GABBROIC AND ECLOGITIC ROCKS AND GARNETS IN THEM

Recalculated to 100 per cent

	Rock			Rock type	Garnet		
	(FeO + MnO)	MgO	CaO		(FeO + MnO)	MgO	CaO
1	28.0	36.0	36.0	Reconstituted gabbro	59.4	27.5	13.1
2	27.0	44.0	29.0	Reconstituted gabbro	57.9	31.8	10.3
3	30.4	35.6	34.0	Reconstituted gabbro	55.6	31.6	12.8
4	22.3	50.0	27.7	Reconstituted gabbro	41.2	42.5	16.3
5	27.0	48.0	25.0	Reconstituted gabbro	40.7	40.3	19.0
6	31.0	37.5	31.5	Reconstituted gabbro	49.0	34.4	16.6
7	24.5	46.2	29.3	Garnet metagabbro	....	....	....
8	31.7	35.0	33.3	Eclogite hornblende gabbro	53.0	33.0	14.0
9	45.1	28.4	26.5	Garnet gabbro	62.0	20.0	18.0
10	23.8	44.0	32.2	Hypersthene garnet granulite	43.4	33.5	23.1
11	30.0	37.7	32.3	Garnet amphibolite	....	....	....
12	16.2	38.0	45.8	Garnet amphibolite	....	....	....
13	32.6	32.7	34.7	Eclogite	44.2	28.6	27.2
14	31.0	33.8	35.2	Eclogite	....	....	....
15	23.6	43.0	33.4	Eclogite	38.9	41.9	19.2
16	30.6	32.0	37.4	Eclogite	....	....	....
17	28.3	31.5	40.2	Eclogite	....	....	....
18	21.2	46.0	32.8	Eclogite	....	....	....
19	23.0	41.4	35.6	Kyanite garnet amphibolite	....	....	....
20	10.4	44.8	44.8	Kyanite eclogite	29.4	48.9	21.7
21	14.2	44.2	41.6	Kyanite eclogite	....	....	....
22	28.0	32.5	39.5	Eclogite	....	....	....
23	24.0	57.8	18.2	Eclogite	....	....	....
24	15.2	37.7	47.1	Garnet-pyroxene-labradorite rock	....	....	....
25	13.8	59.1	27.1	Eclogite	28.0	51.0	21.0
26	16.7	42.3	41.0	Amphibole eclogite	....	....	....
27	29.2	36.4	34.4	Amphibole eclogite	....	....	....
28	22.2	32.3	45.5	Garnet gabbro	38.0	44.0	18.0
29	26.4	34.2	39.4	Eclogite	....	....	....
30	15.3	46.8	37.9	Eclogite	....	....	....
31	11.6	56.3	32.1	Eclogite	23.2	56.1	20.7
32	19.7	42.5	37.8	Plagioclase eclogite	35.7	45.9	18.4
33	18.0	43.3	38.7	Garnetiferous hornblende-diopside-hypersthene rock	....	....	....
34	14.5	47.2	38.3	Plagioclase eclogite	....	....	....
35	31.6	32.2	36.2	Garnet amphibolite	....	....	....
36	38.0	28.9	33.1	Garnet amphibolite	....	....	....
37	27.4	61.3	11.3	Eclogite	....	....	....
38	23.3	33.6	43.1	Eclogite	....	....	....
39	20.0	41.8	38.2	Eclogite	....	....	....
40	14.0	43.6	42.4	Eclogite	....	....	....
41	19.4	36.0	44.6	Eclogite	....	....	....
42	28.2	34.7	37.1	Eclogite	....	....	....
43	12.0	44.1	43.9	Eclogite	....	....	....
44	18.3	34.0	47.7	Eclogite	....	....	....
45	25.7	36.3	38.0	Eclogite	....	....	....
46	41.5	21.3	37.2	Eclogite	....	....	....
47	9.7	40.7	49.6	Eclogite	....	....	....
48	10.2	46.2	43.8	Eclogite	....	....	....
49	33.5	25.4	41.1	Eclogite	....	....	....
50	40.9	29.0	30.1	Eclogite	....	....	....
51	38.0	30.4	31.6	Eclogite	....	....	....
52	32.5	34.9	32.6	Eclogite	....	....	....
53	27.4	30.9	41.7	Eclogite	....	....	....
54	32.0	23.0	45.0	Eclogite	....	....	....
55	29.1	33.3	37.6	Eclogite	....	....	....
56	22.3	41.1	36.3	Eclogite	....	....	....
57	31.4	34.3	34.3	Garnet amphibolite	....	....	....
58	34.7	30.0	35.3	Garnet amphibolite	....	....	....

TABLE 33 (Cont.)

	Rock			Rock type	Garnet		
	(FeO + MnO)	MgO	CaO		(FeO + MnO)	MgO	CaO
59	23.8	35.3	40.9	Garnet amphibolite	....	....	....
60	19.6	36.2	44.2	Garnet amphibolite	....	....	....
61	16.1	21.0	62.9	Garnet amphibolite	....	....	....
62	22.3	38.0	39.7	Garnet amphibolite	....	....	....
63	23.6	36.0	40.4	Garnet norite	....	....	....
64	15.8	58.5	25.7	Drusite (eclogite)	....	....	....
65	17.8	60.8	21.4	Drusite (eclogite)	....	....	....
66	17.5	68.9	13.6	Drusite (eclogite)	....	....	....
67	22.2	34.7	43.1	Drusite (eclogite)	....	....	....
68	32.5	30.6	36.9	Drusite (eclogite)	....	....	....
69	18.0	56.0	26.0	Hornblende eclogite	....	....	....
70	35.0	27.6	37.4	Hyperite	....	....	....
71	38.5	26.3	35.2	Hyperite	....	....	....
72	35.4	29.8	34.8	Hyperite	....	....	....
73	34.0	30.7	35.3	Hyperite	....	....	....
74	37.1	29.1	33.8	Hyperite	....	....	....
75	27.0	41.8	31.2	Hornblende hyperite	....	....	....
76	30.0	40.0	30.0	Hornblende hyperite	....	....	....
77	16.5	54.7	28.8	Bronzitic pyropite	30.6	55.2	14.2

(1–6) Reconstituted gabbros from the Adirondacks (Buddington, 1952, p. 40–45)
(7) Garnet-bearing metagabbro (Buddington, 1939, p. 60)
(8) Eclogite hornblende gabbro (Eskola, 1921, p. 43–44)
(9) Garnet gabbro (Eskola, 1921, p. 88)
(10) Hypersthene-garnet granulite (Chemie der Erde, v. 5, 1930)
(11) Garnet amphibolite (Dengo, 1950, p. 876)
(12) Garnet amphibolite (Briere, 1920, p. 127)
(13) Eclogite (Davidson, 1943, p. 98, 100)
(14) Eclogite (Davidson, 1943, p. 98, 100)
(15) Amphibolized eclogite (Alderman, 1936, p. 508)
(16) Eclogite (Alderman, 1936, p. 508)
(17) Eclogite (Alderman, 1936, p. 508)
(18) Eclogite (Tilley, 1937, p. 560)
(19) Kyanite-garnet amphibolite (Tilley, 1937, p. 560)
(20) Kyanite eclogite (Tilley, 1937, p. 430)
(21) Kyanite eclogite (Briere, 1920, p. 168)
(22) Eclogite (Briere, 1920, p. 168)
(23) Eclogite (Eskola, 1921, p. 36)
(24) Garnet-pyroxene-labradorite rock (Eskola, 1921, p. 92)
(25) Eclogite (Sahlstein, 1935, p. 11)
(26) Amphibole eclogite (Sahlstein, 1935, p. 13)
(27) Amphibole eclogite (Sahlstein, 1935, p. 14)
(28) Garnet gabbro (Gjelsvik, 1947, p. 11)
(29) Eclogite (Hezner, 1903 p. 466)
(30) Eclogite (Schuster, 1878, p. 368)
(31) Eclogite, average analysis, from Williams (1932, p. 343)
(32) Plagioclase eclogite from Sittampundi complex (Rock C. 41)
(33) Garnetiferous hornblende-diopside-hypersthene rock (Rama Rao, 1945, p. 97)
(34) Plagioclase eclogite (Marchet, 1925, p. 244)
(35) Garnet amphibolite (Marchet, 1925, p. 314)
(36) Garnet amphibolite (Marchet, 1925, p. 314)
(37) Eclogite (Switzer, 1945, p. 7)
(38)–(43) Eclogites (Briere, 1920, p. 168)
(44)–(48) Eclogites (Weiseneder, 1935, p. 182, 184, 189, 193, 196)
(49)–(56) Eclogites (Niggli, 1930, p. 103, 105, 197, 211)
(57)–(62) Garnet amphibolites (Niggli, 1930, p. 105, 169, 211, 213)
(63) Garnet norite (Groves, 1935)
(64)–(68) Drusites (eclogites) (Machkovtsev, 1927)
(69) Hornblende eclogite (Erdmannsdorfer, 1938, p. 444)
(70)–(74) Hyperites (Brogger, 1935, p. 108)
(75)–(76) Hornblende hyperite (Brogger, 1935, p. 170)
(77) Bronzitic pyropite, Sittampundi complex (Rock C. 60)

absence of more specific data on paired analyses of garnet-bearing basic rocks and their garnets, the present diagram helps to bring out the general characteristics of the eclogites, as distinct from other garnetiferous basic rocks.

Origin of the eclogites.—Two possible hypotheses may explain the origin of these eclogites: (1) formation under metastable conditions from an original basic gabbro with subsequent diaphthoresis, and (2) formation under dynamothermal metamorphism at moderate depths in the presence of a catalyst, probably H_2O.

HYPOTHESIS 1: Riddle and Foster (1949) suggested that kyanite, generally accepted to be a high-pressure mineral, can be formed metastably. Recent work of Bowen and Tuttle (1949, p. 439–460) on the system MgO-SiO_2-H_2O demonstrated that anthophyllite can also be formed metastably. Dengo (1950, p. 877) postulated that eclogites can be formed metastably, under conditions of regional dynamothermal metamorphism of intermediate grade. However, the evolution of metastable facies in rocks is difficult to explain in the present state of our knowledge. Alderman (1936) thought that the formation of omphacite was conditioned by the composition of the primary pyroxene and the availability of albite molecule; Yoder (1950) stated that the small amount of soda found in the eclogite pyroxene did not justify the assignment of special, extreme conditions for its formation. Wieseneder (1935, p. 208–209) stated that the formation of eclogite may be a function of the bulk composition, a view paralleled in the conclusion of Bowen and Tuttle (1949, p. 450) who stated in connection with the metastable formation of anthophyllite that it may be a function of the total composition of the system MgO—SiO_2—H_2O.

The writer suggests that, under the conditions of metamorphism of the Sittampundi Complex, the formation of eclogite may be conditioned by the total composition of the system and the nature of the garnet formed, which will determine the composition of the remaining minerals to be formed.

However if eclogite is a restricted high-pressure facies for equilibrium, then it may have formed metastably during regional metamorphism from a basic gabbro. It is conceivable that pyropic garnet was formed by reaction between the olivine and a certain proportion of the anorthite molecule from the plagioclase, which readjusts itself to a more sodic composition (Shand, 1945, p. 269). This supports observations made on an analyzed eclogite, which has a normative feldspar An_{79} and modal feldspar An_{50}. Probably 75 per cent of the original plagioclase combined with olivine to form a garnet, leaving behind a more sodic feldspar.

In bronzitic pyropite and bronzitic eclogite, which have very little plagioclase, it is likely that the feldspar present originally may have been of very basic composition, and the small amount of soda molecule liberated during the formation of the garnet may have entered the clinopyroxene structure. The formation of the eclogite may be correlated with the first stage in the transformation of the whole complex during the regional migmatization, resulting in the formation of peninsular gneiss. The writer suggests that the retrograde changes observable in the eclogitic rocks were induced by a lowering of pressure consequent on the elevation of the complex by the intrusion of the younger granite, and aided by access of intergranular fluid.

HYPOTHESIS 2: An alternate suggestion for the formation of these eclogites would be that they were probably formed during the Post-Dharwar regional dynamothermal metamorphism with volatiles acting as catalyst. The process may have been rejuvenated during the intrusion of the younger granite, resulting in an assemblage showing retrograde as well as prograde characters. Further consideration of this hypothesis must await more critical data on stability relationships of garnets and other high-pressure minerals.

Origin of Chromitite

The anorthosites carry conformable layers of chromitite (Pl. 6, figs. 1, 3) extending several miles along the strike and ranging in thickness from a few inches to more than 10 feet. These are significant in proving the igneous origin of the complex as a whole.

The origin of chromite has been discussed by Sampson, Ross, Singewald, Fisher, and others, and in relation to the problem of the chromitites of this complex Sampson's (1932, p. 113–144)

discussion of the South African deposits is significant.

The alternation of felsic and mafic bands of anorthosites and the remarkable persistence of chromitite bands within them bear an unmistakable similarity to the Dwars River section in the Bushveld igneous complex. At other localities in the Bushveld, however, the occurrence of chromitite within the anorthosite s reported (Kupferburger *et al.*, 1937, p. 9) to be exceptional. The mineralogy of the chromitite and related host rock in the Dwars River sequence and in the Sittampundi complex is as ifollows:

Dwars River	*Sittampundi*
Chromitite composed of poikilitic plagioclase, of bronzite, or both with scattered chromite crystals. Biotite present occasionally.	Chromitite composed of poikilitic pargasite or anthophyllite or both with scattered chromite grains, corundum present at contact with anorthosite.
Anorthositic norite	Anorthite or bytownite edenite gneiss
An_{67}	An_{80-100}

Thus the Sittampundi sequence merely represents a metamorphic equivalent of the Dwars River rocks. Sampson (1932, p. 132–133) interpreted the Dwars River sills as fillings of residual chromite-bearing residual magma in cracks developed in the crystallized anorthosite. While this may be a reasonable assumption for sills of limited lateral extent, it is not applicable in the present instance, where individual chromitite layers can be traced for more than 10 miles. It is reasonable to assume that the chromitite bands formed during crystallization of the magma, with settling of chromitite at different levels, attributable to local disturbances in the magma chamber as proposed by Hess (1938, p. 264–268). Hess' theory for the origin of mafic bands in anorthositic and gabbroic rocks may also apply to chromitite bands in anorthosite.

Bateman (1951, p. 407) proposed a theory of "late gravitative liquid accumulation" to account for the presence of oxide ore bodies in basic rocks. He envisaged the enrichment of metallic oxides in the residual magma, which accumulated on a floor of early-crystallized silicates. He believed that under quiescent conditions this would form a stratiform deposit, and under pressure result in late magmatic injections. This theory does not, however, satisfactorily explain the formation of bands of chromitite in anorthosite.

The origin of the chromite cannot be interpreted from thin and polished sections of chromitite as all primary structures and textures have been obliterated by metamorphism. Field evidence indicates that chromite crystallized normally in the regular chromitite layers within the anorthosites toward the bottom of the sheet. The absence of transgressive relationship and the absence of xenolithic anorthosite within the several chromitite layers examined in the field show that the chromitite in this case is not late magmatic.

Equivalent Unmetamorphosed Rocks

It is clear that these rocks have undergone profound mineralogical transformations with little or no change in bulk chemistry. Tables 31 and 32 compare the chemical composition of these rocks with others which have not undergone any metamorphic reconstitution. Rocks similar to Sittampundi anorthosites have been recorded recently from Messina country in Transvaal, South Africa, by Sohnge (1946) and Van Zyl (1950). The corundum-bearing edenite amphibolites from North Carolina described by Hadley (1949, p. 111) also resemble the anorthositic rocks of the Sittampundi complex. Assuming no appreciable change in the bulk composition, the primary nature of the various units of the complex is inferred to be as follows:

Original rock	*Present rock*
Anorthosite	Leucocratic anorthite gneiss and related clinozoisite, garnet assemblages
Gabbroic and noritic anorthosite	Bytownite and anorthite edenite gneisses, anorthite anthophyllite edenite rock
Troctolite	Edenite gneisses and segregations
Olivine gabbro Gabbro	Bronzitic pyropite Eclogite series
Chromitite	Pargasite chromite rock
Bronzitite	Perknites, composed essentially of pargasite and anthophyllite

Hadley (1949, p. 110–111) presented petrographic evidence to support his suggestion that edenite amphibolites have been derived from troctolites. He writes (p. 111):

> "In many of the specimens studied, coronoid texture characteristic of the troctolite is more or less well preserved in the amphibolite. It is most evident in aggregates of clear, fine-grained amphibole, or of amphibole and spinel, surrounding plagioclase grains or masses of recrystallized enstatite. In the coarser-grained amphibolite, however, enstatite and all traces of coronoid texture are absent, and chromite and corundum are almost universal accessories. The edenite-amphibolite thus appears to have resulted from an alteration of troctolite amphibolite, in which the fine-grained enstatite and amphibole of the coronas has been changed to coarser-grained edenite with little change in the feldspar. The two rocks grade into each other by various degrees of change in texture and mineral content and are commonly very hard to distinguish in the field."

Conceivably, such relic structures present in the Sittampundi rocks were obliterated during the second stage of transformation. The metamorphic history of these rocks can be summarized as follows:

Stage 1: Regional metamorphism and migmatization. Original rocks of anorthositic facies transformed to anorthite amphibole assemblages, by reconstitution. Eclogite rocks formed from gabbroic rocks, perhaps metastably. Chromitites amphibolized and reconstituted with elimination of TiO_2 as rutile from chromite framework.

Stage 2: Dynamothermal metamorphism associated with the intrusion of younger granite, rich in mineralizers. Anorthositic rocks undergo further transformation, with resultant formation of clinozoisite, corundum and garnet. Eclogitic rocks develop retrograde character due to the action of mineralizers at elevated temperatures. Amphiboles in the chromitites show alteration to talcose minerals.

Origin of Banding and Lineation

Banding.—The mode of occurrence, and layered character of the complex suggest that some primary banding resulted during the cooling and crystallization of the magma. Cooper (1936), Coats (1936), Hess (1938), Van Zyl (1950), and Turner and Verhoogen (1951) have discussed the problem in some detail.

On the assumption that some of the layering was primary, the explanation offered by Hess appears most apt in the present instance. As has been suggested earlier, the chromitite bands may also have been formed by a similar process.

As this body has undergone metamorphic transformations, it would not be unreasonable to suggest that banding may have been accentuated by metamorphic differentiation.

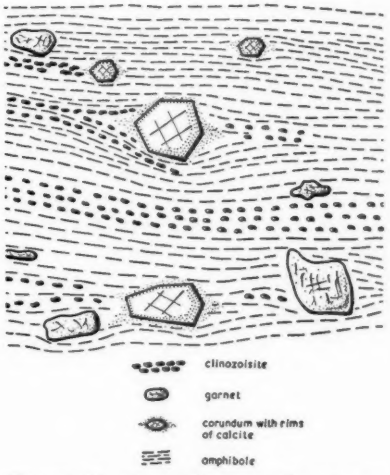

FIGURE 19.—SKETCH SHOWING CORUNDUM CRYSTALS IN META-ANORTHOSITE

Corundum, clinozoisite, garnet, anorthite paragenesis on footwall of old corundum quarry south of Sittampundi. Note hornblende and clinozoisite crystals wrapping around corundum crystals which lie in the plane of foliation with their longer axes perpendicular to the lineation. Note thin rims of calcite around the corundum porphyroblasts.

Preferred orientation of minerals.—The anorthositic rocks are characterized by preferred dimensional orientation of amphiboles and clinozoisite and platy parallelism of the calcic plagioclases. A linear structure as brought out by the dimensional orientation of the hornblende grains plunges southwest, south-southwest, or south, ranging around a generally south-southwest direction parallel to the plunge of the anticlinal fold in which the rocks are inferred to be involved. A similar orientation of the lineation is displayed by the hornblende grains in the country rocks south of the Complex.

In contrast to the amphiboles, the corundum porphyroblasts lie in the foliation with their longer axes perpendicular to the lineation (Fig. 19). It is conceivable that the alumina liberated may have moved along the planes of foliation and crystallized out as corundum crystals with their long axes in the direction of least pressure.

TABLE 34.— COMPARATIVE VERTICAL SEQUENCE IN SOME GRAVITY-STRATIFIED SHEET COMPLEXES

Name	Bushveld	Bay of Islands	Sittampundi
Length	280 miles	65 miles	25 miles
Width	150 miles	10 miles	1½ miles
Thickness	2 to 3½ miles	7 miles	6000 feet
Age	Precambrian	Ordovician	Precambrian
	Acid rocks (granite, granophyre, and felsite)	Roof volcanics	Top eroded
Upper zone	Gabbro in part with interstitial granophyre Andesine anorthosite, diallagite etc. Feldspar An_{45-60}	Gabbro in part banded with some zones of troctolite olivine gabbro feldspathic dunite, etc., with only a little pyroxenite (Upper zone)	Eclogite gabbro series Feldspar An_{45-60} Orthopyroxene En_{84} Garnet Mg_{45-50}
Main zone	Norite, labrodorite anorthosite, hypersthene diallagite, diallage hypersthenite, etc., with ilmenite-magnetite layers Feldspar An_{60-70}	Dunite, peridotite, subordinate pyroxenite, contains zones of interbanded troctolite, gabbro pyroxenite, feldspathic dunite, peridotite, and gabbroic anorthosite (Lower zone)	
Critical zone	Interbanded norite, diallage norite, bronzitite, harzburgite, bytownite anorthosite, etc., with several chromite layers and a platinum horizon. Feldspar An_{70-80}		Anorthosite series with several layers of chromitite Feldspar An_{80-100} Also several thin layers of eclogite, garnet pyroxenite, and bronzitic pyropite Orthopyroxene En_{85}
Transition zone	Basic norite, bronzitite, bytownite anorthosite, minor chromite layers, local sulfide lenses	Several chromite layers	
		Basal group?	Garnet Mg_{50-55}
Chill zone	Basic norite, bronzitite, bytownite anorthosite Feldspar An_{73} Hypersthene En_{88}		Basal group hidden (?)
Mineralogical variation	Feldspar increasing in anorthite content downward. Pyroxene magnesian toward base	Bytownite to labradorite. Olivine Fa_7 to Fa_{20} Orthopyroxenes at the base and clinopyroxenes at top	Feldspar An_{45-100} Orthopyroxene En_{80-86} Garnet Mg_{45-60}
Segregations and dikes		Pyroxenite veins, gabbro pegmatite, feldspathic dunite, basalt prophyry, gabbro, granite	Websterite Pegmatite
Satellitic intrusions	Norite, quartz dolerite, locally pyroxenite, olivine bronzitite, etc.	Ultramafic rocks, gabbro, and hornblende gabbro	Pyroxenite Websterite

This would explain the tendency of amphibole crystals in the rock to wrap around the corundum porphyroblasts, indicating that corundum grew with forceful outward pressure against the surrounding minerals.

Comparison with Stratiform Sheets and Evidence for Igneous Origin

The rocks of this complex are unique; the only other occurrences of similar rocks are in the Messina country of northern Transvaal in South Africa (Sohnge, 1946; Van Zyl, 1950). These African occurrences are considered igneous in origin, and are interpreted to have formed by gravity stratification during differentiation of a basic magma.

During the last 2 decades, several gravity-stratified sheets have been described by Hall (1932), Buddington (1936), Peoples (1936), Cooper (1936), Stewart (1946), and others. In Table 34 the vertical sequence in the Sittampundi complex has been tabulated together with those of the Bushveld and Bay of Island complexes. While it is realized that too close an analogy cannot be drawn, the comparison indicates the Sittampundi complex is probably of the gravity-stratified type. It is difficult to interpret the sequence of crystallization as all the primary minerals have undergone transformation; but in bulk chemistry, the exposed section of the Sittampundi complex corresponds to the transition zone of the Bushveld and the lower zone of the Bay of Island complexes.

The following are some of the salient points which unequivocally point to an igneous origin for these enigmatic rocks.

(1) The whole complex shows a striking resemblance to classical occurrences of gravity-stratified sheets. The bulk chemistry of the various rocks of the complex bear a striking similarity to the chemistry of rocks from other stratiform sheets.

(2) The presence of several layers of chromitite within the anorthosites of the complex, proves conclusively their genetic relationship. The chemical composition of the chromite is similar to those of chromites from other gravity-stratified sheets.

(3) The eclogites carry garnets free from inclusions, which according to Eskola (1920, p. 183) characterizes garnets of eclogites derived from igneous rocks.

(4) The paragenesis of the cordierite-corundum-sillimanite-anthophyllite-bytownite rocks found within the anorthosites, suggests their formation from aluminous sediments by reaction with a basaltic magma. This indirectly points to an unequivocally magmatic origin for the anorthosites.

(5) A statistical analysis of the twin laws of the plagioclase feldspars in these rocks indicates a fair proportion of complex twins. This feature has been considered by Turner and Gorai as indicative of igneous parentage and the complex twins of plagioclase in this instance may be relics preserved during partial recrystallization of the rocks. The presence of skeletal diopside crystals in thin sections of some rocks, indicates that relic features have been preserved, despite their recrystallization.

(6) Very minor amounts of TiO_2, P_2O_5, MnO, and SrO occur in the Sittampundi rocks; this is a characteristic feature of rocks from differentiated sheets.

In assuming an igneous origin for these rocks, as a working hypothesis, the possibility of their derivation by metamorphism of limestones of peculiar composition has not been disregarded. However, the evidence in favour of such a hypothesis is mostly negative, as may be seen from the following points:

(1) It would be difficult to get a section of impure limestone with a gradational compositional range, to give rise to a suite of rocks of varied compositions like anorthosites and eclogites.

(2) While it is possible that small bodies of paraanorthosite may be formed by metasomatism of limestone, it is difficult to visualize an extensive belt of anorthosite, associated with eclogites and chromitites formed by such a process.

(3) If the anorthosites were derived from limy sediments, the corundum-rich zone would have been restricted to a specific horizon, assuming them to be formed from a bauxitic layer in the original sediments. The homogeneous distribution of corundum in the anorthosites is, however, a direct contradiction to the metasedimentary origin of these rocks.

(4) The chromitites are beyond doubt, igneous, and their mineralogy does not indicate them to be metamorphosed placers.

(5) In the region around the complex there are several bands of crystalline limestone and marble, but none within the complex itself.

It may be seen from the above that present evidence favors igneous origin for these rocks.

Summary

Mineralogy

(1) The garnets of the eclogitic rocks are pyralmandites, which are characteristic of eclogites.

(2) The garnet from the anorthosite has a peculiar composition with high grossularite molecule and fair amount of pyralmandite molecule, which according to Ramberg indicates formation under a high-pressure environment.

(3) The plagioclase feldspars of the anorthositic rocks have a unique compositional

range of An_{80} to An_{100}. Anorthites with An_{98} and An_{99} occur in these rocks, and probably represent the nearest approach in nature to synthetic anorthite. Statistical analysis of the laws of twinning of these plagioclases indicates a fair proportion of twins considered characteristic of magmatic rocks. It has been found that the refractive indices of calcic feldspars are critical for fixing their composition, while other methods have an accuracy of only ±5 per cent An.

(4) The monoclinic amphiboles from the anorthosite and chromitite were chemically anayzed and their compositions correlated with the determined optical properties. The amphibole is edenite in anorthosites and pargasite in the chromitites. They represent a pargasite-edenite subseries of hornblende.

(5) The anthophyllite in the anorthosite is rich in alumina and is gedrite, or according to Rabbitt, an aluminian anthophyllite. The value N_Z for this and other aluminian anthophyllites falls above the curve of Rabbitt, indicating identity as a separate sub-group. The anthophyllites in the chromitites have lower values of N_Z, suggesting a magnesian composition. It is conceivable that in the rocks of this complex, anthophyllites varying from magnesian to aluminian types are present.

(6) Cordierite from the rock interpreted as a xenolith is a magnesian variety and optically negative. A review of the literature on cordierites shows that the explanations adduced for the anomalous optical character of some cordierites are unsatisfactory.

(7) The clinozoisite in the anorthosites is generally low in epidote molecule, though compositional variations are noticeable within a single thin section.

(8) The chromite in the chromitite is rich in the spinal molecule falling at the boundary of chromian spinal and aluminian chromite. The presence of exsolved plates of rutile in this chromite is an unusual feature.

(9) Corundum in these rocks is derived from the primary rocks during two periods of metamorphism, associated with the formation of garnet and clinozoisite-epidote.

(10) The writer suggests that the mineral transformations took place during two periods of Archean metamorphism.

Petrology

(1) By analogy with other gravity-stratified sheets, this complex is interpreted as a stratiform sheet.

(2) The bulk chemistry of the rocks agrees with that of rocks from other described stratiform sheets.

(3) Much of the layering is considered primary, and the chromitite horizons are thought to have been formed during the normal fractional crystallization of a basic magma under quiescent conditions, with recurring turbulence or pulsation of the magma within the chamber.

(4) The eclogite series are interpreted as original mafic gabbros of the complex. The writer suggests that they were transformed to eclogites, possibly metastably, during the first period of regional metamorphism. A triangular diagram representing the percentages of (FeO + MnO), MgO, and CaO has been constructed and the analyses of 77 garnet-bearing rocks and the garnets in some of them plotted. The tie lines drawn for the paired analyses indicated differing trends for the eclogites and gabbroic rocks. An eclogite field has been demarcated in the triangular diagram.

(5) The anorthositic rocks fall in the amphibolite facies, though they fall in generally restricted fields of the *A C F* diagram for the cordierite-anthophyllite subfacies. The analyzed eclogite and related garnets fall in their appropriate fields in the *A C F* diagram of Eskola for the eclogite facies.

(6) The following sequence of events is envisaged:

(a) Emplacement of basic magma in Dharwar sediments during a period of quiescence. Fractional crystallization and gravitative differentiation with formation of a layered complex.

(b) Metamorphism and regional migmatization, with consequent chemical and mineralogical transformations in the rocks of the complex.

(c) Elevation of the complex to the level of erosion with accompanying retrograde changes in eclogites. Top of complex eroded.

(d) Forceful intrusion of younger granite domes up the complex, tilting it on its edge. Considerable mineralogical changes, induced by mineralizers from the granite, with consequent formation of epidote minerals, garnet, and

corundum. The eclogites develop retrograde characters.

(7) The name Sittampundi complex is proposed for this body of layered basic rocks.

References Cited

Adams, F. D., and Barlow, A. E., 1910, Geology of the Haliburton and Bancroft areas, Province of Ontario: Geol. Survey Canada Mem. 6, 419 p.

Alderman, A. R., 1936, Eclogites in the neighbourhood of Glenelg, Invernesshire: Geol. Soc. London Quart. Jour., v. 92, p. 488–530.

Backlund, H. G., 1946, Zur genitische Deutung der Eclogite: Geol. Rundschau, Band 27, p. 47–61.

Baker, George, 1952, Opaque oxides in some rocks of the basement complex, Toricelli Mountains, New Guinea: Am. Mineralogist, v. 37, p. 567–577.

Barth, T. F. W., 1952, Theoretical petrology: N. Y., John Wiley and Sons, Inc., 387 p.

Bateman, A. M., 1951, The formation of late magmatic oxide ores: Econ. Geology, v. 46, p. 404–426.

Bateman, J. D., 1945, Composition of the Bird river chromite, Manitoba: Am. Mineralogist, v. 30, p. 596–600.

Berman, H., 1937, Constitution and classification of the natural silicates: Am. Mineralogist, v. 22, p. 342–408.

Birch, F. *et al.*, 1942, Handbook of physical constants: Geol. Soc. America. Special Paper 36, 325 p.

Bournon, de Count, 1802, Description of the corundum stone, and its varieties, commonly known by the names of Oriental Ruby, Sapphire, etc. with observations on some other mineral substances: Royal Soc. London, Philos. Trans. v. 92, pt 2, p. 233–326.

—— 1817, Catalogue de la collection Mineral, particuliere du roi: Paris, 1817.

Bowen, N. L., and Tuttle, O. F., 1949, The system MgO-SiO_2-H_2O: Geol. Soc. America Bull., v. 60, p. 439–460.

Briere, P. Y., 1920, Les eclogites francaisses—leur composition mineralogique et chemique; leur origine: Soc. Franc. Mineralogie Bull., v. 43, p. 72–222.

Brink, W. C., 1950, The geology, structure, and petrology of the Nuwerus area, Cape Province: Univ. Stellenbosch Annals, v. 26, sec. *A*, p. 142.

Brögger, W. C., 1935, On several Archean rocks from the south coast of Norway. 11. The South Norwegian hyperites and their metamorphism: Skrifter Det Norske Videnskaps-Akademie I. Oslo, 1934, 421 p.

Brownell, G. M., 1943, Chromite from Manitoba; Univ. Toronto Studies, Geol. Ser., no. 48, Contributions to Canadian mineralogy, p. 101–102.

Buddington, A. F., 1936, Gravity stratification as a criterion in the interpretation of the structure of certain intrusives of the northwestern Adirondacks: 16th Intern. Geol. Cong. Rept., 1933, p. 347–352.

—— 1939, Adirondack igneous rocks and their metamorphism: Geol. Soc. America Mem. 7, 354 p.

Buddington, A. F., 1952, Chemical petrology of some metamorphosed, Adirondack gabbroic, syenitic, and quartz-syenitic rocks: Am. Jour. Sci., Bowen vol., p. 37–84.

Bugge, J. A. M., 1943, Geological and petrographical investigations in the Kongsberg-Bamble formation: Norges. Geol. Unders. 160, p. 82–103.

Burri, C., and Niggli, P., 1945, Die jungen Eruptivgesteine des mediterranen Orogens: Vulkaninstitut Immanuel Friedlander, Nr. 3, Zurich, p. 620–654.

Chayes, F., 1949, A simple point counter for thin-section analysis: Am. Mineralogist, v. 34, p. 1–11.

Chenevix, R., 1802, Analyses of corundum and some of the substances which accompany it with observations on the affinities which the earths have been supposed to have for each other in the humid way: Roy. Soc. London Philos. Trans. v. 92, pt. 2, p. 327–347.

Coats, R. R., 1936, Primary banding in the basic plutonic rocks: Jour. Geology, v. 44, p. 407–419.

Cooper, J. R., 1936, Geology of the southern half of the Bay of Islands igneous complex: Newfoundland Dept. Nat. Res., Geol. Sec., Bull. 4, 62 p.

Davidson, C. F., 1943, The Archean rocks of the Rodil district, South Harris, Outer Hebrides: Roy. Soc. Edinburgh Trans., v. 61, p. 71–112.

Dengo, G., 1950, Eclogitic and glaucophane amphibolites in Venezuela: Am. Geophys. Union Trans., v. 31, p. 873–878.

Doelter, C., 1917, Handbuch der Mineralchemie: Dresden, Bd. II, p. 979–1000.

Donnay, J. D. H., 1943, Plagioclase twinning: Geol. Soc. America Bull., v. 54, p. 1645–1652.

Düll, E., 1903, Über die Eklogite des Münchberger Gneisgebietes: Geogno. Jahresheften. Munchen, Band 15, p. 65–156.

Du Rietz, Torsten, 1929, Studies on the rocks of Radmunso: Geol. Foren. Forh., Stockholm, v. 51, p. 495–507.

Emmons, R. C., 1943, The universal stage: Geol. Soc. America Mem. 8, 205 p.

Emmons, R. C., and Gates, R. M., 1943, Plagioclase twinning: Geol. Soc. America Bull., v. 54, p. 287–304.

Erdmannsdörffer, O. H., 1938, Eklogit im Schwarzwald und seine retrograde Umwandlung: Jour. Geology, v. 46, p. 438–447.

Eskola, P., 1914, On the petrology of the Orijarvi region in southwestern Finland: Comm. Geol. Finlande Bull. 40, 279 p.

—— 1915, On the relations between chemical and mineralogical composition in the metamorphic rocks of the Orijarvi region: Comm. Geol. Finlande Bull. 44, p. 110–145.

—— 1920, The mineral facies of rocks: Norsk. Geol. Tidsskr., v. 6, p. 143–194.

—— 1921, On the eclogites of Norway: Vidensk. Skr. I, Mat. Naturv. Kl. Kristiania, no. 8, p. 1–118.

—— 1925, On the petrology of eastern Fennoscandia, I, The mineral development of basic rocks in the Karelian formations: Fennia, v. 45, no. 19, p. 1–93.

—— 1939, Die Enstehung der Gesteine (Barth, T. F. W., Correns, C. W., and Eskola, P.) Springer, Berlin, 422 p.

Eskola, P., 1950, Paragenesis of Cummingtonite and Hornblende from Muuruvesi, Finland: Am. Mineralogist, v. 35. p. 728–734.

Fermor, L. L., 1912, Preliminary note on the origin of Meteorites, Jour. and Proceedings: Asiatic. Soc. Bengal, new Ser.; 8, no. 9, p. 316–317.

—— 1936–1940, An attempt at the correlation of the ancient schistose formations of peninsular India: Geol. Survey India Mem., v. 70, pts. 1, 51 p.; pt. 2, 324 p.

Fisher, L. W., 1929a, Chromite, its mineral and chemical composition: Am. Mineralogist., v. 14, p. 341–357.

—— 1929b, Origin of chromite deposits: Econ. Geology, v. 24, p. 691–721.

Fleischer, M., 1937, The relation between chemical composition and physical properties in the garnet group: Am. Mineralogist., v. 22, p. 751–759.

Folinsbee, R. E., 1941, Optic properties of cordierite in relation to alkalies in the cordierite-beryl structure: Am. Mineralogist., v. 26, p. 485–500.

Foslie, S., 1945, Hastingsites and amphiboles from the epidote-amphibolite facies: Norsk. Geol. Tidsskr., v. 25, p. 74–98.

Ghosh, P. K., 1941, The charnockite series of Bastar state and western Jeypore: Geol. Survey of India Rec., v. 75, Prof. Paper 15, 55 p.

Gjelsvik, T., 1947, Anorthosittkomplekset i Heidal: Norsk. Geol. Tidsskr., v. 26, p. 1–58.

Gorai, M., 1950a, Proposal of twin method for the study of the "granite problem": Geol. Soc. Japan Jour. v. 56, no. 655, p. 149–156.

—— 1950b, Method of distinguishing C-twin and A-twin of plagioclase under ordinary polarisation microscope (Abstract): Geol. Soc. Japan Jour. v. 56, no. 660, p. 443.

—— 1950c, The features of plagioclase twinning in various granitic rocks. Geol. Soc. Japan Jour., v. 56, no. 663, p. 515–518.

—— 1951, Petrological studies on plagioclase twins: Am. Mineralogist, v. 36, p. 884–901.

Groves, A. W., 1935, The charnockite series of Uganda, British East Africa: Geol. Soc. London Quart. Jour., v. 91, p. 150–207.

Hadley, J. B., 1949, Preliminary report on corundum deposits in the Buck Creek peridotite, Clay country, North Carolina: U.S. Geol. Survey Bull. 948-E, p. 103–128.

Hall, A. L., 1932, The Bushveld igneous complex of central Transvaal: Geol. Survey South Africa Mem. 28, 554 p.

Hall, A. L., and Nel, L. T., 1926, On an occurrence of corundum-sillimanite rock in the norite of the Bushveld igneous complex, west of Lydenburg: Geol. Soc. South Africa. Trans., v. 29, p. 1–16.

Hallimond, A. F., 1943, On the graphical representation of the calciferous amphiboles: Am. Mineralogist., v. 28, p. 65–89.

Heald, M. L., 1950, Structure and petrology of the Lovewell Mountain quadrangle, New Hampshire: Geol. Soc. America Bull., v. 61, p. 43–90.

Henderson, E. P., 1931, Notes on some minerals from the Rhodolite quarry near Franklin, North Carolina: Am. Mineralogist, v. 16, p. 563–568.

Heritsch, F., 1926, Studien über den Chemismus der Granaten: Neues Jahrb. Min., Abt. A, Beil. Band 55, p. 60–91.

Heritsch, H., 1931, Vorläufiger Bericht über die Minerale der Lieserschlucht bei Spittal an der Drau: Neues Jahrb. Centralblatt Abt. A, no. 8, p. 366.

Hess, H. H., 1938, Primary banding in norite and gabbro: Am. Geophys. Union Trans., v. 19, p. 264–268.

—— 1941, Pyroxenes of common mafic magmas: Am. Mineralogist, v. 26, p. 515–535, 573–594.

—— 1949, Chemical composition and optical properties of common clino-pyroxenes; pt. 1: Am. Mineralogist, v. 34, p. 621–666.

—— 1950, Vertical mineral variation in the Great Dyke of Southern Rhodesia: Geol. Soc. South Africa Trans., v. 53, p. 159–166.

Hess, H. H., and Phillips, A. H., 1938, Orthopyroxenes of the Bushveld type: Am. Mineralogist, v. 23, p. 450–456.

—— 1940, Optical properties and chemical composition of magnesian orthopyroxenes: Am. Mineralogist, v. 25, p. 271–285.

Hezner, L., 1903, Ein Beitrag zur Kenntnis der Eklogite und Amphibolite, mit besonderer Berücksichtigung der Verkommnisse des Mittleren Ötztales: Min. Pet. Mitt., Band 22, p. 437–471, 505–580.

Hills, E. S., 1936, Reverse and oscillatory zoning in plagioclase feldspars: Geol. Mag., v. 73, p. 50–56.

Holland, T. H., 1896, On the origin and growth of garnets and of their micropegmatitic intergrowths: Geol. Survey of India Rec., v. 29, pt. 1, p. 20–30.

—— 1900, The charnockite series, a group of Archean hypersthenic rocks in peninsular India: Geol. Survey India Mem. 28, pt. 2, p. 119–249.

Iyer, L. A. N., 1933, On the corundum-bearing rocks of Namakkal taluk, Salem district, Madras Presidency (Abstract): Indian Sci. Cong, Proc., v. 20.

Johannsen, A., 1937, A descriptive petrography of the igneous rocks: 4 vols. Univ. Chicago Press.

Johnstone, R. W., 1949, Clinozoisite from Camaderry Mountain, Co. Wicklow, Mineralog. Mag., v. 28, p. 505–515.

Kolderup, C. F., and Kolderup, N. H., 1940, Geology of the Bergen Arc system: Bergens Museums Skrifter, no. 20, p. 69–89.

Kranck, E. H., 1935, On the crystalline complex of Liverpool-Land: Moddel. om. Grön., v. 95, no. 7, p. 5–119.

Kratzert, J., 1921, Die Krystallographischen und optichen konstanten des Anorthites vom Vesuvius: Zeits. Krist., v. 56, p. 465–488.

Krishnan, M. S., 1924, Notes on cordierite in a cordierite gneiss from Madura district, Madras, India: Mineralog. Mag., v. 20, p. 248–251.

—— 1949, Geology of India and Burma, Madras: 544 p.

Kupferburger, W., *et al.*, 1937, The chromite deposits of the Bushveld igneous complex, Transvaal, Union of South Africa: Dept. Mines Bull. 10 (Geol. series), 48 p.

Lacroix, A., 1889, Contributions à l'étude des gneiss à pyroxène et des roches à wernerite: Soc. Franc. Mineralogie. Bull., v. 12, no. 4, p. 282–348.

Levin, S. B., 1950, Genesis of some Adirondack garnet deposits: Geol. Soc. America Bull,. v. 61, p. 519–566.

Machkovtsev, S., 1927, Sur les drusites des bords de la Mer Blanche, Travaux: Soc. Natural. Leningrad, v. 57, sec. Geol. Min. p. 79.
Mallet, F. R., 1891, Contributions to the study of the pyroxenic varieties of gneiss and of the scapolite-bearing rocks (translation of the original paper of Lacroix): Geol. Survey India Rec., v. 24, pt. 3, p. 155–200.
Marchet, A., 1924, Zur Kenntnis der Amphibolite des niederösterreichischen Waldviertels: Tscher, Min. Petr. Mitt. Band 36, p. 229–318.
McConnell, D., 1939, Note on the chemical similarity of idocrase and certain garnets: Am. Mineralogist, v. 24, p. 62–63.
Middlemiss, C. S., 1896, Preliminary notes on some corundum localities in the Salem and Coimbatore districts, Madras: Geol. Survey India Rec., v. 29, pt. 2, p. 39–50.
Miller, F. S., 1935, Anorthite from California: Am. Mineralogist, v. 20, p. 139–146.
—— 1937, Petrology of the San Marcos gabbro, southern California: Geol. Soc. America Bull., v. 48, p. 1397–1426.
Newbold, T. J., 1843, Mineral resources of southern India: Jour. Asiatic Soc., London, v. 7, p. 224.
Newhouse, W. H., and Hagner, A. F., 1949, Cordierite deposits of the Laramie Range, Albany County, Wyoming: Wyoming Geol. Survey Bull. 41.
Niggli, P. *et al.*, 1930, Chemismus Schweizerischer Gesteine: Beitr. z. Geologie d. Schweiz, Geotechn, Series 14, Bern, 389 p.
Oppenheimer, L., 1914, Unterschungen an cordierit: Verhandl. d. Heidelb. Naturh. Med. Vereins, N. F. 13, p. 257–303.
Orlov, A., 1926, Sur les membres du groupe zoisite-epidote pauvres en fer: Mem. Soc. Roy. Sci. Bohême, no. 19, p. 1–42.
Pehrman, G., 1932, Uber optisch positiven Cordierit: Acta. Ac. Aboensis Math. et. Phys., Band 6, p. 12.
Peoples, J. W., 1936, Gravity stratification as a criterion in the interpretation of the structure of the Stillwater complex, Montana: 16th Internat. Geol. Cong. Rept., p. 353–360.
Philipsborn, Von H., 1930, Zur chemisch-analytischen Erfassung der iso-morphen variation gesteinbildender Minerale. Die Mineralkemponenten des pyroxengranulits von Hartmannsdorf (Sa): Chemie der Erde, v. 5, p. 233–253.
Rabbitt, J. C., 1948, A new study of the anthophyllite series: Am. Mineralogist, v. 33, p. 263–323.
Rama Rao, B., 1945, The charnockite rocks of Mysore (southern India): Mysore Geol. Dept. Bull. 18, 197 p.
Ramberg, H., 1943, En Udersökelse av Vestrandens Regionalmetamorphe bergarter: Norsk. Geol. Tiddsskr., v. 23, p. 1–174 (English summary 153–174).
—— 1944, Petrological significance of sub-solidus phase transitions in mixed crystals: Norsk. Geol. Tiddsskr., v. 24, p. 42–74.
—— 1952, The origin of metamorphic and metasomatic rocks: Univ. Chicago Press, 317 p.
Ramdhor, P., 1931, Zeits: Prak. Geol., v. 39, p. 90.
—— 1940, Die Erzmineralien in gewohnlichen magmatischen Gesteinen: Pruss. Akad. der Wissen. Abhandl. Math. naturw Klasse, no. 2.
Riddle, F. H., and Foster, W. R., 1949, Sillimanite in "Industrial minerals and rocks:" 2d ed., New York, Am. Inst. Min. Metall. Eng., p. 893–926.
Sahlstein (Sahama) T. G., 1935, Petrographie de Eklogiteinschlüsse in den Gneissen des sud westlichen Liverpool-landes in Ost-Grönland: Medd. om. Grönland, v. 95, no. 5, p. 5–43.
Sampson, E., 1929, May chromite crystallize late?: Econ. Geology, v. 24, p. 632–649 (symposium with contributions by C. S. Ross and J. T. Singewald).
—— 1931, The origin of chromite: Econ. Geology, v. 26, p. 662–669.
—— 1932, Magmatic chromite deposits in southern Africa: Econ. Geology, v. 27, p. 113–144.
Sederholm, J. J., 1916, On synantetic minerals: Comm. Geol. Finlande Bull. 48, p. 1–148.
Shand, S. J., 1945, Coronas and coronites: Geol. Soc. America Bull., v. 56, p. 247–266.
Shibata, H., 1936, Graphic intergrowth of cordierite and quartz in pegmatites from Sasago and Dosi, province of Kai, Japan: Jap. Jour. Geology Geography, v. 13, p. 205.
Silliman, B., Jr., 1849, Description of several American minerals: Am. Jour. Sci., 2d ser., v. 8, p. 391.
Sohnge, P. C., 1946, The geology of the Messina copper mines and surrounding country: Union of South Africa Geol. Survey Mem. 40, 272 p.
Stevens, R. T., 1944, Composition of some chromites of the Western Hemisphere: Am. Mineralogist, v. 29, p. 1–34.
Stewart, F. H., 1942, Chemical data on a silica-poor argillaceous hornfels and its constituent minerals: Mineralog. Mag., v. 26, p. 260–266.
—— 1946, The gabbroic complex of Belhelvie in Aberdeenshire: Geol. Soc. London Quart. Jour. v. 102, pt. 4, p. 465–498.
Sundius, N., 1944, On the substitution relations in the amphibole group: Sveriges. Geol. Undersökning Ser. C. Årsbok 38, no. 460, p. 1–11.
—— 1946, The classification of the hornblendes and the solid-solution relations in the amphibole group: Sveriges. Geol. Undersökning Ser. C Årsbok 40, no. 480, p. 1–31.
Switzer, G., 1945, Eclogite from the California glaucophane schists: Am. Jour. Sci., v. 243 p. 1–8.
Tempel, H. G., 1938, Der Einflus der seltenen Erden und einiger anderer Komponenten auf die physikalisch-optischen Eigenschaften innerhalb der Epidotgruppe: Chemie der Erde, v. 11, p. 525–550.
Thayer, T. P., 1946, Preliminary chemical correlation of chromite with the containing rocks: Econ. Geology, v. 41, p. 202–217.
Thiele, E., 1940, Die Beziehung der chemischen Zusammensetzung zu den physikalisch optischen Eigenschaften ineinigen Mineralien des Kontakts: Chemie der Erde, v. 13, p. 65–91.
Thomas, H. H., 1922, On certain xenolithic Tertiary minor intrusions in the island of Mull: Geol. Soc. London Quart. Jour., v. 78, p. 229–259.
Tilley, C. E., 1936, The paragenesis of kyanite eclogites: Mineralog. Mag., v. 24, p. 422–432.
—— 1937, The paragenesis of kyanite-amphibolites: Mineralog. Mag. v. 24, p. 555–567.
—— 1939, Kyanite gedrite parageneses: Geol. Mag., v. 76, p. 326–330.
—— 1940, A group of gneisses (sillimanitic and cordieritic) from the moraines at Cape Deni-

son: Australasian Antarctic Exp. Rept., ser. A, v. 4, no. 10, p. 339–344.

Tsuboi, S., 1923, A dispersion method of determining plagioclase in cleavage flakes: Mineralog. Mag., v. 20, p. 108.

—— 1935, Anorthite from Wadaki (Idu-Petrological Notes): Jap. Jour. Geology and Geography, v. 12, p. 110–111.

Turner, F. J., 1947, Determination of plagioclase with the four-axis universal stage: Am. Mineralogist, v. 32, p. 389–410.

—— 1948, Mineralogical and structural evolution of the metamorphic rocks: Geol. Soc. America Mem. 30, 342 p.

—— 1951, Observations on twinning of plagioclase in metamorphic rocks: Am. Mineralogist, v. 36, p. 581–589.

Turner, F. J., and Verhoogen, J., 1951, Igneous and metamorphic petrology: N. Y. McGraw-Hill Book Co. Inc., 602 p.

Wieseneder, H., 1935, Beiträge zur Kenntnis der ostalpinen Eklogite: Min. Petr. Mitt., v. 46, p. 174–210.

—— 1937, Eklogite und "Eklogitschale" der Erde: Zentralbl. Mineralogie, Abt. A, p. 149–152.

Wijkerslooth, de P., 1947, The chromite deposits of the Guleman concession: Koninkl Nederland Akademie Wetenschap. 59 p.

Willemse, J., 1938, On the old granite of the Vredefort region and some of its associated rocks: Geol. Soc. South Africa Trans., v. 40, p. 43–119.

Williams, A. F., 1932, The genesis of the diamond: London, pt. 1, p. 352.

Winchell, A. N., 1937, Cordierite: Am. Mineralogist, v. 22, p. 1175–1179.

—— 1938, The anthophyllite and cummingtonite-grunerite series: Am. Mineralogist, v. 23, p. 329–333.

—— 1945, Variations in composition and properties of the calciferous amphiboles: Am. Mineralogist, v. 30, p. 27–50.

—— 1951, Elements of optical mineralogy, pt. 2: 4th ed., N. Y., John Wiley and Sons, Inc., 551 p.

Wright, W. I., 1938, The composition and occurrence of garnets: Am. Mineralogist, v. 23, p. 436–449.

Yoder, H. S., 1950, The jadeite problem: Am. Jour. Sci., v. 248, p. 225–248, 312–334.

—— 1951, Stability relations of clinochlore and cordierite in the system MgO-Al_2O_3-SiO_2-H_2O (Abstract): Geol. Soc. America Bull., v. 62, p. 1493.

Zyl, van J. S., 1950, Aspects of the geology of the northern Soutpansberg area: Univ. Stellenbosch Annals, v. 26, sec. A, p. 1–95.

Geological Survey of India, Calcutta 13, India

Manuscript Received by the Secretary of the Society February 2, 1953

Publication Authorized by the Director, Geological Survey of India

Short Note

BULLETIN OF THE GEOLOGICAL SOCIETY OF AMERICA
VOL. 67, PP. 391-394 MARCH 1956

CAMBRO-ORDOVICIAN AGE OF THE "INWOOD" LIMESTONE AND "MANHATTAN" SCHIST NEAR PEEKSKILL, NEW YORK

BY SIDNEY PAIGE

Introduction

In September 1955 the writer was retained by the Consolidated Edison Company, Inc. of New York to prepare a geological report on a power-house site at Indian Point, Westchester County, New York; Indian Point is on the east bank of the Hudson River about 2½ miles southwest of Peekskill.

Three days were spent in the field. Fortunately the writer had the advantage of a map and report by Berkey and Rice (1921) covering in detail the geology of the West Point quadrangle.

The sole purpose of this communication is to establish the identity of the Cambro-Ordovician sequence—Poughquag quartzite, Wappinger limestone, Hudson River shales—with the stratigraphic sequence "Lowere (?) quartzite", "Inwood" limestone, "Manhattan" schist near Peekskill, within the West Point quadrangle, New York, and to emphasize those geologic principles well recognized and accepted that point to and support such an identification.

No attempt is made to establish a correlation either with distant metamorphic rocks along the Atlantic Piedmont belt or with metamorphic rocks in complex structures to the northeast within the New England highlands. Much work has been done in those areas by many geologists over the decades. Much of the earlier work is published, much of the later work still remains unpublished.

The writer wishes to acknowledge the cooperation of Dr. Arthur N. Strahler who supplied a geologic map of the Tomkins Cove quarry area on which significant stratigraphic relations were displayed; and to thank Dr. Marshall Kay, who as always, generously, out of his wide knowledge, directed attention to pertinent sources of information; to Dr. Walter Bucher, a student of this area for many years, thanks for his support of our position after the work was finished.

The Problem Stated

Figure 1 is the writer's stratigraphic and structural interpretation of the southwest portion of the geologic map of the West Point quadrangle. A narrow strip has been added at the south border in order to include the geology of Stoney Point on the west side of the Hudson River. The geologic boundaries and fault lines on this map, except within the narrow strip, are those displayed on Berkey's map of the West Point quadrangle. Within the areas designated as Precambrian gneiss some geologic details have been omitted, since they do not bear on the problem under consideration.

The important stratigraphic age distinction, so long in question and displayed on the West Point quadrangle, is between a sequence of three formations recognized by everyone as Cambro-Ordovician in age and a sequence of two formations mapped as of "doubtful" age, presumably Precambrian since the sequence appears in Berkey's geologic report (1921, p. 140) as late Grenville in age.

The recognized Cambro-Ordovician strata appear at two places: (1) in a narrow northeast trending strip north of Peekskill, and (2) at Tomkins Cove west of the Hudson River. Southeast of and southwest of Peekskill the late Grenville (?) strata of Berkey's map appear in all outcrops on the east side of the Hudson River.

The Cambro-Ordovician strata include from the bottom up a quartzite at the base (Poughquag quartzite), a formation very diffi-

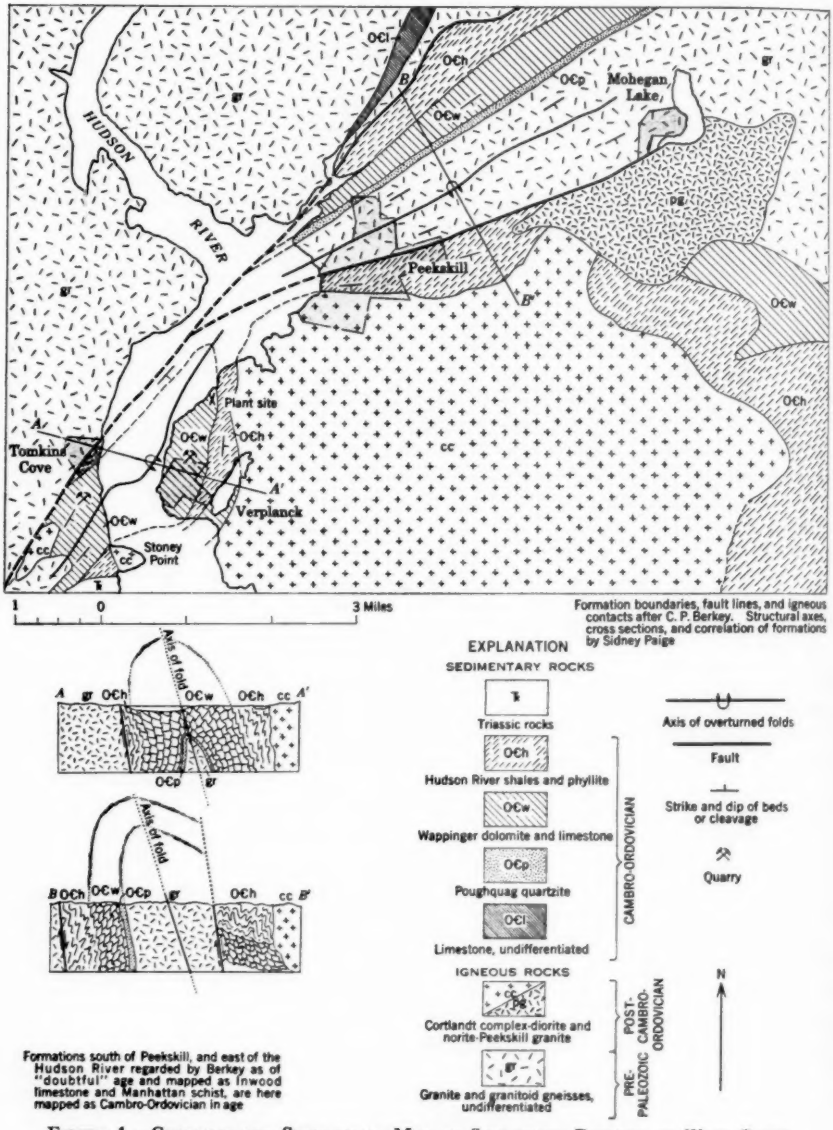
HUDSON RIVER
Mohegan Lake
Peekskill
Plant site
Tomkins Cove
Verplanck
Stoney Point
1 0 3 Miles
Formation boundaries, fault lines, and igneous contacts after C. P. Berkey. Structural axes, cross sections, and correlation of formations by Sidney Paige
EXPLANATION
SEDIMENTARY ROCKS
Triassic rocks
Hudson River shales and phyllite
Wappinger dolomite and limestone
Poughquag quartzite
Limestone, undifferentiated
CAMBRO-ORDOVICIAN
IGNEOUS ROCKS
Cortlandt complex-diorite and norite-Peekskill granite
Granite and granitoid gneisses, undifferentiated
POST-CAMBRO-ORDOVICIAN
PRE-PALEOZOIC
Axis of overturned folds
Fault
Strike and dip of beds or cleavage
Quarry
N
Axis of fold
Formations south of Peekskill, and east of the Hudson River regarded by Berkey as of "doubtful" age and mapped as Inwood limestone and Manhattan schist, are here mapped as Cambro-Ordovician in age

FIGURE 1.—GEOLOGIC AND STRUCTURAL MAP OF SOUTHWEST PORTION OF WEST POINT QUADRANGLE, NEW YORK

cult to find, reported to be several hundred feet in thickness; a dolomitic limestone (Wappinger limestone) 1000 or more feet in thickness; and a phyllite sequence referred to as Hudson River shales and phyllites on Berkey's map. The late Grenville (?) strata are reported to include the "Lowere" quartzite (not shown on Berkey's map, but reported locally elsewhere); "Inwood" limestone; and above it the "Manhattan" schist sequence.

The question raised is, are the Cambro-Ordovician sequence and the Precambrian

sequence identical? If so, how are they connected structurally?

Stratigraphy, Structure, Metamorphism, and Correlation

Geologists caring to pursue this problem independently, but relying only on published papers, should read *The geology of the West Point quadrangle* by Charles P. Berkey and Marion Rice (1921) and papers entitled *Structural and petrographic studies in Dutchess County, N.Y.*, Part I by Robert Balk (1936), Part II by Tom F. W. Barth (1936). Abundant references in these papers point to the studies of earlier workers. There is no need to repeat here the lengthy arguments, pro and con, appearing in these cited papers as to the age of the rocks; they are many and involved. We turn rather to an examination of the geologic relationships displayed in the field, near Peekskill.

Stratigraphy and structure.—A stratigraphic sequence, recognized and accepted as of Paleozoic age (Cambro-Ordovician) by all who have worked in this region, consists of three formations: Poughquag quartzite at the base (200± feet), Wappinger limestone (2000± feet), and Hudson River phyllite and shale (thickness unknown ?) at the top. These beds had been mapped both east and west of the Hudson River (1) in a northeast-trending strip about a mile north of Peekskill and east of the river, and (2) at Tomkins Cove, west of the river.

A second (shown on the West Point quadrangle) stratigraphic sequence, "Inwood" limestone and "Manhattan" schist, appears and had been mapped east of the river, in the city of Peekskill and to the southeast and southwest.

In a region so covered with vegetation and alluvial and glacial debris that it is difficult to follow outcrops, it is indeed fortunate that huge quarries have been opened on both sides of the river, one at Tomkins Cove on the west side, and the other a short distance north of Verplanck on the east bank. These quarries are deep and long and afford an exceptional opportunity to examine the structure and lithology of the dolomites in which they are excavated.

The striking features of the Tomkins Cove quarry are as follows: (1) The dolomites are closely folded, in places isoclinally. There is some evidence of two periods of folding. The axial planes of the main folds and the minor folds are overturned to the northwest. (2) The beds, on the average, strike N. 35°–40° E. and dip 70°± SE. The dip in the eastern limb of the folds is gentler on the average than that in the western limbs. (3) The quarry is limited to the northeast by the appearance of phyllites or mica schists, dipping steeply southeast on the west flank of the major fold. Drill holes confirm this relationship, but the same dips may be observed in the railroad cut north of the quarry at the river's edge.

Mica schists also appear on the eastern limb of the major fold, in the railroad cut at Stoney Point, where schists are invaded by an outlier of the Cortlandt complex. Thus all the stratigraphic elements of a closely appressed overturned fold are present. Along the major fold axis in the southern face of the quarry the rock is so crushed that it is not usable as quarry rock, further evidence of the severity of compression. The dolomites in this quarry strike directly northeast and across the Hudson River, and the contacts of the overlying phyllites or mica schists likewise strike across the river.

In the large quarry north of Verplanck on the east side of the river, the closely folded dolomites dip 70°± E., strike N. 35°–45° E., and bear every evidence of occupying the east limb of an overturned fold. The mica schists that overlie the dolomites appear on the eastern wall and limit the quarry in that direction. These schists also dip 70°± SE.

These beds in the eastern quarry are megascopically indistinguishable from the beds in the western quarry, and examination of thin sections from dolomites of both quarries disclosed no difference in the rock other than that of grain size of recrystallization—a difference of metamorphism reflecting the proximity of a large mass of plutonic rock, the near-by Cortlandt complex.

The writer is firmly convinced that the dolomite east and west of the river is the same stratigraphic unit, and that the phyllites and mica schists are identical units—*i.e.*, the Cambro-Ordovician sequence is identical with the "Inwood", "Manhattan" sequence of the Peekskill area.

Metamorphism.—The work of Balk, Barth, and others has abundantly proved the progressive increase of metamorphic intensity displayed by the Cambro-Ordovician sequence, north of the Hudson Highlands, as the beds are followed eastward. Near Peekskill there is also the fact that the Cortlandt complex has invaded rocks on both sides of the river, but the main mass lies east of the river. There is every reason why phyllites should appear as mica schists near the borders of this large complex intrusive. Students wishing to pursue this matter further should refer to the work of Balk and Barth (1936).

Summary and Conclusions

The reader should keep in mind that all the stratigraphic units involved have been subjected to varying degrees of metamorphism; all are folded, in places isoclinally, and the folds are overturned toward the northwest. All are infolded with, and downfaulted into Precambrian granitoid gneisses.

Age determinations of stratigraphic sequences based on relative degree of metamorphism are generally fallacious.

In the Peekskill region, the stratigraphic units mapped as Cambro-Ordovician north of Peekskill and at Tomkins Cove, west of the Hudson River, are identical with stratigraphic units in and south of Peekskill, mapped as "Inwood" limestone and "Manhattan" schist of "doubtful" age, and referred to by Berkey and Rice (1921, p. 140) as of late Grenville age.

Clearly, New York State east of the Hudson River offers a rich field for stratigraphic and structural studies. Only years of patient, careful work will clarify all the problems that are only too easy to imagine.

References Cited

Balk, Robert, 1936, Structural and petrologic studies in Dutchess County, New York. Part I. Geologic structure of sedimentary rocks: Geol. Soc. America Bull., v. 47, p. 685–774

Barth, Tom. F. W., 1936, Structural and petrologic studies in Dutchess County, New York. Part II. Petrology and metamorphism of the Paleozoic rocks: Geol. Soc. America Bull., v. 47, p. 775–850

Berkey, C. P., and Rice, Marion, 1921, Geology of the West Point quadrangle, New York: N. Y. State Mus. Bull. 225–226, 152 p.

DEPT. GEOLOGY, COLUMBIA UNIVERSITY, NEW YORK 27, N. Y.

MANUSCRIPT RECEIVED BY THE SECRETARY OF THE SOCIETY, DECEMBER 28, 1955